DEPARTAMENTO DE BIOLOGÍA CELULAR, FISIOLOGÍA E INMUNOLOGÍA

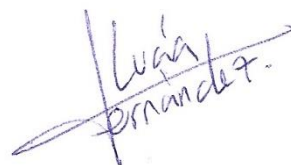Programa de Doctorado en Biomedicina

Regulation of coenzyme Q biosynthesis through nutritional and pharmacological interventions

Regulación de la biosíntesis del coenzima Q a través de intervenciones nutricionales y farmacológicas

Lucía Fernández del Río

Córdoba, 2017

TITULO: *Regulation of coenzyme Q biosynthesis through nutritional and pharmacological interventions*

AUTOR: *Lucía Fernández del Río*

DEPARTAMENTO DE BIOLOGÍA CELULAR, FISIOLOGÍA E INMUNOLOGÍA

Programa de Doctorado en Biomedicina

Regulation of coenzyme Q biosynthesis through nutritional and pharmacological interventions

Memoria de Tesis Doctoral presentada por **Lucía Fernández del Río**, Licenciada en Biología, para optar al grado de **Doctora en Ciencias**.

Los Directores,

Dr. José Manuel Villalba Montoro
Catedrático de Biología Celular
Universidad de Córdoba

Dra. María Isabel Burón Romero
Catedrática de Biología Celular
Universidad de Córdoba

En Córdoba, a 16 de junio de 2017

D. José Manuel Villalba Montoro y Dª María Isabel Burón Romero, Doctores en Ciencias y Catedráticos de Universidad del Área de Biología Celular del Departamento de Biología Celular, Fisiología e Inmunología de la Universidad de Córdoba,

INFORMAN

Que Lucía Fernández del Río, Licenciada en Biología, ha realizado bajo su dirección el trabajo titulado **"Regulation of coenzyme Q biosynthesis through nutritional and pharmacological interventions"**, que a su juicio reúne los méritos suficientes para optar al Grado de Doctora en Ciencias.

Y para que conste, firma el presente INFORME en Córdoba, a 16 de junio de 2017.

Fdo.: José Manuel Villalba   Fdo.: María Isabel Burón
Montoro   Romero

TÍTULO DE LA TESIS: Regulation of coenzyme Q biosynthesis through nutritional and pharmacological interventions

Regulación de la biosíntesis del coenzima Q a través de intervenciones nutricionales y farmacológicas

DOCTORANDA: Lucía Fernández del Río

INFORME RAZONADO DEL/DE LOS DIRECTOR/ES DE LA TESIS

Durante el desarrollo de la presente Tesis Doctoral, llevada a cabo entre los años 2013 y 2017, la doctoranda Lucía Fernández del Río ha superado con creces los objetivos, tanto formativos como de investigación, planteados al comienzo de la misma. El trabajo realizado por la doctoranda ha permitido demostrar que el proceso de biosíntesis de coenzima Q es una diana de diversas intervenciones nutricionales de gran impacto traslacional, como son los polifenoles y los ácidos grasos de la dieta. En el primero de los casos, la doctoranda define por primera vez al kaempferol, presente en muchos alimentos de origen vegetal, como un nuevo sustrato biosintético del coenzima Q que actúa como precursor del anillo isoprenoide de esta molécula antioxidante. En el segundo caso, también por primera vez, se caracteriza a los ácidos grasos poliinsaturados como componentes de la dieta que actúan sobre la ruta del mevalonato estimulando la síntesis de coenzima Q, particularmente de la isoforma con 10 unidades isoprenoides (coenzima Q_{10}). El otro aspecto cubierto en esta Tesis Doctoral ha sido el papel de un agente farmacológico como el zoledronato, bisfosfonato ampliamente utilizado como agente terapéutico en desórdenes óseos, como molécula que también actúa sobre la ruta del mevalonato, en este caso inhibiendo la producción de coenzima Q y alterando notablemente el equilibrio entre las dos isoformas (coenzima Q_9 y coenzima Q_{10}). Los resultados obtenidos en la Tesis son de gran relevancia pues apuntan hacia mecanismos que no había sido definidos hasta el momento y que pueden ayudar a comprender la importancia de la dieta en estados fisiológicos y/o patológicos asociados a una deficiencia en coenzima Q, así como a evidenciar la naturaleza de los efectos asociados a tratamientos a largo plazo con bisfosfonatos. Los resultados obtenidos en la Tesis han sido presentados en algunos de los congresos más prestigiosos relacionados con el tema de estudio, tanto a nivel internacional (*American Society for Biochemistry and Molecular Biology, Oxygen Club of California World Congress*) como nacional (*Sociedad Española de Bioquímica y Biología Molecular*, *Sociedad Española de Biología Celular*). La Tesis ha permitido reunir una cantidad suficiente de información que permitirá publicar los resultados en revistas de alto impacto. De ellos, la parte relativa al papel del kaempferol como sustrato en la biosíntesis de coenzima Q ya ha sido publicada en la revista *Free Radicals in Biology and Medicine*. El resto se encuentran actualmente en preparación. El trabajo se ha desarrollado en el ámbito de un Proyecto de Investigación financiado por el Plan Estatal. La formación de la doctoranda se ha completado con la realización de cursos y colaboraciones de investigación y docentes, así como con la realización de tres estancias cortas internacionales, la primera en la Universidad de California-Davis, y las dos siguientes en la Universidad de California-Los Ángeles. Por todo ello, se autoriza la presentación de la Tesis Doctoral con Mención Internacional.

Córdoba, 19 de Junio de 2017

Firma de los directores

Fdo.: José Manuel Villalba Montoro   Fdo.: María Isabel Burón Romero

Index of contents

Index of figures

Index of tables

Abbreviations

^{13}C-K	^{13}C-kaempferol
2,4-diHB	2, 4-dihydroxybenzoic acid
3,4-diHB	3, 4-dihydroxybenzoic acid
4HB	4-hydroxybenzoic acid
4-HPAC	4-hydroxyphenolacetic acid
a.u.	Arbitrary units
AA	Arachidonic acid
ALA	α-linolenic acid
ATP	Adenosyl triphosphate
BHT	Butylated hydroxytoluene
CLAP	Chymostatin, Leupeptin, Antipain and Pepstatin
CR	Calorie restriction
Cu	Curcumin
D*-GCVLS	Dansyl labeled peptide GCVLS
D_3-FE	D_3-ferulic acid
D_6-Cu	D_6-curcumin
DMAPP	Dimethylallyl pyrophosphate
DMSO	Dimethyl sulfoxide
DNA	Deoxyribonucleic acid
EDTA	Ethylenediaminetetraacetic acid
EFAs	Essential fatty acids
EPA	Eicosapentanoic acid
ER	Endoplasmic reticulum
FBS	Fetal bovine serum
FDPS	Farnesyl diphosphate synthase
FE	Ferulic acid
FOH	Farnesol
FPP	Farnesyl diphosphate
FTase	Farnesyl transferase
GBM	Glioblastoma
GFP	Green fluorescent protein
GGDPS	Geranylgeranyl diphosphate synthase
GGOH	Geranylgeraniol
GGPP	Geranylgeranyl diphosphate
GPP	Geranyl pyrophosphate
HEK 293	Human embryonic kidney cells 293
HeLa	Human cervical cancer cells
Hep G2	Human liver hepatoma cells
Hepa 1.6	Mouse liver hepatoma cells
HL-60	Human promyelocytic leukemia cells
HMG-CoA	3-hydroxy-3-methylglutaryl-coenzyme A
HPLC	High performance liquid chromatography

IDI	Isopentenyl-diphosphate isomerase
IPP	Isopentenyl pyrophosphate
IUPAC	International Union of Pure and Applied Chemistry
K	Kaempferol
LA	Linoleic acid
LXR	Liver X receptor
MCT	Medium-chain triacylglycerol's
MEFs	Mouse embryonic fibroblast
mPT	Permeability transition
MTT	3-(4,5-dimethylthiazol-2-yl)-2,5-diphenyltetrazolium bromide
MUFA	Monounsaturated fatty acids
NAD^+	Nicotinamide adenine dinucleotide (oxidized)
NADH	Nicotinamide adenine dinucleotide (reduced)
NADPH	Nicotinamide adenine dinucleotide phosphate
NAM	Nicotinamide
NAM	Nicotinamide
NBPs	Nitrogen-containing bisphosphonates
Nv	Mitochondrial numerical density
PABA	p-aminobenzoic acid
PBS	Phosphate buffered saline
PDSS1	Polyprenyl diphosphate synthase subunit 1
PDSS2	Polyprenyl diphosphate synthase subunit 2
PMRS	Plasma membrane redox system
PMSF	Phenylmethylsulfonyl fluoride
PTP	Permeability transition pore
PUFA	Polyunsaturated fatty acid
Q	Coenzyme Q
$Q^{\bullet-}$	Ubisemiquinone
QH_2	Ubiquinol
RIPA	Radioinmmunoprecipitation assay
ROS	Reactive oxygen species
SDS	Sodium dodecyl sulfate
SFA	Saturated fatty acids
siRNA	Small interfering RNA
TCA	Trichloroacetic acid
Tkpts	Mouse kidney proximal tubule epithelial cells
UCPs	Uncoupling proteins
VDAC	Voltage-dependent anion channel
Vv	Mitochondrial volume density
ZOL	Zoledronic acid

Abstract

1. Introduction

Coenzyme Q (Q) is a prenylated benzoquinone present in all eukaryotes organisms. It is localized mainly in mitochondria but is also present in all cellular membranes. This molecule, apart from participates as electron carrier in the electron transport chain, has a role in numerous important cellular functions such as metabolism, antioxidant protection and signal regulation. The biosynthesis of Q is a not completely characterized process that can be divided into three main steps: the synthesis of the polyisoprenoid tail through the mevalonate pathway in eukaryotes, the attachment of the tail to the benzoquinone ring precursor and, finally, the subsequent modifications of the ring to yield the final product. The prenylated chain is produced by a trans-polyprenyl transferase (called PDSS1-PDSS2 in mammals), which is specie-specific giving the different lengths of the isoprenoid side chain. For example, *S. cerevisiae* produce Q_6 while bacteria produce Q_8 and rodents and humans produced both, Q_9 and Q_{10}. The well-known ring precursor of Q, 4-hydroxybenzoic acid (4HB), is derived from tyrosine and phenylalanine in mammals, although other phenolic compounds are also able to serve as Q ring precursors. The enzyme COQ2 mediates the condensation of the isoprenoid tail with a quinone ring precursor generating a membrane-bound Q precursor, which is modified by COQ proteins (COQ3-COQ11) in a sequence of enzymatic reactions that includes one decarboxylation, three hydroxylations, two O-methylations and one C-methylation to form the final product. It is well known that tissue levels of Q are regulated in response to a number of physiological, experimental and pathological alterations. Given the essential functions of Q, a deficit in this molecule leads to a number of mitochondrial disorders with heterogeneous clinical symptoms. Q_{10} deficiency is unique among mitochondrial disorders because oral supplementation with exogenous Q_{10} can improve clinical symptoms, however, oral Q has low bioavailability and its final destination is not the inner mitochondrial membrane as in the case of endogenous Q. For these reasons, recent research is focus on alternative procedures able to induce endogenous Q biosynthesis.

The mevalonate pathway, which involve the biosynthesis of the polyisoprenoid side chain of Q, also produces other isoprenoids compounds that are of vital importance for diverse cellular functions. Several regulators of this pathway have been described, being the most important: statins and bisphosphonates. Statins inhibit the HMG-CoA reductase, an upstream enzyme of the pathway, resulting in a depletion of all the downstream

metabolites of the pathway, especially cholesterol, making these compounds a main therapy to lower cholesterol levels. Moreover, numerous studies in animals and humans have stablished the statin-induced Q depletion as a well-documented event. On the other hand, nitrogen-containing bisphosphonates (NBPs) have been used as primary therapy for bone disorders, due their ability to selectively bind bone and impaired the bone reabsorption. NBPs inhibit mainly the so-called *branch point enzyme* of the mevalonate pathway, farnesyl diphosphate synthase (FDPS), but also inhibit other enzymes such as geranylgeranyl diphosphate synthase (GGDPS) and squalene synthase (SQS). The evidence of the role of NBPs on the regulation of Q is limited to a few studies. A decrease of this lipid is described in mice macrophages, in Hep G2 cells treated with risendronate as well as in human plasma of postmenopausal women with osteoporosis treated with zoledronic acid.

Phenolic compounds are secondary metabolites in plants with a common aromatic ring bearing one or more hydroxyl groups. Focusing on their structure, they are classified broadly into simple and complex phenolics (or polyphenols) or, by abundance, in two big groups: flavonoids and non-flavonoids compounds. Polyphenols, which are widely present in foods and beverages of plant origin, have received great interest during the last years due to their positive effects on human health. The beneficial properties of dietary polyphenols have been partially attributed to their antioxidant role as well as to their ability to modulate molecular targets and signaling pathways. Phenolic acids such as 4HB, vanillic acid, protocatechuic acid and *p*-coumarate as well as the stilbenoid resveratrol function as Q ring precursors in yeast and mammals. Moreover, a large list of phenolic acids display an inhibitory effect on upstream enzymes of the mevalonate pathway, when present at high concentrations. Apart from the role that some phenolic compounds play in the biosynthesis of Q, little is known about the possible interaction between more complex polyphenols and the metabolism or regulation of Q.

Fatty acids are biomolecules composed by a carboxyl group linked to a long hydrocarbon chain. They are rarely free in nature but, rather, are found taking part of complex lipid molecules and being the fundamental components of biological membranes. Attending to the presence of double bounds between the carbons of the lateral chain, fatty acids can be classified into saturated (no double bond is present in the hydrocarbon chain) and unsaturated fatty acids (at least one double bound is present between two carbons of the

chain). Within the unsaturated fatty acids, two groups are stablished according to the number of double bonds present in the molecule: monounsaturated fatty acids (MUFA) and polyunsaturated fatty acids (PUFA). Cells are not able to produce all types of fatty acids it requires, but some of them must come from diet. These fatty acids are called "essential fatty acids". There are two known families of essential fatty acids, the n-3 and the n-6 series. Due to essential fatty acids are obtained directly from the diet, it fat and oil composition has important long-term consequences for health. Some studies have described the ability of biological membranes to adapt its phospholipid composition according to the major lipid source present in the diet, so a modification in the lipid pattern could produce biochemical alterations in cells, especially mitochondrial membranes. PUFA sources, such as soybean or fish oil, will generate membranes more susceptible to oxidative stress than a SFA or a MUFA source, like animal fat and olive oil, respectively. Some studies revealed that different dietary fats influenced the mitochondrial levels of Q_9 and Q_{10} in rat liver, being the n-6 PUFA the one that produced the biggest increase. Moreover, previous studies in our group revealed a fast regulation of mice Q biosynthesis, which involved *COQ* genes and COQ proteins, after 1 month of dietary intervention with different fat sources. Concretely, a n-3 PUFA rich diet (based on fish oil) induced the differential expression of *COQ* genes in liver, kidney, skeletal muscle, brain and heart. Additional studies revealed that Q plays an important role in protecting eukaryotic cells from the autoxidation products of PUFA.

Therefore, the main objective of the present Doctoral Thesis was deepen into the regulation of the Q system through nutritional (polyphenols and different fatty acid sources) and pharmacological (statins and NBPs) interventions.

2. Materials and Methods

Different cellular lines of different origins were used, being the two most important Hepa 1.6 (derived from mouse liver hepatoma) and Tkpts (derived from mouse kidney proximal tube epithelium). Mouse embryonic fibroblast (MEFs), human cervical cancer cells (HeLa), human promyelocytic leukemia cells (HL-60), human liver hepatoma cells (Hep G2) and human embryonic kidney cells 293 (HEK 293) were used to complement some results along the whole study.

In order to study the effect of different polyphenols in the Q system we treated the cells with kaempferol, resveratrol, apigenin, quercetin, piceatannol, luteolin, naringenin, curcumin, ferulic acid or 4HB. Three different lipid emulsions were added to the cells to test the influence of fatty acids over Q metabolism: *Lipofundin MCT/LCT* 20% (source of n-6 PUFA), *Lipoplus* 20% (source of n-3 PUFA) and *ClinOleic* 20% (source of n-9 MUFA) Trolox and butylated hydroxytoluene (BHT) were used to discard possible effects of the oxidation of the lipid emulsions used in our studies. Inhibitors of the pathways on study were used. Thus, *p*-Aminobenzoic acid (PABA) was used to depress Q biosynthesis and nicotinamide were used to inhibited sirtuin activity. Lovastatin and zoledronic acid were the selected compounds of the family of statin and NBPS, respectively, to study the influence that a regulation in the mevalonate pathway could produce in Q metabolism. Additionally, direct inhibition of FDPS was carried out using specific siRNAs against this enzyme. The most suitable concentration of all these compounds was stablished after measuring cell viability in a MTT assay. The duration of the treatments was 48 hours.

Additionally, animal models were used to complement some studies. To test the effect of different fat sources we used samples from an experimental mice model with four dietary groups: one control group fed 95 % of a pre-determined *ad libitum* intake (control) and three calorie restriction (CR) groups fed 40 % less than the control. Lipid source for the control and one of the CR groups was soybean oil (high in n-6 PUFA) whereas the two remaining CR groups were fed with diets enriched in fish oil (high in n-3 PUFA) or lard (high in saturated and monounsaturated fatty acids). To study the possible relationship between Sirt3 and Q metabolism we used frozen tissues from Sirt3 knockout mice (*Sirt3-/-*).

In terms of lipid analysis, non saponifiable lipids from the different samples were extracted using SDS, ethanol-isopropanol and hexane, and analyze in HPLC with electrochemical detection, in the case of Q, or HPLC connected to a diode array detector, in the case of cholesterol. Q biosynthesis was indirectly determined using ^{14}C-4HB. This radioactive precursor was synthetized essentially as described by Clarke *et al.* and given to the cells during 48 h. Incorporation of radioactive precursor was determined after precipitation of the samples using 5% trichloroacetic acid and solubilization with 1M NaOH. Radioactivity was quantified in a scintillation counter by mixing with scintillation

liquid. Direct biosynthesis of Q were measured using ^{13}C-4HB and ^{13}C-kaempferol. Q (non-labelled and ^{13}C-labelled) was extracted using methanol and petroleum ether, and measured by HPLC coupled to tandem mass spectrometry (MS/MS).

Additional methodologies were performed to determine levels of intermediary products on Q metabolism study. An adaptation of the protocol developed by Holstein *et al*., which used a GCVLS peptide linked to a fluorescent dansyl group, was used to measure the amount of GPP or FPP in cellular extracts. Relevant enzymes and proteins as COQ2, FDPS, OXPHOS complex, unprenylated Rap1A, total Rap1A, Sirt3, acetylated lysine and VDAC were measured by immunodetection in western blotting. In all cases, protein concentration was determined using the variation introduced by Stoscheck of the traditional protein assay protocol described by Bradford. Planimetric and stereological mitochondrial measurements were performed using electron microscopy micrographs to study the ultrastructure of mitochondria in cells treated with lipid emulsions.

3. Results and Discussion

Plant polyphenols, present in the human diet, are redox active molecules and modulate numerous cellular pathways. In the present study, we tested whether treatment with polyphenols affected the content or biosynthesis of Q. Tkpts cells and HEK 293 were treated with several types of polyphenols, being kaempferol the one that produced the largest increase in Q levels. The increase of Q was related with upregulation of its biosynthetic rate because it was totally inhibited by PABA, a well-characterized inhibitor of COQ2 activity in mammalian cells. Additionally, we studied the role of kaempferol in Q biosynthesis by a competitive assay using radiolabelled ^{14}C-4HB. Kaempferol competed with ^{14}C-4HB as ring precursor of Q and inhibited incorporation of ^{14}C-4HB while simultaneously increasing Q levels. Moreover, our studies with ^{13}C-kaempferol demonstrated a previously unrecognized role of this flavonol as an aromatic ring precursor in Q biosynthesis. The metabolism of kaempferol responsible for its incorporation into the Q biosynthetic pathway remains to be established, although two possibilities can be proposed: (1) kaempferol could act directly as Q precursor being itself a substrate for the COQ2 transferase and would be subsequently metabolized and modified by different COQ proteins until it reaches the final structure of Q; or alternatively (2) kaempferol could be cleaved in the cell to yield potential precursors

which would be then integrated into this pathway. Investigations of the structure-function relationship of related flavonols, derived from the utilization of different products in our cellular model, demonstrated the importance of two hydroxyl groups, located at C3 of the C ring and C4' of the B ring, both present in kaempferol, as important determinants of kaempferol as a Q biosynthetic precursor. Concurrently, our results confirmed the kaempferol mediated increased of the mitochondrial sirtuin Sirt3 through a mechanism not related to the enhancement of Q biosynthesis in Tkpts cells. Determinations of Q levels from different tissues (skeletal muscle, liver, kidney and brain) of Sirt3-KO mice and their respective controls had no significant variation and thus indicated that Q metabolism is not related with Sirt3 activity.

Whatever the metabolic route involved, an increase of alternative Q ring precursors in cells will only turn into higher Q levels if cells have low availability of endogenous 4HB. Tkpts, HEK 293, Hepa 1.6, HL-60, Hep G2 and MEFs were treated with increased amounts of 4HB, to observe whether increased levels of precursor have any effect on Q levels. The increase of Q observed in Tkpts and HEK 293, but not in cells of different origin, confirms that the endogenous availability of this precursor is very low in mouse and human kidney cells. These results indicated that 4HB is a limiting step in the biosynthesis of Q specifically in renal derived cells. A previous report related maximal levels of COQ2 polypeptide with those organs displaying the highest Q concentrations. In accordance, our results showed that Tkpts cells presented higher levels of both Q and COQ2 polypeptide than those encountered in Hepa 1.6 cells. Higher levels of the COQ2 transferase might maintain low cellular concentrations of the ring precursor 4HB due to its rapid use by the COQ2 prenyltransferase activity. Measurements of inner and outer mitochondrial membrane markers suggested that Tkpts cells, in comparison with Hepa 1.6 cells, might have less or smaller mitochondria, but they contain more surface of mitochondrial cristae inside this organelle that could explain the highest levels of Q observed. Increasing the availability of Q precursors in cells, supplementing with 4HB or kaempferol, could move the metabolic flux in favor of the synthesis of Q, helping to ameliorate the phenotype associated with certain Q deficiencies, at least for some organs such as kidney.

Unsaturated fatty acids are basic components of the diet and have, among others, several targets in the mevalonate pathway. Using Hepa 1.6 cells treated with lipid emulsions of

different composition, we have shown that unsaturated fatty acids were able to increase Q and decrease cholesterol levels. The increment of Q is not related with lipid peroxidation because Hepa 1.6 cells displayed the same results to the emulsions in absence and presence of BHT or Trolox, two antioxidants that inhibit oxidation. In the case of PUFA, increased Q levels are directly related with an increment of Q biosynthesis. Moreover, our results indicate that PUFA regulates the different Q isoforms in a different way, promoting the biosynthesis of Q_{10} over Q_9 and decreasing Q_9/Q_{10} ratio. However, MUFA did not alter Q biosynthesis. The regulation of the ratio could be influenced by the decrease of FDPS produced by these lipid sources, which might lead to the accumulation of IPP and DMAPP within the cell. The accumulation of IPP would promote the biosynthesis of Q_{10} over Q_9, a mechanism already proposed for HepG2 cells. However, additional targets of unsaturated fatty acids are necessary to understand the different regulation of cholesterol and Q. GPP and FPP, the two metabolites produced by FDPS, are accumulated in presence of PUFA indicating that FDPS directly do not regulate its metabolites but possibly this is in charge of GPP/FPP-consuming enzymes. Measurements of the prenylated form of Rap1A, a protein that is specifically geranylgeranylated, indirectly indicated that GGDPS, a FPP-consuming enzyme, was not affected by PUFA. Therefore, high levels of FPP in the cells could be the result of a PUFA-mediated inhibition of SQS, the major FPP-consuming enzyme, or other enzyme involved in the cholesterol branch. Decreased levels of cholesterol confirmed this hypothesis but additional experiments will be needed to point the concrete enzyme. Possibly isopentenyl-diphosphate isomerase, the enzyme that convert IPP to its highly nucleophilic isomer dimethylallyl diphosphate (DMAPP), could be a target of fatty acids and its regulation could enhance DMAPP levels that might inhibit the second catalytic reaction of FDPS producing an accumulation of GPP. Taken together these results indicates that PUFA, and to a lesser extent MUFA, were able to increase Q levels but only PUFA acting as regulators of Q biosynthesis. The regulation may involves different steps in the mevalonate pathway, such as FDPS, but possibly a direct target in the biosynthesis branch of Q is also needed to exert the described effects.

A model of calorie-restricted animals of different ages allowed us to study the effect of a different fat type supplementation as well as the effect of aging *in vivo*. We observed that calorie restriction abolished these age-induced changes of Q levels in liver and skeletal

muscle from mice fed PUFA-enriched diets. In a calorie restriction context, liver and skeletal muscle tissues were able to adapt to a PUFA-enriched diet by increasing Q levels and decreasing Q_9/Q_{10} ratio. Taken together, these observations agree with the described protective effect of a saturated fat source in calorie-restricted conditions previously described by our research group. Additionally, it was observed that FDPS is also regulated by a calorie restriction intervention and influenced by the different fat sources, but in a different way from how it is regulated in the hepatocellular model. Further experiments will be needed to fully understand the exact regulation that fatty acids exerts in, both, cellular and animal models.

To deepen into the regulation of Q system through the regulation of FDPS we used two additional approaches: one genetic and one pharmacologic. In the genetic strategy, we utilized specific siRNAs against FPDS and showed that an inhibition of this enzyme is sufficient to increase Q_{10} levels and decrease the Q_9/Q_{10} ratio, without altering Q_9 or total Q levels. This Q regulation might be mediated by an increase of some upstream metabolites in the mevalonate pathway such as IPP. The inhibition of this enzyme did not change the level of its products, GPP and FPP, even when the enzyme levels were very low. Indirect measurement of GGDPS revealed that an inhibition of FDPS did not affect the function of this downstream enzyme.

On the other hand, in the pharmacological approach, we used zoledronic acid (ZOL) to inhibit FDPS. The specific inhibition of FDPS mediated by ZOL is widely described in the literature. We studied the effect of ZOL on Q system in several cell lines, including two murine and two human lines. The inhibition of FDPS due to ZOL is not at the transcriptional level, as we previously described for treatments with PUFA and siRNAs, but it is due to a slow, tight binding process that results in the inactivation of FPDS activity. However, FDPS is not the unique molecular target of this compound. ZOL also inhibits other enzymes in the mevalonate pathway such as SQS and GGDPS. Measuring the unprenylated form of Rap1A we confirmed the inhibition of ZOL over GGDPS in Tkpts and Hepa 1.6 cells. Lower cholesterol levels in Tkpts gave us an indirect proof of the inhibition of SQS but the response in Hepa 1.6 is not the same. However, all the cells treated with ZOL (Tkpts, Hepa 1.6, HeLA and HEK 293) generally decreased Q biosynthesis and Q levels, but also decreased the ratio Q_9/Q_{10}. The same upregulation of IPP seems to be the cause of the regulation of the ratio, however, an additional target in

the Q biosynthetic branch of the pathway should be necessary to explain low levels of Q. GPP and FPP were also measured in ZOL treated cells showing an increase of GPP but no changes in FPP levels. The effect of ZOL in the GPP levels of Hepa 1.6 is higher than in the kidney-derived cell line indicating that the mevalonate pathway is differentially regulated in cells lines from different origins. ZOL binds and remains the DMAPP/GPP site during FDPS inhibition impairing the binds of GPP and possibly leading to the accumulation of this metabolite that could contribute to the cellular functions described for NBPs. However, the general decrease of Q levels cannot be explained by the inhibition of FPDS nor the inhibition of GGDPS. Based on these results, we suggest that ZOL might have an additional target in the biosynthesis branch of Q of the mevalonate pathway, similarly to unsaturated fatty acids, despite their effects are totally opposite. Guo *et al.* described NBPs as inhibitors of hexaprenyl diphosphate synthase (from *Sulfolobus solfataricus*) and octaprenyl diphosphate synthase (from *E. coli*). Whether these long-chain prenyltransferases are potently inhibited by bisphosphonates, PDSS1-PDSS2 become a strong candidate to be the additional target of ZOL that inhibit Q levels in mouse and human cells.

In order to compare an upstream inhibition of the mevalonate pathway with the downstream inhibition describe above we use lovastatin, an inhibitor of the HMG-CoA reductase. Cells treated with lovastatin decrease Q_9, Q_{10} and total Q but did not alter the Q_9/Q_{10} ratio in Tkpts and Hepa 1.6 cells. Moreover, lovastatin treatment decreased cholesterol levels in Tkpts cells. In this context, the whole pathway is inhibited all, thus, all the downstream metabolites are decreased, including IPP which is proposed to be determinant in the regulation of the Q_9/Q_{10} ratio. 4HB, apart from being a well-known Q precursor, is described to act as an upstream inhibitor of the mevalonate pathway. In Hepa 1.6 cells, in which 4HB is not considered a limiting step of Q biosynthesis, 100 µM of 4HB produced a decrease in Q levels possibly acting as inhibitor of the whole route. Our results would indicate that an upstream inhibition of the mevalonate pathway, as that caused by lovastatin, have has different effects of Q system comparing with a downstream inhibition, as that caused by ZOL, fatty acids or specific siRNA against FDPS. Additional research is needed to understand the mechanisms underlying the differential cell-specific effects of several inhibitors on the products of different branches of the mevalonate pathway as Q and cholesterol.

Resumen

1. Introducción

El coenzima Q (Q) es una benzoquinona prenilada presente en todos los organismos eucariotas. Se localiza principalmente en la mitocondria pero está presente en todas las membranas celulares. Esta molécula, además de participar como transportador de electrones en la cadena de transporte de electrones mitocondrial, está implicada en el metabolismo, la protección antioxidante y la regulación de señales celulares. La biosíntesis del Q, mecanismo que aún no ha sido elucidado por completo, se divide en tres pasos: la síntesis de la cola isoprenoide, la unión de esta cola al anillo benzoquinónico y, finalmente, las consecutivas modificaciones del anillo hasta llegar al producto final. La cola isoprenoide es producida por una trans-poliprenil transferasa específica de especie (llamada PDSS1-PDSS2 en mamíferos), que determina las diferentes longitudes de la cadena lateral en los diferentes organismos. Por ejemplo, *S. cerevisiae* produce Q_6, las bacterias producen Q_8 y los roedores y humanos dos isoformas, Q_9 y Q_{10}. El precursor más conocido del Q es el ácido 4-hidroxibenzoico (4HB), que deriva de la tirosina y la fenilalanina en mamíferos, aunque recientemente otros compuestos fenólicos han sido descritos como precursores alternativos del anillo. La enzima COQ2 media la condensación de la cola isoprenoide con el anillo benzoquinónico generando el primer precursor del Q anclado en membrana, que será modificado a continuación por las diferentes proteínas COQ (COQ3-COQ11) mediante una serie de reacciones secuenciales que incluyen una descarboxilación, tres hidroxilaciones, dos O-metilaciones y una C-metilación hasta formar el producto final. Bajo diferentes condiciones fisiológicas, experimentales y patológicas los niveles tisulares de Q pueden estar elevados o disminuidos. Dadas las funciones esenciales del Q, un déficit en esta molécula puede desencadenar varios desórdenes mitocondriales con síntomas de distinta índole. La deficiencia de Q_{10} es única entre los diferentes desórdenes mitocondriales ya que la suplementación oral con Q_{10} exógeno es capaz de mejorar algunos de los síntomas. Sin embargo, el Q tomado de forma oral tiene muy baja biodisponibilidad y su destino final no es la membrana mitocondrial interna, como en el caso del Q endógeno. Por esta razón, en la actualidad las investigaciones están enfocadas hacia procedimientos alternativos capaces de inducir la síntesis endógena de esta molécula.

La ruta del mevalonato, involucrada en la biosíntesis de la cola isoprenoide del Q, produce además otros lípidos isoprenoides muy importantes en diversas funciones celulares.

Varios reguladores de la ruta del mevalonato han sido descritos, siendo los más importantes las estatinas y los bisfosfonatos. Las estatinas inhiben a la HMG-CoA reductasa, una de las primeras enzimas de la ruta, provocando una disminución de todos los metabolitos que se localicen aguas abajo. Uno de los compuestos más inhibidos es el colesterol, propiciando así el uso de éstos compuestos como terapia primaria para bajar los niveles de colesterol en sangre. Numerosos estudios realizados en animales y humanos han documentado el descenso de los niveles de Q como efecto secundario del tratamiento con estatinas. Por otro lado, los bisfosfonatos que contienen nitrógeno (NBPs) han sido utilizados como terapia en enfermedades óseas gracias a su habilidad de unirse selectivamente el hueso e impedir la reabsorción del mismo. Los NBPs inhiben principalmente la enzima central de la ruta del mevalonato, la farnesil difosfato sintasa (FDPS), pero también son capaces de inhibir otras enzimas de la ruta como la geranilgeranil difosfato sintasa (GGDPS) o la esqualeno sintasa (SQS). Las evidencias de la regulación del Q por los NBPs están limitadas a unos cuantos estudios. Un descenso de este lípido está descrito en macrófagos de ratón tratados con ácido zoledrónico, en células Hep G2 tratadas con risendronato y en muestras de plasma de mujeres postmenopáusicas con osteoporosis tratadas con ácido zoledrónico.

Los compuestos fenólicos son metabolitos secundarios vegetales con un anillo aromático común que contiene uno o más grupos hidroxilos. Centrándonos en su estructura, se clasifican en compuestos fenólicos simples o complejos (también llamados polifenoles). Sin embargo, atendiendo a su abundancia podemos clasificarlos en dos grandes grupos: flavonoides y no flavonoides. Durante los últimos años, los polifenoles, que son ampliamente presentes en comidas y bebidas de origen vegetal, han recibido gran atención debido a sus efectos positivos sobre la salud humana. Sus propiedades beneficiosas han sido parcialmente atribuidas a su actividad antioxidante así como a su habilidad como moduladores de diferentes dianas moleculares y vías de señalización. Los ácidos fenólicos como el 4HB, el ácido vanílico, el ácido protocatéquico y el ácido p-coumárico, así como el estilbeno resveratrol pueden funcionar como precursores del anillo del Q en levaduras y mamíferos. Además, una larga lista de ácidos fenólicos, usados a altas concentraciones, han sido descritos como inhibidores de las primeras enzimas de la ruta del mevalonato. Aparte del papel que desempeñan algunos compuestos fenólicos como precursores del Q, se conoce poco acerca de la posible interacción de estos compuestos con el metabolismo y la regulación de este antioxidante.

Los ácidos grasos son biomoléculas compuestas con un grupo carboxilo unido a una cadena larga lateral hidrocarbonada. Estos compuestos no se suelen encontrar libres en la naturaleza sino que se encuentran como componentes fundamentales de las membranas biológicas. Atendiendo a la presencia de dobles enlaces entre carbonos de la cadena lateral, los ácidos grasos pueden ser clasificados en saturados (en los que no hay presencia de dobles enlaces) o insaturados (en los que por lo menos un doble enlace está presente en la cadena). Dentro de los ácidos grasos insaturados se establecen dos grupos según el número de dobles enlaces presentes en la molécula: monoinsaturados (MUFA) o poliinsaturados (PUFA). Las células no son capaces de producir todos los tipos de ácidos grasos que necesitan sino que algunos de ellos se obtienen directamente de la dieta. Estos ácidos grasos son los llamados "ácidos grasos esenciales", y se clasifican principalmente en dos familias: la serie n-3 y la serie n-6. Debido a que los ácidos grasos esenciales se obtienen directamente de la dieta, la composición de grasa y aceite de la misma tiene importantes consecuencias a largo plazo para la salud humana. Algunos estudios han descrito la habilidad de las membranas de adaptar su composición lipídica en función de la grasa predominante en la dieta, por lo que una modificación del patrón lipídico puede producir alteraciones bioquímicas en las células, especialmente en las membranas mitocondriales. Las fuentes de PUFA, como el aceite de soja o el aceite de pescado, generarán membranas más susceptibles al daño oxidativo que las fuentes ricas en ácidos grasos saturados o MUFA, como la grasa animal o el aceite de oliva, respectivamente. Algunos estudios han descrito que las diferentes grasas de las dieta aumentan los niveles mitocondriales de Q_9 y Q_{10} en el hígado de rata, siendo los PUFA n-6 los que producen el mayor incremento. Estudios previos realizados en nuestro grupo de investigación con ratones alimentados durante un mes con diferentes fuentes grasas, mostraron una regulación rápida de la biosíntesis del Q, tanto a nivel génico como a nivel de proteína. Concretamente, dietas enriquecidas en aceite de pescado (y, por tanto, enriquecidas en n-3) inducen la expresión de los genes *COQ* en hígado, riñón, músculo esquelético, cerebro y corazón. Estudios adicionales mostraron que el Q juega, además, un papel fundamental en la protección de las células eucariotas de la autooxidación de los PUFA.

Por tanto, el objetivo principal de la presente Tesis Doctoral es profundizar en la regulación del sistema del Q a través de intervenciones nutricionales (como son el uso de polifenoles o diferentes fuentes grasas) y farmacológicas (como el uso de estatinas y NBPs).

2. Materiales y métodos

Líneas celulares de diferentes orígenes han sido utilizadas a lo largo del estudio, siendo las más importantes: Hepa 1.6 (derivadas de hepatoma de ratón) y Tkpts (derivadas de túbulo contorneado proximal de riñón de ratón). Fibroblastos embrionarios de ratón (MEFs) así como células humanas derivadas de cáncer de cérvix (HeLa), células de leucemia promielocítica humana (HL-60), células derivadas de hepatoma humano (Hep G2) y células embrionarias de riñón humano (HEK 293) se utilizaron para complementar diferentes resultados a lo largo de todo el estudio.

Para estudiar los efectos que diferentes compuestos fenólicos pueden tener sobre el sistema del Q las células fueron tratadas con kaempferol, resveratrol, apigenina, quercetina, piceatannol, luteolina, naringenina, curcumina, ácido ferúlico o 4HB. Además, tres emulsiones lipídicas de diferente composición fueron añadidas a los cultivos para evaluar la influencia que las diferentes fuentes de ácidos grasos pueden tener sobre el metabolismo del Q. Las tres emulsiones son: *Lipofundina MCT/LCT* 20% (fuente de PUFA n-6), *Lipoplus* 20% (fuente de PUFA n-3) y *ClinOleic* 20% (fuente de MUFA n-9). Tratamientos con Trolox e hidroxitolueno butilado (BHT) fueron usados para descartar una posible influencia de la peroxidación lipídica en los resultados obtenidos con las emulsiones lipídicas. Varios inhibidores de las rutas de estudio fueron utilizados: el ácido *p*-aminobenzoico (PABA) para inhibir la biosíntesis de Q y la nicotinamida para inhibir la actividad de sirtuinas. La lovastatina y el ácido zoledrónico fueron seleccionados como representantes de la familia de las estatinas y los NBPs, respectivamente, para estudiar la influencia que una regulación sobre la ruta del mevalonato puede tener sobre el sistema del Q. Adicionalmente, una inhibición específica de la FDPS fue llevada a cabo usando siRNAs diseñados específicamente para esta enzima. La concentración adecuada de cada uno de los compuestos se definió después de medir la viabilidad celular en un ensayo MTT. La duración de los tratamientos fue, en todos los casos, de 48 horas.

Diferentes modelos animales fueron utilizados para complementar algunos de los estudios llevados a cabo. Para evaluar el efecto de la composición de varias fuentes grasas se usó un modelo animal compuesto de cuatro grupos dietéticos: un grupo control alimentado con el 95% de la previamente calculada ingesta *ad libitum* de los ratones y tres grupos en

40 % de restricción calórica (RC). La fuente grasa del grupo control y de uno de los grupos en RC fue aceite de soja (rica en PUFA n-6), mientras que las fuentes grasos de los otros dos grupos en RC fueron aceite de pescado (rico en PUFA n-3) y manteca (rica en ácidos grasos saturados y MUFA n-9). Para estudiar la posible relación entre la sirtuina mitocondrial Sirt3 y el metabolismo del Q usamos tejidos congelados de ratones Sirt3 knockout (*Sirt3-/-)*.

Los lípidos no saponificables de las diferentes muestras fueron extraídos usando SDS, una mezcla de etanol-isopropanol y hexano, y analizados en HPLC con detección electroquímica, en el caso del Q, o con HPLC conectado a un detector *diode array*, en el caso del colesterol. La biosíntesis del Q fue medida de forma indirecta usando ^{14}C-4HB. Este precursor radioactivo fue sintetizado previamente usando el protocolo descrito por Clarke *et al.*, y añadido a las células durante 48 horas. La incorporación del precursor radiactivo de determinó tras la precipitación de las muestras con ácido tricloroacético al 5% y la solubilización de las mismas con NaOH 1M. La radiactividad se cuantificó en un contador de centelleo tras añadir cóctel de centelleo. A su vez, la biosíntesis del Q fue determinada de forma directa usando ^{13}C-4HB y ^{13}C-kaempferol. El Q (no marcado y marcado con ^{13}C) fue extraído usando metanol y éter de petróleo, y medido mediante HPLC acoplado a espectrometría de masas.

Metodologías adicionales fueron llevadas a cabo para complementar los estudios centrados en elucidar el metabolismo del Q en diferentes contextos. Una adaptación del protocolo desarrollado por Holstein *et al*., que utiliza un péptido de secuencia GCVLS unido a un grupo dansilo fluorescente, fue llevada a cabo para determinar los niveles de GPP y FPP en extractos celulares. Los niveles de varias enzimas y proteínas relevantes como COQ2, FDPS, los diferentes complejos de la cadena de transporte de electrones mitocondrial, Rap1A prenilado y total, Sirt3, lisina acetilada y VDAC se midieron mediante inmunodetección por western-blot. En todos los casos, la concentración proteica de las muestras se determinó usando la variación descrita por Stoscheck del método tradicional de determinación de proteína descrito por Bradford. Medidas planimétricas y estereológicas de la mitocondria fueron llevadas a cabo usando imágenes tomadas mediante microscopía electrónica para estudiar la ultraestructura de este orgánulo en células tratadas con las diferentes emulsiones lipídicas.

3. Resultados y discusión

Los polifenoles vegetales presentes en la dieta humana son moléculas redox muy activas capaces de modular numerosas rutas celulares. En nuestro estudio, hemos evaluado el efecto de diferentes polifenoles sobre los niveles y la biosíntesis del Q. Células Tkpts y HEK 293 fueron tratadas con diferentes polifenoles, siendo kaempferol el que produce el mayor incremento en los niveles de este antioxidante. Este aumento de los niveles de Q mediado por kaempferol está relacionado con el incremento de la tasa de biosíntesis de esta molécula ya que es totalmente inhibido por PABA, un inhibidor muy conocido de la actividad COQ2 en células de mamífero. Además, el papel del kaemperol en la regulación de la biosíntesis de Q se estudió de forma indirecta en un ensayo competitivo con [14]C-4HB, en el que se observó que este polifenol compite con el [14]C-4HB como precursor del anillo benzoquinómico del Q inhibiendo la incorporación del precursor radiactivo. A modo de confirmación, los estudios llevados a cabo usando ^{13}C-kaempferol demostraron una nueva función de este flavonol como precursor del anillo aromático en la biosíntesis de Q. El metabolismo del kaempferol responsable de su incorporación en la ruta de biosíntesis del Q aún no ha sido establecido, sin embargo, podemos proponer dos posibilidades: (1) el kaempferol puede actuar directamente como precursor del Q siendo él mismo sustrato de la transferasa COQ2 para ser, a continuación, modificado por las diferentes proteínas COQ hasta llegar a la estructura final del Q; o alternativamente (2) el kaempferol puede ser metabolizado en la célula dando lugar a precursores potenciales del Q que pueden integrarse en la ruta de biosíntesis. Investigaciones que relacionan la estructura y la función de los flavonoles, derivadas de la utilización de diferentes productos en nuestro modelo celular, han demostrado la importancia de los dos grupos hidroxilos (localizados en las posiciones C3 del anillo C o C4' del anillo B) como estructuras determinantes en la actuación del kaempferol como precursor del Q. Paralelamente, nuestros resultados han confirmado que el incremento de la sirtuina mitocondrial Sirt3 producido por el kaempferol es independiente del aumento de la biosíntesis del Q producido por este flavonol en células Tkpts. Determinaciones de los niveles de Q en tejidos (músculo esquelético, hígado, riñón y cerebro) de ratones Sirt3 *knockout* y en sus correspondientes controles, no presentan variaciones de ningún tipo indicando de nuevo que el metabolismo del Q no está relacionado con Sirt3.

Independientemente de la ruta involucrada, un aumento de los precursores de anillo en las células solo tendrá efecto sobre los niveles de Q si esas células tienen una baja disponibilidad de 4HB. Las células Tkpts, HEK 293, Hepa 1.6, HL-60, Hep G2 y MEFs fueron tratadas con cantidades crecientes de 4HB, para ver el efecto que un aumento del precursor podía tener sobre los niveles de Q. El incremento de los niveles de Q observado en Tkpts y HEK 293, pero no en células de otros orígenes, confirma que la disponibilidad endógena de este precursor es muy baja en células de riñón, tanto humanas como de ratón. Nuestros resultados indican que el 4HB es un paso limitante en la biosíntesis del Q específicamente en células derivadas de riñón. Estudios previos relacionan los niveles máximos de COQ2 con aquellos órganos que poseen los mayores niveles de Q. En consecuencia, nuestros resultados mostraron que las Tkpts presentaban mayores niveles tanto de Q como de COQ2 en comparación con las células hepáticas Hepa 1.6. Unos niveles altos de COQ2 pueden ayudar a mantener niveles bajos de precursores como el 4HB debido a una elevada tasa de consumo de sustrato por esta enzima. Las medidas de marcadores de membrana mitocondrial interna y externa sugieren que las células Tkpts, en comparación con las células Hepa 1.6, poseen menos mitocondrias o más pequeñas pero con una mayor superficie de crestas dentro del orgánulo que puede explicar los elevados niveles de Q observados. Incrementando la biodisponibilidad de precursores del Q en las células, suplementando con 4HB o kaempferol, podría derivar flujo metabólico a favor de la biosíntesis del Q, ayudando a mejorar el fenotipo asociado con ciertas deficiencias de Q al menos en algunos órganos como el riñón.

Los ácidos grasos insaturados son componentes básicos de la dieta y tienen, entre otras, varias dianas en la ruta del mevalonato. Usando células Hepa 1.6 tratadas con emulsiones lipídicas de diferente composición, observamos que los ácidos grasos insaturados son capaces de incrementar el Q y de disminuir los niveles de colesterol. Este incremento no está influenciado por la peroxidación lipídica ya que las células Hepa 1.6 muestran los mismo resultados en respuesta a las emulsiones lipídicas en ausencia o presencia de BHT o Trolox, dos antioxidantes capaces de inhibir la oxidación de las moléculas. En el caso de los PUFA, el incremento de los niveles de Q está directamente relacionado con un aumento de la tasa de biosíntesis de este antioxidante. Además, nuestros resultados indican que los PUFA regulan de forma independiente las diferentes isoformas del Q, promoviendo la biosíntesis de Q_{10} sobre la de Q_9 y, por tanto, disminuyendo el ratio Q_9/Q_{10}. Sin embargo, los MUFA no alteran la biosíntesis de Q. La regulación del ratio

Q_9/Q_{10} puede estar influenciada por el descenso de la FDPS producido por los ácidos grasos insaturados, que promueve la acumulación de IPP y DMAPP, metabolitos aguas arriba en la ruta, dentro de la célula. La acumulación de IPP puede estimular la biosíntesis de Q_{10} sobre la de Q_9, como ya ha sido descrito para células Hep G2. Sin embargo, los ácidos grasos insaturados deben tener dianas adicionales que justifiquen la diferente regulación observada para el colesterol y para el Q. GPP y FPP, los dos metabolitos producidos por la FDPS, se acumulan en presencia de PUFA indicando que la FDPS no regula directamente sus metabolitos sino que probablemente se regulen por las enzimas que los consumen. Las medidas que hemos realizado de la forma no prenilada de Rap1A, una proteína que es específicamente geranilgeranilada, indican de forma indirecta que la GGDPS, una de las enzimas consumidoras de FPP, no se afecta por los PUFA. Por tanto, los niveles altos de FPP observados en las células pueden ser el resultado de una inhibición mediada por PUFA de la SQS, la principal enzima consumidora de FPP, o de otra enzima involucrada en la rama de biosíntesis del colesterol. El hallazgo de un descenso de los niveles de colesterol confirma esta hipótesis aunque serán necesarios experimentos adicionales para indicar la enzima concreta. La isopentenil difosfato isomerasa, la enzima que convierte el IPP en su isómero DMAPP, puede ser diana de los ácidos grasos y su regulación puede desencadenar un incremento de los niveles de DMAPP que inhiba la segunda reacción de la FDPS produciendo la acumulación de GPP. En conjunto, nuestros resultados indican que los PUFA, y en menos medida los MUFA, son capaces de incrementar los niveles de Q, pero solamente los PUFA actúan como reguladores de la biosíntesis de esta molécula. Esta regulación involucra diferentes niveles de la ruta del mevalonato, como la FDPS, aunque la existencia de una diana adicional en la rama de biosíntesis del Q se hace necesaria para explicar algunos de los resultados descritos.

El modelo de animales en RC de diferentes edades nos permitió estudiar el efecto de la suplementación con distintos tipos de grasas así como el efecto de estas intervenciones dietéticas sobre el envejecimiento *in vivo*. Se observó que la RC elimina los cambios inducidos por la edad en los niveles de Q en hígado y músculo esquelético de ratones alimentados con dietas enriquecidas con PUFA n-6. En un contexto de RC, el hígado y el músculo esquelético son capaces de adaptarse a dietas enriquecidas en PUFA incrementando los niveles de Q y disminuyendo el ratio Q_9/Q_{10}. De forma conjunta, nuestras observaciones están de acuerdo con el efecto protector, descrito previamente por

nuestro grupo, de las fuentes grasas saturadas en condiciones de RC. Además, hemos observado que la FDPS es también regulada en condiciones de RC y se influencia por las diferentes fuentes grasas, aunque de una manera diferente a la que hemos descrito en el modelo celular. Serán necesarios experimentos adicionales para entender la regulación exacta que los ácidos grasas ejercen tanto en modelos animales como celulares.

Para profundizar en la regulación del sistema del Q a través de la regulación de la FDPS hemos utilizado dos aproximaciones: una genética y otra farmacológica. En la estrategia genética, utilizamos siRNAs específicos diseñados contra la FDPS y observamos que la disminución en los niveles de esta enzima es suficiente para incrementar los niveles de Q_{10} y bajar el ratio Q_9/Q_{10} ratio, sin afectar a los niveles de Q_9 o de Q total. Todo ello posiblemente debido a la acumulación de precursores aguas arriba en la ruta del mevalonato, como el IPP. La inhibición de esta enzima no altera sus productos (GPP y FPP), incluso cuando los niveles de la enzima son muy bajos. Medidas indirectas de la GGDPS revelan que la inhibición de la FDPS no afecta a su función de geranilgeranilación.

Por otro lado, en la aproximación farmacológica, hemos usado ácido zoledrónico (ZOL) para inhibir la FDPS. La inhibición de la FDPS mediada por ZOL es ampliamente descrita en la bibliografía. Hemos estudiado el efecto del ZOL en el sistema del Q en varias líneas celulares, incluyendo dos líneas humanas así como dos líneas murinas. La inhibición de la FPDS mediada por ZOL no ocurre a nivel transcripcional, como en el caso de los tratamientos con PUFA o con el uso de siRNAs, sino que es debida a una inhibición lenta y estrecha que resulta en la inactivación de la actividad de la FDPS. Sin embargo, la FDPS no es la única diana de este compuesto. El ZOL inhibe también otras enzimas de la ruta del mevalonato como la SQS y la GGDPS. Medidas de la forma no prenilada de Rap1A nos permitieron confirmar la inhibición del ZOL sobre la GGDPS en células Tkpts y Hepa 1.6. Los bajos niveles de colesterol en presencia de ZOL en células Tkpts nos indican de forma indirecta una regulación sobre la SQS. En células Hepa 1.6 los niveles de colesterol no se afectan con el tratamiento de ZOL. Sin embargo, en todas las células tratadas con ZOL (Tkpts, Hepa 1.6, HeLA and HEK 293) se observa un descenso generalizado de la biosíntesis y de los niveles de Q, disminuyendo a su vez el ratio Q_9/Q_{10}. De nuevo, el incremento de los niveles de IPP parece ser la causa de la regulación del ratio aunque, sin embargo, una diana adicional en la rama de biosíntesis del Q es necesaria para explicar

los bajos niveles observados de esta molécula. Medidas de los niveles de GPP y FPP mostraron que el ZOL incrementa los niveles de GPP sin afectar a los niveles de FPP. El efecto del ZOL sobre los niveles de GPP en Hepa 1.6 es mayor que el observado en la línea celular derivada de riñón, lo que sugiere que la ruta del mevalonato es regulada de forma diferencial en líneas celulares de diferentes orígenes. El ZOL se une al sitio de unión del DMAPP/GPP durante la inhibición de la FDPS propiciando la acumulación de GPP en la célula, el cual posiblemente pueda contribuir a las funciones celulares descritas para este fármaco. Sin embargo, el descenso general de Q no se explica mediante la inhibición de la FDPS o de la GGDPS, por lo que es posible que este fármaco tenga una diana adicional en la rama de biosíntesis del Q de igual forma similar a los PUFA aunque sus efectos sean completamente opuestos. Guo *et al.* describen los NBPs como inhibidores de la hexaprenil difosfato sintasa (de *Sulfolobus solfataricus*) y la octaprenil difosfato sintasa (de *E. coli*), lo que nos lleva a pensar en que si estas preniltransferasas de cadena larga son reguladas por NBPs, la PDSS1-PDSS2 podría ser una diana potencial del ZOL, inhibiendo así los niveles de Q en células de mamífero.

Para comparar una inhibición aguas arriba de la ruta del mevalonato con la previamente descrita inhibición aguas abajo se usó la lovastatina, un inhibidor de la HMG-CoA reductasa. Las células Tkpts y Hepa 1.6 tratadas con este fármaco disminuyeron sus niveles de Q_9, Q_{10} y Q total, sin afectar el ratio Q_9/Q_{10}. Además, el tratamiento con lovastatina disminuye los niveles de colesterol en Tktps. En este contexto, toda la ruta del mevalonato está inhibida así como todos sus metabolitos, incluyendo el IPP, que se ha propuesto como determinante en la regulación del ratio Q_9/Q_{10}. Por otro lado, el 4HB, además de ser bien conocido como precursor del Q, se describe como inhibidor de las primeras enzimas de la ruta del mevalonato. En las células Hepa 1.6, en las que el 4HB no es considerado un paso limitante en la biosíntesis del Q, una concentración de 100 µM de este compuesto produce un descenso en los niveles de Q, posiblemente actuando como inhibidor de la ruta. Nuestros resultados indican que una regulación aguas arriba de la ruta del mevalonato causada por la lovastatina tiene efectos diferentes sobre el sistema del Q al de una inhibición sobre la FDPS (observada con PUFAs, siRNA y ZOL). Será necesaria una experimentación adicional para entender los efectos específicos del tipo celular observados con los diferentes inhibidores sobre diferentes ramas de la ruta del mevalonato, como la del Q o la del colesterol.

Introduction

1. Coenzyme Q

1.1. Structure and chemical properties

Coenzyme Q (also named ubiquinone, 2,3-dimethoxy-5-methyl-6-polyprenyl-1,4-benzoquinone or simply Q) was firstly discovered by Festenstein *et al.* in 1955 [1] and then isolated by Crane *et al.* in 1957, who also described its redox capacity as well as its presence in the complexes of the electron transport chain [2]. One year later, Wolf and collaborators determined the complex structure of Q, being a lipid composed by a benzoquinone ring connected to a long isoprenoid side chain (Figure I1) [3], which required a specific position in the biological membranes. In living organisms, Q exists in a number of different forms depending on the length of the isoprenoid side chain. For example, *Saccharomyces cerevisiae* produces Q_6, *Candida utilis* produces Q_7, *Escherichia coli* produces Q_8, *Candida albicans*, *Arabidopsis thaliana* and rodents produce Q_9 and *Schizosaccharomyces pombe* and humans produce Q_{10} [4-6]. One type of Q is dominant in each organism, but (a) minor type(s) of Q can be also detected. This happens, for example, in rodents and humans where Q_9 and Q_{10} are synthetized, or in the lung pathogen *Pneumocystis* which synthetizes *the novo* Q_7, Q_8, Q_9 and Q_{10} [7].
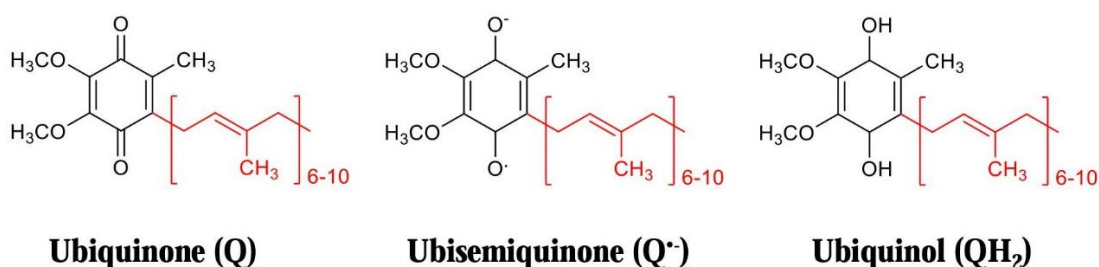
Figure I1. <u>**Coenzyme Q chemical structure**</u>. Chemical structure of Q in its three possible redox states: ubiquinone (fully oxidized), ubisemiquinone (intermediate) and ubiquinol (fully reduced). The benzoquinone ring is represented in black while the isoprenoid side chain is represented in red.

As a redox compound, Q can exist in three different redox states and a different name is given in each case. Fully oxidized Q is called ubiquinone (Q) and possesses two ketone groups in *para* position. However, when one of the ketone groups is reduced we have

partially reduced Q or ubisemiquinone ($Q^{\bullet-}$), and when the molecule is fully reduced we named it ubiquinol (QH_2) which bears two hydroxyl groups instead (Figure I1) [8].

1.2. Cellular, tissue and species distribution

Biosynthesis of Q occurs in all tissues and cells in the organism, and the lipid is present in all cellular membranes. However, several studies have described that Q distribution is not homogenous neither in membranes nor in tissue or among different species [9, 10].

In membranes, polyisoprenoid chains of Q are present in the central hydrophobic region, between the double layers of phospholipid fatty acids, while the benzoquinone ring turn out to the outer or inner surface of the membrane depending on the functional requirements. The effective ordering effect of Q is the consequence of the methoxy groups on the benzoquinone ring and also of the interaction between quinone head groups and phospholipid molecules by hydrogen bonds [11]. This central localization of Q in the membranes results in an increased fluidity and permeability [10], contrary to the effect that cholesterol exerts in the membranes. Membranes need to be saturated with the appropriate lipids to develop optimal functions and, thus, the deficiency of one of them will have deleterious consequences. If the lipid exceeds the optimal amount, a non-membranous distribution will be needed. Despite Q is synthetized in mitochondria, this organelle it is not its unique destination. Q is reported to be present in Golgi apparatus, in similar concentrations to the ones found in mitochondria, but also in microsomes, plasma membrane, nuclear envelope and peroxisomes. Approximately 30% of the membrane-located Q of rat liver appears to be associated with extra-mitochondrial membrane compartments [10, 12, 13].

Moreover, Q distribution is not uniform among the various tissues and organs, indicating that Q levels are adapted to the particular physiology of the tissue. Due to its short half-life, a coordinated balance between synthesis and degradation, processes that occur in all tissues, probably determines Q levels in the different tissues. In mice, rats and humans, maximal Q concentrations are present in kidney, liver and especially in heart, whereas lower amounts can be detected in brain and skeletal muscle. Others organs possess small amounts of Q, for instance, lung and spleen with only the 10 % of the levels detected in heart [12, 14]. Because Q redistribution between organs seems insignificant, tissue-specific mechanisms must exist to determine actual levels of Q in any given tissue.

In rodents and humans, the same isoforms, Q_9 and Q_{10}, are present but the total amount of Q changes within the two species. In brain, spleen and lung, total Q levels are the same in human and rats but, in most of the other organs, human amount of Q is 2 to 5 fold lower than the observed in rats. Moreover, the proportion between the different isoforms also varies among species. In rats Q_9 is the major isoform, however, a relative high amount of Q_{10} is detected. In brain, spleen and intestine as much as one-third and, in other tissues, 10-20 % of the total Q is Q_{10}. In contrast, the major isoform in humans is Q_{10} and only a smaller portion (2-7 %) of the total Q has an isoprenoid chain length of nine units [11, 14, 15].

1.3. Biological functions

Several functions have been described for Q from its discovery to the present, including mitochondrial and extramitochondrial ones:

1.3.1. Mitochondrial functions
1.3.1.1. Electron transport

The first role described to Q was its capacity to serve as electron carrier in the electron transport chain, thus, participating in the generation of ATP, the energetic molecule in the cell [16]. The electron transport chain consists of four major multi-subunit complexes designated NADH-ubiquinone oxidoreductase (complex I), succinate-Q dehydrogenase (complex II), QH_2-cytochrome *c* reductase (complex III), cytochrome *c* oxidase (complex IV), and two connecting redox-active molecules: Q and cytochrome *c*. Finally, a mitochondrial ATP synthase (also called complex V) create ATP while using the proton motive force created by the electron transport chain as a source of energy (Figure I2) [17]. Q is the unique compound that transfers electrons between either Complex I or Complex II to Complex III by receiving electrons from NADH or succinate, respectively. Other minor sources of electrons are dihydroorotate dehydrogenase, electron transfer flavoprotein dehydrogenase and glycerol-3-phosphate dehydrogenase, enzymes that support key aspects of the metabolism [18].

For many years, mitochondrial respiratory complexes were supposed to move freely in the membrane linked by the two connecting molecules. However, in recent years, this

fluid model has changed due to the demonstration that all the complexes, except complex II, were able to associate in supercomplexes. Nowadays, it is proposed that the respirasome (formed by complexes I, III, and IV), other supercomplexes (I + III or III + IV), as well as free respiratory complexes coexist and allow a better adaptation of cells to the environment [17, 19, 20]. In this context, two distinct Q pools were defined: one dedicated to reduce equivalents coming from NADH and trapped in the supercomplexes that contains complexes I + III, and an independent second Q pool dedicate to reduce equivalents coming from $FADH_2$, freely located along the inner mitochondrial membrane [8, 20]. These pools compete for the delivery of electrons to complex III.
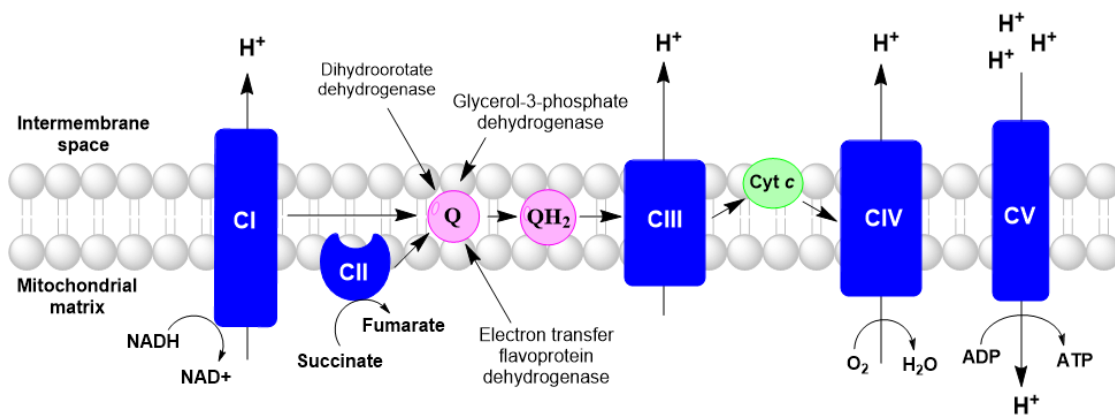
Figure I2. Central role of Q in the electron transport chain. Schematic representation of the different components of the respiratory chain as well as the electron sources of Q. The figure do not show the real structural organization of the respiratory chain. Adapted from [18].

1.3.1.2. Uncoupling proteins

Uncoupling proteins (UCPs) are present in plants and animals constituting a subfamily of the mitochondrial carrier family. Situated in the inner mitochondrial membrane they can translocate H^+ from the outside to the inside of the mitochondria and, thus, in a controlled process the proton gradient built by the electron transport chain is uncoupled from oxidative phosphorylation, and heat rather energy is produced [10]. These protons are delivered from fatty acids to the H^+ acceptor group of the uncoupling proteins with the assistance of oxidized Q, which is an obligatory cofactor in this process [21]. In addition to thermogenesis, UCPs could be involved in suppression of oxygen radicals.

1.3.1.3. Mitochondrial transition permeability pore

In order to facilitate the trans-membranous transport, the inner mitochondrial membrane contains a number of macromolecule transporters and ion channels. These are necessary because this membrane has a low permeability to solutes and ions to permit energy conservation in form of an electron and a pH gradient [10]. Under conditions of increased Ca^{2+} loading, especially when accompanied by oxidative stress and a fall in adenine nucleotides, mitochondria undergo a phenomenon known as permeability transition (mPT). The mPT is traditionally defined as a phenomenon associated with the opening of a proteinaceous permeability transition pore (PTP) located in the inner mitochondrial membrane allowing solutes with molecular masses of up to 1,500 Da to enter or exit the mitochondrial matrix [22]. However, the translocation of these large molecules leads to a collapse of mitochondrial functions. Several analogues of Q as well as Q_{10} are some of the compounds that prevent the opening of the PTP counteracting apoptotic events such as ATP depletion, release of cytochrome *c* into the cytosol or caspase activation [21].

1.3.1.4. Final acceptor in *the novo* synthesis of pyrimidines

The conversion of dihydroorotate to orotate, catalyzed by dihydroorotate dehydrogenase is the single redox reaction in the biosynthesis of pyrimidine nucleotides. Dihydroorotate dehydrogenase is located in the inner mitochondrial membrane and linked to the electron transport chain through Q, which acts as electron acceptor receiving the two electrons released in the production of orotate and being thus reduced to ubiquinol [23].

1.3.2. Extramitochondrial functions
1.3.2.1. Plasma membrane redox system

Analogously to mitochondria, plasma membrane develops active redox functions [24]. The plasma membrane redox system (PMRS) transfers electrons from either intra- or extracellular donors to extracellular acceptors. It is based principally in the participation of three components: (1) one or more NADH-Q reductase enzymes located on the cytosolic side of the plasma membrane (as NADH-cytochrome b5 oxidoreductase and DT-diaphorase), which regulate the cytosolic NAD^+/NADH ratio and ascorbate reduction [25], (2) the Q present in the plasma membrane and (3) hydroquinone oxidases (ECTO-

NOX or ENOX proteins) located on the outer surface of the plasma membrane that function as terminal oxidases involved in the regulation of cell growth and differentiation [26]. PMRS plays a key role in maintaining the levels of $NAD^+/NADH$ and oxidized and reduced Q in cells. Moreover, in mitochondria-deficient cells, survival is dependent on PMRS activity because under these conditions this system is largely responsible for the life sustaining regeneration of NAD^+ from NADH required for glycolytic ATP production, an important pathway even in cells containing mitochondria [13].

1.3.2.2. Antioxidant function

Mitochondria are considered the mayor source of reactive oxygen species (ROS) in the cells. The production of these molecules is important because it underlies oxidative damage in many pathologies and contributes to retrograde redox signalling from the organelle to the cytosol and nucleus [8, 27]. Superoxide ($O_2 \cdot^-$) generation results from single-electron premature reduction of oxygen by electrons moving through the electron transport chain. Complex I generates $O_2 \cdot^-$ within the mitochondrial matrix only, whereas complex III generates $O_2 \cdot^-$ both in the intermembrane space and in the matrix [28]. Another source of ROS is the production of H_2O_2 by monoamine oxidases in the mitochondrial outer membrane, the various flavin oxidases in peroxisomes and the leakage of electrons from cytochrome P-450 in the endoplasmic reticulum (ER) [10]. Other ROS producers are plasma membrane NADPH oxidases, a family of enzymes that are distinguished by their membrane-spanning catalytic "NOX" or dual oxidase ("DUOX") subunit that it uses to transfer electrons from NADPH to molecular oxygen. Seven members of the NADPH oxidase family have been identified in mammals, including NOX1- through 5- as well as DUOX1- and DUOX2-containing oxidases [29, 30]. Unlike NOX2 and NOX1, which produce superoxide and then H_2O_2 after dismutation of superoxide by SOD, NOX4, DUOX1, and DUOX2 enzymes generate H_2O_2 directly [31].

Free radicals formed in the cells are able to damage lipids, proteins and DNA, a concept known as oxidative stress. The oxidative stress is defined as an imbalance between the systemic manifestation of ROS and a biological system's ability to readily detoxify the reactive intermediates or to repair the resulting damage [32, 33]. Lipid peroxidation starts when a hydrogen atom is subtracted from a polyunsaturated fatty acid (PUFA) and results

in the formation of carbon-centered free radical, peroxyl radical, lipid hydroperoxide, alkoxyl radical and degradation to hydrocarbons, ethers, alcohols, aldehydes and epoxides. Protein oxidation affects to certain amino acid residues of a particular protein generating hydroxyl radicals that progress within the same protein or to another proteins or lipids. Meanwhile, DNA is also affected by ROS, especially mitochondrial DNA which is more sensitive due to the lack of protective histones and its limited repairing capacity [10]. To protect against the oxidative damage caused by ROS cells produce antioxidants, which include enzymes and non-enzymatic agents that can prevent the formation ROS or can directly eliminate them [34]. Superoxide dismutase, glutathione peroxidase, catalase, thioredoxin reductase and peroxiredoxin are part of the antioxidant enzyme group. On the other hand, within the non-enzymatic antioxidants agents we found vitamin C and E, carotenoids, glutathione, α-lipoic acid, flavonoids and ubiquinol [10].

Several studies described the role of Q as an endogenous antioxidant protecting against lipid peroxidation, protein carbonylation and DNA damage. Q inhibits lipid peroxidation by preventing the production of peroxyl radicals and, moreover, ubiquinol reduces the initial perferryl radical forming the ubisemiquinone and H_2O_2. The removal of the initiating perferryl radical protects both lipids and proteins from oxidation. In addition, the reduced form of Q regenerates vitamin E from α-tocopheroxyl radicals [8, 21]. Complementary studies reveals that the administration of ubiquinol, *in vitro* or *in vivo*, prevents the DNA oxidation and breakdown in mouse liver and human lymphocytes [35, 36].

Ascorbate is another antioxidant that protects cellular components from oxidative damage by a direct quenching of various soluble free radicals or by reducing tocopheroxyl radicals to tocopherol. As humans and different animals cannot synthetize this vitamin, the mechanisms to maintain the ascorbate obtained from the diet are a basic objective for cells [37]. Participation of Q in the plasma membrane NADH-ascorbate free radical reductase indicated a similar role in ascorbate stabilization by whole cells. This activity has been demonstrated in yeast and some animal cell types [38-40]. Q also contribute to ascorbate regeneration in endomembranes [37]. However, ascorbate it is not the only cellular antioxidant protected by Q. α-Tocopherol (or vitamin E), present in membranes and lipoproteins, is known to scavenge free radicals providing antioxidant protection in cells. Previous studies showed that Q protect α-tocopherol against oxidation in a

concentration-dependent manner, and take part in the recycling of α-tocopherol from its phenoxyl radical [41, 42].

1.4. Biosynthesis

The biosynthesis of Q is still a not completely characterized process. It is divided into three steps: the synthesis of the polyisoprenoid tail, the attachment of the tail to the benzoquinone ring precursor and, finally, the subsequent modifications of the ring to yield the final product [21, 43].

1.4.1. Synthesis of polyisoprenoid tail of Q. The mevalonate pathway

The isoprenoid tail of Q is synthetized through the mevalonate pathway, which represents the initial steps in a series of enzymatic reactions that have been established to account for production of polyisoprenoids (e.g. dolichol) and sterols.

In eukaryotes, the first step of this pathway involves the condensation of two acetyl-CoA molecules to form acetoacetyl-CoA catalyzed by acetoacetyl-CoA thiolase. Then, HMG-CoA synthase condenses another unit of acetyl-CoA with acetoacetyl-CoA synthetizing 3-hydroxy-3-methylglutaryl-coenzyme A (HMG-CoA). Successive reduction steps, catalyzed by HMG-CoA reductase, produce mevalonate as a final product. Mevalonate is subsequently phosphorylated in two steps by mevalonate kinase and phosphomevalonate kinase. Then, ATP dependent decarboxylation of mevalonate-5-diphosphate, mediated by mevalonate diphosphate decarboxylase, yields isopentenyl pyrophosphate (IPP), which is the building block for the biosynthesis of isoprenoids. IPP can isomerize giving dimethylallyl pyrophosphate (DMAPP) by the isopentenyl pyrophosphate isomerase. A head-to-tail condensation of IPP to DMAPP results in the formation of geranyl pyrophosphate (GPP) and the addition of another IPP unit gives farnesyl pyrophosphate (FPP). In mammals, the same enzyme, farnesyl diphosphate synthase (FDPS), catalyses these last two steps (Figure I3) [43-45]. All enzymes responsible for the conversion of mevalonate to FPP are greatly enriched in the cytoplasm with the exception of HMG-CoA reductase, that is an integral component of the ER membrane with the C-terminal catalytic region located completely in the cytosol. Therefore, mevalonate pathway occurs mainly in the cytosol but it is closely linked to the ER [46].
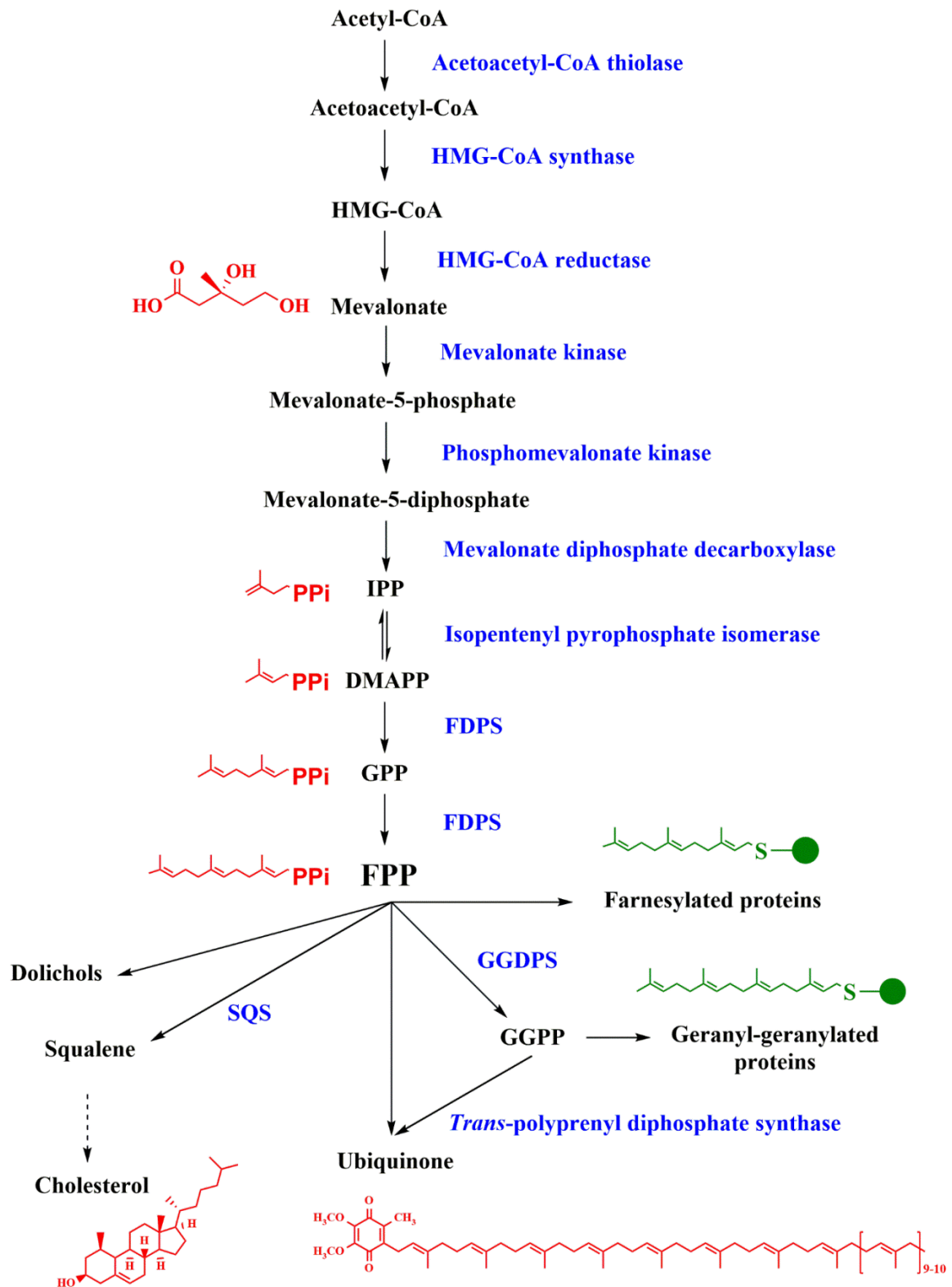
Figure I3. **Schematic representation of the mevalonate pathway in eukaryotes.** We summarize the different steps of the mevalonate pathway as well as its principal final products. The enzymes involves are represented in blue and the chemical structure of some important metabolites in red. A schematic representation of isoprenylated protein is represented in green.

FPP represent the branch point metabolite of the pathway being substrate of multiple enzymes. As substrate of squalene synthase, FPP will ultimately be converted to sterols, such as cholesterol. Long-chain E-isoprenyl synthases use FPP as primer for the formation of the side chain of Q. FPP also serves as a substrate for dehydrodolichyl diphosphate synthases whose products function as sugar carriers in the formation of glycoproteins and glycolipids. Moreover, FPP is also used as a primary substrate for the synthesis of geranylgeranyl diphosphate (GGPP), mediated by geranylgeranyl diphosphate synthase (GGDPS). GGPP and FPP are respectively substrates of protein geranylgeranyl or farnesyl transferase that catalyze lipid isoprenylation of proteins with a CAAX box at their C-terminus [47]. All these enzymes are considered to be rate-limiting in the terminal part of their biosynthetic process [10].
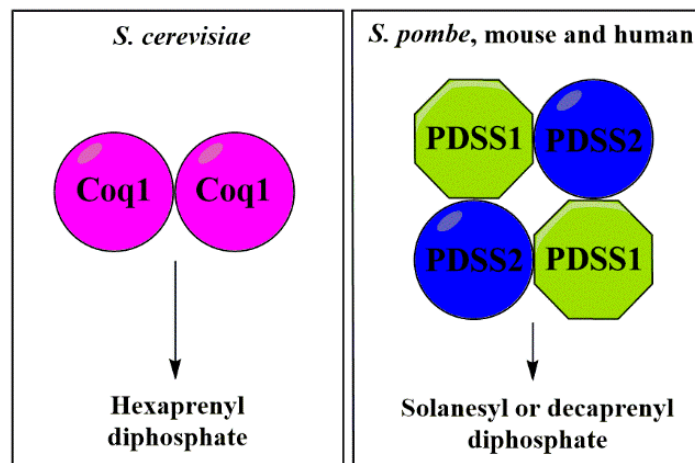
Figure I4. **Classification of *trans*-prenyl diphosphate synthase in eukaryotes**. While in *S. pombe*, mice and humans these enzymes are heterotetrameric, in *S. cerevisiae* the equivalent enzyme is believed to be homodimeric. Adapted from [48].

Focusing on Q, its long isoprenoid side-chain is synthetized by trans-polyprenyl diphosphate synthase that condense FPP or GGPP with several molecules of IPP, all in trans configuration [21, 48]. Additionally, GPP is observed to serve as precursor in the polyisoprenoid synthesis in in vitro studies with rat liver microsomes, but no evidences of this fact are observed in vivo [10, 49]. Trans-polyprenyl transferase in S. cerevisiae is a homodimer called Coq1p (encoded by COQ1 gene) whereas in mammals the enzyme is a heterotetramer called PDSS1-PDSS2 (encoded by PDSS1 and PDSS2 genes) (Figure I4) [48]. The mature Coq1 protein is localized at the mitochondrial matrix peripherally

associated with the inner mitochondrial membrane and, therefore, the elongation of the polyisoprenoid chains starting from FPP or GGPP occurs in the mitochondria. Trans-polyprenyl transferases are species-specific enzymes and responsible for determining the correspondent tail length of Q in each organism [50].

1.4.2. The benzoquinone ring and its attachment to the isoprenoid tail

Little is known about the biosynthesis of the ring of Q in non-plant organisms. 4-Hydroxybenzoic acid (4HB) was considered to function as the main ring precursor of Q for more than 40 years. In mammals, this phenolic compound is derived from tyrosine and phenylalanine, two essential amino acids in cells [51]. During these years, only a study in 1976 described vanillic acid and protocatechuic acid as alternative precursors in Q biosynthesis in mammals [52]. However, in the last decade several alternative compounds have been described to serve as Q ring precursors. In 2010, two independent studies identified *p*-aminobenzoic acid (PABA) as a novel Q precursor in yeasts [53, 54]. PABA differs from 4HB only by one substituent of benzoic acid, an amine (NH_2) rather than a hydroxyl group (OH). PABA is converted into Q via the same Q biosynthetic pathway, but needs an additional step(s) to replace NH_2 by OH at C4 [55]. Then, in 2014, Block *et al*. described that *Arabidopsis* is able to use *p*-coumarate, but not PABA, as another ring precursor in Q biosynthesis [51]. Recently, in 2015, Xie *et al.* have described that human and *E. coli* cells do not utilize PABA as precursor in the biosynthesis of Q while both *p*-coumarate and resveratrol, another polyphenol structurally similar to *p*-coumarate, can serve as a ring precursors of Q biosynthesis in *E. coli*, yeasts and human cells [56] (Figure I5). Interestingly, unnatural compounds analogues of 4HB (such as 2,4-diHB or 3,4-diHB) are also able to serve as alternative precursors in Q synthesis in yeast as well as in mammalian, both human and mouse, cells [57-59].

The *COQ2* gene encodes for the enzyme 4-hydroxybenzoate polyprenyl transferase (Coq2 or COQ2 in yeast and mammals, respectively) which mediates the second step in Q biosynthesis: the condensation of the isoprenoid tail with a quinone ring precursor generating the first membrane-bound Q precursor that resembles the final product of the pathway (Figure I5). Genetic and biochemical analyses have revealed that this enzyme has broad substrate specificity [6]. COQ2 is located inside the mitochondria, concretely in the inner mitochondrial membrane [60], therefore, this step of Q biosynthesis is
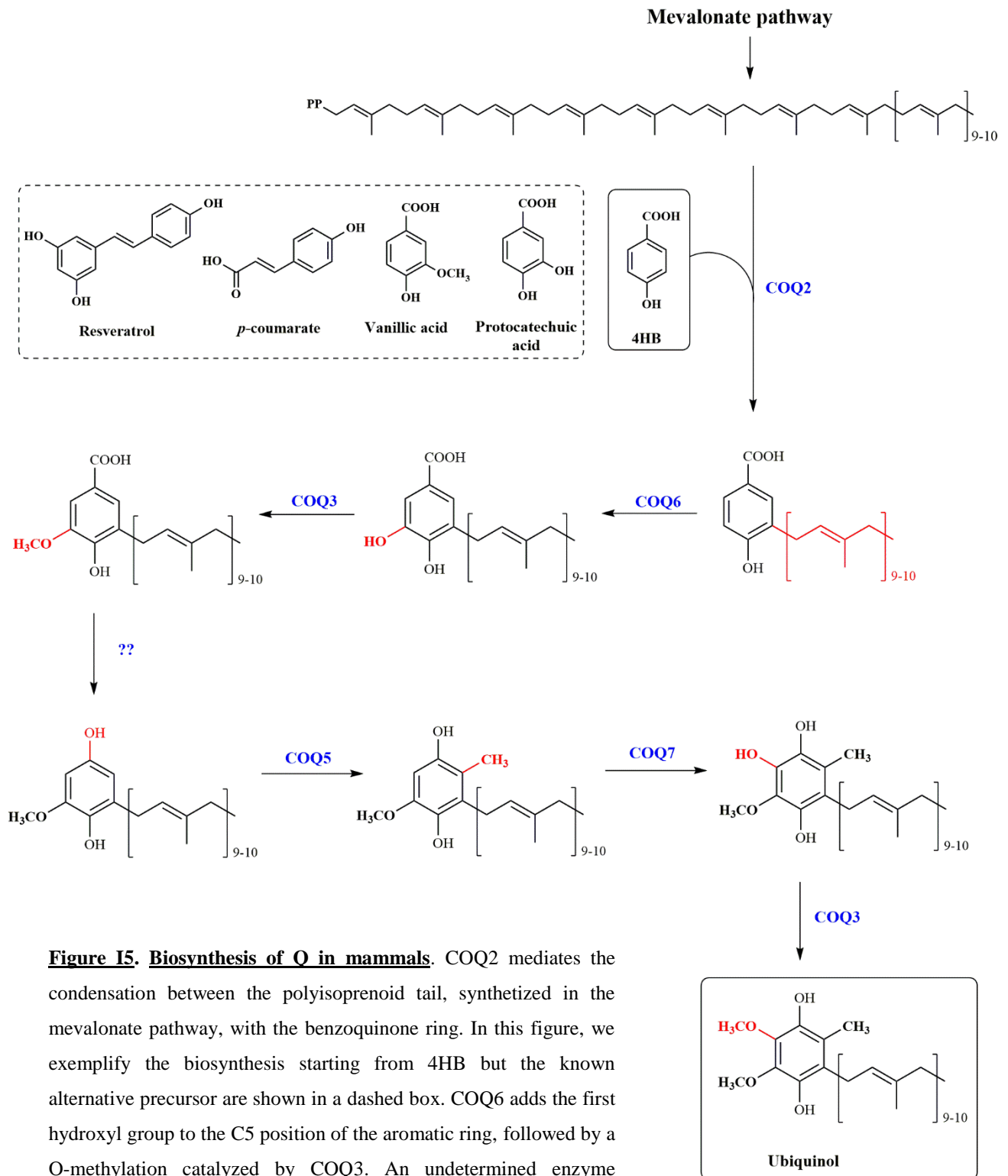
Figure I5. <u>Biosynthesis of Q in mammals</u>. COQ2 mediates the condensation between the polyisoprenoid tail, synthetized in the mevalonate pathway, with the benzoquinone ring. In this figure, we exemplify the biosynthesis starting from 4HB but the known alternative precursor are shown in a dashed box. COQ6 adds the first hydroxyl group to the C5 position of the aromatic ring, followed by a O-methylation catalyzed by COQ3. An undetermined enzyme catalyzes the decarboxylation step and COQ5 catalyzes the C-methylation at the C2 position of the ring. Then, COQ7 adds the second OH group to the C6 position and COQ3 catalyzes the second O-methylation to synthetize ubiquinol. COQ4, COQ9, COQ10, and COQ11 are required for efficient Q biosynthesis, but their functions are yet to be determined.

supposed to take place in the mitochondria. However, a recent study has reported the existence of a new decaprenyl diphosphate transferase named UBIAD1 that synthesizes Q_{10} and is present in the Golgi complex of humans [61]. Loss of UBIAD1 apparently reduces the cytosolic pool of CoQ_{10}. As most of other enzymes involved in Q biosynthesis are located in mitochondria, the mechanism by which UBIAD1 assists with Q production in the Golgi is still unclear [6]. Moreover, the role of UBIAD1 is controversial since *in vivo* studies have identified this enzyme as responsible for the synthesis of vitamin K_2, but not Q_9 or Q_{10} in mice [62].

1.4.3. Modifications of the benzoquinone ring

After the condensation of the polyisoprenid chain with the quinone ring precursor, a number of additional reactions take place to produce the final molecule of Q (Figure I5). These reactions take place only in mitochondria based on the presence of mitochondrial targeting signals in COQ genes and the products of these genes in mitochondria. The use of ^{14}C-labelled 4HB reveals that, after its biosynthesis in mitochondria, Q will be transport to other membranes and blood lipoproteins [13, 18].

This sequence of enzymatic steps is not yet completely understood in mammals but includes one decarboxylation, three hydroxylations, two O-methylations and one C-methylation to form the final product. The major part of the studies carried out to elucidate the genes involved in this final step of Q biosynthesis were performed using *S. cerevisiae coq* mutants, and thus, the family of *COQ* genes was established. The proteins encoded by *COQ* genes are in charge of these reactions [6, 43]. All *COQ* genes have mammalian homologues and, some of them, more than one. A briefly description of its function is made below.

COQ3 gene encodes for an O-methyltransferase (Coq3p/COQ3, refers to yeast and mammals, respectively) that catalyzes two O-methylation steps at positions 5 and 6 of the ring structure, an activity that is regulated by phosphorylation. *COQ5* gene encodes a C-methyltransferase (Coq5p/COQ5) that catalyzes the C-methylation step in the Q biosynthetic pathway. Coq5p, additionally, have a role in the structural integrity of the Q biosynthetic complex through the stabilization of Coq3p and Coq4p polypeptides. The *COQ6* gene encodes for one monooxygenases required for Q biosynthesis, Coq6p/COQ6, which catalyzes both the C5 and C1 hydroxylation steps. The mitochondrial ferredoxin

Yah1p and the ferredoxin reductase Arh1p (FDX1L and FDXR in mammals [43]) have been found to be required for the C5 hydroxylation as electron donors. The *COQ7* gene encodes for the other monooxygenase required in Q biosynthesis, which is responsible for the C6 hydroxylation step. Moreover, Coq7p has an important function in the stabilization of the biosynthesis complex. PKA-mediated phosphorylation and Ptc7-mediated dephosphorylation of Coq7p and other Coq proteins have been reported in *S. cerevisiae* [6, 43, 60].

If functions of COQ3, COQ5, COQ6 and COQ7 are well stablished, the functions of the rest of proteins involved in Q biosynthesis are still partially obscure. *COQ4* gene encodes for a protein with an unknown function that apparently plays a regulatory role in the assembly of the Q biosynthetic complex in yeast. *S. cerevisiae* Coq8p and *H. sapiens* ADCK3 (or ADCK4) (encoded by *COQ8* and *ADCK3* genes, respectively) are atypical protein kinases involved in Q synthesis. It is hypothesized that Coq8p phosphorylates Coq3p, Coq5p and Coq7p stabilizing them in the Q biosynthetic complex. Coq9p/COQ9 (the protein encoded by *COQ9* gene) is a lipid-binding protein described as a component of the biosynthetic complex that directly interacts with Coq4p, Coq5p, Coq6p and Coq7p. A role controlling the deamination of Q intermediates that derive from PABA is also proposed [63]. Coq10p/COQ10 (encoded by *COQ10* gene in yeast and *COQ10A and B* gene in mammals) is a START polypeptide that binds Q and facilitates both *de novo* Q biosynthesis and respiratory electron transport probably directing the localization of Q within the mitochondrial membrane [64]. Coq11p (encoded by *COQ11* gene) appears to be necessary for *de novo* Q synthesis in yeast, with a predicted role as a FMN-dependent decarboxylase but it has no clear human orthologue [65]. Finally, there are three more genes (*ADCK1*, *ADCK2,* and *ADCK5*) which have been postulated to participate in the biosynthetic process but there is currently no experimental proof of their involvement.

1.4.4. Multifunctional protein complex in Q biosynthesis

In yeast Coq1 to Coq9 polypeptides are localized in the mitochondrial matrix associated to the inner mitochondrial membrane and in mammals we observed a mitochondrial localization for most of their orthologues [43]. Coq proteins in yeast assemble in a multi-subunit complex (termed the Q-synthome) (Figure I6), which is destabilized by the absence of a single Coq polypeptide [66]. In this complex, Coq2p spans the inner

membrane and the other enzymes are peripherally associated with this membrane on the matrix side. Coq3p, Coq4p, Coq5p, Coq6p, Coq7p and Coq9p take part in this complex. Moreover, Coq8p is observed to have a closer associating with Coq6 helping to stabilize the complex and Coq11 is shown in association with Coq4p, Coq5p, and Coq7p. Coq1p and Coq2 function separately. It has been shown that Q itself and the latest metabolites of the pathway can associate to the Q-synthome playing a role in it stability [67]. Some evidences of complex association have been described to some human *COQ* genes orthologues and due to the majority of complexed proteins retained their interactions from yeast to human, it is expected Q complex to be conserved in mammalian cells [65].
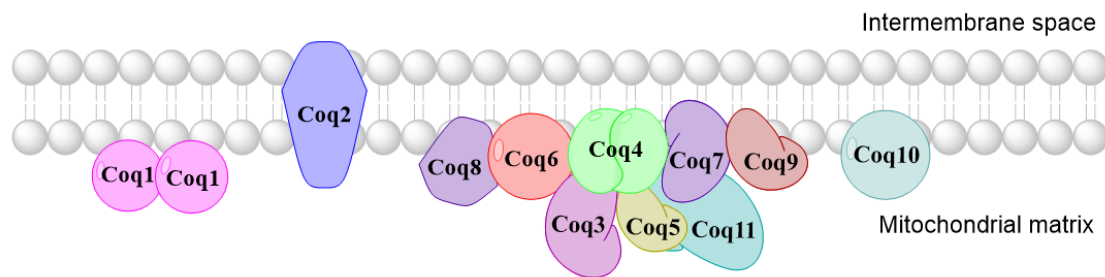
Figure I6. **Model of the Q-synthome in *S. cereviasie* proposed by Allan *et al*. [65].** In the proposed model Coq3, Coq4, Coq5, Coq6, Coq7, Coq8, Coq9 and Coq11 take part in the complex while Coq1, Coq2 and Coq10 do not associate with the rest of polypeptides. Adapted from [65].

1.5. Coenzyme Q regulation

A coordinated balance between the synthetic and catabolic enzymes of Q determines its levels in the different tissues. However, despite the advances in the understanding of the Q biosynthetic pathway, there are still few data concerning its regulation. Studies suggest that phosphorylation and dephosphorylation of Coq proteins represent key events in the modulation of Q biosynthesis, a notion supported with the discovery of the putative kinase Coq8 [43, 68]. The expression of the proteins involved is also regulated by transcriptional factors. In addition, due to the polyisoprenoid tail of Q is synthetized *via* the mevalonate pathway, the regulation of this pathway, at any level, may have a direct effect on Q levels. On the other hand, this lipid is rapidly broken down, as reflected it short half-life of 49-125 hours, and the initial steps in this degradation involve ω-oxidation and subsequent oxidation of the side chain.

Under a number of physiological, experimental and pathological conditions tissue levels of Q are either elevated or depressed. For instance, Q levels are enhanced in cold adaptation or exercise, due to squalenes and epoxides, thyroxin, PPARα and LXRα agonists, vitamin E treatments or in diseases such as Alzheimer's, diabetes or prion diseases. Moreover, Q levels are decreased in aging, with treatments with vitamin A, statins treatments or RXRα deficiency or in diseases such as liver cancer, cardiomyopathy or Parkinson's disease [21].

1.6. Human coenzyme Q_{10} deficiencies

Q_{10} deficiency is a biochemical finding first described in 1989 [69]. Given the essential functions of Q, a deficit in this molecule leads to a number of mitochondrial disorders with an unexplained heterogeneous clinical spectrum that encompasses at least five major phenotypes: (1) an encephalomyopathy, characterized by recurrent myoglobinuria, (2) a severe infantile multisystem disorder with encephalopathy, (3) an ataxic syndrome with cerebellar atrophy, (4) an isolated myopathy, and (5) a steroid-resistant nephrotic syndrome (SRNS) [70]. The identification of the underlying genetic defects has allowed to distinguish primary or secondary forms of deficiency. Primary Q_{10} disorders are rare conditions with an autosomal recessive mode of inheritance. These disorders are caused by disruption of genes involved directly in the biosynthetic pathway of Q. Mutations in *PDSS1*, *PDSS2*, *COQ2*, *COQ4*, *COQ6*, *COQ9*, *ADCK3* and *ADCK4* have been identified to date [43]. On the other hand, secondary Q_{10} disorders are associated to mutations caused in genes not directly involved in Q biosynthesis or to other disorders such as mitochondrial DNA depletion, dietary insufficiency or the use of pharmacotherapeutic agents such as statins [70]. Moreover, this type of deficiency could also be a secondary effect of a disease already present in the patient.

Primary Q_{10} deficiency is unique among mitochondrial disorders because oral supplementation with exogenous Q_{10} can improve clinical symptoms. Moreover, in some secondary deficiencies Q_{10} supplementation is also effective. Renal, CNS, and muscular symptoms respond very well to treatment. However, it should be noted that Q_{10} should be administered as soon as possible because although the treatment can stop the progression of the clinical manifestations, once severe kidney or CNS damage is established, it cannot be recovered [71]. Many different aspects may influence the

variability of the clinical response to Q_{10} supplementation. Obvious factors are the therapeutic dosages, the pharmaceutical formulation employed, the severity of the underlying illness and the progression of tissue damage [72], but there are probably many other components, genetic, environmental, and even epigenetic [73], that modulate the response to treatment.

However, the long polyisoprenoid chain renders Q_{10} highly lipophilic and difficult to absorb by cells, so due to its low bioavailability, other treatments are being investigated. Reactivation of endogenous synthesis is a promising approach because endogenously produced Q_{10} will be delivered to the appropriate subcellular compartments, while with exogenous supplementation the distribution of Q_{10} is not controlled and it may have difficulties to efficiently reach mitochondria. As examples, we can highlight the bypass of the enzymatic defect achieved in yeast expressing a human COQ6 mutation using vanillic acid [74] or the restoration of Q biosynthesis in patient fibroblast cells completely lacking the enzymatic activity of COQ7 using the unnatural biosynthesis precursor 2,4-dihydroxybenzoate [57]. However, due to the existence of high variability of mutations not all the treatment are effective for all the patients.

2. Inhibitors of the mevalonate pathway

As we described above, the mevalonate pathway produces isoprenoids that are vital for diverse cellular functions, ranging from the cholesterol or Q biosynthesis to mechanisms of growth control. Several regulators of this pathway have been described, being the most important: statins and bisphosphonates. While statins inhibit the HMG-CoA reductase, an upstream enzyme of the pathway, bisphosphonates inhibit mainly the so-called *branch point enzyme*, FDPS.

2.1. Statins

2.1.1. Structure and classification

Structurally, statins are characterized by the presence of a conserved lactone ring. This family of compounds can be divided into two broad classes: type 1 and 2. Type 1 statins are lipophilic and possess a butyryl side chain. Lovastatin, pravastatin, and simvastatin are examples of type 1 statins. Type 2 statins are are distinguished from type 1 by the

replacement of the butyryl side chain with a fluorophenol group and, typically, possess larger side chains. Atorvastatin, cerivastatin, fluvastatin, pitavastatin and rosuvastatin are examples of type 2 statins [75]. In Figure I7 some statins examples of both classes were represented, all of them licensed for clinical treatments.
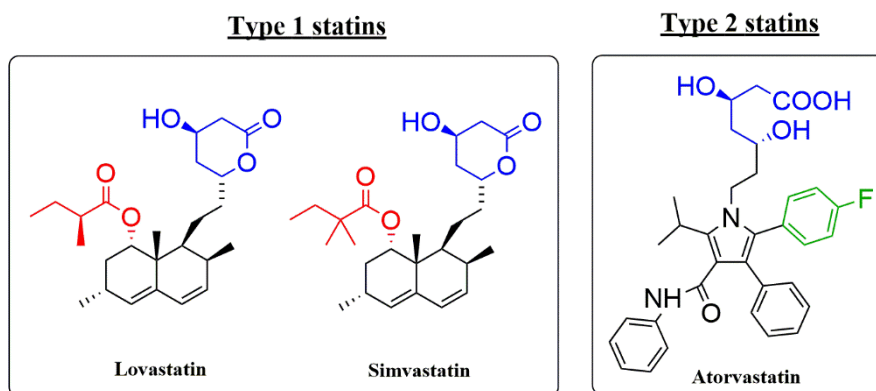
Figure I7. **Statins chemical structure.** The conserved lactone ring of statins is represent in blue. A butyryl side chain (represented in red), which is different in each statin, characterizes type 1 statins. Type 2 statins differ from type 1 statins due to the replacement of the butyryl side chain with a fluorophenyl group (green).

2.1.2. Functions and molecular targets

Statins competitively inhibit HMG-CoA reductase, one of the most relevant enzyme of the mevalonate pathway, blocking the conversion of HMG-CoA to mevalonic acid by a catalytic mechanism. In other words, statins molecules occupy the catalytic portion of HMG-CoA reductase, specifically the binding site of HMG-CoA, thus blocking access of this substrate to the active site [76]. The inhibition of this enzyme results in a depletion in all the downstream metabolites of the mevalonate pathway, especially cholesterol, making these compounds a primary therapy to lower cholesterol levels. Therefore, statins have shown strong evidence-based proved capacity of decreasing the cardiovascular morbidity and mortality.

However, statins present cholesterol-independent or pleiotropic effects because of the inhibition of the synthesis of important isoprenoid intermediates of the mevalonate pathway, such as FPP or GGPP. Between the observed pleiotropic effects we found: improvement of endothelial function, atherosclerotic plaque-stabilizing effects, anti-inflammatory and immunomodulatory effects, antithrombotic properties, effects on bone

metabolism, on risk of dementia, induction of apoptosis and anti-proliferative effects [76]. All these functions make statins to be potential treatments of some disorders such as autoimmune diseases, rheumatoid arthritis or cancer.

2.1.3. Statins and Q

Q derives its isoprenyl tail from the mevalonate pathway so the depletion of metabolic intermediates caused by statins may affect the levels of this antioxidant leading to some adverse events. From 1990 up to now, numerous studies in animals (involving six different species) and humans stablished the statin-induced Q depletion as a well-documented event [60, 70, 77-81]. Q depletion was observed in plasma as well as in different tissues such as liver, heart and muscle. Some of these studies also looked specifically the adverse consequences of this stain-induced Q depletion: decreased ATP production and impairment in mitochondrial bioenergetics events, increased production of free radicals with consecutive damage of mitochondrial DNA, increased injury after ischemia/reperfusion, defective activity of cells division, increased mortality in cardiomyopathy and heart failure, and skeletal muscle injury and dysfunction. Moreover, statin-induced Q depletion is also considered one of the mechanisms responsible for statin-therapy related new onset diabetes [80]. Therefore, Q supplementation is widely used and studied as a treatment of choice for preventing this induced deficiency.

2.2. Bisphosphonates
2.2.1. Structure and classification

Structurally, bisphosphonates are chemically stable derivatives of inorganic pyrophosphate. In their structure, a non-hydrolyzable carbon atom has substituted the central oxygen of pyrophosphates, but the phosphate groups flanking this central carbon are maintained (Figure I8). The flanking phosphate groups provide bisphosphonates with a strong affinity for hydroxyapatite crystals in bone. Linked to the central carbon we found the long side-chain (R^2 in the diagram), which determines the chemical properties, the mode of action and the strength of bisphosphonate drugs, and the short side-chain (R^1) that mainly influences binding process and pharmacokinetics. A hydroxyl group in the R^1 position is highly recommendable in bisphosphonates used for medical treatments because it highly increases their ability to bind calcium. Moreover, the presence of a

nitrogen or amino group in the R^2 position increases bisphosphonate's potency by 10 to 10,000 relative to early non–nitrogen-containing bisphosphonates. Early non–nitrogen-containing bisphosphonates, such as etidronate, clodronate, and tiludronate, are considered first-generation bisphosphonates. The addition of nitrogen in the R^2 position results in the second- and third-generation of bisphosphonates, with compounds like alendronate, risedronate, ibandronate, pamidronate, and zoledronic acid [82].
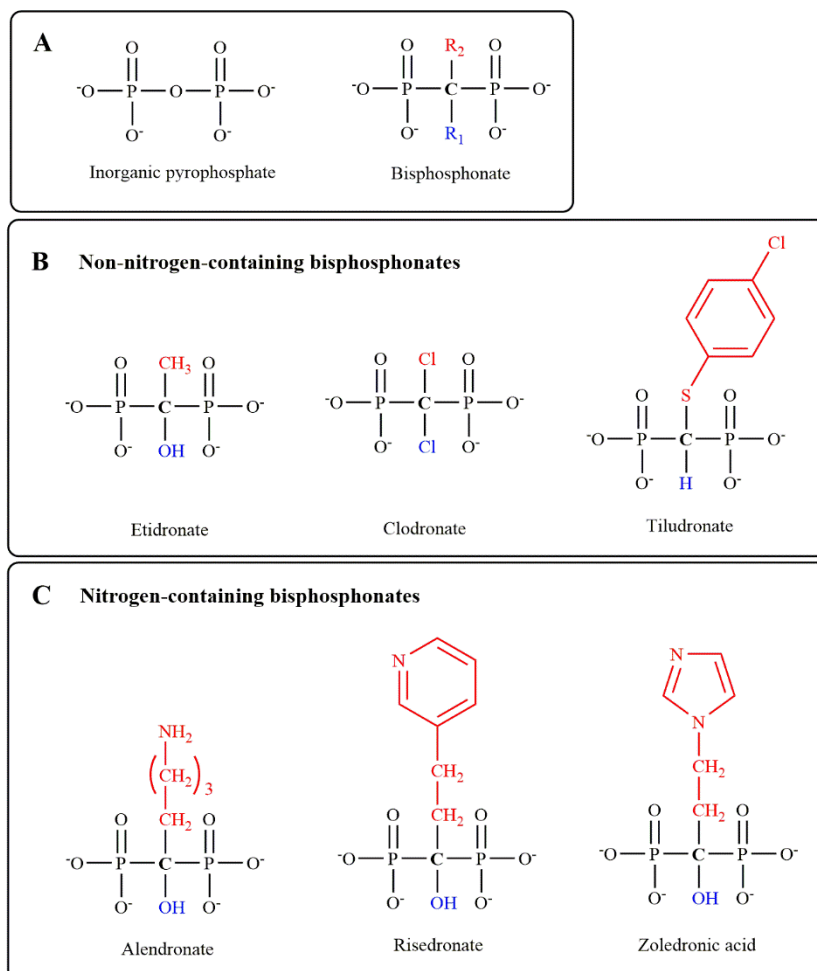
Figure I8. **Bisphosphonates chemical structure**. **(A) Inorganic pirophosphate vs bisphosphonates.** The chemical structure of these compounds is represented. In bisphosphonates we can observe the central carbon as well as the short-side chain R^1 (in blue) and the long-side chain R^2 (in red). Similar colour pattern is maintained in the rest of the compounds. **(B) Non-nitrogen-containing bisphosphonates.** Etidronate, clodronate and tiludronate are some examples. **(C) Nitrogen-containing bisphosphonates.** Alendronate, risedronate and zoledronic acid are some examples. Adapted from [82].

Zoledronic acid (ZOL) is a third-generation compound, highly potent and widely used for medical applications. Having the general structure described above for this type of compounds, it is the heterocyclic imidazole group attached to the R^2 position the characteristic that distinguishes zoledronic acid from other bisphosphonates (Figure I7) [83].

2.2.2. Functions

The ability of bisphosphonates to bind selectively the hydroxyapatite crystals of the bone, and it subsequent selective deposition in this tissue, linked to the pro-apoptotic function on osteoclasts, results in the utilization of these compounds as primary therapy for bone disorders. These pathologies, that include osteoporosis, Paget's disease of osteogenesis imperfecta, hypercalcemia or osteolysis associated with multiple myeloma and metastatic cancers, are characterized by excessive or imbalanced skeletal remodelling, in which osteoclastic and osteoblastic activities are not tightly coupled, leading to excessive osteoclast-mediated bone resorption [82, 84]. Moreover, in the last years, nitrogen-containing bisphosphonates (NBPs) have been used as treatment for disorders non-related with bone. For example, ZOL have demonstrated a potent anti-proliferative effect against glioblastoma (GBM) cell lines, breast cancer cells and patient-derived GBM lines. In cancer clinical studies, ZOL improves disease-free survival, decreases residual invasive tumor size, and reduces circulating tumor cells [85].

2.2.3. Molecular targets

Given the fact that NBPs are the most potent and the most used nowadays, we will focus on this more recent class of compounds. These compounds exert their cellular effects by interference with the mevalonate pathway.

The most studied fact is that NBPs are proposed to selectively bind and inhibit FDPS, the enzyme that represent the branch point in the mevalonate pathway [86]. This presumably selective inhibition produce a loss of posttranslational isoprenylation of proteins (including the small guanosine triphosphate–binding proteins Rab, Rac, and Rho, which play central roles in the regulation of core osteoclast cellular activities including stress fiber assembly, membrane ruffling, and survival), leading to osteoclast apoptosis and,

thereby, inhibiting the bone-destroying function of these cells [82]. According to several studies, the NBPs exert a slow, tight binding inhibition on FDPS [87-89]. In other words, first, the inhibitor binds rapidly to an open formation of the DMAPP/GPP site of FDPS producing a slow conformational change that locks the enzymatic-NBPs complex. Secondly, IPP binds to the complex and induce a full closure, preventing further catalysis (Figure I9).
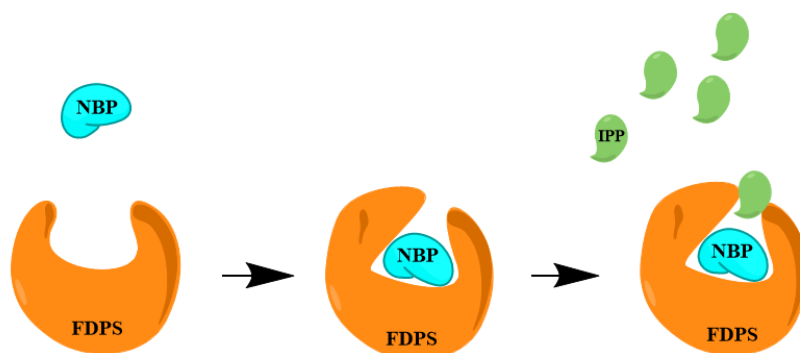
Figure I9. **Mechanism of FDPS inhibition by bisphosphonates.** First, NBPs bind rapidly the DMAPP/GPP site of FDPS producing a slow conformational change that locks the enzymatic-NBPs complex. Secondly, IPP binds to the complex and induce a full closure, blocking other substrates (such as DMAPP) from accessing and displacing the N-BP inhibitor. Adapted from [87].

Conversely, some *in vivo* studies suggested that the inhibition of the mevalonate pathway by N-BPs lies downstream the FPP synthesis step due to several cellular effects of N-BPs such as inhibition of osteoclast formation, inhibition of ovarian cancer cell migration or inhibition of breast cancer cell invasion, were reversed only by geranylgeraniol (GGOH) but not by farnesol (FOH) [90]. In accordance, some of the biological activities of ZOL are sustained by its inhibitory effect of protein geranyl-geranylation, which is influenced by an inhibition of FDPS, but mainly produced by a direct inhibition of geranylgeranyl diphosphate synthase (GGDPS). Several studies have support the ability of NBPs to selectively bind and inhibit geranylgeranyl diphosphate synthase (GGDPS) and geranylgeranyl transferase I [85, 91, 92]. However, the mechanism is unclear and needs to be further explored.

Moreover, NBPs are potent inhibitors of squalene synthase [93]. This enzyme catalyse the formation of squalene, the first committed step of the sterol branch in the mevalonate pathway, so its inhibition results in a decrease of cholesterol and sterol biosynthesis [90].

2.2.4. Bisphosphonates and Q

Despite Q is a final product of the mevalonate pathway, the information of its regulation by NBPs is limited to a few studies. Coscia *et al.* described a Q decrease after treatment with ZOL in cells derived from a mammary tumor of a BALB-neuT female (TUBO cells), as well as in macrophages obtained from 18-week-old mice [94]. This decrease was restricted to Q_9 in Hep G2 cells treated with risendronate [95]. Complementary, a clinical study reveals that postmenopausal women with osteoporosis treated with ZOL compromised Q_{10} levels and vitamin E status in plasma [96].

2. Dietary phenolic compounds

2.1. Structure and classification

Phenolic compounds are secondary metabolites in plants with a common aromatic ring bearing one or more hydroxyl groups. Phenylalanine and/or tyrosine are the precursors for the synthesis of phenolic acids through shikimate pathway, being the addition of hydroxyl groups into the phenyl ring a key step of the biosynthesis [97]. More than 8000 natural phenolic compounds have been identified to date [98]. Due to the diversity and wide distribution of these compounds in plants, they can be categorized according to different parameters. Phenolic compounds have been classified by their source of origin, biological function, and chemical structure.

Focusing on their structure, they are classified broadly into simple and complex phenolics (or polyphenols). Simple phenolics contain a carboxylic group attached to the benzene ring with one or more hydroxyl or methoxyl groups attached to it, whereas polyphenols are compounds with higher molecular weight due to the presence of more than one benzene ring. More concretely, phenolic compounds have been classified into five major chemical families, namely flavonoids, phenolic acids, stilbenes, lignans and curcuminoids (Figure I10-A) [99] or, by abundance, in two big groups: flavonoids and non-flavonoids compounds.

2.1.1. Flavonoids

Flavonoids are polyphenolic compounds comprising 15 carbons with two aromatic rings connected by a three-carbon bridge. They are the most numerous of the phenolics and are found throughout the plant kingdom [100]. The basic flavonoid skeleton can have numerous substituents resulting in the establishment of subclasses, being the principals: flavones, flavonols, flavan-3-ols, isoflavones, flavanones, and anthocyanidins (Figure I10-B). Moreover, other flavonoid subgroups also exist with a minor presence in the diet such as chalcones, dihydrochalcones, dihydroflavonols, flavan-3,4-diols, coumarins and aurones.

A   Classification of phenolic compounds

Phenolic acids   Stilbenoids   Flavonoids

Lignans   Curcuminoids

B   Classification of flavonids

Flavonol   Flavone   Flavan-3-ol

Isoflavone   Flavanone   Anthocyanidin
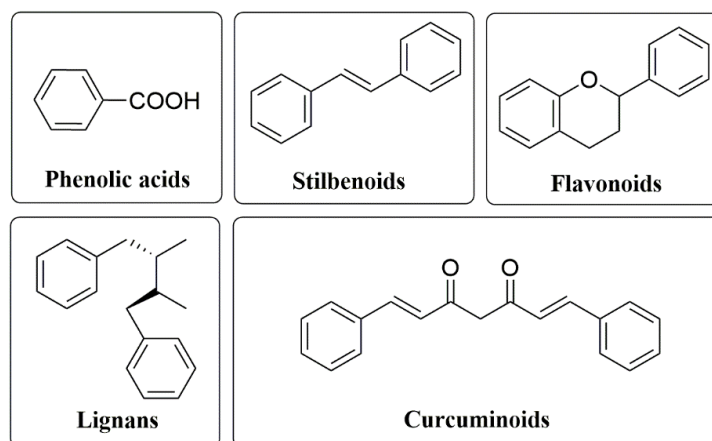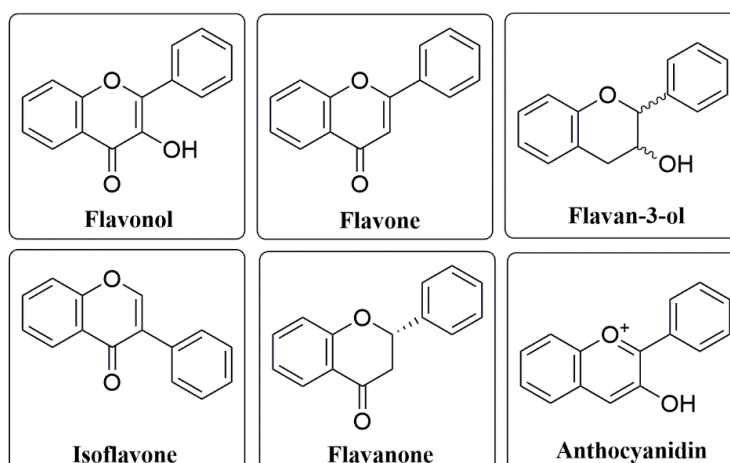
Figure I10. Classification of phenolic compounds according to their chemical structure. **(A) General classification of phenolic compounds.** The general structure of the main groups of phenolic compounds, phenolic acid, stilbenes, flavonoids, lignans and curcuminoids, is represented. **(B) Classification of flavonoids.** The general structure of the most abundant subgroups of flavonoids is represented: flavonols, flavones, flavan-3-ols, isoflavones, flavanones and anthocyanidins.

2.1.2. Non-flavonoids compounds

The main non-flavonoids of dietary significance are the phenolic acids, the hydroxycinammates and their conjugated derivatives, and the polyphenolic stilbenes. Moreover, due it extensive use as condiments and flavouring in the food industry we can also stand out the curcuminoid group.

2.2. Therapeutic potential

Polyphenols, which are widely present in foods and beverages of plant origin, have received great interest during the last years due to their positive effects on human health. Fruits, vegetables, olive oils, whole grains and other types of foods and beverages such as tea, chocolate and wine are examples of rich sources of polyphenols [98]. Several studies have strongly supported a role for polyphenols in the prevention of important diseases such as cancer, cardiovascular disease, chronic inflammation and neurodegenerative disease [101]. The beneficial properties of polyphenols have been partially attributed to their antioxidant role as well as to their ability to modulate molecular targets and signaling pathways. For instance, they can exerts anti-carcinogenic effects due to the ability to: (a) induce cell cycle arrest; (b) inhibit oncogenic signaling cascades controlling cell proliferation, angiogenesis and apoptosis; (c) modulate ROS levels; (d) promote tumor suppressor proteins such as p53; and (e) enhance the ability to differentiate and transform cancer cells into normal cells [97]. Their antioxidant capacity is widely linked to their ability to reduce free radical formation and to scavenge free radicals, but other mechanisms of action serving to elevate endogenous antioxidants are also important. For example, polyphenols can induce antioxidant enzymes such as glutathione peroxidase, catalase and superoxide dismutase and inhibit the expression of enzymes such as xanthine oxidase [102]. Moreover, they can elicit cellular signaling and modulate pathways that determine activity of the mitochondrial electron transport chain, membrane potential and biogenesis, intra-mitochondrial oxidative status and, ultimately, mitochondria-triggered cell death [103]. Another important factor is the molecular structure of these compounds, which can modulate their properties and functions. Of note, the 3-hydroxyl group in flavonols is considered especially important for their antioxidant activities [98].

However, polyphenols can behave as a double-edged sword; on the one hand, when used properly in the form of foods or functional foods, they are strong antioxidants the exert their action against oxidative stress, being thus beneficial to health. On the other hand, they can also display pro-oxidant activity when consumed in high doses, such as when taking supplements [104].

2.3. Dietary phenolic compounds and Q

As we described above, some (poly)phenolic acids exerts a key role as precursor of the benzoquinone ring of Q. Concretely, phenolic acids such as 4HB, vanillic acid, protocatechuic acid and *p*-coumarate as well as the stilbenoid resveratrol function as Q ring precursors in yeast and mammals [52, 56]. Moreover, a large list of phenolic acids such as *p*-coumaric acid, *m*-coumaric acid, isoferulic acid, ferulic acid, tyrosine, *p*-hydroxyphenyl-lactic acid, *p*-hydroxyphenylacetic acid, 4HB, anisic acid, *p*-hydroxybenzaldehyde and *p*-hydroxyphenylpyruvic acid display an inhibitory effect on phosphomevalonate kinase and mevalonate diphosphate decarboxylase, when present at high concentrations [105] (see Figure I3). This study revealed that some of the phenolic acids compete with the substrates, mevalonate 5-phosphate and mevalonate 5-pyrophosphate, whereas others inhibit uncompetitively. Therefore, the inhibition of these enzymes, that participate in the early stages of the mevalonate pathway, may regulate the biosynthesis of Q.

Apart from the role that some phenolic compounds have over the biosynthesis of Q, little is known about the possible interaction of more complex polyphenols in Q metabolism or regulation. A significant number of polyphenols have been shown to interact strongly with the lipid domains of cell membranes, altering the properties of the immediate lipid environment in which a representative number of crucial protein receptors are embedded. Moreover, it is described that mitochondria is a target for polyphenols [103, 106]. Linking these facts, a possible direct or indirect interaction of these compounds and Q is easy to come up with. An example is given by the flavonol quercetin. Quercetin is the most efficient polyphenol exerting a protective effect against mitochondrial dysfunction probably due to its ability to enter cells and accumulate in mitochondria. The ubiquinone/ubiquinol-like behaviour of quercetin allows preserving mitochondrial function. The polyphenol will prevent the formation of H_2O_2, even when the H_2O_2

production rate is stimulated by mitochondrial inhibitors like rotenone. Quercetin joins the Q-binding site of complex I instead of the inhibitor avoiding the impairment of the mitochondrial function. These findings suggest a new mitochondrial protective function for dietary polyphenols, independent of their antioxidant properties [107, 108]. A similar mechanism was also proposed for epichatechin, kaempferol and apigenin [109].

3. Dietary fatty acids

3.1. Fatty acids

Fatty acids are biomolecules composed by a carboxyl group linked to a long-chain hydrocarbon side groups. Most fatty acids have an even number of carbon atoms because they are usually biosynthesized by the concatenation of C_2 units and commonly the length oscillates between 14 and 22 carbons. They are rarely free in nature but, rather, are found taking part of complex lipid molecules and being the fundamental components of biological membranes. The nomenclature of fatty acids are made according the rules created and developed by the International Union of Pure and Applied Chemistry (IUPAC). However, their importance in biological process have made that, on one hand, traditional names of the most common or important compounds have been maintained and, on the other hand, the development of alternative nomenclatures have been promoted. Thus, despite for the IUPAC the C1 of the molecule is the one that belongs to the carboxyl group, an alternative nomenclature start to count from the carbon of the terminal methyl group of the chain (named carbon ω). Therefore, using this alternative nomenclature the third carbon from this side is the ω-3. This alternative is normally used in the biomedical literature.

Attending to the presence of double bound between the carbons of the lateral chain as well as it number and location, fatty acids can be classified as (see examples in Figure I11):

- **Saturated fatty acids** (SFA). In these molecules, no double bond is present in the hydrocarbon chain, resulting in an elevated fusion point. They can be identified with the abbreviate formulation of n:0, where n is the number of carbons present in the chain (for example, palmitic acid, 16:0).

- **Unsaturated fatty acids**. In these molecules, at least one double bound is present between two carbons of the chain. According to the number of double bonds two groups are stablished: monounsaturated fatty acids (MUFA) and polyunsaturated fatty acids (PUFA). The major part of these lipids have a double bound between C9 and C10 and, if more than one is present, the additional doubles bounds tend to occur at every third carbon atom toward the methyl terminus of the molecule. Two important classes of PUFA are denoted ω-3 (or n-3) and ω-6 (or n-6). This nomenclature allows to identity perfectly each fatty acid in a simple manner. For instance, eicosapentanoic acid (EPA) is named 20:5 ω-3 denoting its 5 double bonds, the first between ω-3 and ω-4 carbons.

Fatty acids are the structural units to the establishment of more complex molecules. One, two or three fatty acids can be esterified with glycerol to form monoglycerides, diglycerides, and triglycerides, respectively. Moreover, the combination of acylglicerols with a phosphate group and an aminoalcohol form phospholipids, the structural components of the cellular membranes.
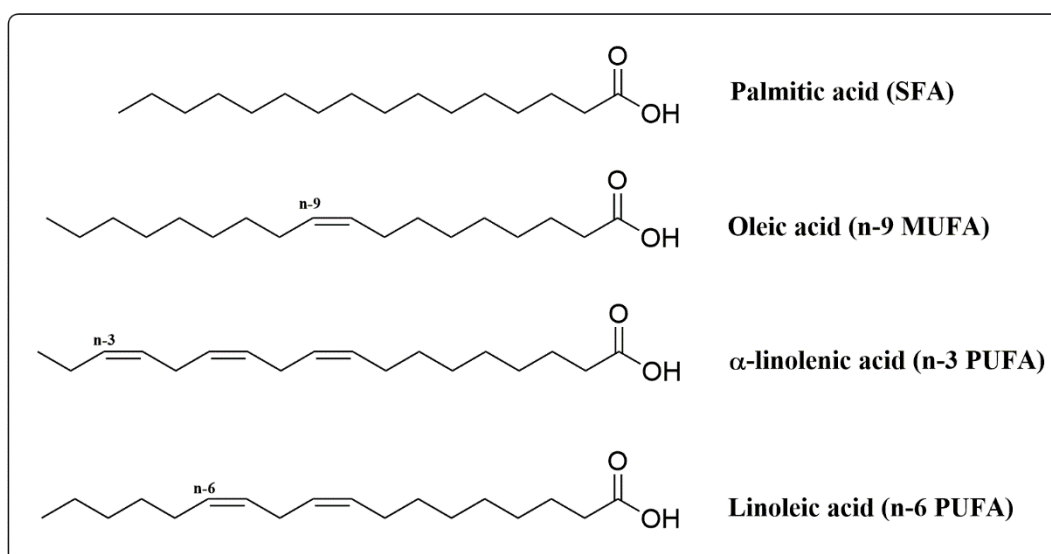
Figure I11. Classification of fatty acids attending to the presence of double bonds. We represent the main group of fatty acids: saturated fatty acids (SFA), monounsaturated fatty acids (MUFA) and polyunsaturated fatty acids (PUFA). One of the most important fatty acid of each group is selected to act as example. For PUFA, we have represented the two principal series of these compounds.

3.2. Essential fatty acids

Cells are able to synthetize fatty acids in the cytoplasm from acetyl-CoA and NADPH through the reactions of enzymes called fatty acid synthases. These fatty acids are known as the "non-essential fatty acids". However, cells are not able to produce all types of fatty acids it requires, but some of them must come from diet. These fatty acids are called "essential fatty acids" or EFAs [110]. The fact that mammal's cells cannot synthetize *ex novo* some types of fatty acids were elucidated in rats fed with a totally fat-free diet. Because of this feeding, among other problems, rat had growing alterations, dermatitis and reproductive disorders [111]. However, mayor advances in the understanding of the essential fatty acids are obtained, unfortunately, due to health problems developed in patients fed with fat-free total parenteral nutrition [112].

There are two known families of EFAs, the n-3 and the n-6 series. Both, are synthetized in plants through reactions related directed with the chlorophyll biosynthesis, where a type of desaturases, not synthetized in animals, are in charge of the insertion of a double bond in n-3 or n-6 positions of the hydrocarbon chain of the fatty acid. α-Linolenic acid (ALA) is the primary n-3 EFA whereas linoleic acid (LA) in the primary n-6 EFA (see their structures in Figure I11). Both n-3 and n-6 fatty acids exert important roles in the biophysics properties of the lipid bilayers, increasing its fluidity and affecting its oxidation pattern. Moreover, these lipids are beneficially associated with some pathological disorders. The n-3 series, apart from being a structural component of the membranes, plays an important protective role against cardiovascular diseases, psychiatric disorders [113], immune alterations and some types of cancer [114]. On the other hand, the n-6 series is associated with a beneficial influence over cardiovascular diseases [115].

Moreover, EFA are actually precursors to hormone like substances called "eicosanoids". The n-6 fatty acids, especially arachidonic acid (AA), are the primary source of the n-6 eicosanoids that are produced from oxygenation of AA by cyclooxygenase, lipoxygenase, and epoxygenase enzymes to produce prostaglandins, leukotrienes, lipoxines, and P-450 compounds, which acts as prolific cell messengers [110].

3.3. Dietary lipids

Due to essential fatty acids are obtained directly from the diet, it fat and oil (which differ only in that fats are solid and oils are liquid at room temperature) composition has important long-term consequences for health. Some studies have described the ability of biological membranes to adapt its phospholipid composition according to the major lipid source present in the diet [116-118], so a modification in the lipid pattern could produce biochemical alterations in cells, especially mitochondrial membranes [119]. PUFA sources, such as soybean or fish oil, will generate membranes more susceptible to oxidative stress than a SFA or a MUFA source, like animal fat and olive oil, respectively. Therefore, these alterations in the membranes could affect the oxidative damage rate and its related process such as aging [120]. Optimal cellular functions will require an adequate incorporation of PUFA through the diet as basic elements of the cellular membranes without exceeding the correct balance to avoid its negative activities.

3.4. Dietary fatty acids and Q

Huertas *et al*. provided the first evidences of the interaction of dietary fat and Q levels [116]. The different dietary fats used (virgin olive oil, refined olive oil and corn oil) did not produce any effect on microsomes but all of them influenced the mitochondrial levels of Q_9 and Q_{10} in rat liver. Higher mitochondrial Q content is observed in a corn oil-based diet (a source of n-6 PUFA) in comparison with an olive oil-based diet (a MUFA source). This difference in the amount of Q can also be supported by the fact that the mitochondrial membrane is more unsaturated in animals fed corn oil, and a higher antioxidative defense is therefore needed. It also been described that after an unnatural induction of oxidative stress a significant decrease of coenzyme Q_9 content was reported in the corn oil group but not in the olive oil group [121]. The high Q_9 turnover possibly stems from the oxidative damage that is induced in highly unsaturated mitochondrial membranes as a result of the corn oil intake. It is also described that Q levels in liver mitochondrial membranes of rats are significantly affected by the supplementation of olive oil with 200 mg/kg of vitamin E in comparison with a simple supplementation of olive oil. These differences suggest that vitamin E content in olive oil had a direct effect on Q levels, possibly due to a synergism between vitamin E and Q [122].

Moreover, previous studies in our Group reveals a fast regulation of mice Q biosynthesis, which involve *COQ* genes and COQ proteins, after 1 month of dietary intervention [123]. In this study, different sources of SFA and PUFA, as well as calorie restriction (CR), alter Q metabolism. Concretely, a n-3 PUFA rich diet (based on fish oil) induce the expression of *COQ* genes in liver, kidney, skeletal muscle, brain and heart. The incorporation in the membranes of fatty acids more sensitive to oxidation activates the biosynthesis pathway of Q as a defense mechanism to face a redox disarrangement. On the other hand, short-term calorie restriction use the biosynthesis pathway of Q to alter the energetic metabolism, although adaptation of *COQ* genes transcription is tissue-dependent.

From another point of view, Q is also related with fatty acids and diet when used as a dietary supplemental antioxidant. Exogenous Q is used as a supplement to alleviate the oxidative stress produced by PUFA-enriched diets. Ochoa *et al.* showed that heart mitochondria in rats fed a polyunsaturated fatty acid (PUFA)-rich diet and supplemented with Q_{10} present a lower hydroperoxide levels; higher content and/or activity of α-tocopherol, Q, and catalase; and a slightly lower decrease in mitochondrial function. According to that, previously reported positive effects of Q supplementation on the lifespan of rats fed a PUFA-rich diet [124] might be a consequence, at least in part, of a lower oxidative stress level [125]. Moreover, Quiles *et al.* described that MUFA can protect cardiomyocyte mitochondria from age-related changes, and that Q supplementation to a n-6 PUFA-enriched diet partially resembles MUFA benefits [126]. In liver, the supplementation with exogenous Q_{10} increased Q levels in both, total homogenates and plasma membranes, but rats fed with sunflower oil as fat source showed higher amounts of Q than those fed with olive oil, indicating a more protective antioxidant effect of olive oil dietary fat with respect to sunflower oil [127].

Fatty acids can suffer autoxidation reactions generating lipid peroxides and peroxyl radicals, which are chemically reactive and result in many products that are toxic to cells. A previous study performed in Coq3-deleted yeast revealed that these Q-deficient mutants are hypersensitive to the autoxidation products of linolenic acid and other polyunsaturated fatty acids, while the monounsaturated oleic acid, which is resistant to autoxidative breakdown, has no effect. The hypersensitivity of the Q-deficient mutants can be rescued by the addition of antioxidants, concretely, butylated hydroxytoluene, α-tocopherol or trolox, an aqueous soluble vitamin E analog. The results indicate that

autoxidation products of polyunsaturated fatty acids mediate the cell killing and that Q plays an important role in protecting eukaryotic cells from these oxidative products [128].

Objectives

The main objective of this work is to analyze the regulation of the coenzyme Q system through nutritional and pharmacological interventions. For this purpose, we include three partial objectives corresponding to the study of how coenzyme Q metabolism is influenced by three different groups of compounds:

1. **Phenolic acids**. In this partial objective, we will study the effect of different flavonoids and non-flavonoids compounds on coenzyme Q levels and their role as coenzyme Q precursors.

2. **Fatty acids**. To evaluate the effects of fatty acids on Q metabolism we will use an *in vitro* model of cell lines treated with lipid emulsions that differ in their composition as well as an *in vivo* model of animal fed with different fat sources.

3. **Farnesyl diphosphate synthase inhibitors**. In this case, the objective is the study of this key enzyme of the mevalonate pathway as a potential regulator of Q metabolism. We will use different strategies to inhibit this enzyme: specific siRNAs and zoledronic acid, as example of the nitrogen-containing bisphosphonate family. Q metabolism will be determined in the farnesyl diphosphate synthase depleted cells.

Materials and Methods

The brand of all the products used in the present work are summarized in Appendix 1.

1. Cellular model

1.1. Cell cultures

All cultures were maintained at 37ºC in sterile conditions and in a humidified atmosphere of 5% CO_2. Routinely, cells were replated every 3-4 days to maintain the culture using the appropriate cell culture media. Cell lines used in the present work (see images in Figure M1) are:

- **Human embryonic kidney cells 293 (HEK 293).** Cells were grown in DMEM: F12 with 1 g/L glucose supplemented with 10% FBS, 2mM L-glutamine and gentamicin-amphotericin B (125 µg/ml and 5 mg/ml, respectively).

- **Human liver hepatoma cells (Hep G2**). Cells were maintained in MEM containing 1g/L glucose and supplemented with 10% FBS, 1% sodium pyruvate, 2mM L-glutamine and gentamicin-amphotericin B (125 µg/ml and 5 mg/ml, respectively).
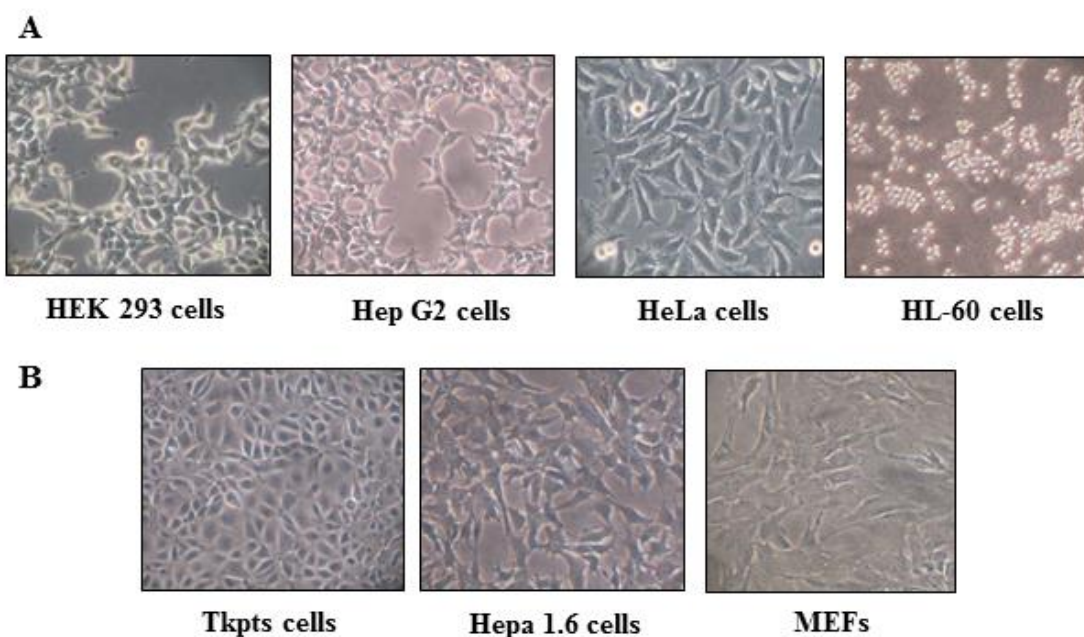
Figure M1. Cell cultures used along the study. (A) Human cell lines. HEK 293, HepG2, HeLa and HL-60 cells. **(B) Mouse cells.** Tkpts, Hepa 1.6 and MEFs. Images were taken directly from the inverted microscope.

- **Human promyelocytic leukemia cells (HL-60).** Cells were grown in RPMI-1640 supplemented with 10% FBS, 2mM L-glutamine and gentamicin-amphotericin B (125 µg/ml and 5 mg/ml, respectively).

- **Human cervical cancer cells (HeLa).** Cells were grown in DMEM with 4,5 g/l glucose supplemented with 10% FBS, 4mM L-glutamine and gentamicin-amphotericin B (125 µg/ml and 5 mg/ml, respectively).

- **Mouse kidney proximal tubule epithelial (Tkpts) cells**. Cells were grown in 1:1 DMEM: F12 with 4.5 g/L glucose supplemented with 10% FBS, 2mM L-glutamine and gentamicin-amphotericin B (125 µg/ml and 5 mg/ml, respectively).

- **Mouse liver hepatoma cells (Hepa 1.6).** Cells were culture in the same culture medium described above for Tkpts cells.

- **Mouse embryonic fibroblast (MEFs).** Cells were culture in DMEM 2g/L glucose supplemented with 10% FBS, 2mM L-glutamine and gentamicin-amphotericin B (125 µg/ml and 5 mg/ml, respectively).

All cell lines were obtained from ATCC except for Tkpts and MEFs. Tkpts cells [129] were kindly provided by Dr. Elsa Bello-Reuss (Texas Tech University Health Science Center) and Dr. Judit K. Magyesi (University of Arkansas for Medical Sciences, Little Rock, AR) whereas MEFs were obtained in our own laboratory by repeated subculture of cells derived from mouse embryos following a standard 3T3 immortalization protocol [130].

1.2. Viability assay

Final concentration of each product used in this work was selected on the basis of previous MTT viability assays. NAD(P)H-dependent cellular oxidoreductases enzymes present in viable and metabolic active cells are capable of reducing the 3-(4,5-dimethylthiazol-2-yl)-2,5-diphenyltetrazolium bromide (MTT) to its insoluble formazan, which has purple color. Non-viable cells has lost this ability so the color formation serves as a useful marker of viability [131]. To perform these assays, a convenient number of cells were plated into 24 well-plates and treated with the correspondent compound during 48h. Then, 50 µl/ml of a 5 mg/ml stock of MTT were added to the cultures. After 2 hours of incubation at 37ºC in 5% CO_2, the culture medium was removed, the converted dye solubilized with

0.04M HCl in absolute isopropanol, and the absorbance measured at 590 nm in a plate reader (Optic Ivymen System 2000-C).

1.3. Treatments

Generally, unless otherwise specified, the same experimental conditions were used to test all the compounds in mouse and human cells. Each product was dissolved according to the manufacturer's information. Assays were performed in 6 well-plates with an initial amount of 50,000-100,000 cells/well. Cells were incubated with the selected compounds for 48h under standard culture conditions (37ºC, 5% CO_2).

1.3.1 Phenolic compounds

Several phenolic compounds were used to test their effects on Q metabolism. Cells were treated with kaempferol, resveratrol, apigenin, quercetin, piceatannol, luteolin, naringenin, curcumin, ferulic acid or 4HB. In viability assays the concentration range was 5nM to 100µM. Some of the higher concentrations were found non-viable for cells, so in the following experiments the concentration range of all the phenolic compounds was decreased to 5 nM to 10µM, excepting for 4HB which did not affect cell viability at any of the concentrations tested. These compounds were mainly used in Tkpts cells but, in some cases, other cells lines such as HEK 293, HL-60, Hep G2, Hepa1.6 and MEFs were also used to complement these studies.

1.3.2. Lipid emulsions

To study the effect of different fat sources in Q metabolism we treated the cells with commercial lipid emulsions, traditionally used in parenteral nutrition. *Lipofundin MCT/LCT* 20%, *Lipoplus* 20% and *ClinOleic* 20% were added to the cells at a concentration of 7 µl/ml. *Lipofundin MCT/LCT* 20% is a source of n-6 PUFA due its composition is based on soybean oil. It contains 100g/L of soybean oil and 100g/L of medium-chain triacylglycerol's (MCT). As a source of n-3 PUFA (characteristic of a diet enriched in fish oil) we used *Lipoplus* 20% composed by 100g/L of MCT, 80g/L of soybean oil and 20g/L of n-3 triacylglycerol's. As a source of n-9 MUFA we used *ClinOleic* 20% mainly composed of purified olive oil (160g/L) and soybean oil (40g/L). The treatments with the described emulsions were performed in Hepa1.6 and Tkpts cells,

with the precaution of plating the cells at high density (15,000 cells/cm^2). Other cellular lines were also tested, such as Tkpts and HEK 293, but these lipids were extremely toxic for them, making it impossible to perform any study with lipid emulsions on these kidney-derived cell lines.

During the development of this study, B. Braun Melsungen AG stopped the commercialization of *Lipofundin MCT/LCT* 20%. The used of this lipid emulsion was restricted to a short period and so, *Lipofundin* only appears in some of the presented experiments. These experiments do not necessarily have to be the first ones because the workflow, in which the work was performed, was not the same that the one that is presented in this document.

1.3.3. Antioxidants

To discard the possible effect of the oxidation of the lipid emulsions used in our studies we made a co-treatment with two antioxidants: trolox (6-hydroxy-2,5,7,8-tetramethylchroman-2-carboxylic acid), an analogue of vitamin E, and butylated hydroxytoluene (BHT). To discard cellular toxicity, a viability curve for each compound was performed at a concentration range from 500 nM to 2 mM. According to the obtained results, trolox was used at 250 µM and BHT at 50 µM. Corresponding determinations were carried out in Hepa 1.6 cells.

1.3.4. Inhibitors

1.3.4.1. *p*-Aminobenzoic acid

To test if the effect of the compounds tested was related with ubiquinone biosynthesis we used *p*-aminobenzoic acid (PABA), a polyprenyltransferase Coq2 inhibitor, as an indirect approach. This compound was used at 1 mM in Tkpts cells, a concentration previously shown by our Group to produce an effective inhibition of ubiquinone biosynthesis [132].

1.3.4.2. Nicotinamide

Nicotinamide, a well-known inhibitor of sirtuin deacetylase activity [133], was used in some of our experiments in Tkpts cells, either by itself or in a combined treatment with the polyphenol kaempferol. In both cases, this product was used at 10 mM

1.3.4.3. Zoledronic acid

This third generation bisphosphonate is a well-known inhibitor of the enzyme farnesyl diphosphate synthase [89], which plays a major role in the mevalonate pathway. The toxicity of this chemical was tested in a concentration range from 0.5 µM to 200 µM in Tkpts, Hepa1.6, HEK 293 and HeLa cells. Each cellular line showed a different tolerance to this product, and we selected the highest concentration that did not affect cellular viability. Thus, we used ZOL at 20 µM in Hepa 1.6 and Tkpts cells, at 10 µM in HeLa cells and at 5 µM in HEK 293 cells.

1.3.4.4. Lovastatin

Lovastatin is part of a family of compounds named statins, well known as inhibitors of the HMG-CoA reductase. The inhibition of this enzyme suppress the conversion of HMG-CoA to mevalonic acid, an important step in the mevalonate pathway [134]. This compound was tested in Hepa 1.6 and Tkpts cells at a final concentration of 1µM, which was previously defined in a toxicity curve for each cell line.

1.4. Transient cellular transfections

1.4.1. Plasmids

Hepa 1.6 and Tkpts cells were transfected using Lipofectamine® 2000 according to the manufacturer's instructions. 100,000 cells were seeded in 12-well plates and cultures overnight at 37% and 5% CO_2 until a 70-90% of confluence was reached before starting the transfection procedure. To measure the efficiency of transfection (Transfection index, see below) of our cellular lines by flow cytometry, 1 µg of phrGFP-N1 vector (Agilent Technologies) was mixed with 3 or 6 µl of Lipofectamine® 2000 in 0.5 ml of Opti-MEM and incubated for 5 min at room temperature. Cell media were withdrawn and the new transfections complexes were added to the cells and incubated at 37% and 5% CO_2 for 24 hours. After this time, Opti-MEM that contained the lipid complexes was replaced by 1 ml of complemented media and cells were incubated another 24h hours.

1.4.2. siRNAs

Two commercial 27mer siRNA duplexes designed against mouse FDPS as well as a universal scramble negative control (all from OriGene[TM] Technologies) were used to transfect Hepa1.6 cells. 250,000 cells were plated in 6-well plates and incubated overnigth at 37% and 5% CO_2. For each transfection we used 6 µl of Lipofectamine® 2000 in 1 ml Opti-MEM and siRNAs at a final concentration of 20 nM. Cultures were incubated for 48 h post-transfection (with a media change at 24 hours) in order to allow siRNAs to achieve the appropriate inhibition of FDPS. After this time, cells were recovered and processed for lipid measurements and western-blotting (see below). siRNA effectiveness was validated for each experiment by western-blot using a specific antibody raised against FDPS.

Identification	Sequence
SR411924-**A**	rArGrArGrGrUrArCrArArArUrCrGrArUrUrGrUrCrArArGTA
SR411924-**B**	rCrArUrGrUrGrGrArUrCrUrUrGrGrUrArGrArUrArCrArCTG

Table M1. **SiRNA identification and sequence.** We summarize here the sequence of both 27mer siRNA duplexes used to deplete the amount of FDPS in Hepa 1.6 cells.

To test the effect of *Lipoplus 20%* over cells in which the FDPS had been silenced using siRNAs, cells were replated 48 hours after transfecction and treated with 7 µl/ml of *Lipoplus 20%* for another period of 48 hours. When cells were replated we doubled the numbers of wells, including a set of wells to be treated with 7 µl/ml *Lipoplus 20%* alone and a similar set to be used as untreated control.

1.5. Whole cell extracts

1.5.1. For lipid determinations

Once the corresponding treatment was completed, cells were washed with Hanks' balanced salt solution and detached from culture plates, using a cell scraper, in 1ml of the same solution. Cell suspensions were pelleted by low-speed centrifugation and the dry cell pellets were stored at -80ºC until use for extraction of lipids as described below.

1.5.2. For electrophoresis and western-blotting

Cells were washed with Hanks' balanced salt solution twice and detached using a cell scraper directly in a small volume (100-200 µl) of radioimmunoprecipitation assay (RIPA) buffer (50mM Tris-HCl pH8, 150mM NaCl, 0.5% deoxycholate, 0.1% SDS, 1mM DTT, 1% Triton X-100). In order to enhance the preservation of the samples, RIPA buffer was always supplemented with 20µg/ml of each of the following protease inhibitors: chymostatin, leupeptin, antipain and pepstatin (CLAP) and 1mM of phenylmethylsulfonyl fluoride (PMSF). The cell suspension was centrifuged at 10,000 g for 15 minutes to remove non-solubilized debris and the supernatants were saved for future determinations of protein levels by western-blot. All the procedure was carried out at 4ºC.

2. Animal model.

2.1. Calorie restriction and dietary fat intervention in mice

C57BL/6 male mice were used in the present study. Mice were cared according with the *Guide for care and use of laboratory animals (*National Research Council*, United States)*, the *Animal Welfare Act* (PL 89-544, United States) and the Real Decreto 1201/2005, October 10, about protection of animals used in research projects and science. The ethic committees of animal experimentation of the University of California, Davis (United States) and the University Pablo de Olavide (Seville, Spain) approved all the protocols. Animals were maintained at the Andalusian Center of Developmental Biology (University Pablo de Olavide) in individual cages to ensure the correct intake control. Dark-light cycles had a duration of 12 hours, the temperature was 22 ºC and the animals had unlimited access to water. The daily average intake was calculated along three weeks in a group of 30 mice, in order to select a criterion to calculate the amount of calories we should administer in the different diets.

At the age of ten weeks, mice were randomly assigned to one of the different diet groups (one group and the remaining three groups under calorie-restricted conditions) and fed with a purified AIN-93M diet (Research Diets, New Jersey, United States) (composition described in Table M2 and M3). In order to avoid an excessive weight gain and obesity, the control group (Ctrl) was fed with the 95 % of the daily average intake previously

calculated. In calorie-restricted groups (CR), food was reduced to 60 % of the daily average intake. The only difference between diets was the main fat source. While in the Ctrl group the diet contained soybean oil (high in n-6 polyunsaturated fatty acids, Super Store Industries, Lathrop, CA) the three CR groups were fed with diets containing soybean oil, fish oil (high in n-3 polyunsaturated fatty acids: 18% eicosapentaenoic acid and 12% docosahexaenoic acid; Jedwards International, Inc., Quincy, MA) or lard (high in saturated and monounsaturated fatty acids, ConAgra Foods,Omaha, NE), respectively. Two age groups were constituted for each dietary intervention: one for an intervention lasting 6 months and another one for a longer intervention of 18 months.

Ingredients	Lard diet (g/kg)	Soybean oil diet (g/kg)	Fish oil diet (g/kg)
Casein	200	200	200
Corn starch	397.48	397.49	397.50
Maltodextrin	132	132	132
Sucrose	100	100	100
Cellulose	50	50	50
Soybean oil	0	70	0
Lard	70	0	0
Fish oil	0	0	60
t-butyl hydroquinone	0.014	0.015	0.016
Mineral mix	35	35	35
Vitamin mix	10	10	10
L-cysteine	3	3	3
Choline bitartrato	2.5	2.6	2.7

Table M2. Composition of the different diets used in this study. The soybean oil diet was used in the RC-Soy group as well as in the control diet. Diets contain mineral mix (S10022G) and vitamin mix (V10037). Data obtained from [135].

Fatty acids	Lard (%)	Soybean oil (%)	Fish oil (%)
Saturates	40.3	14.8	28.3
Monounsaturated (n-9)	39.2	21.2	8.7
Total n-6	16.0	55.0	3.2
Total n-3	0.7	8.1	33.9
n-6/n-3 ratio	24.4	6.8	0.1

Table M3. Fatty acid composition of the fats present in the different diets used in this study. Data are represent in %. Data obtained from [136].

Animals were sacrificed in the installations of University Pablo de Olavide by cervical dislocation after the corresponding intervention. Tissues were extracted and preserved in freezing buffer (0.21 M mannitol, 0.07 M sucrose and 20 % DMSO). All tissue samples were stored at - 80ºC until use.

2.1.1 Preparation of tissue homogenates.

Muscle and liver from Ctrl and CR animals were already processed in previous studies developed by our Group to obtain whole homogenates [137, 138]. Hind limb skeletal muscles were chopped and homogenized at 4 °C in ice-cold buffer containing 20 mM Tris–HCl pH 7.6, 40 mM KCl, 0.2 M sucrose, 1 mM PMSF, 10 mM EDTA and 20 μg/ml CLAP with a Teflon-glass tissue homogenizer. A second step of homogenization were carried out using a high-performance dispersing instrument (Ultra-Turrax T25, IKA, Staufen, Germany) and the resultant total homogenates were stored at -80 ºC until use. In the case of liver, the same procedure was performed but a suitable buffer was used (5mM Tris-HCl pH 7.4, 0,225 M mannitol, 0.075 M sucrose, 0.5 mM EGTA, 10mM EDTA, 1mM PMSF and 20 μg/ml CLAP).

2.2. Sirt3 knockout model

Frozen tissues from Sirt3 knockout mice (*Sirt3-/-)*, as well as from the corresponding matched controls (wt), were provided by Dr. Verdin (Gladstone Institute, San Francisco, CA, USA) and used in the present study. These male knockout mice were developed as described [139] in a genetic C57Bl/6 background. Mice were maintained on a standard chow diet (5053 PicoLab diet, Ralston Purina Company, St. Louis, MO) and sacrificed at the age of 3 months. The organs were collected and quickly frozen in liquid nitrogen.

2.2.1 Preparation of tissue extracts

A thin slice weighing approximately 50 mg, was directly cut off the frozen tissue and lysed in RIPA buffer supplemented with protease inhibitors, as indicated above. A pellet pestle motor (Kimble® Kontes) was used to aid in tissue disruption. Lysates were centrifuged at 10,000g for 15 min in a tabletop microfuge at 4°C and supernatants were transferred to new vials and conserved at -80 °C. For this study, we prepared tissue homogenates from liver, kidney, skeletal muscle and brain.

3. Lipid extractions

3.1. For HPLC with electrochemical or diode array detection measurements

Cellular pellets (approx. 10^6 cells) from the different treatments or 20mg of tissue homogenate were collected and resuspended in 90µl of Hanks' balanced salt solution. Samples were then solubilized using 10 µl of 10% SDS followed by 200 µl of 95:5 ethanol-isopropanol. After vortexing vigorously, 500 µl of hexane were added and the samples were centrifuged for 5 min at 10,000 g at 4 ℃. Lipids were recovered within the upper hexane phase, and the last step was repeated twice. Hexane phases were combined and the solvent evaporated under vacuum. Lipid extracts were stored frozen at -80℃ until use.

3.2. For HPLC-MS/MS measurements

After treatments, di-propoxy-Q_{10} was added to the pellets as internal standard in mouse and human samples. Cell pellets were resuspended in 1ml of methanol followed by 1ml of petroleum ether. Samples were vortexed for 1 minute and, after removal of the organic upper layer, another 1ml of petroleum ether was added. Samples were vortexed again and the combined organic phase was dried under nitrogen. Lipid dry extracts were stored at -20℃ until use.

4. Determination of protein concentration

Protein concentration of all the samples were determined using the variation described by Stoscheck [140] of the traditional protein assay protocol described by Bradford [141]. Samples were mixed with 50 µl of 1M NaOH in order to facilitate the solubilization and then, 1ml of Bradford reagent was added. Samples were vortexed and incubated for 10 minutes at room temperature in the dark. The absorbance of each sample was measured at 595 nm in a DU-640 spectrophotometer (Beckman Coulter, USA). A standard curve with known concentrations of γ-globulin (from 0 to 20 µg/ml) was used to calculate the final protein concentration of the samples.

5. Measurements of non saponifiable lipids levels by HPLC

5.1. Ubiquinone

HPLC analysis was carried out on a Beckman System Gold (Beckman Coulter, USA) connected to a Coulochem II electrochemical detector (ESA, Chelmsford, MA, USA). The chromatographic separation was performed on a C18 reverse phase analytical column (4.6 mm × 25 cm, Ultrasphere ODS, 5 μm particle) with a mobile phase composed of 53:45:2 methanol-isopropanol-1M pH 4.4 ammonium acetate at a flow rate of 1ml/min. The analytical cell (ESA, Model 5010) was set at potentials of -500 mV and +300 mV in electrodes 1 and 2, respectively. The entire procedure was performed at room temperature. Lipids extracts were dissolved in 30 µl of methanol, and the sample was subjected then to a reduction step by adding 1 µl of freshly prepared 50mM sodium borohydride just before injection into the system.
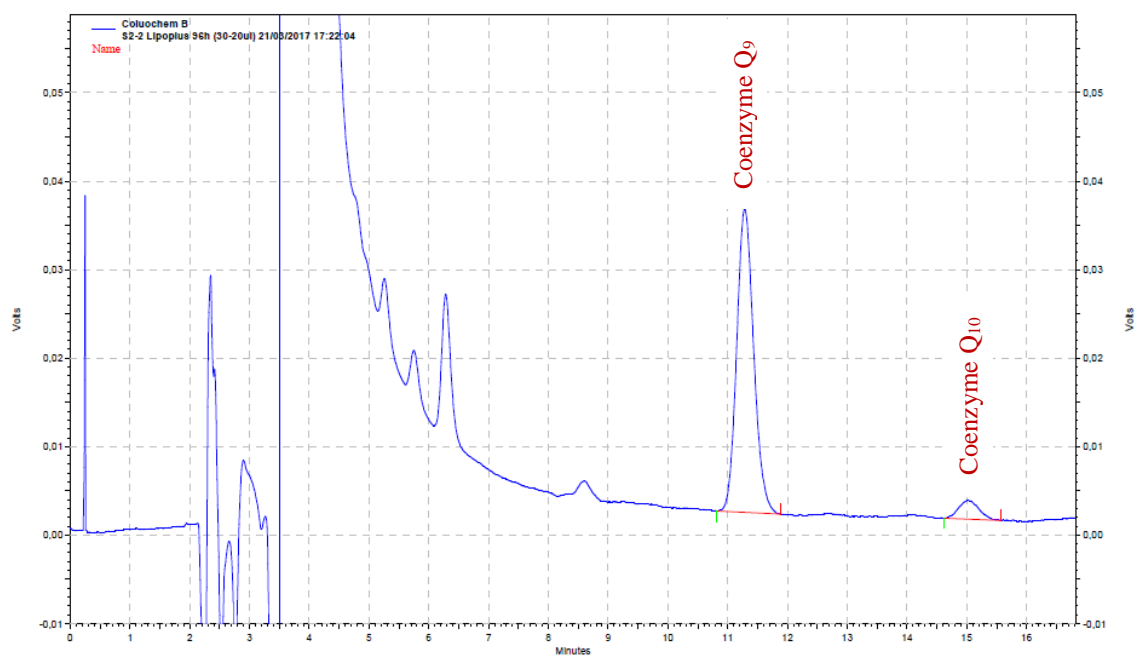
Figure M2. Chromatographic separation of Q_9 and Q_{10}. This figure show a representative chromatogram of Q_9 and Q_{10} levels in Hepa1.6 cells. Alterations in baseline observed between the start of the chromatogram and minute 5 correspond with the alteration caused by the injection of the sample and the presence of sodium borohydride as a reducing agent.

This procedure results in the reduction of the quinones to their corresponding hydroquinones (which are detected at the second electrode with maximal sensitivity) and it allows a significant shortening of chromatography time. Retention times were 10-11

min for reduced Q_9 and 14-15 min for reduced Q_{10} (Figure M1). The area units of hydroquinone peaks were integrated and referred to the reduced Q_{10} standard. Normalized values were obtained by referring to the amount of protein of each sample.

5.2. Cholesterol

HPLC analysis was performed on a Beckman System Gold (Beckman Coulter, USA) connected to a diode array detector (Module 168, Beckman Coulter, USA). A C18 reverse phase analytical column (4.6 mm × 25 cm, Ultrasphere ODS, 5 μm particle) was used to perform the chromatographic separation, with a mobile phase composed of 70% ethanol-30% methanol at a flow rate of 1ml/min. Although maximum absorption of cholesterol is at 202 nm, this compound was monitored at 210 nm as recommended Arnezeder *et al*. [142] to avoid interference with solvents in the mobile phase that would give a noisier base line. Diode array detector allows checking of the absorption spectrum of the cholesterol peak in every single sample, in order to double check the specificity of the method. Lipids extracts were dissolved in 30 μl of methanol and injected directly into the system. Retention times was approximately 6.7 minutes (Figure M2). The area unit of cholesterol peak was integrated and referred to a commercial cholesterol standard. Normalized values were obtained by referring to the amount of protein of each sample.
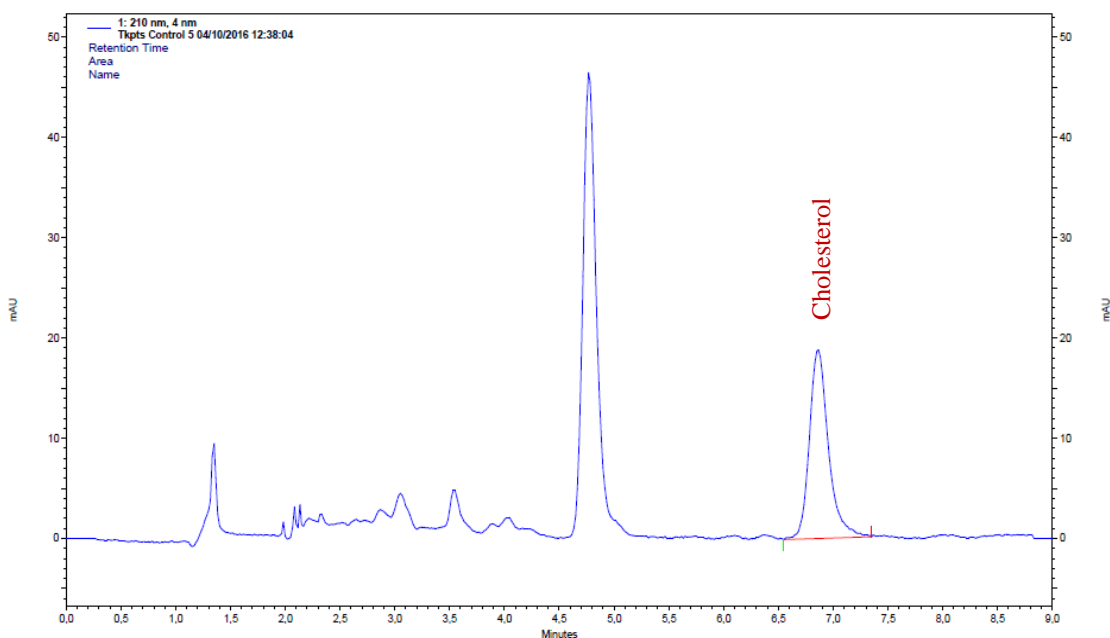
Figure M3. Chromatographic separation of cholesterol. This figure show a representative chromatogram of cholesterol levels in Tkpts cells.

6. Synthesis of radiolabeled 4-hydroxybenzoic acid

In order to measure the rates of Q biosynthesis we synthetized the radiolabeled precursor 4-hydroxy-(U-^{14}C) benzoate (^{14}C-4HB) starting from (U-^{14}C)-tyrosine, essentially as described by Clarke *et al.* [143] with minor modifications. 250μCi of (U-^{14}C)-tyrosine in 2.5 ml of 2% ethanol was blown to dryness under nitrogen. Then, 25 µl of 10M KOH and 17.5 µl of 10M NaOH freshly prepared were added and the resulting mixture were, again, blown to dryness under nitrogen. To perform the alkaline fusion, tubes were heated in a mineral oil sand bath for 6 minutes at 272ºC. After this time, tubes were allowed to cool to room temperature and 400 µl of H_2SO_4 25% (v/v) were added to acidify the sample. After vortexing, tubes were transferred to an ice bath and 1.5 ml of 100% ethyl acetate were added. Tubes were mixed vigorously and centrifuge 10 minutes at 2,000-3,000 rpm in a table top centrifuge (Mixtasel 7000575, Selecta). After this step, 2 phases were clearly differentiated. ^{14}C-4HB was recovered with ethyl acetate in the upper phase while remaining (U-^{14}C)-tyrosine stayed in the bottom aqueous phase. Ethyl acetate was added two more times and the combined organic phase was washed twice with water and dried under vacuum. Final product was dissolved in 1ml of 100% ethanol and stored at -20ºC.
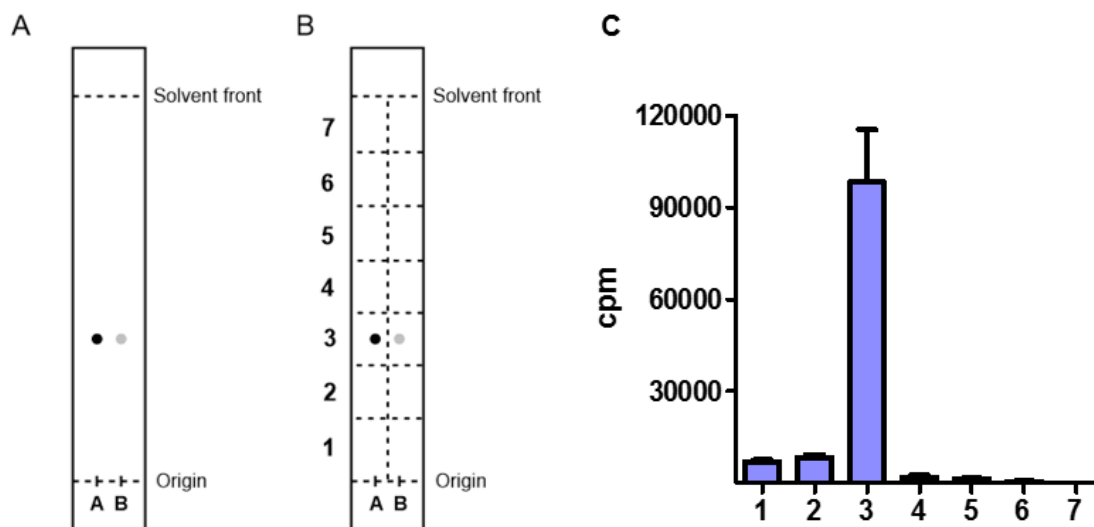
Figure M4. **Scheme of the thin layer chromatography of ^{14}C-4HB on silica gel plates**. Letter A represents the 4HB standard while letter B represents the product synthetized during this protocol. **A)** Two spots represent the co-migration of both standard 4HB and ^{14}C-4HB on the TLC plate. **B)** Dashed lines represent the sections we scratched separately and measured in a scintillation counter. **(C)** Cpm extracted of each section delimited in the silica plate. The synthetized ^{14}C-4HB migrated till section 3 and, in this section of the TLC we detected almost all the radioactivity.

The purity of the synthetic product was checked by thin layer chromatography on silica gel plates which were developed with isopropanol: ammonium hydroxide: water (8:1:1). All detectable radioactivity was contained in a single peak with co-migrated with an authentic 4HB standard. Spots were observed under UV light and radioactivity was double checked scratching section by section the silica of the plates and measuring the radioactivity in a Beckman scintillation counter after mixing each sample with 4ml of scintillation liquid.

7. Ubiquinone biosynthesis assays

7.1. Incorporation of a radiolabeled precursor

^{14}C-4HB (100.000 CPM) was added to the cells during the 48h incubation with the corresponding treatment. Samples were processed as described previously by Córdoba-Pedregosa *et al.* [144]. Briefly, cells were rinsed twice with Hanks' balanced salt solution and fixed for 15 min in 1ml of 5% trichloroacetic acid (TCA). The radioactivity was directly extracted from each well with 1ml of 1M NaOH for 2h at room temperature with gentle stirring. Radioactivity was quantified in a Beckman scintillation counter by mixing 900 µl of each sample with 4ml of scintillation liquid. The CPM values so obtained were then referred to the total amount of protein in each sample.

7.2. Incorporation of ^{13}C labeled or deuterated precursors

Lipid extracts, from cells treated with the corresponding product, were measured by HPLC-tandem mass spectrometry (MS/MS) analyses as previously described by Xie *et al.* [56]. A binary HPLC solvent delivery system with a Luna phenyl-hexyl column (particle size 3 µm, 50 × 2.00 mm, Phenomenex) connected to a 4000 QTRAP linear MS/MS spectrometer from Applied Biosystems (Foster City, CA) was used in all the determinations. Applied Biosystem software, Analyst version 1.4.2, was used for data acquisition and processing. Samples were resuspended in 200µl of 1mg/ml benzoquinone in order to oxidize all the lipids prior to chromatographic separation with a mobile phase composed of 90% solvent A (95:5 mixture of methanol:isopropanol containing 2.5mM ammonium formate) and 10% solvent B (isopropanol containing 2.5mM ammonium formate) at a constant flow rate of 1ml/min during the whole chromatography. All samples were analyzed in multiple reaction-monitoring mode. Transitions monitored are

described in **Table M2**. The area value of each peak, normalized with the correspondent standard curve of Q_9 and Q_{10} and internal standard (di-propoxyQ$_{10}$), was referred as well to the initial amount of protein.

Molecule	*m/z* (+ H)	*m/z* (+ NH$_3$)
Q$_9$	795.6/197.08	812.6/197.08
D$_3$-Q$_9$	798.6/200.08	815.6/200.08
^{13}C$_6$-Q$_9$	801.6/203.08	818.6/203.08
Q$_{10}$	863.6/197.08	880.6/197.08
D$_3$-Q$_{10}$	866.6/200.08	883.6/200.08
^{13}C$_6$-Q$_{10}$	869.6/203.08	886.6/203.08
Dipropoxy-Q$_{10}$	919.7/253.1	936.7/253.1

<u>**Table M4**</u>. **HPLC-MS-MS transitions for each analyte.** We summarize here the transitions used for each molecule in the HPLC-MS/MS. We monitored both the protonated and the ammoniated transitions.

8. Determination of GPP and FPP

The ability of FTase to prenylate proteins with a consensus sequence CAAX in the carboxyl terminus where C is cysteine, A is any aliphatic amino acid and X is the C-terminal amino acid, such as methionine, serine, cysteine, or alanine [145] was used as a tool to determine metabolites such as GPP and FPP. This method combines the specificity of enzymatic reactions, the selective separation of HPLC, and the sensitivity of fluorescence detection to measure low levels of GPP and FPP in cultured cells. Combining a consensus peptide (GCVLS for GPP and FPP), linked to a fluorescent dansyl group, with the enzyme able to perform the isoprenylation (FTase, in the case of GPP and FPP) we are able to measure the amount of GPP or FPP in our samples. The protocol used is an adaptation of that developed by Holstein *et al.* [146].

8.1. Extraction of GPP and FPP from cell cultures

Approximately 10×10^6 cells, conveniently treated, were rinsed, scratched directly in Hank's balanced salt solution and pelleted by low-speed centrifugation. Cell pellets were resuspended in 1ml of cold PBS and centrifuged at 100,000 g during 5min at 4ºC. The buffer (PBS) was aspirated and 0.5 ml of extraction solvent (isopropanol/75 mM

ammonium hydroxide/acetone, in 1:1.5:5 proportion) was added to the cell pellet. Samples were vortexed for 1 min and centrifuged at 10,000 g during 5 min at 4ºC. The extraction was repeated twice and the combined supernatants were dried under nitrogen at 30ºC and stored at -80ºC.

8.2. Enzymatic reaction

Just before to start the enzymatic reaction, the residue was dissolved in 40 µl of 50 mM Tris-HCl pH 7.5 containing 5 mM DTT, 5 mM $MgCl_2$, 10 µM $ZnCl_2$ and 1% octyl-β-D-glucopyranoside. To start the reaction, 0.25 nmoles of D*-GCVLS (dansyl-labeled peptide GCVLS) and 1 µl of FTase (50 µg/µl) were added and the mixture was incubated for 2 hours at 38ºC. The reaction was terminated by the addition of 60 µl acetonitrile. Denatured proteins were removed by centrifugation at 100,000 g at 4 ºC for 5 min and the supernatant was analyzed by HPLC.
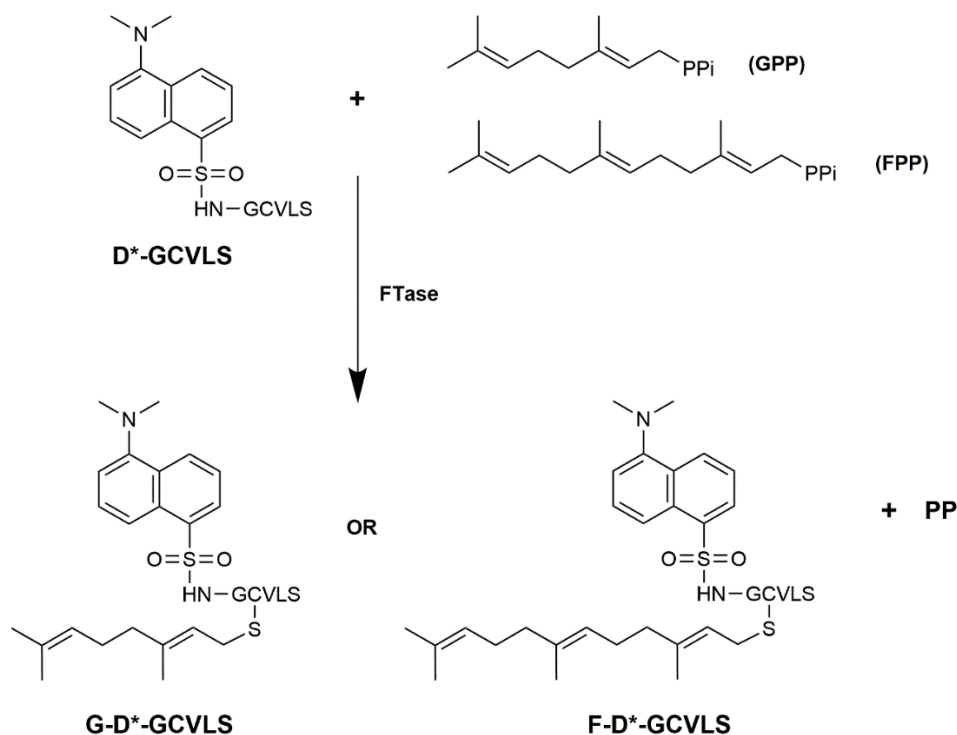
Figure M5. **Reaction catalyzed by FTase.** GPP and FPP reacts with D*-GCVLS peptide to form G-D*-GCVLS and F-D*-GCVLS, respectively. These reaction products can be measured by HPLC-fluorescence. Scheme adapted from [147].

After this reaction, the GPP and FPP present in the sample will be conjugated with the dansyl labeled peptide added forming geranyl/farnesyl-conjugated dansyl peptides (G-D*-GCVLS and F-D*-GCVLS, respectively) that could be separated and quantified using HPLC with fluorescence detection.

8.3. Quantification

HPLC analysis was carried out on a Beckman Gold System (Beckman Coulter, USA) connected to a FP-2020 Plus intelligent fluorescence detector (Jasco Co., Tokyo, Japan). To separate prenylated peptides (G-D*-GCVLS, F-D*-GCVLS) a C18 reverse phase analytical column (4.6 mm × 25 cm, Ultrasphere ODS, 5 μm particle) was used. The mobile phase was composed by two solvents: solvent A, 20 mM ammonium acetate in 40% acetonitrile and solvent B, 20 mM ammonium acetate in 90% acetonitrile. The program was initiated at 26% B for 2 min and then solvent B was brought to 60% by a linear gradient in 3 min. An isocratic 60% solvent B was run up to 15 min, then the solvent B was brought back to 26% B by a linear gradient in 1 min.
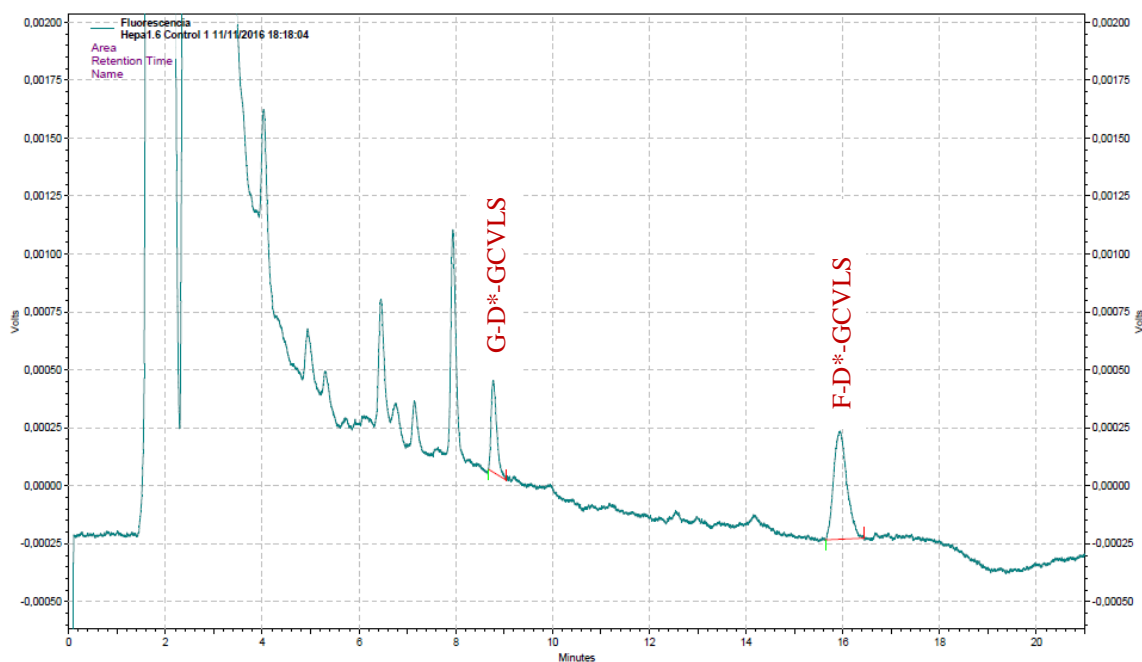
Figure M6. Chromatographic separation of prenylated dansyl-labeled peptides. This figure show a representative chromatogram of G-D*-GCVLS and F-D*-GCVLSPP levels in Hepa1.6 cells. The saturating increase in minute 2-3 corresponds with the non-prenylated dansyl peptide.

The total run time was 21 min. A flow rate of 1.16 ml/min was kept throughout all the analysis. Geranyl- and farnesyl- adducts were monitored by fluorescence at the excitation wavelength of 335 nm and the emission wavelength of 528 nm. The retention time for the G-D*-GCVLS and F-D*-GCVLS peaks were approximately 9 and 16 min, respectively (Figure M5). Their area units were integrated and referred to GPP and FPP commercial standards, previously subjected to the same extraction and enzymatic reaction as the rest of the samples. Normalized values were obtained by referring to the amount of protein of each sample.

9. Protein electrophoresis and western-blot

9.1. Sample preparation

In order to measure proteins not embedded in cellular membranes, 50 µg of the whole cells extract described above were mixed with 1X SDS-dithiothreitol loading buffer (60 mM Tris-HCl pH 6.8, 10 % sucrose, 2 mM EDTA, 1.5 % SDS, 20 mM dithiothreitol and 0,01 % bromophenol blue) and heated for 5 minutes at 100ºC. However, to measure membrane proteins 50 µg of protein extract were mixed with a mixture composed by 1X loading buffer containing CLAP (5mg/ml) and PMSF (100mM) in proportions 18:1:1. In this case, the heating of the samples was limited to 45ºC for 15 minutes to avoid aggregations of membrane proteins that would be otherwise promoted by SDS at higher temperatures. The only exception were those samples prepared to measure levels of the OXPHOS complexes, which cannot be heated more than 37ºC in order to preserve the complex IV signal.

9.2. Electrophoresis, transfer and loading control

TGX 4-20% polyacrylamide gradients gels (Bio-Rad) were used to determine the protein abundance by western-blot. Gels of 10, 18 or 26 wells were used according to the needs of each experimental design and, always, at least one well was used to load the molecular weight marker (Dual Color Precision Plus Protein Standards, Bio-Rad). Proteins were separated in a Criterion system (Bio-Rad) at a constant voltage of 180-200 V.

Once the electrophoresis was completed, proteins were transferred to nitrocellulose membranes included in the Trans-Blot Turbo kit (Bio-Rad) using a program of 25V and

7 minutes included in the Trans-Blot Turbo Tranfer System (Bio-Rad). To have a loading control, membranes were stained with Ponceau S (0.1% Ponceau S red dye diluted in 1% acetic acid) for 5 minutes and gentle stirring at room temperature. The excess of staining was removed by rinsing the membrane several times with 1% acetic acid. Protein patterns so obtained were digitalized using a ChemiDoc^{TM} Imaging System (Bio-Rad). Then, the membranes were blocked with TTBSL buffer (50 mM Tris-HCl pH 7.6, 0.85% NaCl, 0.05% Tween-20 and 5% skimmed milk powder) during 1-5 hours, including a buffer change. After this step, membranes were either used immediately for immunostaining or stored at -20ºC until use.

9.3. Inmunostaining, developing and quantification

Blocked membranes were incubated with the corresponding primary antibody at 4 ºC overnight with gentle stirring. Primary antibodies were diluted in TTBSL at the concentration indicated in **Table M3**. After the incubation, membranes were washed three times with TTBS (50 mM Tris-HCl pH 7.6, 0.85% NaCl and 0.05% Tween-20) at room temperature and gentle stirring. Afterwards, the corresponding species-specific secondary antibody diluted in TTBSL (see specific concentration in **Table M3**) and coupled to horseradish peroxidase was added and the membrane incubated for 1 hour at room temperature with moderate agitation.

Primary antibody	Dilution	Reference	Secondary antibody	Dilution	Reference
Acetylated-lysine	1:1000	9441S	Rabbit anti-IgG	1:2000	sc-2004
COQ2	1:1000	[15]	Chicken anti-IgG	1:5000	Sigma A-9046
FDPS	1:1000	ab153805	Rabbit anti-IgG	1:2000	sc-2004
OXPHOS complex	1:2000	458099	Mouse anti-IgG	1:5000	Sigma A-9044
Rap1 C-17	1:1000	sc-1482	Goat anti-IgG	1:5000	Sigma A-5420
Rap1 E-6	1:1000	sc-398755	Mouse anti-IgG	1:2000	Sigma A-9044
Sirt3	1:1000	sc-99143	Rabbit anti-IgG	1:2000	sc-2004
VDAC	1:1000	sc-98708	Rabbit anti-IgG	1:2000	sc-2004

Table M5. Antibodies used for immunodetection in western blotting. Each primary antibody was used in combination with the corresponding secondary antibody as referred in the table. References denoting "sc" refers to antibodies obtained from Santa Cruz Biotechnologies, "ab" denote an antibody obtained from Abcam and "Sigma A" denote antibodies from Sigma Aldrich. Acetylated-lysine antibody was obtained from Cell Signalling while OXPHOS complex antibody is from Thermo Fisher Scientific.

Then, the antibody was removed and the membrane was washed 3 times with TTBS at room temperature and gentle stirring. Finally, membranes were washed once with TBS (50 mM Tris-HCl pH 7.6 and 0.85% NaCl).

Developing of images was performed by enhanced chemiluminiscence (ECL Plus, Amersham Bioscience). Luminescence derived from the horseradish peroxidase-catalyzed reaction was recovered using a ChemiDoc[TM] Imaging System (Bio-Rad). Images obtained were quantified and normalized with Ponceau S staining, to correct for minor differences in protein loading, using Image Lab[TM] Software (Bio-Rad).

10. Flow cytometry

Hepa 1.6 and Tkpts cells were transfected with phrGFP-N vector and, at the same time, controls cells for each type were subjected to the same transfection procedure but in the absence of plasmid. 48 hours post-transfection, cells were washed with Hank's balance salt solution and detached from the culture plates using non-enzymatic Cell Dissociation Solution. Each cell suspension was directly injected and analyzed in an EPICS XL flow cytometer (Beckman Coulter) equipped with a 488 nm argon laser. After excitation at 488nm, the fluorescence emission was registered at 525 nm (FL1 channel). At least the signal of 20,000 cells were recovered.

The data were obtained in a logarithmic scale and represented in histograms using the EXPO32 ADC Analysis software (Beckman Coulter). Using control cells, we delimited a region in which fluorescence signal was absent and, then, we quantified the % of transfected cells which emitted a fluorescent signal above this region. Using these data, we calculated the transfection index for each cellular line.

11. Electron microscopy

11.1. Sample preparation

Hepa 1.6 cells treated with lipid emulsions were detached from the plates using trypsine for 2-3 minutes before neutralizing with completed culture medium. Cell suspension was mixed with fixing solution (2.5% glutaraldehyde in 0.1 M pH 7 cacodylate buffer) at 1:1 proportion in Eppendorf tubes and incubated for 1 hour at 4 ºC. Afterwards, cells were centrifuged and the supernatant discarded. Fresh fixing solution was added to the pellet

and incubated for 4-6 hours at 4 ℃. Each cell pellet was washed twice with 0.1 M cacodylate buffer, pH 7 prior to postfixation in 1% osmium tetroxide in the same buffer for 1 hour at 4 ℃. A couple of washes were carried out and, then, cells were dehydrated in an ascendant series of ethanol (50%, 70%, 90% and 100%). Pellets were transferred to propylene oxide and then gradually infiltrated in Embed 812 resin using a propylene oxide:resin sequence of 2:2, 1:1 and 1:2 along 48 hours. Samples were transferred to pure resin for 24 hours and, afterwards, allowed to polymerize for 48 hours at 65 ℃. Blocks were removed from the tubes and sculpted prior to the cut in an Ultracut Reicher ultramicrotome to get ultrathin sections (about 50nm width). Sections were recovered on nickel grids and stained with aqueous 2% uranyl acetate for 2 minutes and Reynold's lead citrate for 5 minutes. Sections were photographed in a Philips CM-10 transmission electron microscope. From this material, we obtain high and low magnification images (25,000 X and 5,800-7,900X, respectively) that were subjected to several quantitative analyses as described below.

11.2. Planimetric and stereological calculations

Using Image J software and high magnification images, we measured several ultrastructural mitochondrial parameters such as area, perimeter, maximum and minimum diameter and circularity in a population of 100 mitochondria. Moreover, additional parameters were calculated from the previous measurements. For instance, mitochondrial volume was calculated using maximum and minimum radius assuming the volume mathematical formula of the prolate spheroid, the geometric figure more similar to mitochondria.

Complementary, using the low magnification images we performed a stereological analysis of the samples in order to obtain 3-dimension information of mitochondria inside the cells. Mitochondrial volume density (Vv) as well as mitochondrial numerical density (Nv) were calculated following a point analysis according to the previously described method of Weiber [148]. Briefly, 15 images of whole cells were selected and included into a virtual grid, mitochondria were encircled and a point-counting method was performed, that is, we counted all the grid points that concurred with a mitochondria. Moreover, we also counted the total number of mitochondria present inside a single cell and measured all the planimetric parameters described above in relation to the whole cell.
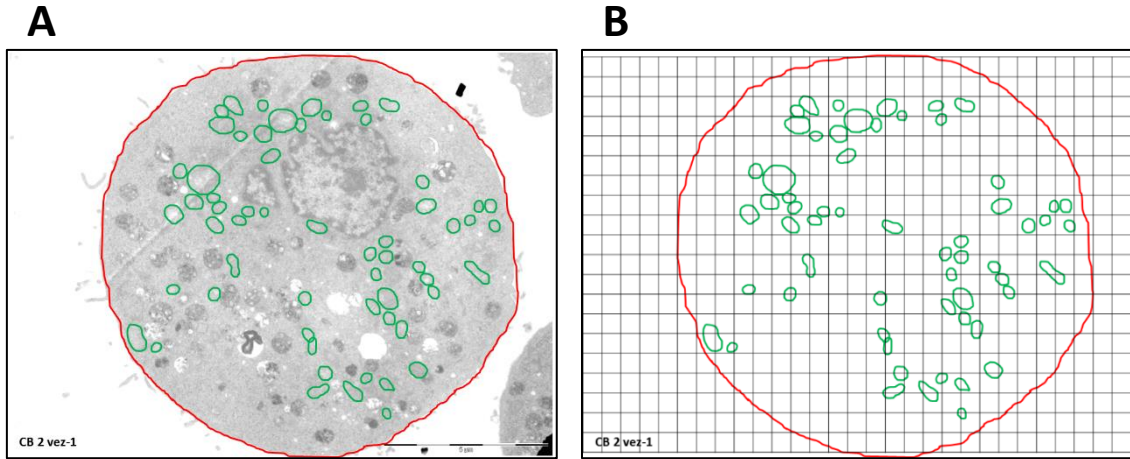
Figure M7. **Example of the stereological mitochondrial measurements.** In red, we observed the limit of the cell while, in green, we observed the limits of all the mitochondria present. **(A)** Electron micrograph were contours had been delimited. **(B)** Overlap of the contours and the virtual grid to perform the point analysis described by Weiber [148].

Therefore, referring the number of points that concur with mitochondria with the total number of points of the grid we calculated the mitochondrial density volume (Vv) and using the following formula

$$Nv = \frac{K}{\beta} \frac{Na^{3/2}}{Vv^{1/2}}$$

We also calculated the mitochondrial numerical density (Nv). "Na" in the numerical profile density (number of mitochondria/μm^2 of cell), and k and β the mitochondrial size distribution and shape coefficients. These coefficients were calculated using the previous planimetric measurements and assimilating the mitochondrial shape to a prolate spheroid as we previously described. Finally, the number of mitochondria per cell was calculated multiplying Vv and Nv by mean cell volume.

12. Statistical analyses

Statistical analyses were performed using GraphPad Prism 5.03 (GraphPad Software Inc., San Diego, CA, USA). All the data shown are mean ± standard error (SEM) from at least four replicates. Normality of data was checked by Kolmogorov-Smirnov test with the Dallal-Wilkinson-Lilliefor corrected p value. Means were compared using either the

parametric two-tail Student's t test or non-parametric Mann-Whitney t test depending on the results of the normality test. Significant differences were referred as * (p<0.05), ** (p<0.01) and *** (p<0.001).

Results

Chapter 1: _Regulation of Q metabolism by phenolic compounds_

1. 1. Q levels in cultured kidney cells treated with different phenolic compounds.
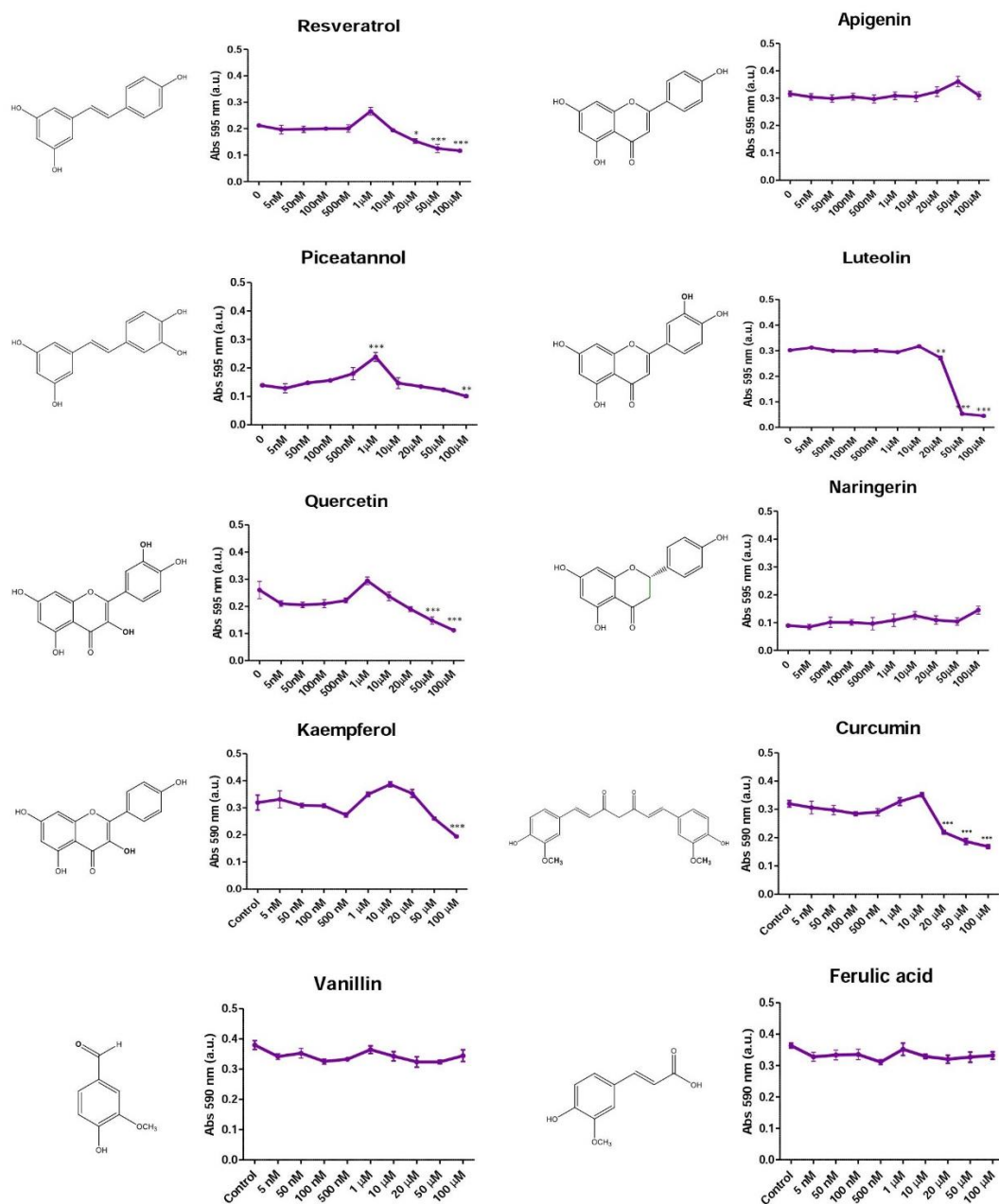
Figure R1. Molecular structures and assessment of toxicity for all phenolic compounds tested in Tkpts cells. A viability assay was performed for each phenolic compound with MTT. The resulting values of A_{590nm} were used to select a concentration range that did not affect cell viability, and was then used for subsequent experiments to determine Q content. Data are represented as mean ± SEM of 8 replicates. Statistically significant differences between control and treatments are represented by * (p<0.05), ** (p<0.01) and *** (p<0.001).

We determined the effect of several polyphenols on Q content and biosynthesis. Each compound used in this study was first added to Tkpts cells at concentrations ranging from 5 nM to 100 µM over a period of 48 h, and tested with the MTT assay to determine possible effects on cellular viability (Figure R1). Kidney cells responded differently to the compounds tested. Neither vanillin nor apigenin, naringenin or ferulic acid produced any toxicity in Tkpts cells in the concentration range used. However, resveratrol, piceatannol, quercetin, kaempferol, luteolin and curcumin decreased cellular viability when used at high concentrations. Based on these data, we chose to test phenolic compounds at concentrations ranging from 5 nM to 10 µM to detect possible effects on Q content. Within this range, none of the polyphenols under study decreased viability significantly, and only a small increase in viability was observed at 1µM piceatannol.

In the same way, during the development of the study we had used HEK 293 cells as a complementary model of human renal cells. The toxicity of the compounds was also assessed in this cellular line and results are shown in Figure R2. Kaempferol, curcumin, vanillin and ferulic acid impaired cell viability of HEK 293 at high concentrations. These observations allowed us to use concentrations of each compound that did not affect cellular viability in the experiments carried out with this cell line.
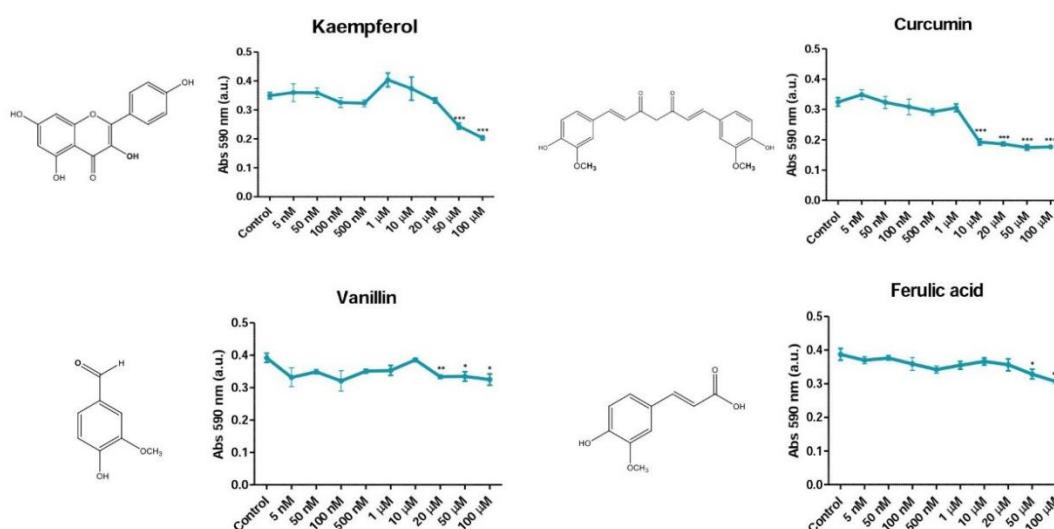
Figure R2. Molecular structures and assessment of toxicity for all phenolic compounds tested in HEK 293 cells. A viability assay was performed for each phenolic compound with MTT. The resulting values of A_{590nm} were taking into account to select a concentration in further experiments carried out with this cell line. Data are represented as mean ± SEM of 8 replicates. Statistically significant differences between control and treatments are represented by * ($p<0.05$), ** ($p<0.01$) and *** ($p<0.001$).
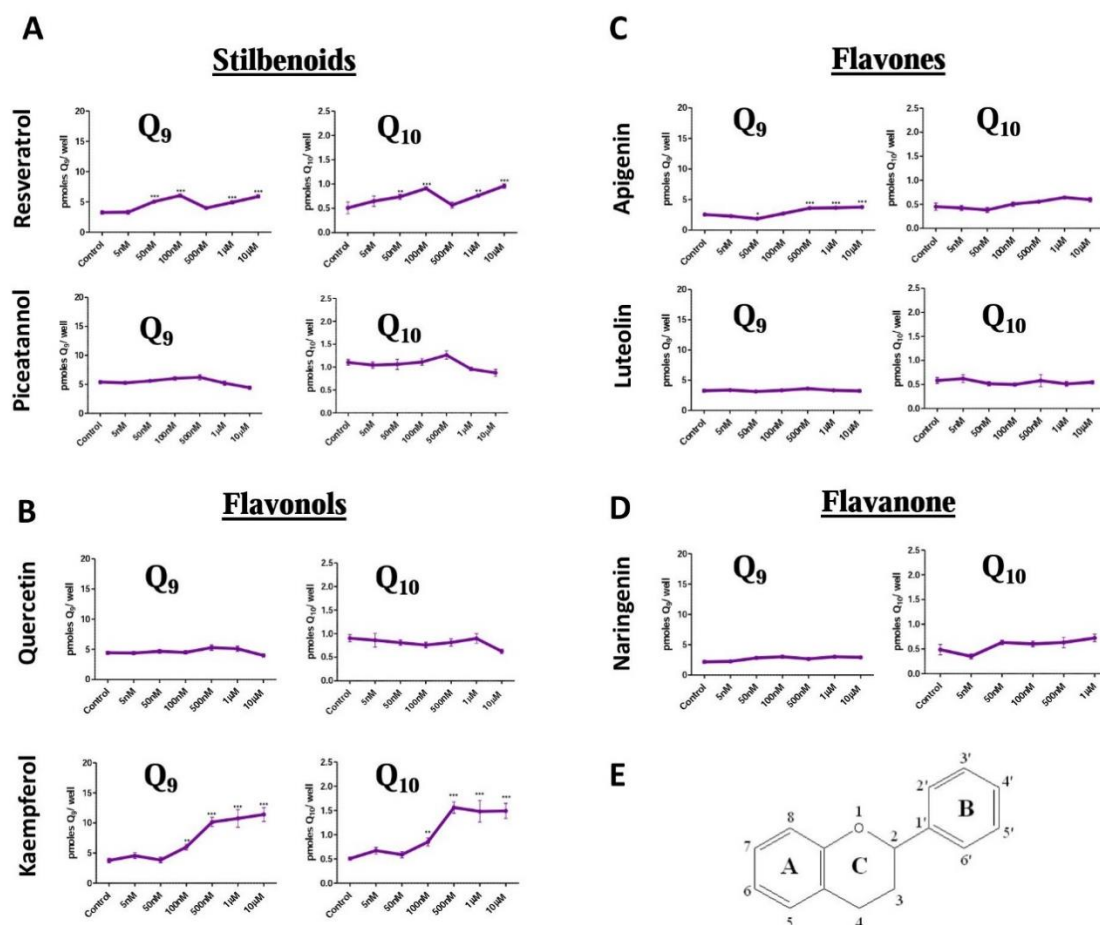
Figure R3. **Effect of different polyphenols on Q levels of Tkpts cells.** Q_9 and Q_{10} levels were determined in Tkpts cells treated with different polyphenols at the given concentrations for 48 h. After the incubation period, lipids were extracted and Q levels quantified. **(A) Stilbenoids**. Resveratrol, but not piceatannol, produced a modest increase of Q_9 and Q_{10} levels. (**B**) **Flavonols**. Quercetin did not affect Q levels, but kaempferol produced a dramatic increase of both Q_9 and Q_{10}. **(C-D) Flavones and a flavanone**. Apigenin, but not luteolin or naringerin, slightly increased Q_9 and Q_{10} levels. **(E) Basic chemical skeleton of flavonoids**. Data are represented as mean ± SEM of 6 replicates. Statistically significant differences between control and treatments are represented by ** ($p<0.01$) and *** ($p<0.001$).

Once we selected the range of concentrations of phenolic compounds, we next focused on the study of Q levels. For these assays, we first tested how two stilbenoids (resveratrol and piceatannol) and two flavonols (quercetin and kaempferol) affected Q levels in Tkpts cells. As shown in Figure R3-A, resveratrol produced a slight increase of Q_9 and Q_{10} levels at most concentrations above 50 nM, whereas the other stilbenoid tested, piceatannol, and the flavonol quercetin had no effect on Q levels (either Q_9 or Q_{10}) at any of the concentrations tested. In contrast, kaempferol produced a dramatic increase of both

Q_9 and Q_{10} at 100 nM and higher concentrations, producing a plateau at concentrations between 500 nM and 10 µM (Figure R3-B). We also confirmed a substantial increase of Q_9 and Q_{10} levels in Tkpts cells treated with kaempferol at concentrations above 100 nM when specific values were calculated on a protein basis (Figure R4).
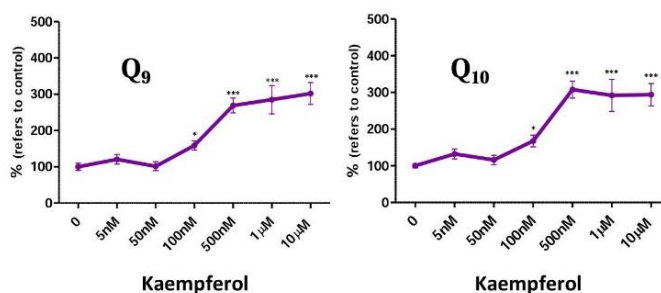
Figure R4. **Kaempferol also increases Q levels when calculated on a protein basis**. Values of Q levels were referred to protein (Bradford assay) to obtain specific values. The figure depicts the percentage of change in specific levels of Q compared to the untreated control. Data are represented as mean ± SEM of 6 replicates. Statistically significant differences between control and treatments are represented by $*p<0.05$ and $***p<0.001$.

Given the differential effects of kaempferol and quercetin (which differ only in one hydroxyl group), we hypothesized that the chemical structure of the flavonoids could influence their effect on Q content (see chemical structures of the compounds used in Figure R1 and the basic chemical skeleton of flavonoids in Figure R3-E). Thus, we tested how additional polyphenols of the flavonoid group affected Q levels in Tkpts cells. For these experiments, we chose two flavones: apigenin, luteolin (Figure R3-C), and one flavanone: naringerin (Figure R3-D). Among these three flavonoids, only apigenin produced a slight increase in Q at concentrations between 500 nM and 10 µM, although a concentration of 50 nM was found inhibitory and statistically significant differences were observed for Q_9 but not for the Q_{10} isoform (Figure R3-C).

The following experiments, aimed on elucidating how flavonoids can increase Q levels, were focused on kaempferol, as this polyphenol was by far the most efficient in augmenting the amounts of cellular Q.

1. 2. Possible implication of the mitochondrial sirtuin Sirt3 on the increased Q levels produced by kaempferol.

Kaempferol has been reported to up-regulate Sirt3 [133, 149], a mitochondrial sirtuin that plays an important role in regulating cellular processes like homeostasis, oxidative stress and aging [150]. Up-regulation of mitochondrial Sirt3 optimizes redox processes linked to the electron transport chain and boosts antioxidant defense in this organelle by activating ROS-scavenging systems [151].
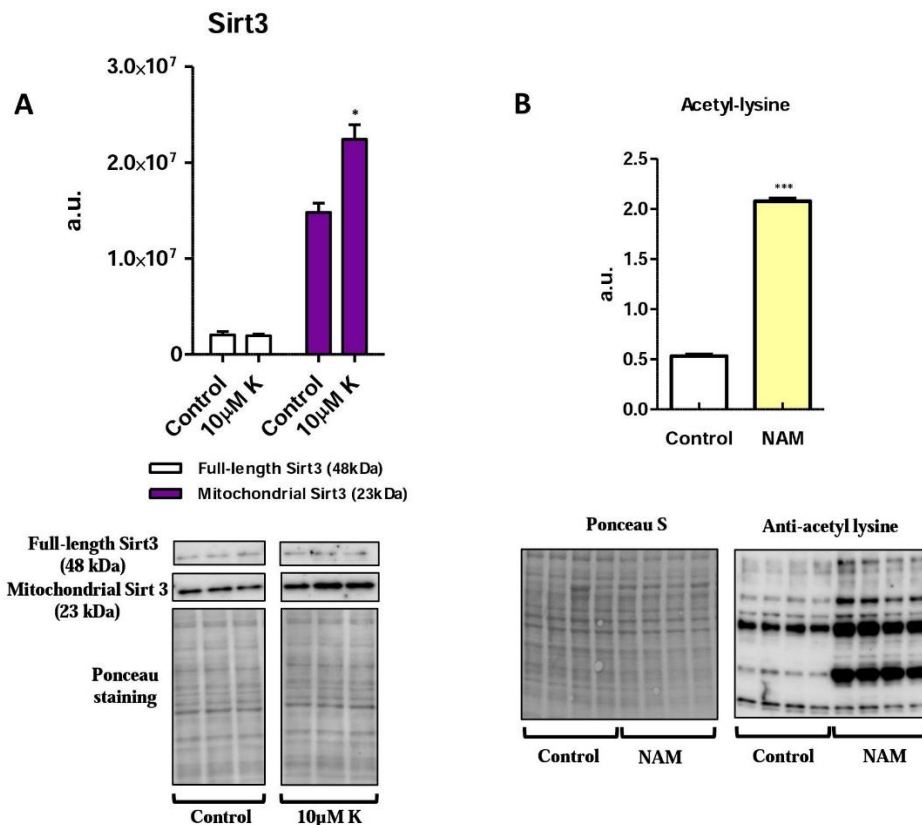
Figure R5. **Effect of sirtuin activators and inhibitors in Tkpts cells.** **(A) Kaempferol increases mitochondrial Sirt3**. A western-blot against Sirt3 shows that the mitochondrial form of Sirt3 is upregulated by kaempferol at 10 μM. **(B) Nicotinamide inhibits deacetylase activity in Tkpts cells**. Anti-acetyl lysine antibody was used to confirm the inhibitory effect of nicotinamide (NAM). As expected, acetylation levels were significantly increased in presence of nicotinamide. In (A) and (B), arbitrary units depicted in the graph relate directly to the immunoblots shown underneath, and the immunoblots derive from the same film. Ponceau S staining was used to correct for minor differences in protein loading between samples. Data are represented as mean ± SEM of 4 replicates. Statistically significant differences between control and treatments are represented by *p<0.05 and ***p<0.001.

Thus, it seemed possible that Sirt3-mediated changes might affect Q levels by providing an antioxidant environment that would diminish oxidative Q degradation. To investigate this, Tkpts cells were treated with kaempferol and the up-regulation of mitochondrial Sirt3 was then assessed. As depicted in Figure R5-A, treatment of Tkpts cells with kaempferol increased significantly the levels of the mitochondrially-targeted (cleaved) form of Sirt3 at concentrations that also increased Q_9 and Q_{10} levels. We next proceeded to verify whether this up-regulation of Sirt3 mediated the increase in Q levels or, on the contrary, it was an independent event.
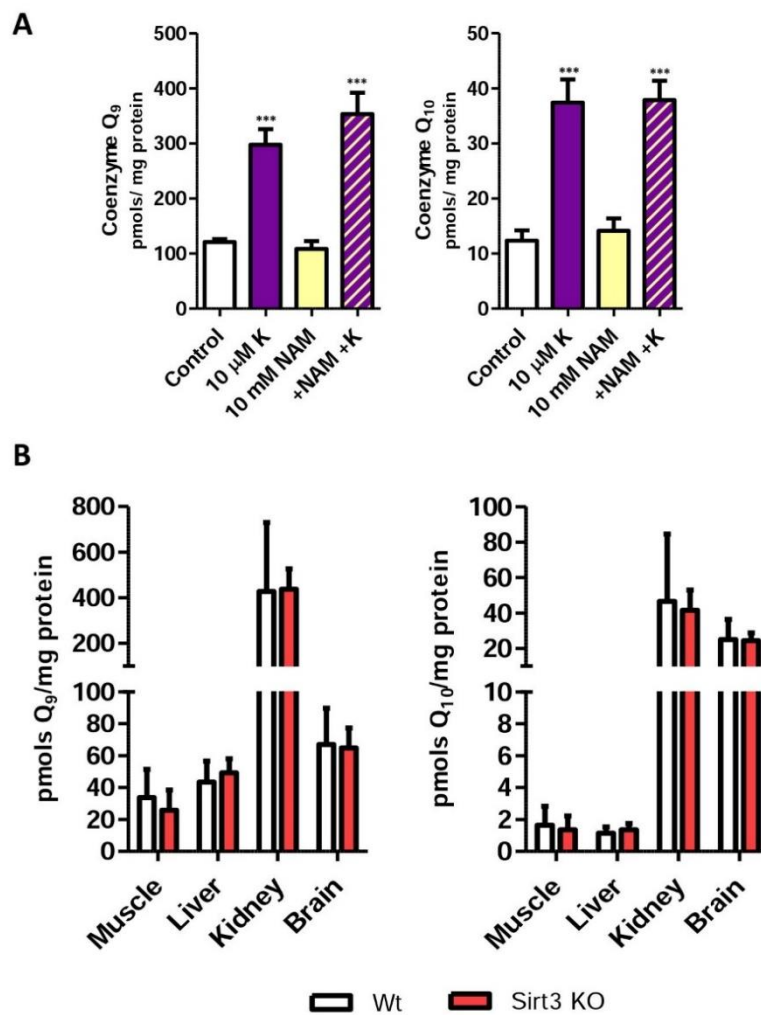
Figure R6. **Study of the Sirt3 role on the regulation of Q levels**. **(A) Tkpts cells.** General inhibition of sirtuin desacetylases by nicotinamide (NAM) at 10 mM did not prevent the increase of Q levels in Tkpts cells treated kaempferol (K) at 10 µM. **(B) Sirt3 KO mice.** Q levels are not altered in tissues (skeletal muscle, liver, kidney and brain) obtained from Sirt3 knockout mice in comparison with age-matched controls. Data are represented as mean ± SEM of at least 5 replicates. Asterisks denote statistically significant differences (***$p<0.001$).

110

To this purpose, we tested whether simultaneous treatment with nicotinamide (NAM), a well-known inhibitor of sirtuin deacetylase activity [133], had any impact on Q levels in Tkpts cells treated with kaempferol. As shown in Figure R6-A, treatment with 10 mM NAM did not alter basal levels of Q in Tkpts cells, and the kaempferol-mediated increase of Q_9 and Q_{10} was completely unaffected by NAM. A western-blot using an anti-acetyl lysine antibody confirmed that, under our experimental conditions, deacetylase activity was significantly inhibited by 10 mM NAM since this treatment produced a substantial increase of protein acetylation (Figure R5-B).

Furthermore, we also determined Q levels in several tissues obtained from Sirt3 knockout mice. In each tissue examined, including muscle, liver, kidney, and brain, Q levels from Sirt3 knockout mice were not significantly different from their background-matched controls (Figure R6-B). Thus, although similar concentrations of kaempferol can indeed up-regulate Sirt3-dependent mitochondrial functions and increase amounts of Q, the increase in Q content does not appear to be related to the upregulation of Sirt3 activity.

1. 3. Effect of kaempferol on Q biosynthesis in mouse and human kidney cells.

We considered the possibility that the increase of Q levels caused by kaempferol could be a consequence of a higher Q biosynthetic rate. To test this possibility, we followed two different approaches. First, we studied how PABA, a well-characterized inhibitor of Coq2 activity in animal cells [10, 132], affected Q levels in control and in Tkpts cells that had been treated simultaneously with 10 µM kaempferol. As expected, PABA decreased Q levels in the control cells. Moreover, PABA abolished the increase of Q in response to kaempferol treatment, indicating a direct link between kaempferol and Q biosynthesis (Figure R7-A).

Secondly, we measured Q biosynthesis with an assay based on the incorporation of exogenous ^{14}C-labeled 4HB as Q ring precursor. Our results showed that kaempferol produced a substantial decrease in the incorporation of ^{14}C-4HB (Figure R7-B). The simultaneous increase of Q levels and decrease of ^{14}C-4HB incorporation into Q by kaempferol implies that this compound competes with the substrate 4HB to behave as a ring precursor for Q biosynthesis.
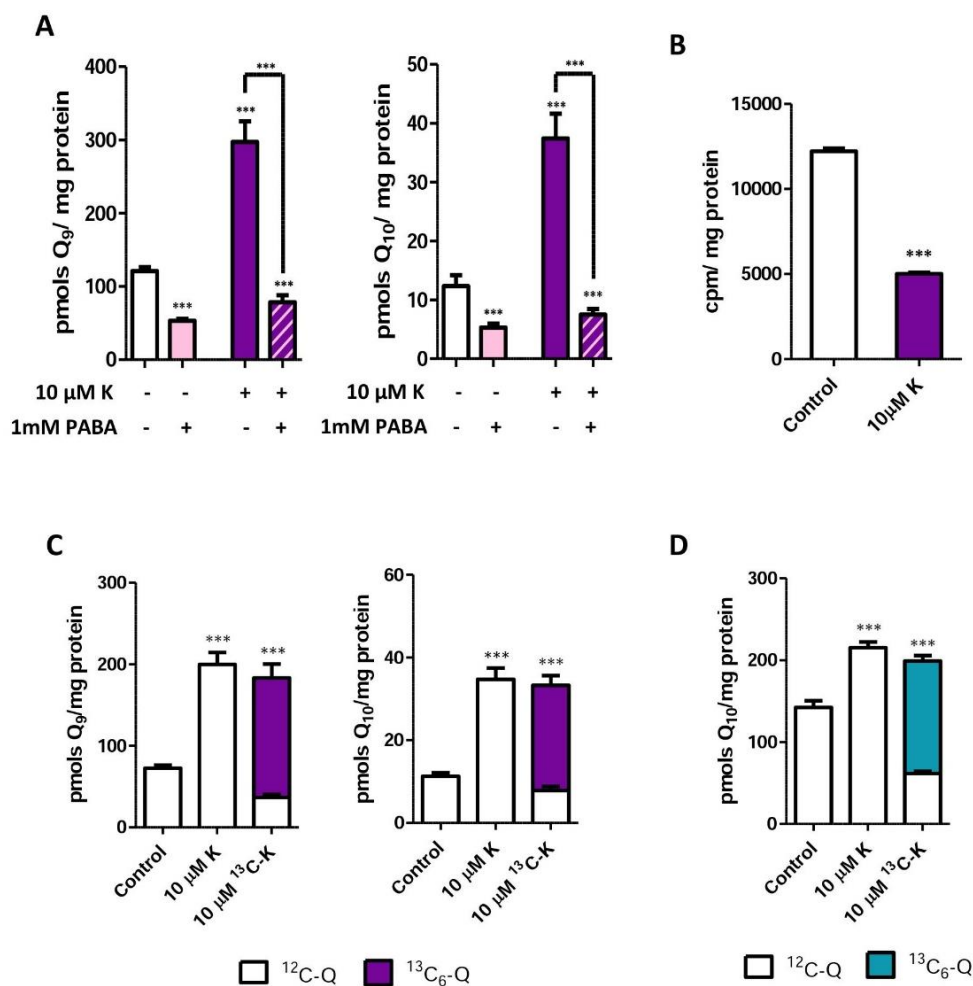
Figure R7. __Role of kaempferol on Q biosynthesis__. **(A) An indirect implication of Q biosynthesis using PABA.** Cells were cultured for 48 h in the presence of 10 μM kaempferol and /or 1mM PABA. Inhibition of the Coq2 polyprenyltransferase with PABA decreased Q levels in control Tkpts cells and abolished the increase of Q_9 and Q_{10} in cells treated with kaempferol (K). **(B) Competition assay of ^{14}C-4HB incorporation into Q**. Treatment of cells with 10 μM kaempferol (K) inhibited the incorporation of ^{14}C-4HB into Q, which indicates competition of kaempferol and 4HB as Q ring precursors. **(C) Demonstration of the role played by kaempferol in Tkpts cells.** Cells were cultured for 48 h in the presence of unlabeled (K) or ^{13}C-labeled kaempferol (^{13}C-K) at 10 μM. Unlabeled (^{12}C, *open bars*) and ^{13}C$_6$-labeled (*closed bars*) Q were then measured with HPLC-MS/MS. The majority of Q measured in cells treated with ^{13}C-kaempferol was ^{13}C$_6$-Q, demonstrating the role of kaempferol as a novel Q ring precursor. **(D) Demonstration of the role played by kaempferol in HEK 293 cells.** Kaempferol is confirmed as a Q ring precursor which also increased Q levels in human kidney cells. Data are represented as mean ± SEM of 6 replicates. Asterisks denote statistically significant differences (***p<0.001).

To confirm this possibility, we cultured Tkpts cells in the presence of ^{13}C-labeled kaempferol and then measured the levels of ^{12}C-Q and ^{13}C$_6$-Q with HPLC-MS-MS. This technique allows the simultaneous measurement of the amount of cellular Q derived from endogenous 4HB (^{12}C-Q) and the amount of newly synthesized Q derived from ^{13}C-kaempferol (^{13}C$_6$-Q). Total levels of Q obtained in the presence of ^{13}C-kaempferol were also compared with those obtained when cells were grown in the presence of the non-labelled polyphenol. We found that Q$_9$ and Q$_{10}$ levels increased equally with both non-labeled and ^{13}C-kaempferol. Of note, when the ^{13}C-labeled precursor was used, nearly all the Q present in Tkpts cells was ^{13}C$_6$-Q, identifying kaempferol as an efficient novel Q ring precursor (Figure R7-C). Similar experiments were carried out to test the effects of kaempferol in human HEK 293 cells, another kidney cell line and, as observed for Tkpts cells, Q levels were also increased by 10 µM kaempferol treatment. Furthermore, when ^{13}C-kaempferol was used, almost all the Q present in HEK 293 cells was ^{13}C$_6$-Q (Figure R7-D). In sum, our results demonstrate a role for kaempferol as a Q ring precursor both in murine and human kidney cell lines.

We do not have any evidence of how kaempferol is included into Q metabolism to serve as Q ring precursor in our cellular model. However, literature described that mammals colonic microflora metabolize kaempferol to 4-hydroxyphenylacetic acid (4HPAA) and 4-methyphenol (or *p*-cresol) [152, 153]. We wonder if a fragmentation that also yielded these compounds might occur in kidney cells and thus, we decided to investigate whether or not these two compounds could also serve as Q ring precursors.

A MTT assay ruled out any toxicity of these compounds in concentrations ranging from 5 nM to 100 µM (Figure R8-A) and no decline in Tkpts viability was observed at any of the concentrations tested. On the contrary, we even observed an increased MTT signal with 4HPPA at concentrations to 10-100µM and at 20 µM *p*-cresol. Thus, we decided to use both 4HPAA and *p*-cresol at a similar concentration as that used in our previous experiments with kaempferol (10 µM). Our results showed that neither 4HPAA nor *p*-cresol increased Q levels, and they were also unable to compete with ^{14}C-4HB in a Q biosynthesis competition assay (Figure R8-B/C). Together, these results argue against 4HPAA and *p*-cresol as metabolites mediating the effect of kaempferol on Q biosynthesis in kidney cells.
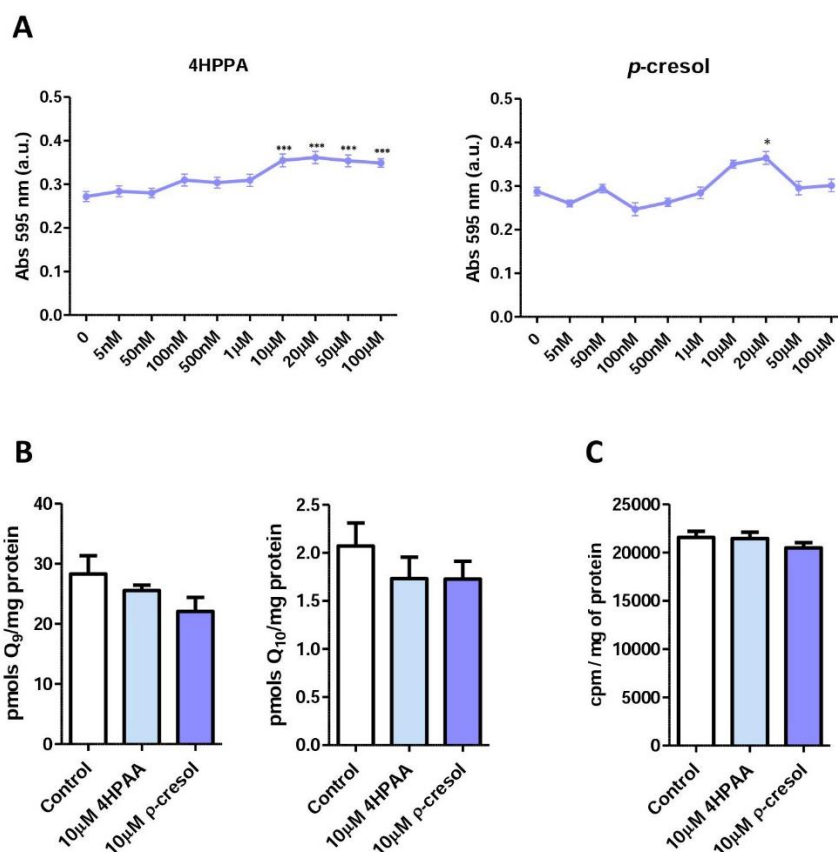
Figure R8. **Effect of 4HPAA and *p*-cresol in viability and Q metabolism of Tkpts cells.** **(A)** **MTT assays.** Viability assays were performed for each product with no toxicity being observed at any of the tested concentrations. Contrary, we observed an increase of MTT absorbance at some concentrations between 10 µM and 100 µM. **(B)** **Q levels.** Neither 4HPAA nor *p*-cresol increased Q levels in Tkpts cells. **(C)** **Radiolabeled Q biosynthesis assay**. A combined treatment with ^{14}C-4HB and 4HPAA or *p*-cresol shows that none of these products compete with ^{14}C-4HB as Q precursor. Data are represented as mean ± SEM of 6 replicates. Asterisks denote statistically significant differences (*p<0.05 and ***p<0.001).

1. 4. Role of other phenolic compounds as Q ring precursors

To further study the ability of other dietary phenolic substances to act as precursors in Q biosynthesis we tested curcumin and ferulic acid, which have a quite different structure in comparison with the stilbenoids and flavonoids we already tested. We also analyzed vanillin, a simpler molecule that shares the same ring structure as curcumin, and ferulic acid (see Figure R1). Vanillic acid, which also bears hydroxyl and methoxy groups in the same position of the ring, has been previously described as Q ring precursor in mammals [52]. As shown in Figure R9-A, total Q_9 levels were decreased when Tkpts cells were treated with both unlabeled or $^{13}C_{12}$-labeled curcumin, with no $^{13}C_6$-Q being detected in
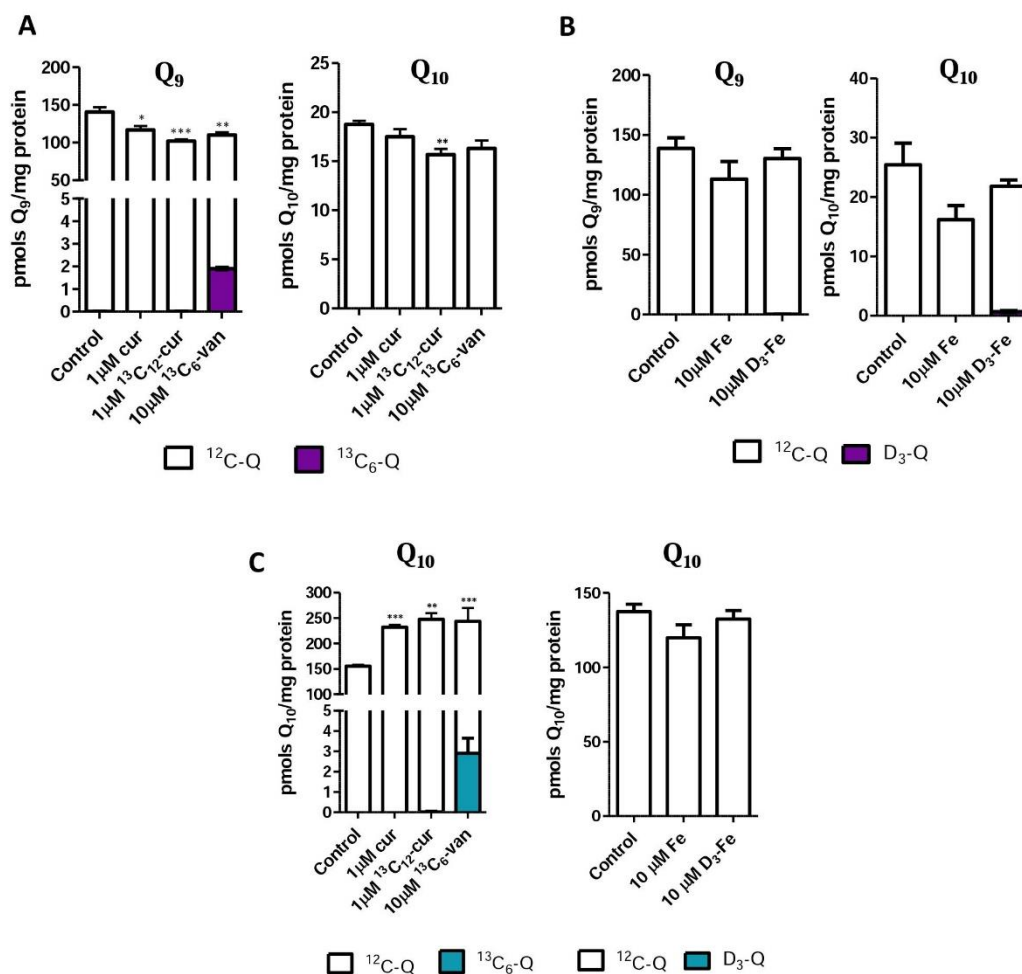
Figure R9. **Effect of curcumin, ferulic acid and vanillin on Q biosynthesis in Tkpts and HEK 293 cells**. **(A) Effect of curcumin and vanillin in Tkpts cells.** Q levels were slightly decreased in Tkpts cells treated with curcumin and vanillin. A small amount of $^{13}C_6$-Q was detected when Tkpts cells were treated with $^{13}C_6$-vanillin, but not with $^{13}C_{12}$-curcumin, indicating that curcumin does not act as Q ring precursor. **(B) Effect of ferulic acid in Tkpts cells.** Ferulic acid did not alter Q levels and a minimal deuterated signal was recovered after the treatment with D_3-ferulic acid, indicating that ferulic acid does not serve as Q ring precursor. **(C) Effect of curcumin, vanillin and ferulic acid in HEK 293 cells.** $^{13}C_6$-Q_{10} is not detected when HEK 293 cells were treated with $^{13}C_{12}$-labeled curcumin, demonstrating that curcumin does not act as Q ring precursor. Ferulic acid does not serve as Q ring precursor because no deuterated signal is recovered after treat HEK 293 cells with D_3-ferulic acid. Data are represented as mean ± SEM of 6 replicates. Statistically significant differences in total Q_9 or Q_{10} between control and treatments are represented by * ($p<0.05$), ** ($p<0.01$) and *** ($p<0.001$).

the latter case. The same trend was observed for Q_{10} levels, although a statistically significant decrease was observed only in the case of $^{13}C_{12}$-labeled curcumin. Vanillin also produced a decrease of Q_9 levels, and the same trend was observed for Q_{10} although

without statistical significance. Strikingly, even when total Q levels were decreased, we were able to detect a signal for $^{13}C_6$-Q_9, although not for $^{13}C_6$-Q_{10}, in lipid extracts obtained from Tkpts cells cultured in the presence of $^{13}C_6$-vanillin (Figure R9-A). However, the proportion of $^{13}C_6$-Q_9 present in cells treated with $^{13}C_6$-vanillin was only about 2%, which is much lower than that produced by ^{13}C-kaempferol (see Figure R7-C). Ferulic acid did not produce any significant change of total Q levels, and deuterated forms of Q_9 or Q_{10} only accounted for a minor portion of total Q after treatment of Tkpts cells with D_3-ferulic acid (Figure R9-B).

Treatments were also carried out in human HEK 293 cells and, in this case, we found that both curcumin and vanillin increased Q_{10} levels. We were unable to detect any $^{13}C_6$-Q_{10} in cells cultured for 48 h in the presence of $^{13}C_{12}$-labeled curcumin (Figure R9-C), which indicated that the increase of Q levels is not related to augmented Q biosynthesis. Total amounts of Q were also increased in HEK 293 cells cultured in the presence of $^{13}C_6$-labeled vanillin, but $^{13}C_6$-Q_{10} was only about 1% of total Q (Figure R9-C), making it unlikely that augmented Q biosynthesis plays a prominent role for the increase of Q levels observed in this cell type. Treatment with ferulic acid did not alter Q levels and the deuterated form of Q_{10} (D_3-Q_{10}) was not detected (Figure R9-C).

In summary, we demonstrate that neither curcumin nor ferulic acid serve as ring precursor for the Q biosynthetic pathway in mouse or human kidney cells, whereas vanillin plays only a minor role in comparison with kaempferol or with the endogenous substrate 4HB.

1. 5. Is 4HB a limiting step for Q biosynthesis in mammal cells?

The efficient utilization of kaempferol by kidney cells as a Q ring precursor could be linked to a limited availability of endogenous ring precursors in these cells. In accordance, Pierrel *et al.* [54] described that availability of the ring precursor (4HB or PABA) was a rate-limiting step for the biosynthesis of Q_6 in yeasts cultured in PABA-free medium. To test whether the effect of kaempferol-mediated increase in Q levels in mammalian cells resulted from limiting amounts of endogenous ring precursors, we measured Q levels in cells that had been treated with exogenous 4HB. For these determinations, we compared the response of the two kidney-derived cell types (mouse Tkpts and human HEK 293) with that of non-kidney cell lines, including mouse liver hepatoma Hepa 1.6, MEFs, human liver hepatoma Hep G2, and human promyelocytic leukemia HL-60 cells.

Previous results of our research group had revealed that 4HB is not toxic even at high concentrations (1-2 mM) so performing a MTT viability assay was not necessary to determine the range of concentrations to use in the experiments.
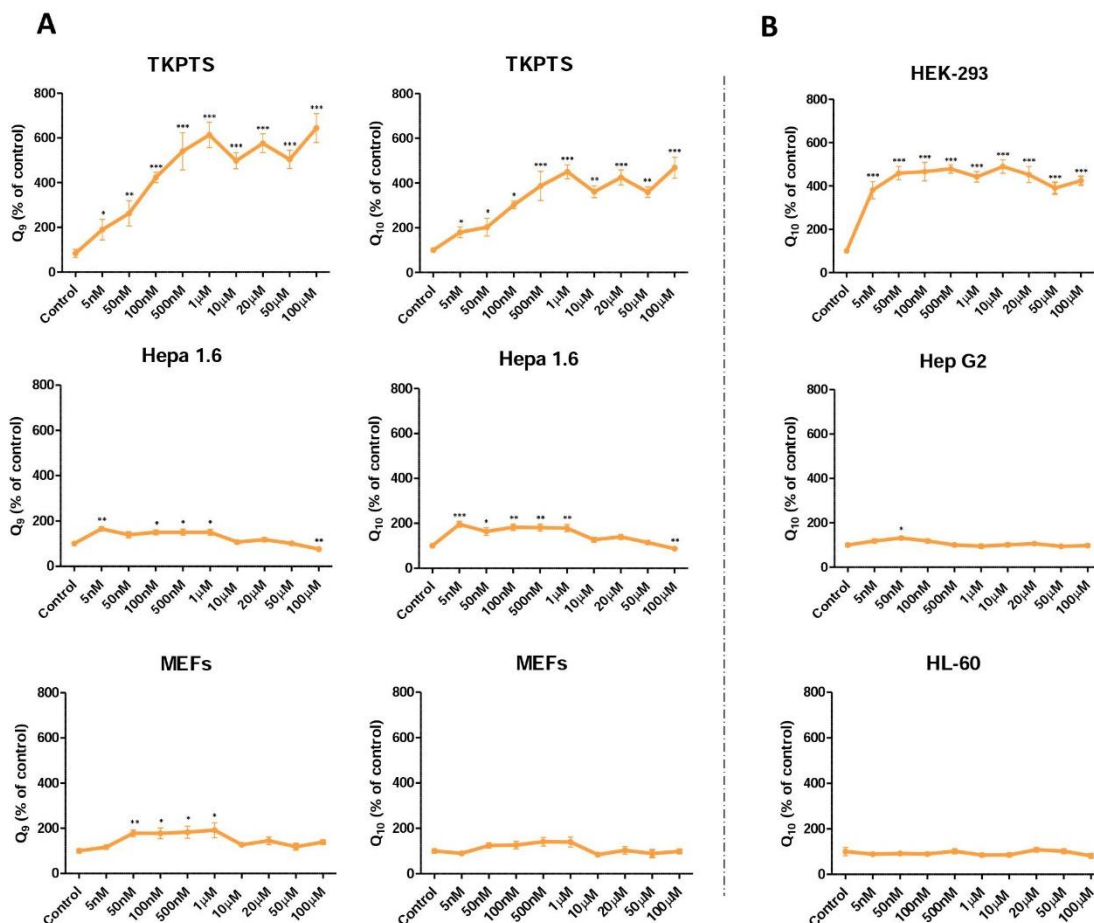
Figure R10. **4HB as a limiting step in the biosynthesis of Q in kidney cells.** Cells of different origin were treated with increasing concentrations of 4HB. **(A) Murine cells**. Tpkts cells exhibited a dramatic increase in Q_9 and Q_{10} levels. However, only a slight increase at some concentrations of 4HB was observed for Hepa 1.6 and MEFs. **(B) Human cells**. Human kidney-derived cells (HEK 293) displayed a significant increase of Q_{10} levels, but this effect was not found in human lines from another origin, such as Hep G2 or HL-60. Data are represented as mean ± SEM of 6 replicates. Statistically significant differences in total Q_9 or Q_{10} between control and treatments are represented by * ($p<0.05$), ** ($p<0.01$) and *** ($p<0.001$).

As depicted in Figure R10, Q levels were dramatically increased in the two kidney-derived cell lines when cultured in the presence of 4HB, and attained levels four- to six-fold higher as compared to the corresponding no-addition controls. HEK 293 cells were particularly sensitive to supplementation of culture medium with 4HB, with a close to

maximal response being already achieved at concentrations as low as 5 nM 4HB. In the mouse Hepa 1.6 cell line, Q levels were increased two-fold by 4HB concentrations between 5 nM and 1 µM but, strikingly, this response was lost at concentration of 10 µM and higher. In the case of MEFs, a slight increase was obtained for the Q_9 isoform at concentrations of 4HB between 50 nM and 1 µM, but no significant changes were observed for Q_{10}. Excepting a slight increase of Q_{10} levels at 50 nM 4HB in Hep G2 cells, no further alteration of Q levels by exogenous 4HB supplementation was observed in this cell line or in HL-60 cells at any concentration.

Taken together, these results support that availability of endogenous 4HB is a limiting step for Q biosynthesis in kidney cells, which favors the incorporation of exogenously applied ring precursors, such as polyphenols (particularly kaempferol) or exogenous 4HB. This could be due to a very active flow of metabolites towards Q biosynthesis, which maintains very low levels of upstream substrates such as endogenous 4HB specifically in kidney cells. This interpretation was further supported by the comparison of Q levels in Tkpts and Hepa 1.6 cells, the former containing much higher amounts of Q, particularly Q_{10} (Figure R11-A), and of the polyprenyltransferase Coq2, the enzyme that catalyzes the condensation reaction between ring and hydrophobic tail precursors, which was found also significantly enriched in Tkpts in comparison with Hepa 1.6 cells (Figure R11-B). This situation resembles that of kidney and liver tissues in the mouse [154].

As Q is synthetized in mitochondria, we wants to ascertain if the results we observed comparing Hepa 1.6 and Tkpts cells could be influenced by a different amount of mitochondria in the cells. To this purpose, we used specific antibodies as markers of outer and inner mitochondrial membrane. The voltage-dependent anion channel (VDAC) is a pore located at the outer membrane of the mitochondrion allowing the entry and exit of numerous ions and metabolites between the cytosol and the mitochondrion [155]. Using this protein as marker of the outer mitochondrial membrane, we have observed that VDAC levels were drastically decreased in Tkpts cells comparing to Hepa 1.6 (Figure R11-C). Moreover, as marker of the inner mitochondrial membrane we have used an antibody mixture that binds specifically to some subunits of all the complexes of the electron transport chain. In this case, we observed a significant increase in complex I, III
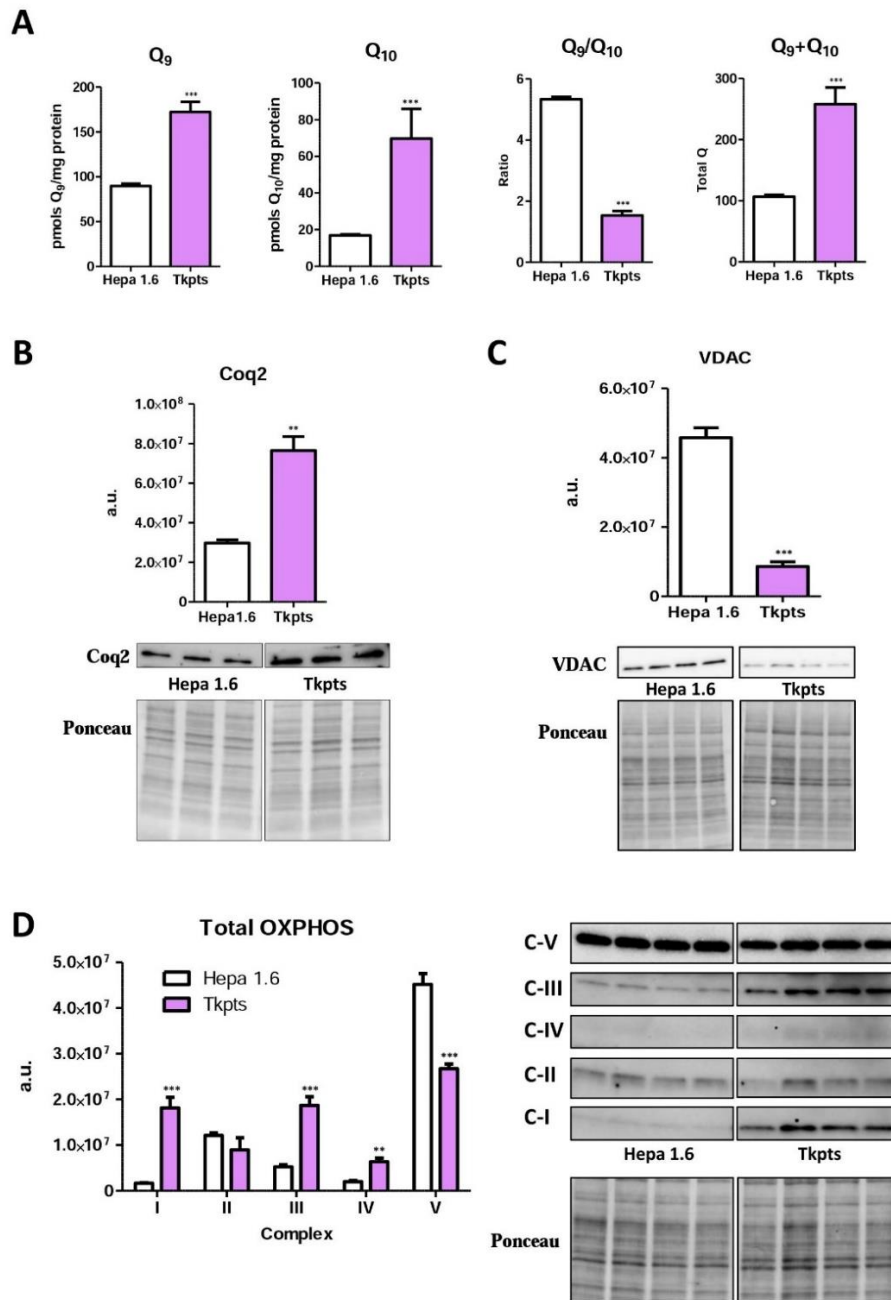
Figure R11. **Comparison of different mitochondrial parameters between kidney-derived Tkpts cells and hepatic Hepa1.6 cells**. **(A) Q levels.** Q levels were higher and Q_9/Q_{10} ratio lower in Tkpts than in Hepa 1.6 cells. **(B) Coq2 prenyltransferase levels**. Tkpts cells displayed higher levels of Coq2 polypeptide. **(C) VDAC levels.** This outer mitochondrial membrane marker was significantly decreased in Tkpts cells. **(D) OXPHOS complexes levels.** Complex I, III and IV were increased while complex V was decreased in Tkpts cells. Arbitrary units depicted in the graph relate directly to the immunoblots shown next to each graph, and the immunoblots derive from the same film. Ponceau S staining was used to correct for minor differences in protein loading between samples. Data are represented as mean ± SEM of at least 3 replicates. Statistically significant differences between both cell types are represented by ** ($p<0.01$) and *** ($p<0.001$).

and IV in Tkpts cells (Figure R11-D). No changes were observed in complex II and a decrease was observed in complex V in this cell line.

Chapter 2: *Role of different fatty acids in Q metabolism*

2.1. Effect of different lipid sources in an in vitro model

Lipid emulsions, traditionally used for parenteral nutrition, were used to study the effect of different lipid sources on Q system. *Lipofundin*, *Lipoplus* as well as *ClinOleic,* a source of n-6 PUFA, n-3 PUFA and n-9 MUFA respectively, were used in Hepa 1.6 cells, a mouse hepatocellular model. First, a viability curve was performed in order to select the most suitable concentration to carry out the following experiments. Figure R12-A represent a MTT assay for each lipid emulsion where it can be observed that Hepa 1.6 cells were apparently affected by these lipids. Despite a decrease in MTT signal was observed from the lowest concentration used of all lipid emulsions (1µl/ml), cells in culture looked perfectly healthy, indicating that the decrease in absorbance obtained after performing a MTT assay refers to a lower growth rate instead of cellular toxicity.

However, it was noted that both low cellular density and the oxidation state of lipid emulsion increased differences in growth rate when we compared control cells with cells treated with lipid emulsions. In Figure R12-B we show a comparison between control cells (no treatment with emulsions) with cells treated with *Lipoplus* (either fresh or aged for more than 3 months) and seeded at different cellular densities. As depicted in this Figure, an oxidized emulsion impaired dramatically the growth rate of the cells, but this effect was significantly attenuated as the cell density increased. When we used a fresh emulsion the growth rate was also affected but to a lesser extent. Again, the decrease of the growth rate could be prevented by increasing the cellular density. Thus, our results show that a higher cellular density has a protective effect against the inhibition of the cell growth caused by emulsions. Although we cannot avoid completely this fact, we can minimize it by using high cellular densities in our experiments. Considering our observations, we decided to use 7 µl/ml of each emulsion and a cellular density of 20,000 cells/cm^2 for all the following experiments.

Complementary, based on our previous investigations focused on polyphenols (see previous chapter) we decided it would be interesting to study the effects of lipid emulsions in renal cells lines as human HEK 293 and mouse Tkpts. However, when these cells were treated with the emulsions it was found that the lipids were extremely toxic, making impossible to perform any comparative study. As an example, we have represented the

MTT toxicity curves for HEK 293 cells in Figure R12-C, showing significant decrease in the absorbance for the three lipid emulsions.
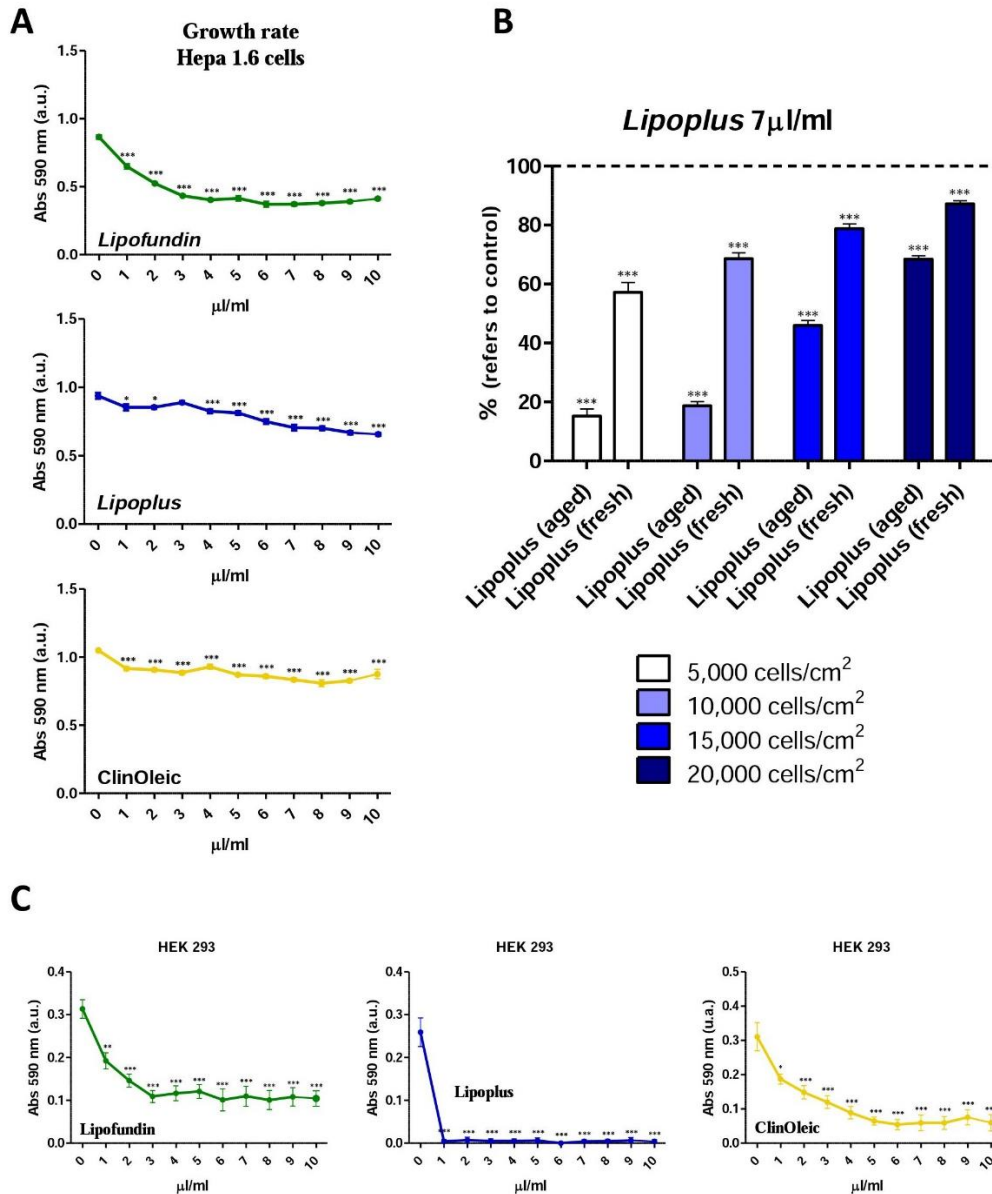
Figure R12. <u>Effect of different lipid emulsions on the growth/viability of Hepa1.6 cells</u>. (A) MTT assay performed in Hepa1.6 cells after treatments with different amounts of *Lipofundin*, *Lipoplus* and *ClinOleic*. Absorbance at 590 nm decreased from the lowest concentration (1µl/ml). **(B) MTT assay performed in Hepa1.6 seeded at different cellular densities after the treatment with aged or fresh *Lipoplus* emulsion.** The oxidized emulsion potentiates the decrease in the growth rate. However, culturing at higher densities protects cells from the effect of the lipids, both for aged and fresh emulsions. **(C) MTT assay in HEK 293 cells after treatments with the three emulsions.** Lipid emulsion are extremely toxic in renal cell lines. Data are represented as mean ± SEM of 8 replicates. Differences are represented as * (p < 0.05) and *** (p < 0.001).

2.2. Effect of different lipid sources on Q levels of Hepa1.6 cells

Q levels were measured to evaluate whether *Lipofundin*, *Lipoplus* or *ClinOleic* have some effect on the levels of this antioxidant. These three emulsions were included in our experiments either under high-glucose or under low-glucose condition. While high-glucose (4.5 g/L glucose) is the standard culture condition for this hepatic cell line, the low-glucose availability (1 g/L) represents a restricted intake for these cells. We decided to use both conditions to test if a lower energetic intake modifies the effect of a different fat source in our *in vitro* model.

Figure R13 shows Q levels after the 48 hours treatment with 7 µl/ml of each lipid emulsion. Focusing on Q_9 levels in cells grown under high-glucose conditions (Figure R13-A) we can observe that *Lipofundin*, *Lipoplus* and, to a lesser extent, *ClinOleic* increase Q_9 in comparison with the untreated controls. Moreover, the increase observed with *Lipoplus* was significantly higher than that produced by *ClinOleic*. When cells were cultured in low-glucose medium, none of the emulsions cause an increment on Q_9 levels, most likely, because the control in this restricted glucose condition already displayed increased levels of the antioxidant. Although, we should note that, even under low-glucose condition, *Lipoplus* treatment led to higher Q_9 levels comparing with *ClinOleic*, as we previously observed when cells were treated with lipid emulsion in high-glucose medium.

Figure R13-B shows Q_{10} levels in cells treated with the lipid emulsions. In this case, despite the control in low glucose also increased Q_{10} levels comparing with the corresponding control cultured in high-glucose medium, the effect of the lipid emulsions was similar independently of the availability of glucose for the cells. Both PUFA sources, *Lipofundin* and *Lipoplus*, increased drastically Q_{10} levels when comparing with the control with no emulsion, indicating that both, n-6 and n-3 fatty acids have a similar effect on regulating Q_{10} levels. *ClinOleic*, which is composed mainly by n-9 MUFA, but it also contains n-6 PUFA, also caused a slight increase of Q_{10} levels compared to control but, in this case, the effect was only observed, since the increase of Q_{10} levels attained by culturing cells under glucose limiting conditions abated any further increase by *ClinOleic*. Moreover, the massive increase of Q_{10} observed when cells were cultured in the presence of PUFA was significantly higher than the slight increase observed with *ClinOleic* in a high-glucose condition.
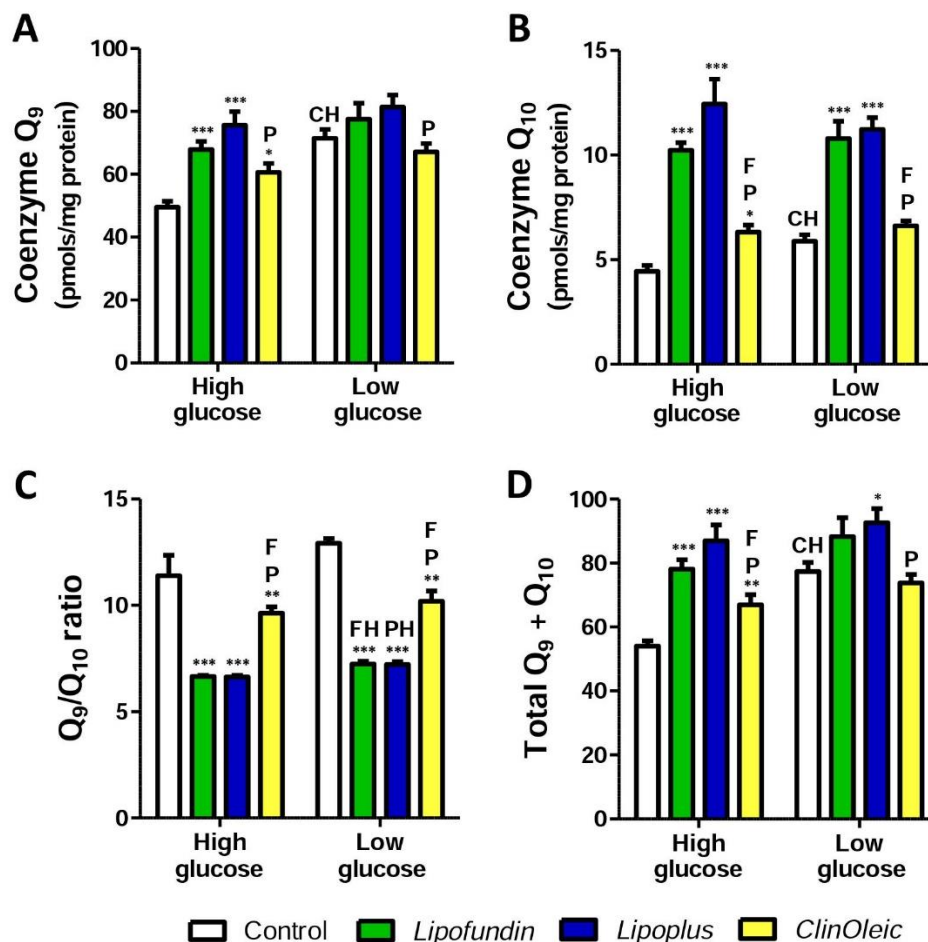
Figure R13. **Effect of different lipid sources on Q levels of Hepa1.6 cells**. **(A) Q_9 levels.** *Lipofundin, Lipoplus* and, to a lesser extent, *ClinOleic* increased Q_9 levels in high-glucose medium. Culturing cells in low glucose already increased Q_9 level in such a way that the effect of lipid emulsions on Q_9 levels was abated. **(B) Q_{10} levels.** Independently of the glucose availability, *Lipoplus*, *Lipofundin* and, to a lesser extent, *ClinOleic* increased Q_{10} levels in comparison with the control without emulsion. **(C) Q_9/Q_{10} ratio.** Independently of the glucose availability, PUFA decreased drastically the ratio while MUFA caused only a slightly decrease when compared to the control without emulsion. **(D) Total Q levels.** *Lipofundin, Lipoplus* and, to a lesser extent, *ClinOleic* increased total Q levels in cells cultured under high-glucose conditions. In low-glucose, Q levels were already increased in comparison with high-glucose, although *Lipoplus* further increased Q levels in comparison with the corresponding control. Data are represented as mean ± SEM of 6 replicates. Differences are represented as * ($p < 0.05$), ** ($p < 0,01$) and *** ($p < 0.001$). "**F**" and "**P**" refers to differences between *Lipofundin* or *Lipoplus* ($p < 0.05$), respectively, under the same condition regarding glucose availability. "**CH**", "**FH**" or "**PH**" refers to differences between control, *Lipofundin* or *Lipoplus* in low-glucose compared with the same treatment but under conditions of high-glucose availability.

The ratio between Q_9 and Q_{10} levels is represented in Figure R12-C as Q_9/Q_{10} ratio. Again, results in this parameter were similar independently of the glucose availability. Exposure of cells to PUFA decreased the Q_9/Q_{10} ratio drastically compared to control and to *ClinOleic* treatment, as a consequence of the dramatic increase of Q_{10} levels already described. Treating the cells with MUFA also decreased the Q_9/Q_{10} ratio, but the decrease was not so pronounced, in accordance to the effect on Q_{10} levels.

Total Q levels in Hepa 1.6 cells treated with different lipid sources are represented in Figure R13-D. Since Q_9 is the main Q isoform presents in mouse cells, total Q levels are often an accurate reflection of Q_9 levels. However, in this case, the dramatic increase of Q_{10} levels attained under some conditions led to a significant contribution to the total Q levels. In high glucose, a large increase of Q levels was observed with *Lipofundin* and *Lipoplus*, whereas only a slight increase was observed with *ClinOleic* in comparison with the control without emulsion. The increase of Q levels caused by exposure to the two PUFA sources was significantly higher than that observed when cells were treated with *ClinOleic*. Under low-glucose conditions, only *Lipoplus* increased significantly Q levels in comparison with the control, which already displayed increased levels of Q, likely due to a low energetic availably. Thus, the increase of Q caused by lipid emulsions was of less magnitude under these conditions of restricted energy.

Taken together, these results indicate that different lipids sources contribute to the regulation of Q levels in the cells, especially Q_{10} leading to significant alterations of Q_9/Q_{10} ratio. Several repetitions of this experiment evidence the specificity of fatty acids to regulate Q_{10} and Q_9/Q_{10} ratio, however, the influence on Q_9 levels is more variable and always lower than the observed for the minority isoform. Moreover, the unsaturation index of the lipids might be a key factor in this regulation.

2.3. Effect of PUFA in mitochondrial morphology and ultrastructure.

Since lipid emulsions produced significant changes of Q levels, and this molecule is intimately related with the mitochondria, we decided to study mitochondrial ultrastructure in cells treated with lipid emulsions, by using electron microscopy. Since electron microscopy in a very laborious and time-consuming technique, we decided to focus on the effect of *Lipoplus*, the emulsion that produced the highest effect on Q, as an example of a PUFA source. Control Hepa 1.6 cells, as well as cells treated with *Lipoplus* were

incubated with the emulsion in high- and low-glucose conditions. After a 48 hours treatment cells were fixed and embedded in resin. Ultrathin sections were then cut in the ultramicrotome, stained and visualized at the electron microscope to obtain micrographs (see Material and Methods). For these ultrastructural studies, we took low-magnification micrographs, in which whole cells could be observed (Figure R14), as well as high-magnification micrographs where mitochondrial ultrastructure could be observed in detail (Figure R15).
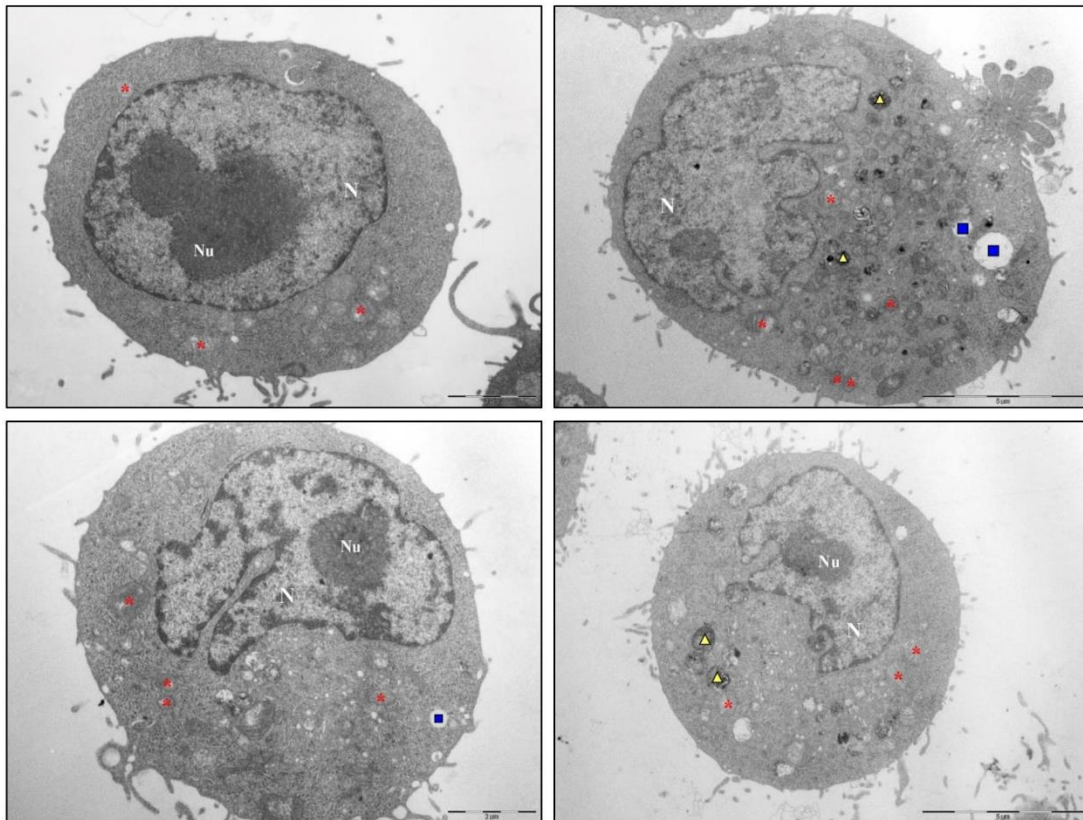
Figure R14. **Ultrastructure of whole Hepa 1.6 cells cultured under control conditions or treated with** ***Lipoplus*****. A) High-glucose control. B) Low-glucose control. C) High-glucose, *Lipoplus* treatment. D) Low-glucose, *Lipoplus* treatment.** Low magnification images (original magnification in the microscope was 5,800X or 7,900X. The bar attached to the micrograph (2 or 5 µM) give the real magnification). N = nucleus; Nu = nucleolus; * = mitochondria; ▲ = autophagy figures; ■ = lipid droplets.

We can observe that, independently of the treatment, Hepa 1.6 cells detached from the culture surface displayed a spherical shape with a prominent nucleus slightly displaced to a pole (Figure R14). Rarely, we found binucleated cells. Although we acknowledge that

this is not the natural shape of these cells, but they show this appearance because of the use of trypsine to detach cells from the culture plate, we found this methodology more appropriate for the subsequent quantitative estimations of mitochondrial abundance per cell (see below). In these micrographs, we were able to distinguish numerous mitochondrial profiles along the cytoplasm, as well as lipid droplets and autophagy figures. The analysis of high-magnification micrographs allowed us to distinguish several features aspects of the mitochondrial ultrastructure (Figure R15). This organelle exhibited an elliptical shape with transverse to the major axis cristae.
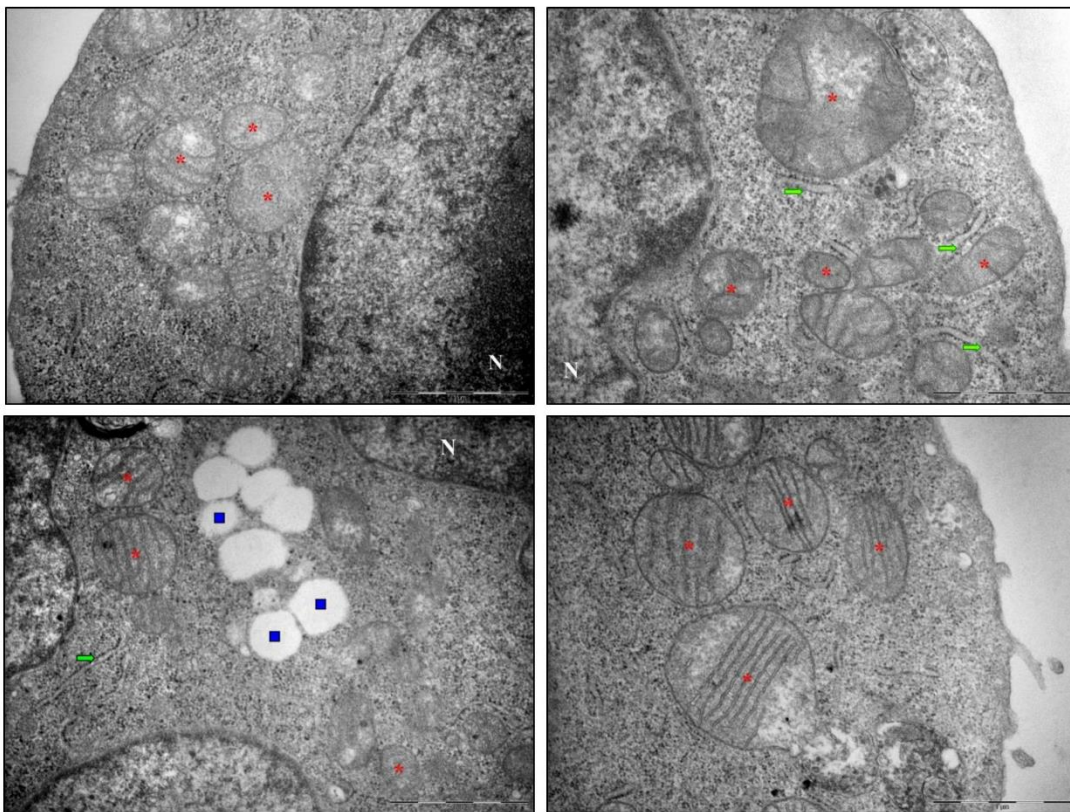
Figure R15. **Detailed section of control and PUFA-treated Hepa 1.6 cells** . **A) High-glucose control. B) Low-glucose control. C) High-glucose plus *Lipoplus* treatment. D) Low-glucose plus *Lipoplus* treatment.** High-magnification images (original magnification in the microscope was 25,000X. The bar attached to the micrograph (1 µM) give the real magnification). N = nucleus; Nu = nucleolus; * = mitochondria; ■ = lipid droplets; →: endoplasmic reticulum.

Planimetric measurements, performed with high-magnification images, revealed addition information about mitochondrial ultrastructure such as mitochondrial area, perimeter,

maximal and minimum radius and circularity. Using the maximal and minimum radius, we also calculated mitochondrial volume. Since all planimetric parameters related to mitochondrial size are related, we will only represent here mitochondrial volume and circularity (Figure R16-A). Mitochondrial volume was only affected by PUFA when given to cells under high-glucose conditions, with a slight increase in cells treated with *Lipoplus*. Moreover, mitochondrial circularity was not affected by neither PUFA nor glucose availability (Figure R16-A).
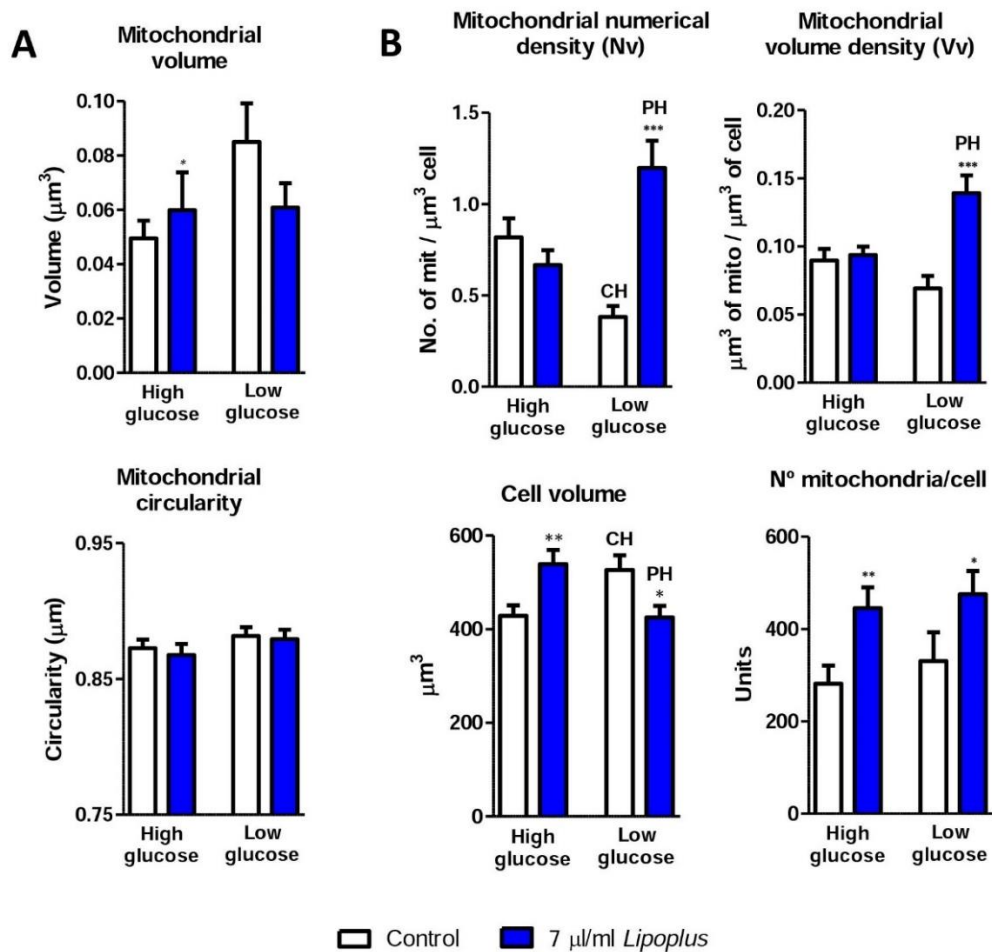
Figure R16. **Mitochondrial ultrastructure parameters in Hepa1.6 cells**. **(A) Planimetric parameters**. PUFA increased mitochondrial volume in high-glucose but not in low-glucose conditions. Mitochondrial circularity was not affected by either PUFA or energetic intake. **(B) Stereological parameters**. PUFA increased Nv and Vv in low-glucose conditions. Cell volume was affected by PUFA and by restricted energetic availability. PUFA increased the no. of mitochondria/cell independently of the energetic availability. Data are represented as mean ± SEM of at least 16 images per experimental condition. Differences with the control are represented as * (p < 0.05), ** (p < 0.01) and *** (p < 0.001). "**CH**" and "**PH**" refers to differences between control and *Lipoplus*, respectively, comparing with the same treatment under high-glucose availability.

Complementary, a stereological analysis were also performed using low-magnification micrographs. Mitochondrial numerical density (Nv), mitochondrial volume density (Vv), cell volume and number of mitochondria per cell were calculated and the results are shown in Figure R16-B. Mitochondrial numerical density (Nv) refers the number of mitochondria present in an area unit of the cell. According to our results, Nv was not influenced by PUFA when cells were cultured under standard conditions (high-glucose). However, Nv was decreased in cells cultured under low-glucose conditions but increased drastically when *Lipoplus* was incorporated into the culture medium (Figure R16-B). As stereological parameter related to relative mitochondrial abundance, we represent the mitochondrial volume density (Vv), a value that reflects the portion of cell volume that is occupied by mitochondria (both in μm^3). Results obtained for Vv were similar to those of Nv (Figure R16-B). Since both Nv and Vv are parameters referred to cellular volume, we also wanted to elucidate if this parameter was also affected by PUFA. Cell volume increased significantly when cells were grown in standard medium (high-glucose) in the presence of PUFA, but also by culturing cells in low-glucose medium. However, the combination of PUFA and low-glucose resulted in a decrease in cellular volume to reach values that were similar to those found in control cells cultured in standard medium (Figure R16-B). Changes observed in cell volume could explain the effect previously described for Nv and Vv in low-glucose condition. Finally, we also calculated the no. of mitochondria per cell and found that PUFA increased significantly the number of mitochondria in a given cell independently of glucose availability. However, changes observed in high-glucose were more noticeable.

As major changes in Q system have been observed in standard glucose conditions, hereinafter we decided to use only the high-glucose condition in further experiments.

2.4. Effect of pro-oxidant status in the increase of Q caused by different lipid sources.

We wanted to elucidate whether the increase of Q in cells treated with PUFA-containing emulsions is a consequence of lipid autoxidation. To this purpose, we combined the 48 hours treatment with two different antioxidants. For these experiments, we decided to use *Lipoplus* because it is the PUFA-containing emulsion that gave a greater response in terms of Q levels. BHT and Trolox, two antioxidant previously used for this purpose [156], were selected and a toxicity curve for each one was performed to choose the appropriate

concentration (Figure R17). BHT did not affect cell viability at concentrations under 50 µM but it revealed extremely toxic for the cells at higher concentrations (Figure R17-A). On the other hand, Trolox did not affect cellular viability at none of the concentrations tested but produced a higher MTT signal at concentrations of 1 and 2 mM (Figure R17-B). According to these data, we chose 50 µM BHT and 250 µM Trolox to perform the following experiments.
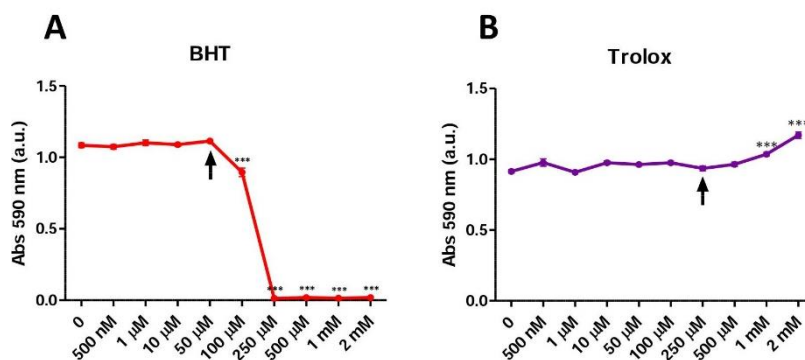
Figure R17. Effect of different antioxidants on the viability of Hepa1.6 cells. **(A) MTT assay performed in Hepa1.6 cells after treatment with BHT.** BHT did not affect cellular toxicity at concentrations lower than 50 µM, but higher concentrations were extremely toxic. **(B) MTT assay performed in Hepa1.6 cells after treatment with Trolox**. This antioxidant did not produce cellular toxicity at all. Data are represented as mean ± SEM of 8 replicates. Differences with the control are represented as *** ($p < 0.001$).

Using the selected concentrations of the two antioxidants, Hepa 1.6 cells were treated during 48 hours with *Lipoplus* in the presence of BHT or Trolox. Cells without any treatment or with *Lipoplus* but without antioxidants were also cultured in parallel to serve as controls. Lipids were extracted from cells grown under the different experimental conditions and Q levels were then measured by HPLC with electrochemical detection and represented in Figure R18. In general, the antioxidants treatment did not affect Q levels in control cells, apart from a slightly decrease in Q_9/Q_{10} ratio observed with BHT (Figure R18-C). However, as expected, the mayor regulation of Q levels is observed on Q_{10} levels, which increased after the treatment with *Lipoplus* in absence or presence of the selected antioxidants (Figure R18-B). Therefore, the Q_9/Q_{10} ratio is decreased independently of the co-treatment with BHT or Trolox (Figure R18-C). A minor regulation is observed on Q_9 or total Q levels. Despite, *Lipoplus* increase Q levels in absence of antioxidants, the co-treatment did not show the same effect (Figure R18-A/D). Together, these data

strongly support that the effect on Q mediated by PUFA is independent of lipid autoxidation.
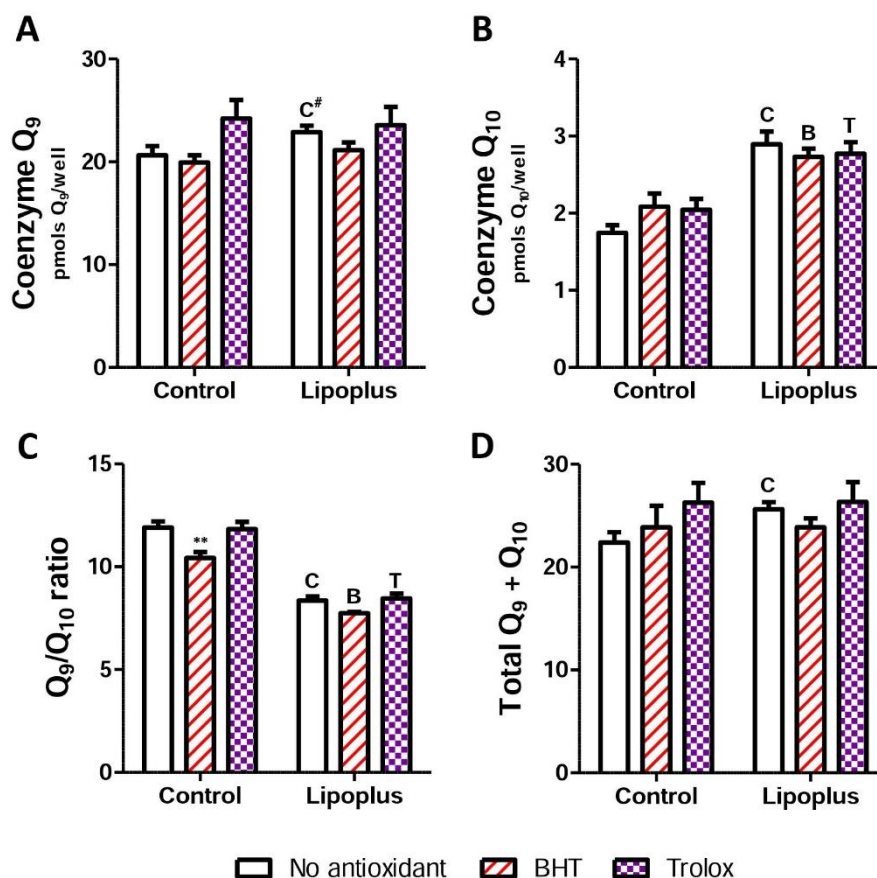
Figure R18. Effect of different antioxidants in combination with PUFA on Q levels of Hepa1.6 cells. **(A) Q_9 levels.** Q_9 levels increase with *Lipoplus*, but nor BHT neither Trolox had effect on Q_9 levels in absence or presence of emulsion. **(B) Q_{10} levels.** Q_{10} increase widely with *Lipoplus* in comparison to control and, also, in the co-treatment with the antioxidants. **(C) Q_9/Q_{10} ratio.** *Lipoplus* decrease the ratio, to the same extent, in presence or absence of antioxidants. **(D) Total Q levels.** The same response described for Q_9 is observed. Data are represented as mean ± SEM of 6 replicates. Differences with the corresponding control are represented as ** (p < 0.01). "**C**", "**B**", and "**T**" refers to differences between control, BHT or Trolox, respectively, comparing control conditions with the response in presence of *Lipoplus*.

2.5. Effect of fatty acids on Q biosynthesis.

We wondered if the increase of Q levels in cells treated with PUFA could be related with a modification of the biosynthesis rate of this molecule. Thus, we measured directly newly-synthesized Q with the aid of $^{13}C_6$-labeled 4HB. Hepa 1.6 were cultured in presence of $^{13}C_6$-4HB for 48 hours, and then the Q already present in the cells (^{12}C-Q)

could be differentiated from the Q that was newly synthetized during our treatment ($^{13}C_6$-Q) by using HPLC-MS/MS. The treatment with the labelled precursor was combined with *Lipoplus* and *ClinOleic* as examples of PUFA and MUFA lipid sources, respectively.
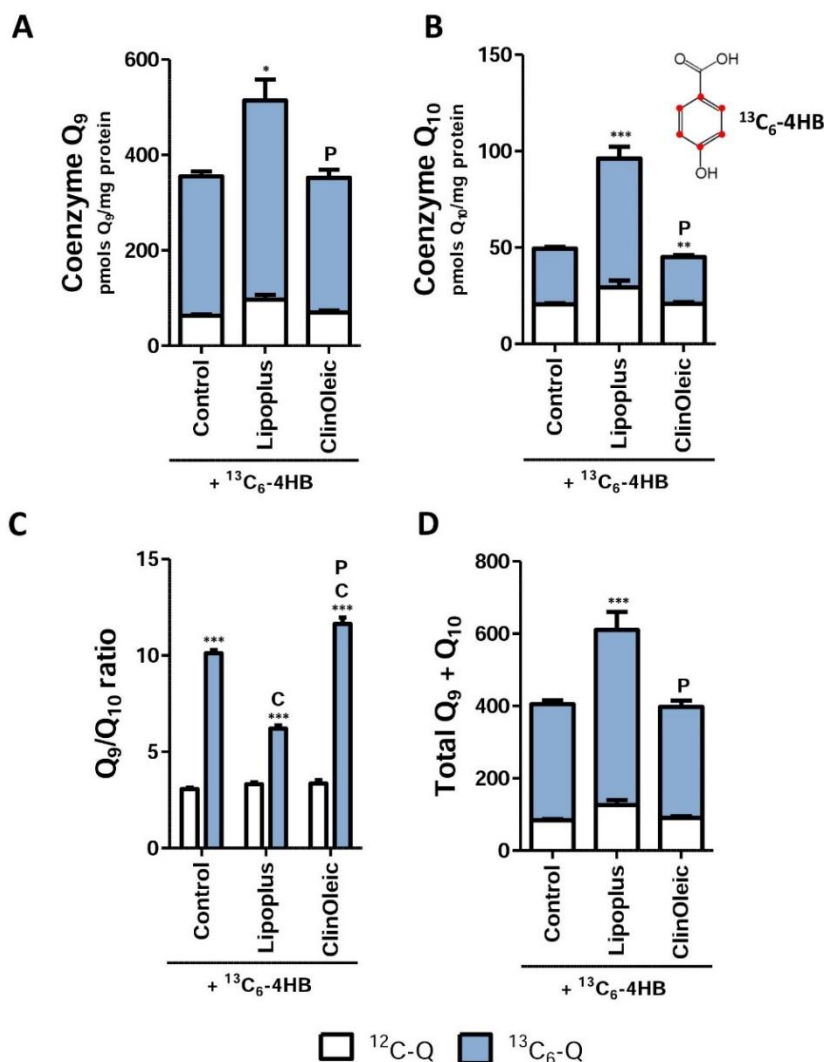
Figure R19. Effect of fatty acids on Q biosynthesis of Hepa1.6 cells. Adding the labeled Q precursor, $^{13}C_6$-4HB, we can measure specifically the amount of Q that is newly synthetized during treatments. **(A) Q9 levels.** *Lipoplus* increased Q_9 biosynthesis comparing to control and *ClinOleic*, which had no effect. **(B) Q10 levels.** Q_{10} biosynthesis was highly increased with *Lipoplus* but slightly decreased with *ClinOleic*. **(C) Q9/Q10 ratio.** ^{12}C-Q ratio did not change during the treatments while $^{13}C_6$-Q ratio significantly decreased with *Lipoplus* and slightly increased with *ClinOleic*. **(D) Total Q levels.** *Lipoplus* increased total Q biosynthesis comparing to control and *ClinOleic*, which again did not display any significant effect. Data are represented as mean $\pm$ SEM of 6 replicates. Differences to the correspondent control are represented as * ($p < 0.05$), ** ($p < 0.01$) and *** ($p < 0.001$). "**C**" and "**P**" refers to differences between control and *Lipoplus*, respectively.

As depicted in Figure R19, under all experimental conditions the majority of Q was ^{13}C-labelled, which is indicative of an active biosynthesis during the 48 hours treatment. ^{13}C$_6$-Q$_9$ levels, and thus, the biosynthesis of Q$_9$ increased significantly in presence of *Lipoplus* compared to control and to *ClinOleic*-treated cells, which maintained ^{13}C-Q$_9$ levels similar to those observed in the control (Figure R19-A). Similar results were observed for ^{13}C$_6$-Q$_{10}$ levels (Figure R19-B), although in this case the increment was substantially higher than the observed for ^{13}C$_6$-Q$_9$. The larger increase observed for ^{13}C$_6$-Q$_{10}$ is in accordance with a predominant effect on the levels of this isoform, as observed in previous experiments. However, *ClinOleic* did not increase ^{13}C$_6$-Q$_{10}$ levels but it even decreased this isoform comparing to the control. Our results suggest that the increase of Q mediated by PUFA is consequence of an increase biosynthetic rate, but changes in the biosynthetic rate are not responsible of the slight increase of Q levels observed after the treatment with MUFA. Q$_9$/Q$_{10}$ ratio of cells cultured under the different experimental conditions is represented in Figure R19-C. We have calculated independently the ratio for ^{12}C-Q and for ^{13}C$_6$-Q. Of note, treatments did not alter the Q$_9$/Q$_{10}$ ratio in the case of the non-labelled isoforms (of ^{12}C-Q) since this Q was already present in the cells before emulsions were added. However, the Q$_9$/Q$_{10}$ ratio calculated for the ^{13}C$_6$-labeled isoforms (and hence, synthesized during the treatment) demonstrated a significant decrease with *Lipoplus* treatment in comparison with control conditions or in the presence of *ClinOleic*, indicating that culturing cells in medium containing PUFA determines an greater increase in the synthesis of the Q$_{10}$ isoform than that of Q$_9$. As expected, total ^{13}C$_6$-Q levels (Figure R19-D) showed a similar pattern to ^{13}C$_6$-Q$_9$ levels. Nevertheless, the increment of Q$_9$ biosynthesis described for *Lipoplus* ($p < 0.05$) together with to the large increase of Q$_{10}$ biosynthesis observed with this emulsion ($p < 0.001$) determines that statistical significance of differences between control and *Lipoplus* is higher ($p < 0.001$) in the case of total Q. No differences of total Q biosynthesis was observed in a treatment with *ClinOleic* indicating that this process is not targeted significantly by MUFA.

2.6. Role of fatty acids as regulators of the mevalonate pathway.

Hepa 1.6 cells, treated with *Lipoplus* and *ClinOleic* during 48 hours, were recovered and processed to perform western-blot and lipid determinations in order to study FDPS and cholesterol levels, two important components of the mevalonate pathway. Using a specific antibody against FDPS we observed that both lipid emulsions, *Lipoplus* and

ClinOleic, inhibited the protein expression of FDPS (Figure R20-A). A 25% of inhibition was observed with *Lipoplus* in contrast with a 49% inihibition observed with *ClinOleic*. Our results confirm the effect of PUFA over the FDPS described in the literature. Moreover, we should take into account that results observed with *ClinOleic* could be influenced by the 1/5 part of soybean oil present in its composition.
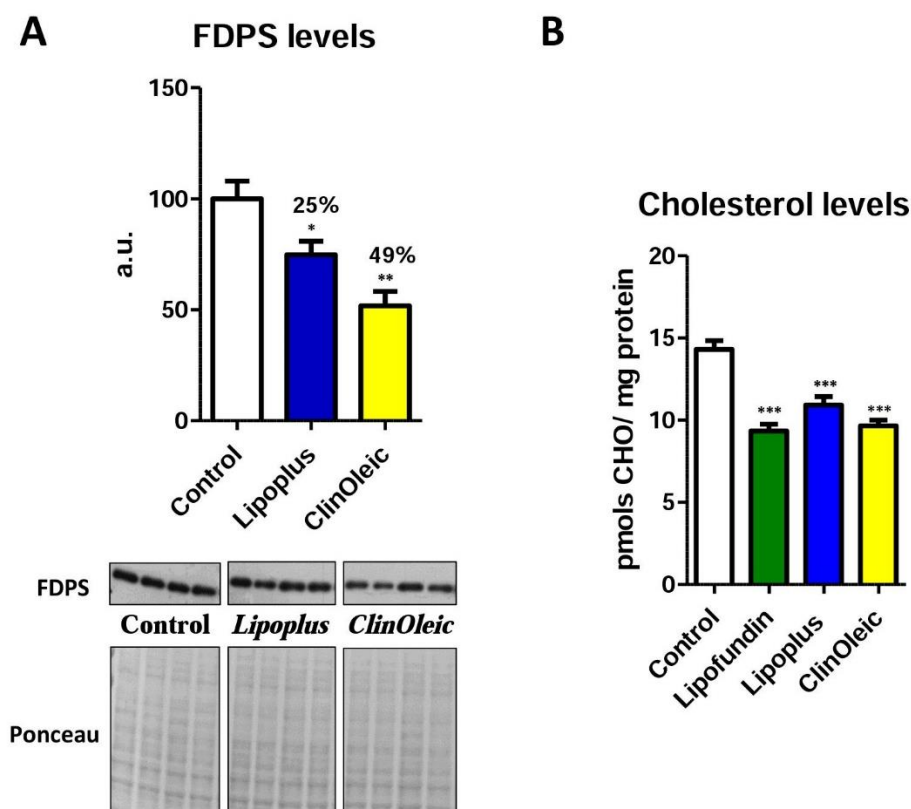
Figure R20. Fatty acids as regulators of some steps of the mevalonate pathway. **(A) FDPS levels.** *Lipoplus* and, even more, *ClinOleic* decreased FDPS in Hepa 1.6 cells. **(B) Cholesterol levels.** *Lipofundin*, *Lipoplus* and *ClinOleic*, in a similar extent, decreased cholesterol. Data are represented as mean ± SEM of at least 4 replicates. Differences with the corresponding control are represented as * ($p < 0.05$), ** ($p < 0.01$) and *** ($p < 0.001$).

On the other hand, cholesterol levels were measured by HPLC coupled with UV detection (Figure R20-B). Results showed that *Lipofundin*, *Lipoplus*, and also, *ClinOleic* decreased cholesterol levels compared to Hepa 1.6 control cells, all of them to a similar extend. Again, our results are in accordance with the described inhibition of cholesterol caused by PUFA. However, the results obtained with *ClinOleic* would indicate that different fatty

acids (PUFA or MUFA) might regulate the mevalonate pathway at different levels, since this emulsion affected cholesterol in the same way as *Lipofundin and Lipoplus* by its effect on Q levels and Q biosynthesis was quite different.

We further investigate if the levels of some isoprene intermediate metabolites from the mevalonate pathway are modified by lipid emulsions. Using HPLC with fluorescence detection, we were able to quantify the cellular levels of GPP and FPP (Figure R21). In animal cells, FDPS catalyzes the synthesis of both GPP and FPP *via* sequential adduction reactions [146]. Thus, provided that PUFA and MUFA decreased FDPS levels (see above), it might be expected that isoprenes produced by this enzyme would be also decreased after the treatment with the lipid emulsions. However, contrary to this hypothesis, our results showed a significant increase of GPP levels in presence of both *Lipoplus* and *ClinOleic*. FPP levels, which were substantially higher than the levels of GPP, were only increased in presence of *Lipoplus.* The increase of these metabolites has been already described in cells treated with bisphosphonates, a family of FDPS inhibitors (see Chapter 3).
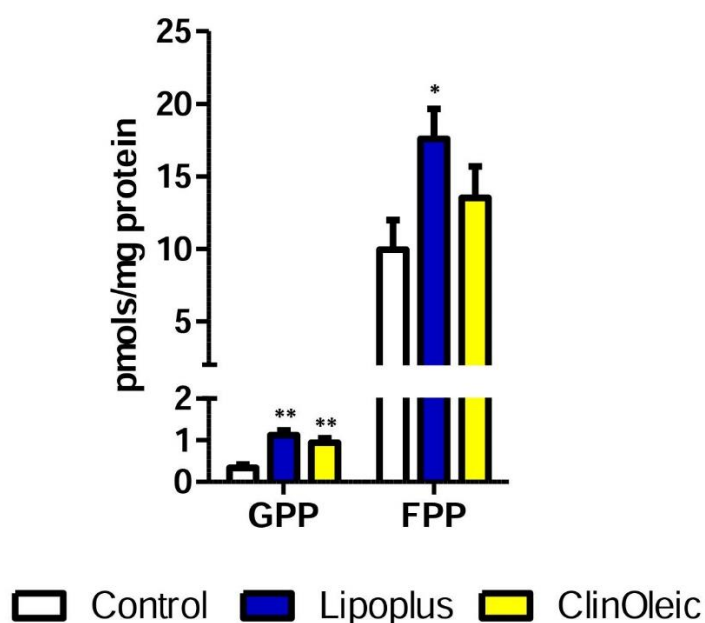
Figure R21. **Effect of fatty acids on GPP and FPP levels of Hepa 1.6 cells.** Both *Lipoplus* and *ClinOleic* increased GPP levels in Hepa 1.6 cells while only *Lipoplus* increased FPP levels. In Hepa 1.6 cells, FPP levels are substantially higher than those of GPP. Data are represented as mean ± SEM of 4 replicates. Differences to the corresponding control are represented as * ($p < 0.05$) and ** ($p < 0.01$).

Downstream from FPP in the mevalonate pathway we found GGPP, an isoprene responsible of the isoprenylation of several proteins in the cell. Rap-1A is a small GTPase, which is exclusively geranylgeranylated [90], and can be used to indirectly study the possible effect of lipid emulsions on GGDPS activity. In Figure R22 we can observe the levels of both unprenylated and total (unprenylated plus prenylated) amount of Rap1A. Unprenylated Rap1A (Figure R22-A) was difficult to detect in Hepa 1.6 cells indicating that the major part of this protein is present in its geranylgeranylated form. However, in this small unprenylated protein fraction we can observe that, while *Lipoplus* did not affect the isoprenylation of the protein, higher levels were indeed detected in cells treated with *ClinOleic*. This increase may be indicative of GGDPS inhibition caused by this treatment. Moreover, our results show that the total form of this protein is not affected by any of the lipids (Figure R22-B).
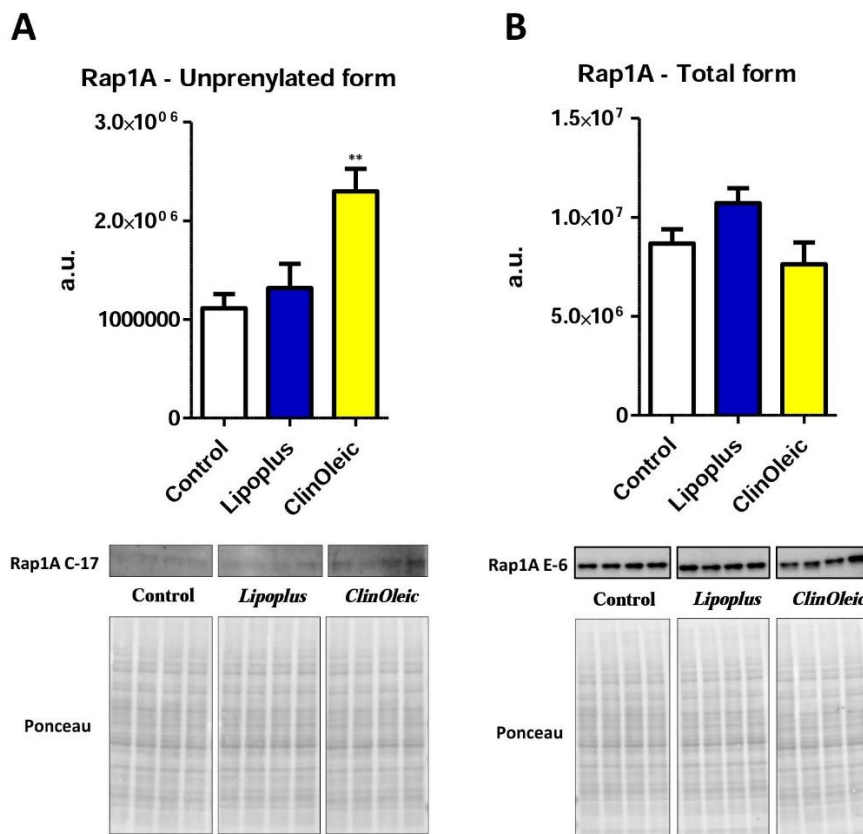
Figure R22. **Effect of fatty acids on the expression of Rap1A in Hepa 1.6 cells.** **(A) Unprenylated Rap1A.** *Lipoplus* does not affect levels of the non-prenylated Rap1A while *ClinOleic* increases this form significantly. **(B) Total Rap1A**. None of the tested emulsions modified total Rap1A levels. Data are represented as mean ± SEM of 4 replicates. Differences with the corresponding control are represented as ** ($p < 0.01$).

2.7. Effect of calorie restriction and fatty acids on Q levels of mice liver and skeletal muscle.

Based on the effects mediated by fatty acids in the hepatocellular model we wondered whether Q levels could be influenced by energetic intake or dietary fat in an *in vivo* model. Our group had previously developed an *in vivo* model in which mice were fed with 95 % of the mean intake (controls) or in 40 % calorie restriction with a diet supplemented with soybean oil. Moreover, different groups of calorie-restricted animals were fed with diets that differed in the principal fat source: soybean oil, fish oil and lard. Samples were collected after a nutritional intervention of 6 months or 18 months, so this model would also allow us to study different parameters with aging. Total homogenates of liver and skeletal muscle, a mitotic and post-mitotic organ respectively, of these mice were used to determine the endogenous levels of Q_9 and Q_{10}, as well as, the Q_9/Q_{10} ratio and the total amount of Q.

In Figure R23, we can observe the effect of age on Q levels and Q_9/Q_{10} ratio in the liver of calorie-restricted animals, in comparison with the controls, in both cases with a diet containing soybean oil as the predominant fat source. Liver Q_9 and Q_{10} levels significantly increased in the 18-month control group compared with the 6-month group. The greater increase of Q_{10} observed with age in control animals produced a decrease in the Q_9/Q_{10} ratio. However, when we analyzed the effect of age in calorie-restricted animals it was found that the increment of Q was abated. Consequently, changes in liver Q_9/Q_{10} ratio also disappeared in animals fed under calorie restriction. Total Q levels were similar to those of Q_9, as Q_{10} is a less represented isoform in mouse tissues. These results indicate that calorie restriction abolishes age-induced changes in Q levels of mouse liver.

We were also interested in studying the effect of different lipid sources in a calorie restriction context. In Figure R24, we can observe the effects of the age combined with the effect of different dietary lipid sources: lard, soybean oil or fish oil, in liver of animals fed in 40% calorie restriction. A 6-month dietary intervention with a diet supplemented with fish oil (CR-fish) increased Q_9 and Q_{10} levels significantly compared with a diet based on lard (CR-lard) or soybean oil (CR-soy). Young CR-soy animals displayed higher levels of Q_{10} compared with a diet based on lard. However, after 18 months of dietary intervention we found an increase of Q_9 in CR-fish compared with CR-lard.
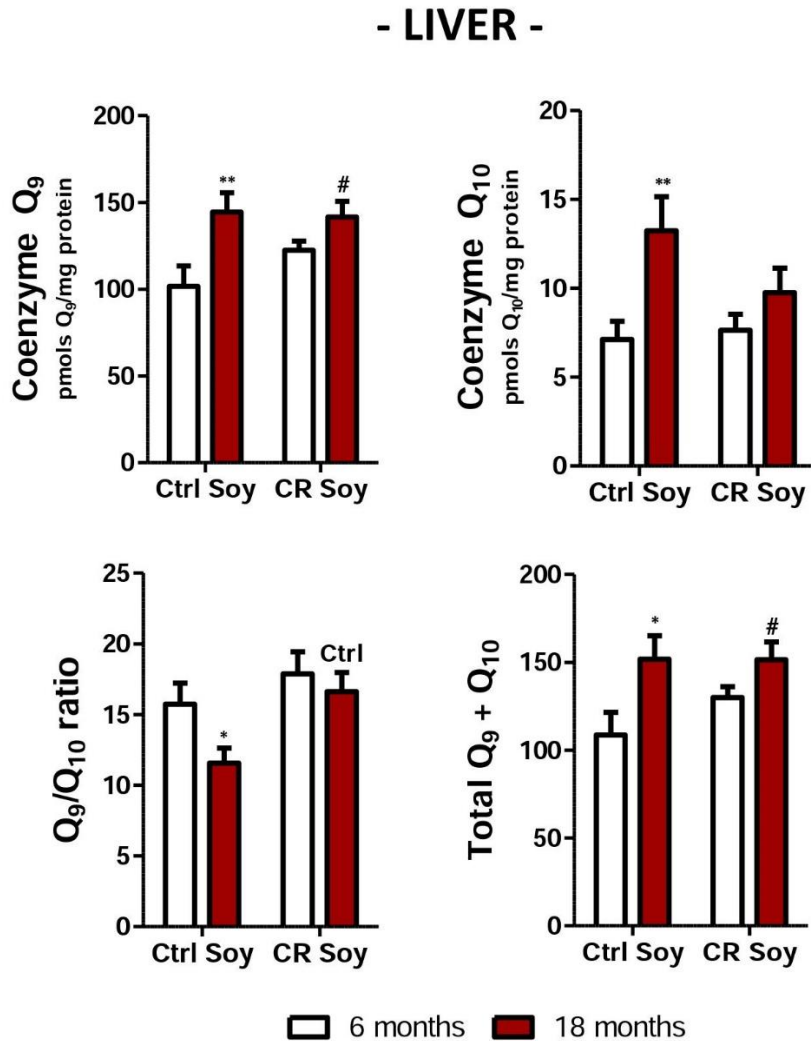
- LIVER -

Figure R23. **Effect of age and calorie restriction on Q levels of mouse liver**. Q_9 and Q_{10}, as well as total Q, increased with age in control conditions whereas CR abolished these age-related changes. Age decreased the Q_9/Q_{10} ratio in control conditions. Q_9, Q_{10} levels, Q_9/Q_{10} ratio and total Q are represented as mean $\pm$ SEM of a minimum of 8 animals. Differences among age of the same diet are represented as * ($p < 0.05$) and ** ($p < 0.01$). "Ctrl" refers to differences between the control diet and the CR-soy diet ($p < 0.05$).

Attending to the Q_9/Q_{10} ratio, we observed that both soybean and fish oil decreased this ratio in comparison with lard diet after 6 months of dietary intervention. However, in a longer nutritional intervention (18 months) the Q_9/Q_{10} ratio was similar among the different fat sources. Again, total Q levels in the liver were similar to those of Q_9, previously described, being CR-fish animals the ones with highest levels of Q along life.
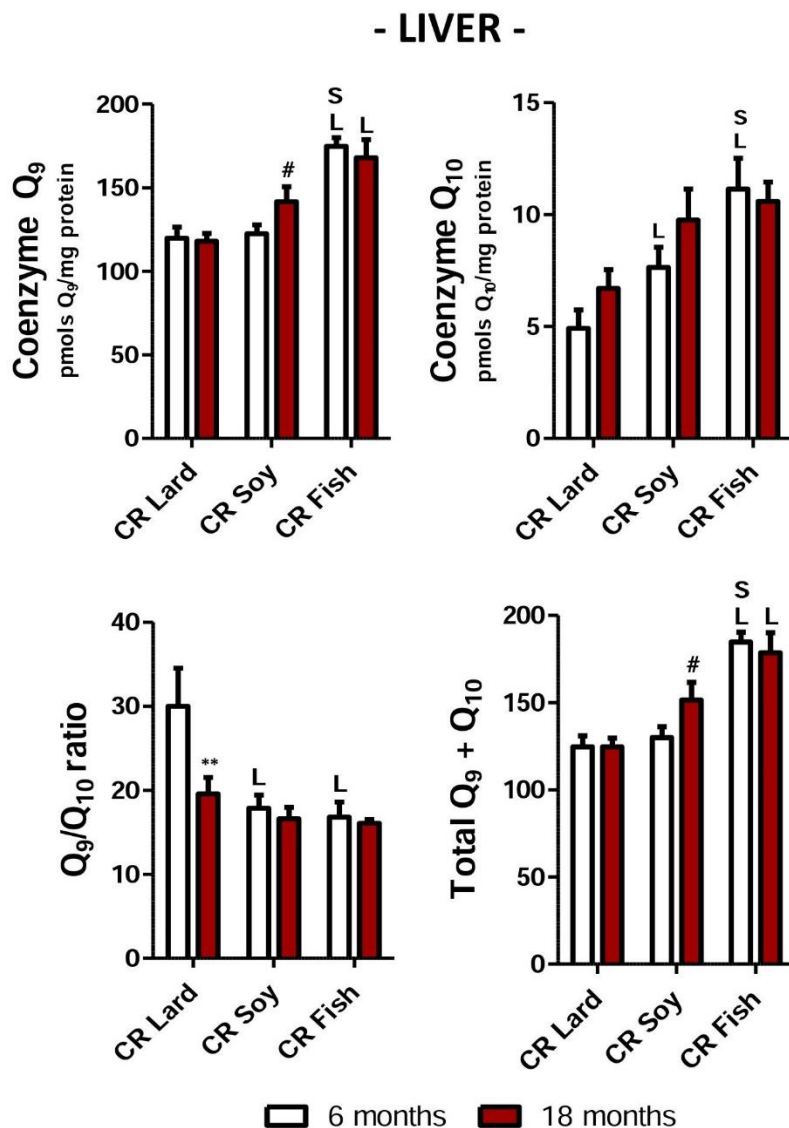
- LIVER -

Figure R24. Effect of different fat sources on Q levels in liver from calorie-restricted mice. The figure depicts Q_9 levels, Q_{10}, Q_9/Q_{10} ratio and total Q. CR-fish group displayed the highest levels of Q_9 in young animals. Old animals increased Q_9 levels with both PUFA, although statistical significance was not reached in CR-soy group. Similar results were observed for total Q. CR-fish diet in young animals also increased significantly Q_{10} levels. Q_9/Q_{10} ratio decreased drastically in CR-lard after 18 months of nutritional intervention, while PUFA maintained a lower ratio in both young and old animals. Data are represented as mean ± SEM of a minimum of 8 animals. Differences among age of the same diet are represented as * (p < 0.05) and ** (p<0.01). "**S**" refers to significant differences (p<0.05) comparing with CR-soy. "**L**" refers to significant differences (p<0.05) comparing with CR-lard. "#" indicate a trend between two ages of the same diet.

- SKELETAL MUSCLE -
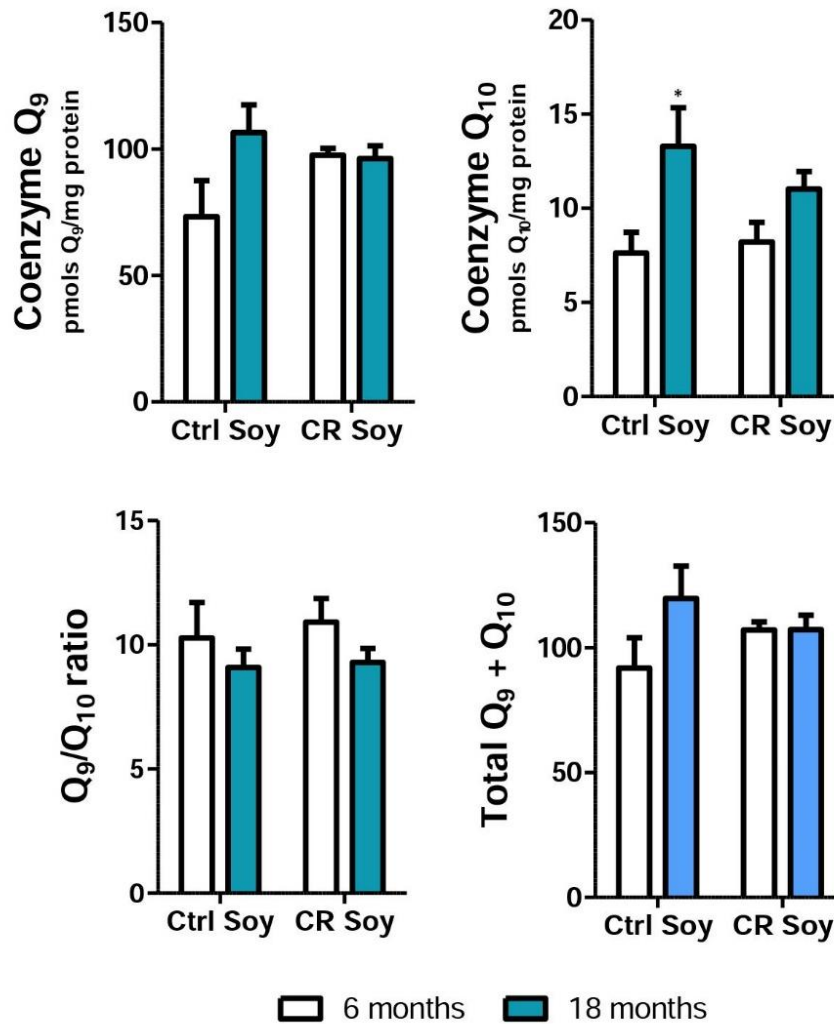
Figure R25. **Effect of age and calorie restriction on Q levels of mouse skeletal muscle.** The only change detected was the age-dependent increase of Q_{10} levels in control conditions. Q_9, Q_{10} levels, Q_9/Q_{10} ratio and total Q are represented as mean ± SEM of a minimum of 8 animals. Differences among age of the same diet are represented as * ($p < 0.05$).

Q levels in total homogenate of skeletal muscle were also studied as an example of post-mitotic tissue. The effect of age in calorie-restricted animals in comparison with control animals was summarized in Figure R25. Neither age nor CR caused any significant change in Q_9, Q_9/Q_{10} ratio or total Q. However, a significant increase in Q_{10} was observed in old control mice in comparison with the young counterparts. Although, in skeletal muscle the differences appeared to be rather small, again, as previously observed in liver, CR seemed to abolish the increase of Q caused by age.
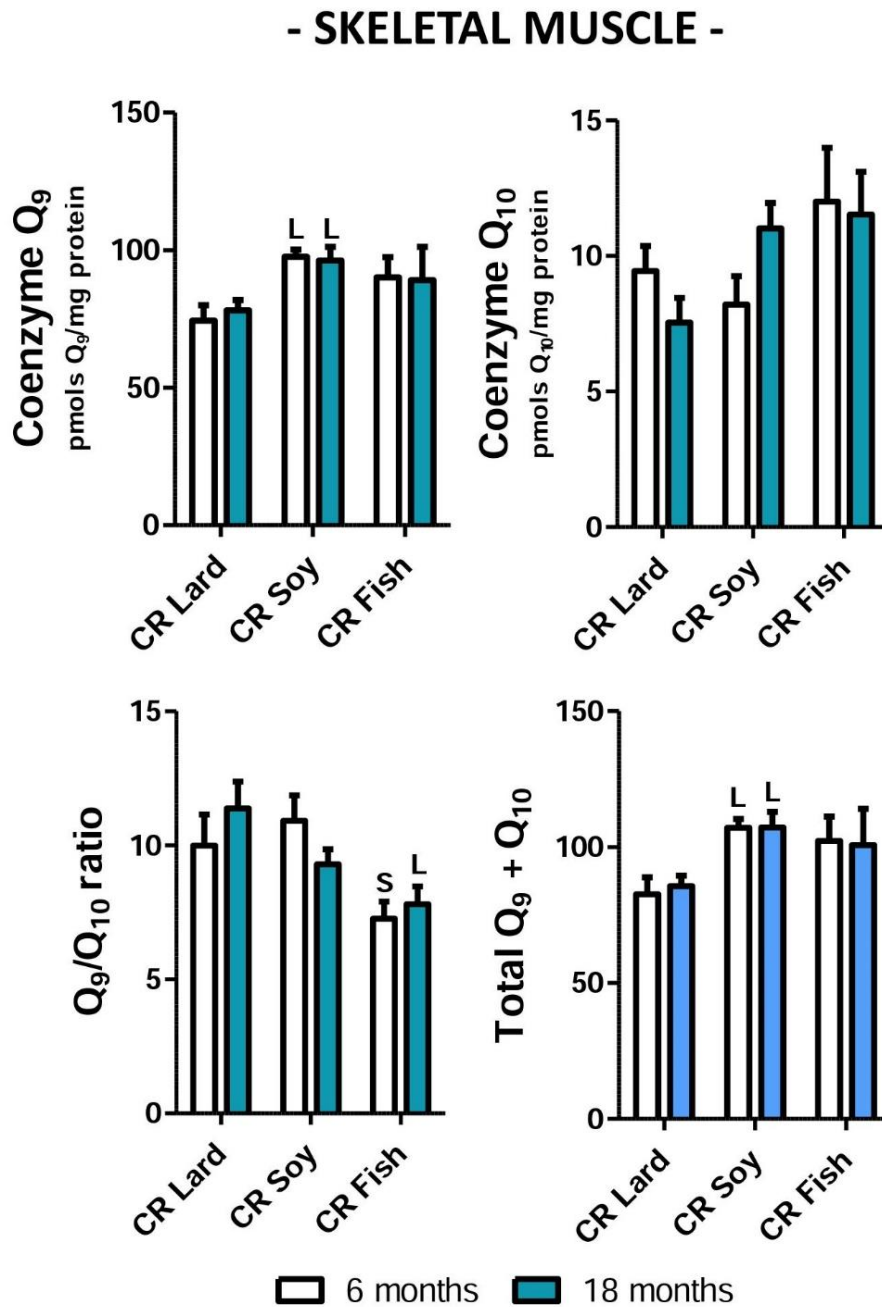
- SKELETAL MUSCLE -

Figure R26. Effect of different fat sources on Q levels of skeletal muscle from calorie-restricted mice. CR-soy, both in young and old mice, increased Q_9 levels when comparing with a diet enriched in lard. This increment was also reflected in total levels of Q. Different dietary sources did not cause significant differences in Q_{10} levels at any age. Q_9/Q_{10} ratio decreased drastically in CR-fish, in both young and old animals. Q_9 and Q_{10} levels, Q_9/Q_{10} ratio and total Q are represented as mean $\pm$ SEM of a minimum of 8 animals. "**S**" refers to significant differences (p<0.05) comparing with CR-soy. "**L**" refers to significant differences (p<0.05) comparing with CR-lard.

The effect of the different fat sources in skeletal muscle is represented in Figure R26. An increase of Q_9, which is also reflected in the total content of Q in muscle, was observed only with CR-soy groups in both young and old animals. No significant changes were observed in Q_{10} levels but a decrease of Q_9/Q_{10} ratio could be recognized for CR-fish, denoting slightly higher Q_{10} levels.

2.8. Effect of calorie restriction and fatty acids on FDPS levels of mice liver and skeletal muscle.

Previous observations using the cellular model related changes in Q levels with the alteration of FDPS levels. As we have observed several changes in Q levels of liver and skeletal muscle of mice fed calorie restricted diets containing lipid from different sources, we decided to determine FDPS levels in this *in vivo* model.

In Figure R27-A, we can observe the changes in hepatic FDPS levels associated with aging and calorie restriction. FDPS levels were increased in young animals fed under calorie restriction comparing to the controls. Moreover, FDPS levels were significantly increased in old control animals while a significantly decrease in old animals was observed for calorie-restricted mice, comparing with young animals fed the same diet. In a calorie restriction context, young animals fed a diet containing soybean oil (CR-soy group) displayed the highest levels of FDPS comparing with animals of the same age fed with other lipid sources. Again, we observed here the decrease of FDPS levels associated with age in a CR diet supplement with soybean oil (Figure R27-B) while there were no changes with age in the remaining dietary groups (CR-lard and CR-fish). Levels of FPDS in old mice from CR-soy group were statistically lower than those measured in old CR-lard mice.

Similar measurements were performed with total homogenates of skeletal muscle. The effect of age and calorie restriction is represented in Figure R28-A. No differences of FDPS levels were observed with age in control mice. However, an increase was observed in old calorie-restricted mice compared with young animals subjected to the same intervention. Attending to calorie-restricted animals fed diets containing different lipids from different sources, young CR-soy animals had increased levels of FDPS comparing with the other two diets (Figure R27-B). On the other hand, old CR-lard mice showed

higher levels than young mice fed the same diet. Moreover, FDPS levels in old CR-lard mice are the highest observed within the three diets.
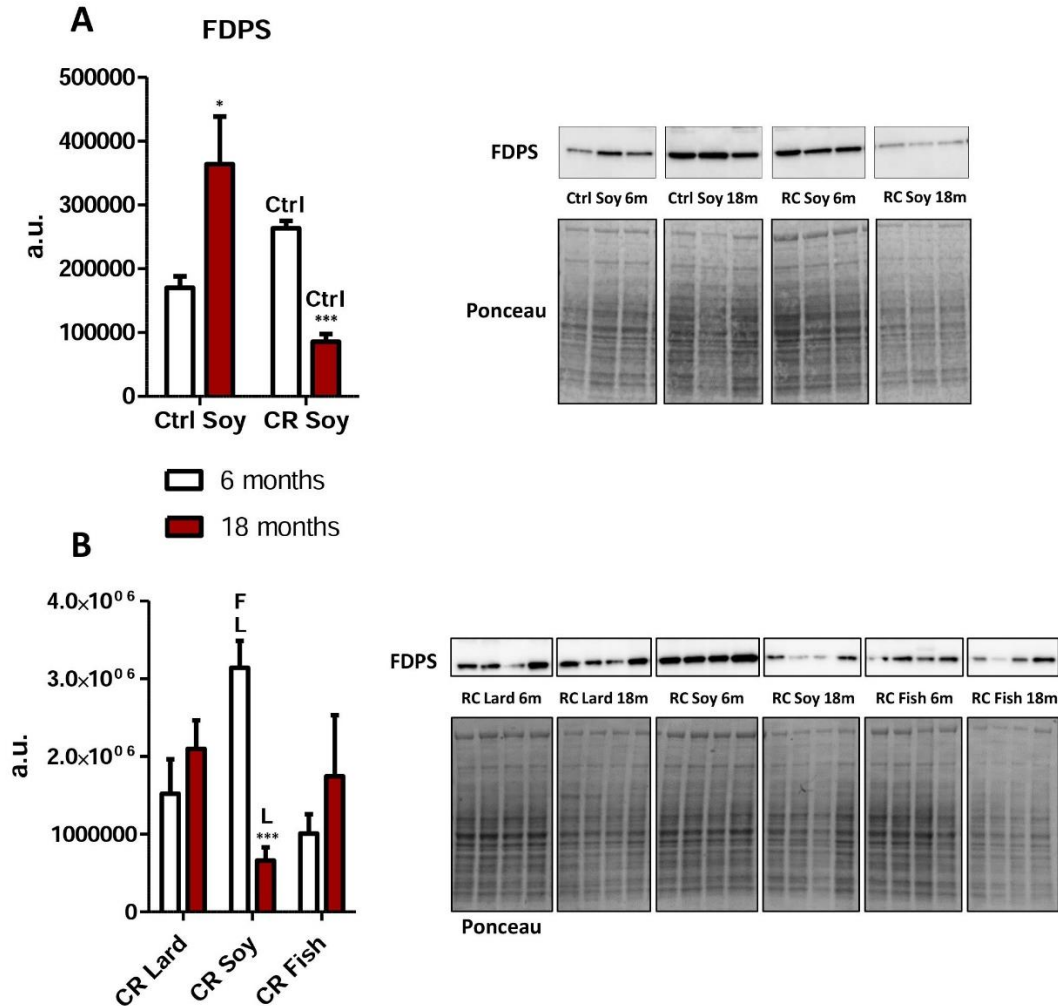
Figure R27. **Effect of age, calorie restriction and dietary lipid source on FDPS levels of mouse liver.** A specific antibody against FDPS was used to measure protein levels of this enzyme. **(A) Effect of age and CR.** FDPS levels was increased in young calorie-restricted mice comparing with the control. Within the same diet, old control animals increased FDPS levels while a decrease was shown in old calorie restricted mice showed it. **(B) Effect of different fat sources in calorie restricted conditions.** Young CR-soy animals showed the highest levels of FDPS comparing to CR-lard and CR-fish animals. Data are represented as mean ± SEM of at least 3 replicates. Differences among age of the same diet are represented as * (p < 0.05) and *** (p < 0.001). "**Ctrl**" refers to differences between the control diet and the CR-soy diet (p < 0.05), "**L**" refers to significant differences (p<0.05) comparing with CR-lard and "**F**" refers to significant differences (p<0.05) comparing with CR-fish. Arbitrary units depicted in the figure relate directly to the immunoblots shown aside, and the immunoblots derive from the same film. Ponceau' staining is shown as protein loading control.
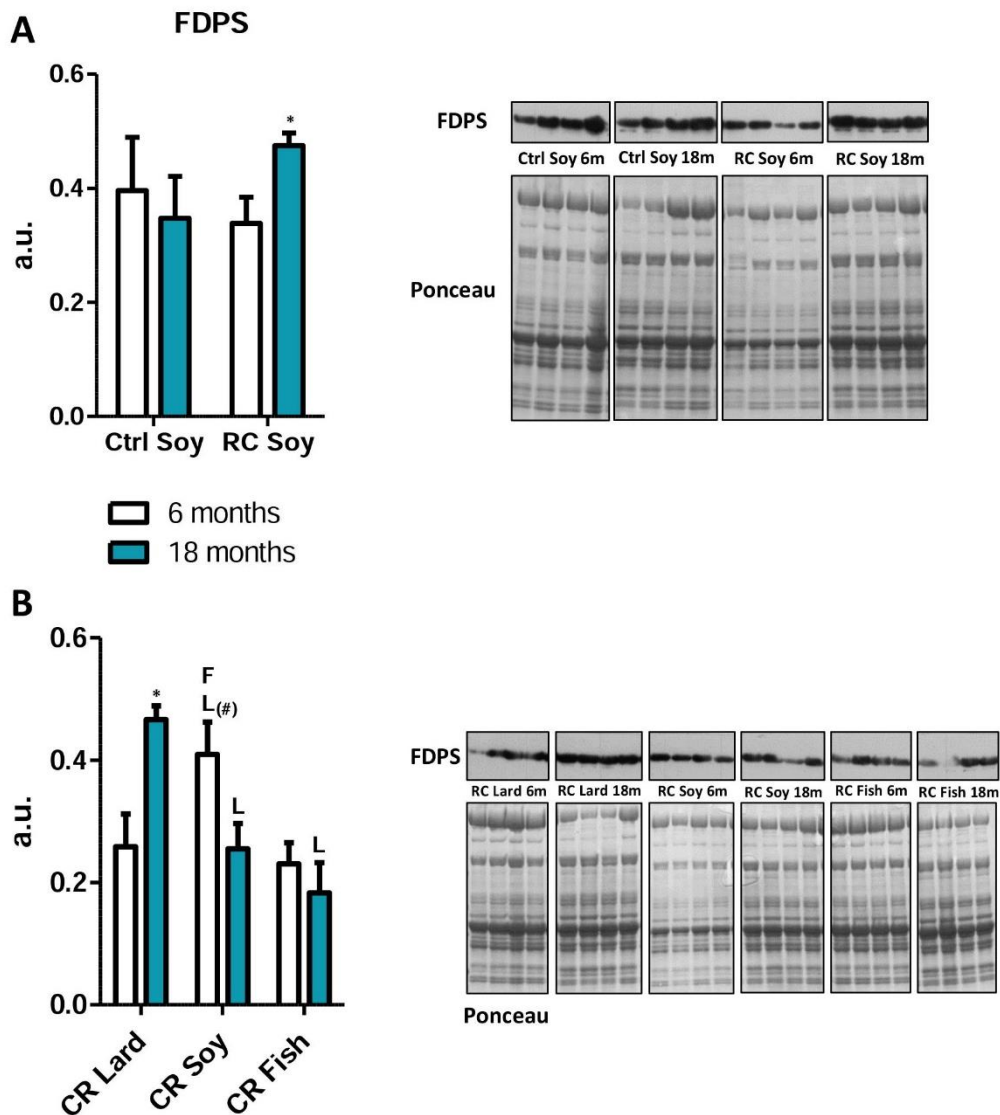
Figure R28. **Effect of age, calorie restriction and lipid source on FDPS levels of mouse skeletal muscle.** A specific antibody against FDPS was used to measure protein levels of this enzyme. **(A) Effect of age and CR.** No changes associated with age are observed in control animals. FDPS levels were increased in old CR-soy mice comparing with young animals fed the same diet. **(B) Effect of different fat sources in calorie-restricted conditions.** The highest levels of FDPS in young animals were observed in the CR-soy group, while the highest levels in old mice were observed in CR-lard group. Within mice fed the CR-lard diet, FDPS levels increased with age. Data are represented as mean ± SEM of 4 replicates. Differences among age of the same diet are represented as * ($p < 0.05$). "L" refers to significant differences ($p<0.05$) comparing with CR-lard and "F" refers to significant differences ($p<0.05$) comparing with CR-fish. Arbitrary units depicted in the figure relate directly to the immunoblots shown aside, and the immunoblots derive from the same film. Ponceau' staining it shown as loading control.

Chapter 3: *Effect of specific FDPS inhibition on Q metabolism*

In order to deepen the regulation of FDPS on Q metabolism we decided to inhibit this enzyme using two different mechanisms: a genetic approach and a pharmacological one.

3.1. Genetic approach to deepen the alteration of the Q metabolism mediated by FDPS.

In order to carry out this approach we decided to use small interfering RNAs (siRNAs), double-stranded RNA molecules that interfere with the expression of specific genes with complementary nucleotide sequences, resulting in an inhibition of the translation. Specifically, we used a couple of siRNAs, named A and B, designed specifically against different sequences of the *FDPS* gene (see Table M1 in Material and Methods). A universal scramble siRNA was used as a control in all the experiments.

As siRNA are used in transient transfections, we needed to know if our cells had a suitable transfection index to perform the experiments. Cells transfected with a phrGFP-N1 vector were cultured during 48 hours and the transfection index was calculated from the green fluorescence of cells measured by flow cytometry (FL1). In Figure R29, we can observe the transfection index (%) for both cellular lines, Hepa 1.6 and Tkpts, with two different doses of Lipofectamine® 2000, our transfection agent. Independently of the Lipofectamine amount, Hepa 1.6 reached an average transfection index of 33% in contrast with the 3% observed in Tkpts cells. Attending to the histograms we observed that while transfected Tkpts (dashed blue line) did not show almost any differences respect to the control (red), the signal of transfected Hepa 1.6 cells increased significantly in the selected region. Thus, we decided to continue our experiments only with the hepatocellular model.

The first step was to optimize the transfection with the siRNAs against FDPS, both A and B, in Hepa1.6 cells. Using a specific antibody to check FDPS levels after transfecting with the siRNAs we observed that the inhibition we achieved in these previous determinations was always lower than 55%. However, this decrease in protein levels was variable among each experiment. For this reason, we decided to check FDPS levels in each experiment and the corresponding western-blot is represented together with each result (see below).
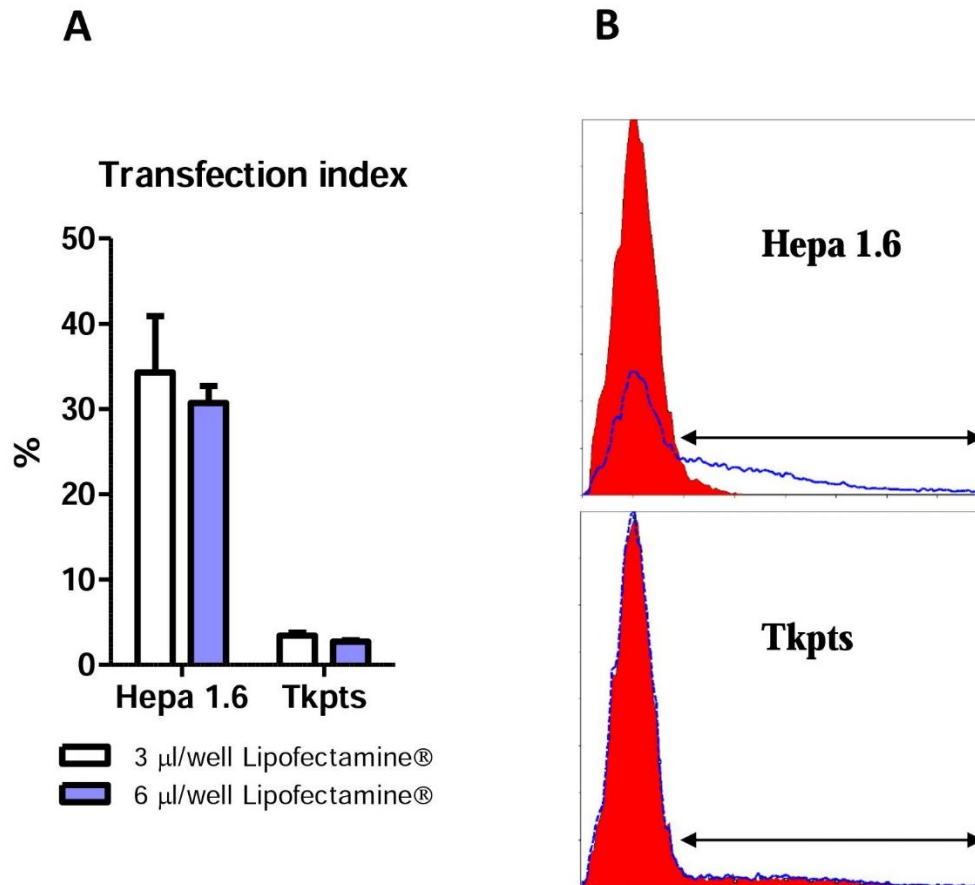
Figure R29. **Transfection index in Hepa 1.6 and Tkpts cells.** **(A) Transfection index.** Hepa 1.6 cells showed a transfection index of about 33% in contrast with the 3% observed in Tkpts cells. Results are independent of the used dose of Lipofectamine® 2000. Data are represented as mean ± SEM of 3 replicates **(B) Flow cytometer histograms**. Histograms of both cells lines were represented. The big initial peak correspond with control cells and no transfected cells. Transfection index was calculated measuring the signal recover in the delimited segment. Data are represented as mean ± SEM of 3 replicates.

3.1.1. Coenzyme Q levels in FDPS-depleted Hepa 1.6 cells.

Q levels measured in cells treated with siRNAs against FDPS are represented in Figure R30. Both siRNAs, A and B, depleted FDPS levels in Hepa 1.6 cells in comparison with the scramble siRNA (Figure R30-A). Q_9 levels measured in these cells revealed a clear trend towards a decrease when FDPS was inhibited, while Q_{10} levels were increased significantly under the same conditions (Figure R30-B/C). Genetic interference of FDPS also affected the Q_9/Q_{10} ratio that decreased in cells treated with the siRNAs (Figure R30-D). Moreover, total Q was not affected by the inhibition of the FDPS, because the decrease of Q_9 was compensated by a similar increase of Q_{10} (Figure R30-E). These

146

results were similar independently of the siRNA used and of the % of inhibition achieved by them.
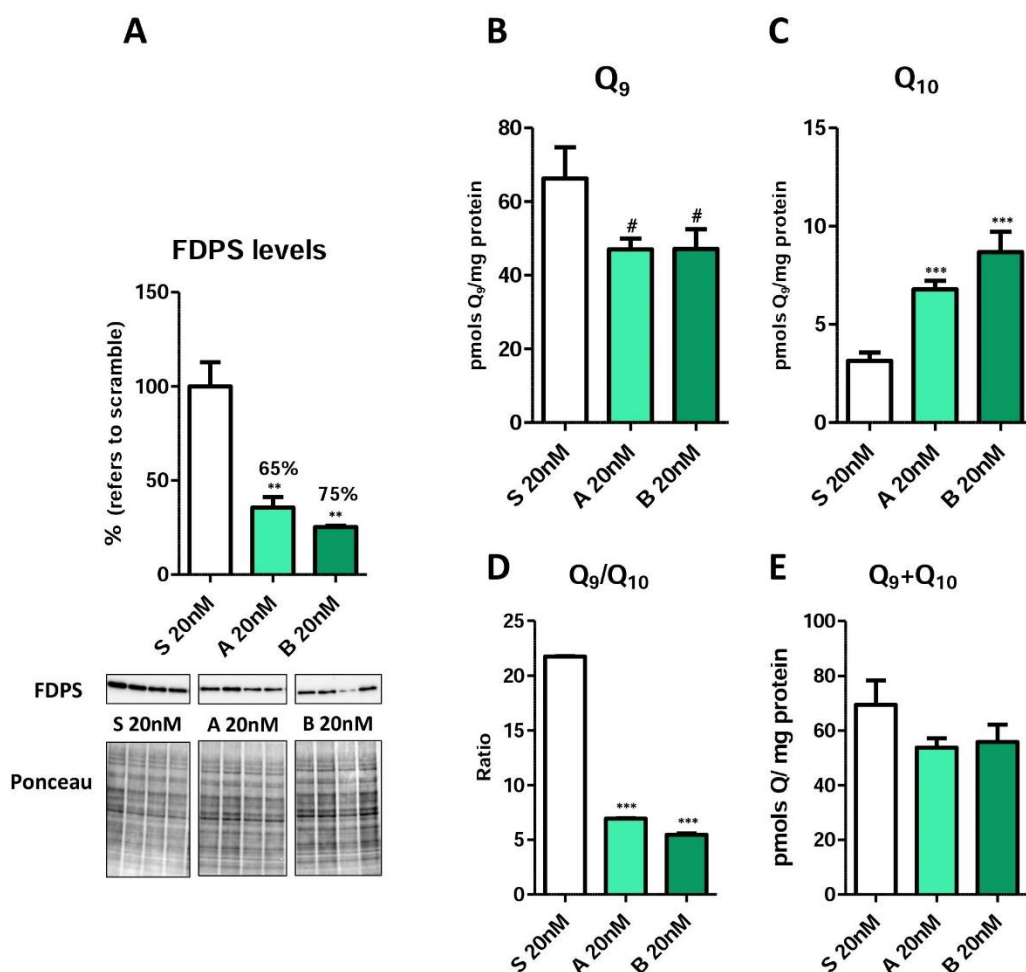
Figure R30. Effect of genetic silencing of FDPS on Q levels in Hepa 1.6 cells. **(A) FDPS levels.** A western-blot shows FDPS levels in the same siRNA-transfected Hepa 1.6 cells used for determining Q levels by HPLC. Both siRNAs, A and B, achieved a high inhibition of FDPS levels. The % depicted in the graph relates directly to the immunoblots shown underneath, and the immunoblots derive from the same film. Ponceau' staining it shown as protein loading control. **(B) Q_9 levels**. The inhibition of FDPS does not cause statistically significant changes in Q_9 levels, however, a clear downward trend could be observed with both siRNAs. **(C) Q_{10} levels.** The inhibition of FDPS caused a large increase in Q_{10} levels. **(D) Ratio Q_9/Q_{10}.** A dramatic decrease of Q_9/Q_{10} ratio was observed in cells depleted from FDPS. **(E) Total Q levels.** Although the different isoforms were influenced by the inhibition of FDPS, total Q levels did not change. Data are represented as mean ± SEM of at least 4 replicates. Differences to the corresponding control are represented as ** ($p < 0.01$) and *** ($p < 0.001$). # denotes a trend compared to the control.

3.1.2. Alterations of several steps of the mevalonate pathway in FDPS-depleted Hepa 1.6 cells.

Contrary to our expectations, we had previously observed an increase of GPP and FPP in cells cultured in the presence of PUFA. Using our genetic model for depletion of FDPS, the levels of these isoprenes were also measured and results are represented in Figure R31. Due to the complexity of the experiment, only siRNA B was used for this determination. Here siRNA B produced an 83% inhibition in the levels of FDPS (Figure R31-A). Strikingly, neither GPP nor FPP changed when FDPS was inhibited, although a non-significant increasing trend was observed for FPP (Figure R31-B).
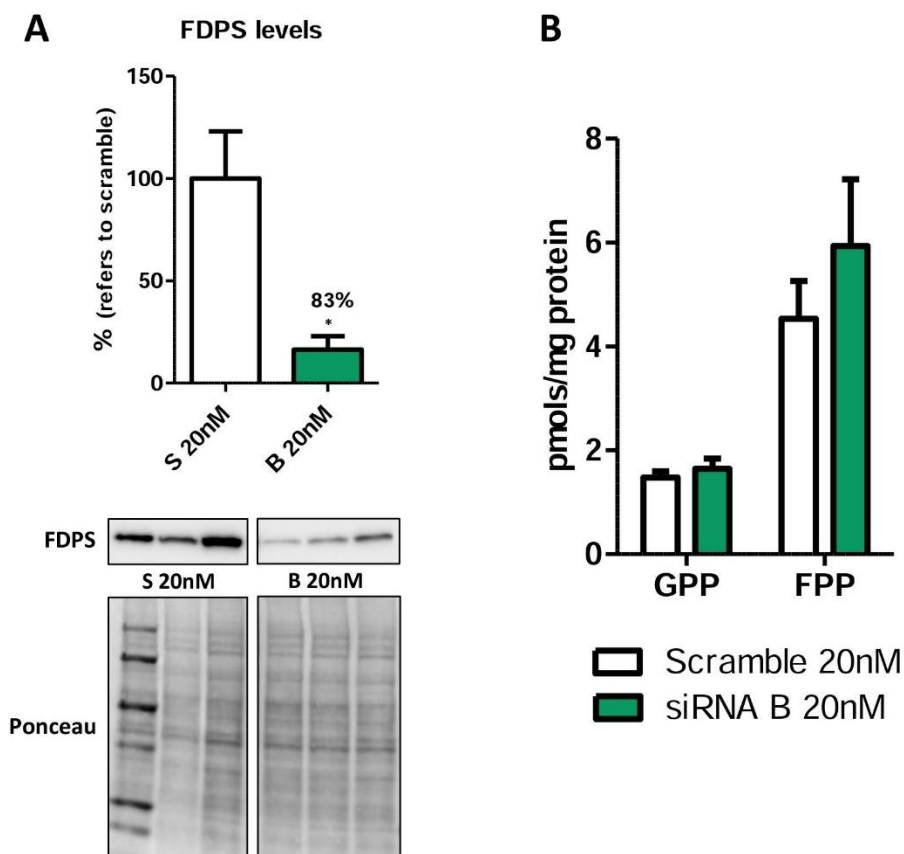
Figure R31. GPP and FPP levels in FDPS silenced Hepa 1.6 cells. **(A) FDPS levels.** A western-blot shows FDPS levels in siRNA transfected Hepa 1.6. SiRNA B achieved a high inhibition of FDPS levels. The % depicted in the graph relates directly to the immunoblots shown underneath, and the immunoblots derive from the same film. Ponceau' staining is shown as loading control. **(B) GPP and FPP levels**. Neither GPP nor FPP were affected by the inhibition of FDPS. Data are represented as mean ± SEM of 3 replicates**.**

Rap1A levels were also studied in samples treated with the siRNAs against FDPS. Again, in this experiment both siRNAs achieved a good inhibition rate (55-60%) (Figure R32-A). Our results are indicative that total Rap1A do not change despite FDPS is inhibited in the cells, although, a downward trend was observed with siRNA B (Figure R32-B). A signal for the non-prenylated form of Rap1a could not be even detected, indicating that the inhibition of FDPS does not affect protein geranylgeranylation and Rap1A remains completely prenylated.
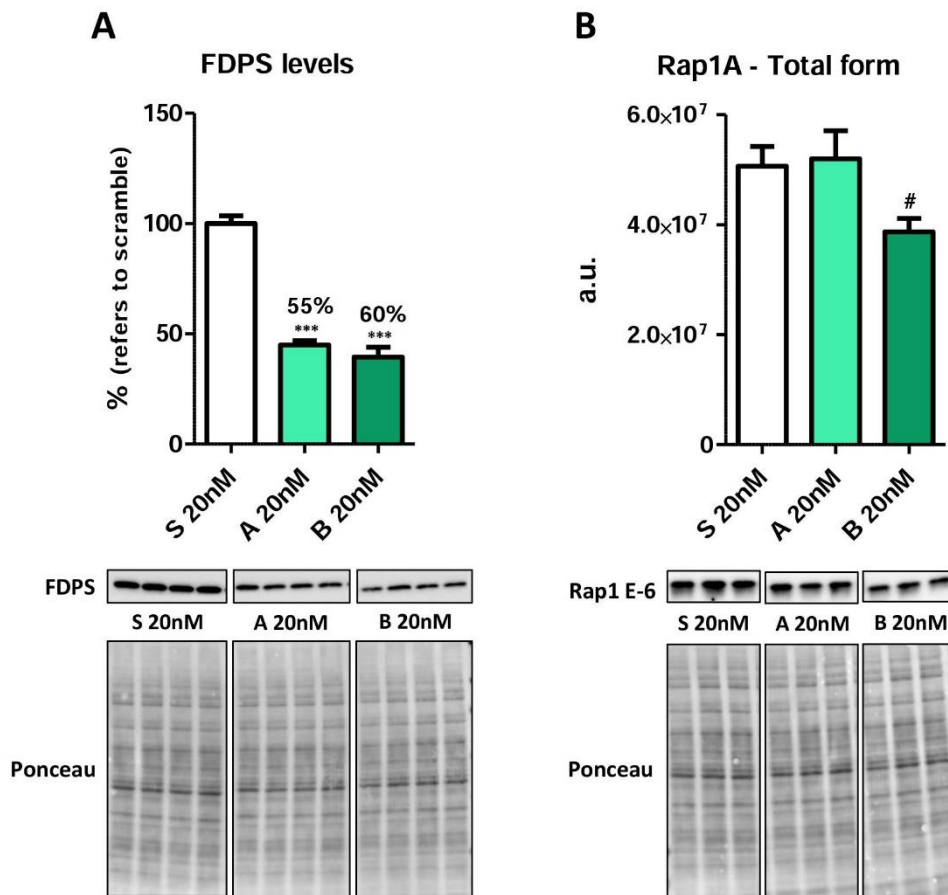
Figure R31. **Total Rap1a levels in FDPS-silenced Hepa 1.6 cells.** (A) **FDPS levels.** A western-blot shows FDPS levels in siRNA-transfected Hepa 1.6. Both siRNAs achieved a correct inhibition of FDPS levels. **(B) Total Rap1a levels**. Total Rap1 levels were not affected by the inhibition of FDPS, although a downward trend was observed with siRNA B. The % of arbitrary units depicted in the graph relates directly to the immunoblots shown underneath, and the immunoblots derive from the same film. Ponceau' staining is shown as loading control. Data are represented as mean ± SEM of at least 3 replicates. Differences with the corresponding control are represented as *** (p < 0.001). # represents a trend compared to the control.

3.1.3. Combined effect of PUFA and siRNA on Q levels in Hepa 1.6 cells.

PUFA as well as the inhibition of FDPS by siRNAs generated similar results in relation to Q_{10} levels and Q_9/Q_{10} ratio indicating that the decrease in FDPS levels might regulate in some way these parameters. We asked ourselves if the combination of both interventions, PUFA and siRNA, could have an enhanced effect over Q levels. Hepa 1.6 cells were transfected with siRNA B against FDPS or scramble during 48 hours and, then, these cells were further treated with *Lipoplus* during another 48 hours incubation period, being 96 hours the total time of the intervention.

First, we checked the inhibition on FDPS levels (Figure R33-A) to observe that, surprisingly, *Lipoplus* (combined with the scramble siRNA) did not affect FDPS levels, but the treatment with siRNA B decreased 75% its expression, both in absence and in presence of PUFA. Q_9 levels, represented in Figure R33-B, decreased only when FDPS levels were decreased by siRNA B. However, the decrease observed with the combination of siRNA B and *Lipoplus* was higher than that observed with the single siRNA treatment. Meanwhile, Q_{10} levels highly increased in cells transfected with siRNA B comparing to the scramble, and this increase was even higher when cells were also treated with *Lipoplus* (Figure R33-C). A substantial inversion of the Q_9/Q_{10} ratio was clearly observed in FDPS-depleted cells and, again, the effect was more pronounced in cells that had been also treated with *Lipoplus* (Figure R33-D). Total levels of Q ($Q_9 + Q_{10}$) decreased with siRNA B, independently of the presence of *Lipoplus*, but the effect was less pronounced than the decrease observed for Q_9, probably due to the simultaneous augmentation of Q_{10} levels (Figure R33-E).

Taken together these results suggest that *Lipoplus* potentiates the effect observed in Q_9 and Q_{10} levels and Q_9/Q_{10} ratio.
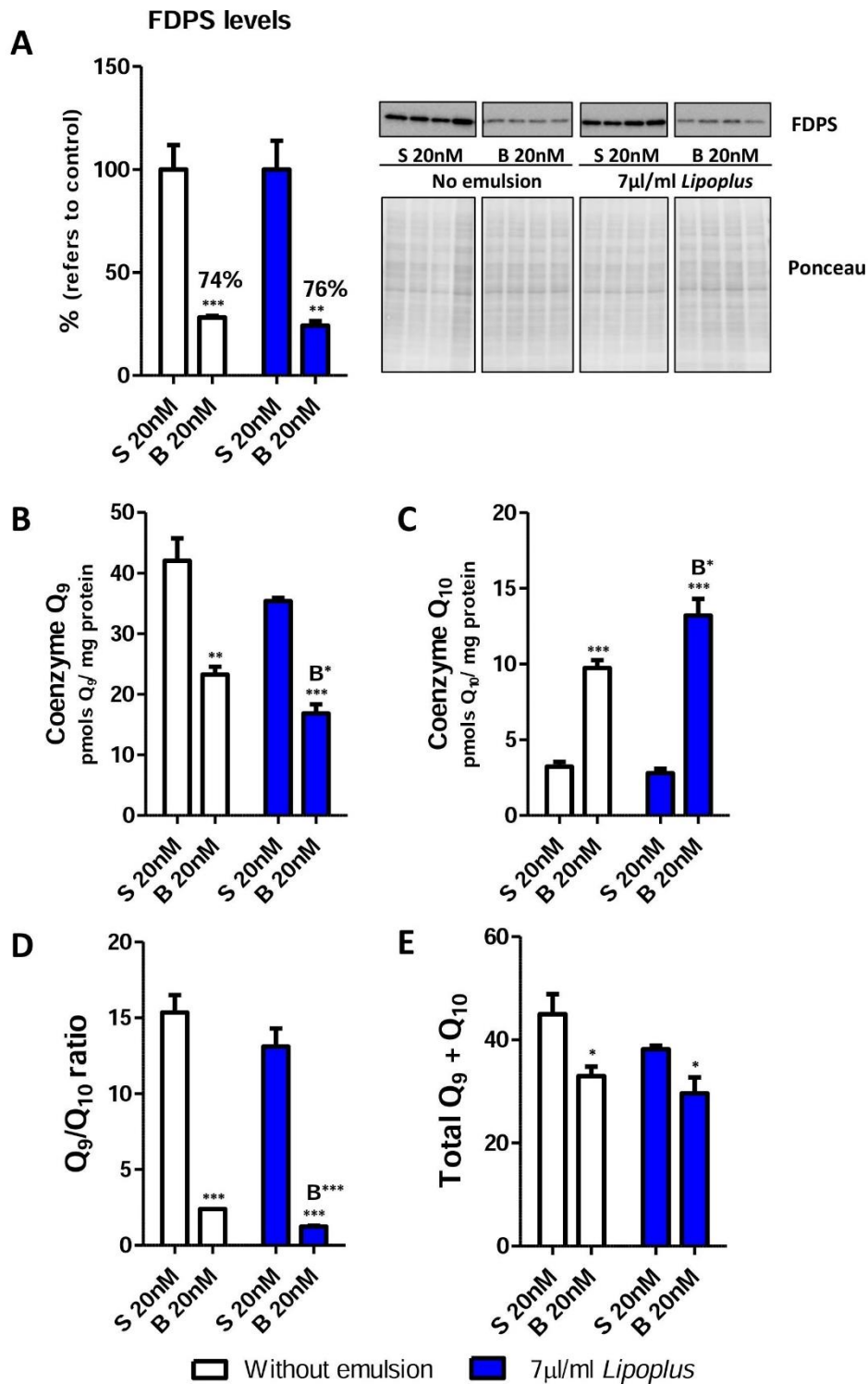
Figure R33. Q levels in Hepa 1.6 cells after a combined treatment with siRNAs and *Lipoplus*. (A) FDPS levels. A western-blot shows FDPS levels in siRNA transfected Hepa 1.6. About a 75 % inhibition of FDPS levels was achieved by siRNA B in absence or presence of *Lipoplus*. The % of arbitrary units depicted in the graph relates directly to the immunoblots shown underneath, and the immunoblots derive from the same film. Ponceau' staining it shown as loading control. **(B) Q_9 levels**. The inhibition of FDPS by siRNA B decreased Q_9 levels, and this effect was significantly potentiated when combined with

Lipoplus. **(C) Q$_{10}$ levels.** An increase in Q$_{10}$ levels was observed with siRNA B, and again, this effect was potentiated by *Lipoplus.* **(D) Q$_9$/Q$_{10}$ ratio.** A large decrease was observed in cells depleted from FDPS by siRNA B. Again, the decrease was potentiated by the presence of *Lipoplus.* **(E) Total Q levels.** A slight decrease was observed in FDPS-depleted cells, independently of the presence or absence of PUFA. Data are represented as mean ± SEM of at least 4 replicates**.** Differences to the corresponding control are represented as * ($p < 0.05$), ** ($p < 0.001$) and *** ($p < 0.001$). **"B"** refers to significant differences ($p < 0.05$) comparing with single siRNA B treatment.

3.2. Pharmacological approach to study the alteration of Q metabolism mediated by FDPS.

Complementary, we decided to use a pharmacological approach to inhibit FDPS levels. Using ZOL we achieved an inhibition at post-translational level, so we used this drug to study the effect of this inhibition on the Q system.

3.2.1. Effect of zoledronic acid in cellular viability.

Before starting our experiments, we studied the viability of the cells after a 48 hours treatment with ZOL. In this study, we maintained our hepatocellular model but also included Tkpts cells, and other two human cell lines: HEK 293 and HeLa cells. MTT curves for each cell line after a ZOL treatment are represented in Figure R34. Cell viability was compromised at concentrations of 50 µM and higher in Hepa 1.6 cells and at 80 µM and higher in Tkpts cells (Figure R34-A/B). Moreover, HEK 293 and HeLa were more sensitive to this drug, and started to show a decreased viability from 10 µM and 20 µM, respectively (Figure R34-C/D). According to the described results, a different concentration of ZOL was selected to treat each cellular line, according to its particular tolerance to this drug. Thereby, ZOL at 20 µM were used to treat both, Hepa 1.6 and Tkpts cells. However, lower concentrations were needed in the experiments performed with human cell lines. In this case, 5 µM ZOL was used to treat HEK 293 while HeLa cells were treated with 10 µM ZOL.
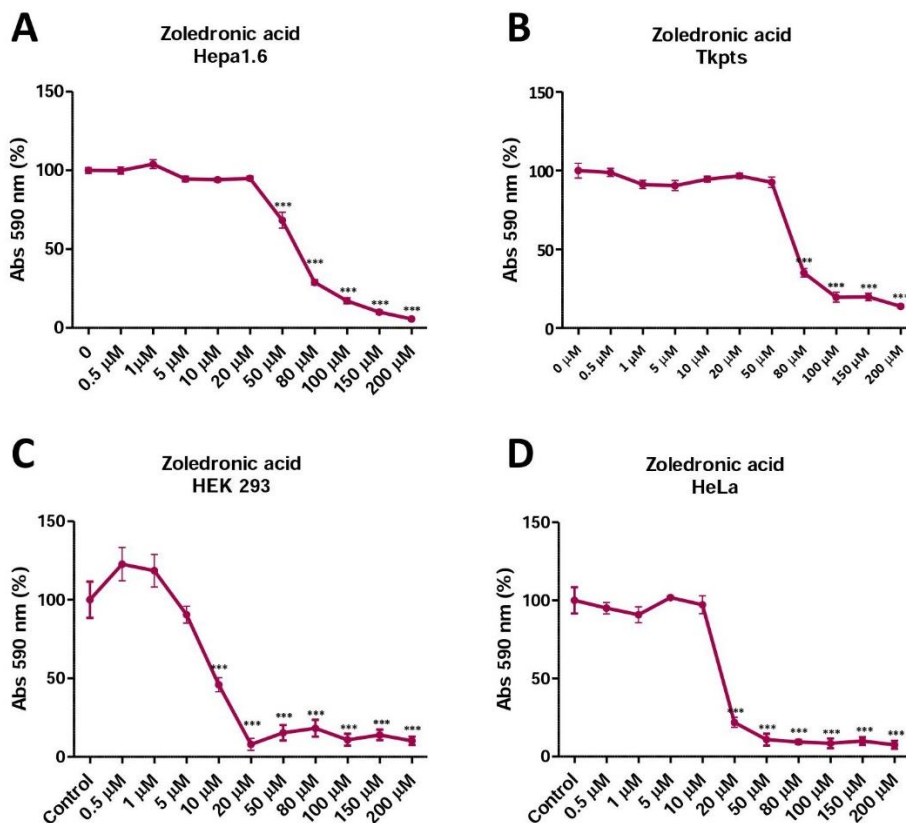
Figure R34. **Cellular tolerance to zoledronic acid.** A MTT curve using increasing concentrations of ZOL was performed in each cell line. **(A) Hepa 1.6 cells.** Viability of the cells was affected at concentrations of 50 µM and higher. **(B) Tkpts cells**. Viability of the cells was affected at concentrations of 80 µM and higher. **(C) HEK 293 cells**. Viability of the cells was affected at concentrations of 10 µM and higher. **(D) HeLa cells.** Viability of the cells was affected at concentrations of 20 µM and higher. Data are represented as mean ± SEM of 8 replicates**.** Differences with the corresponding control are represented as *** (p < 0.001).

3.2.2. Zoledronic acid as an efficient inhibitor of FDPS.

Despite ZOL is well-known as inhibitor of FDPS [89, 157], we wanted to check whether this property is maintained in our cellular models. Since ZOL inhibits FDPS in a post-translational way, FDPS levels should not be modified with the treatment. Verification of this fact is represented in Figure R35-A. As expected, FDPS levels were not modified in cells treated with ZOL, neither in the case of Hepa 1.6 nor in Tkpts cells.
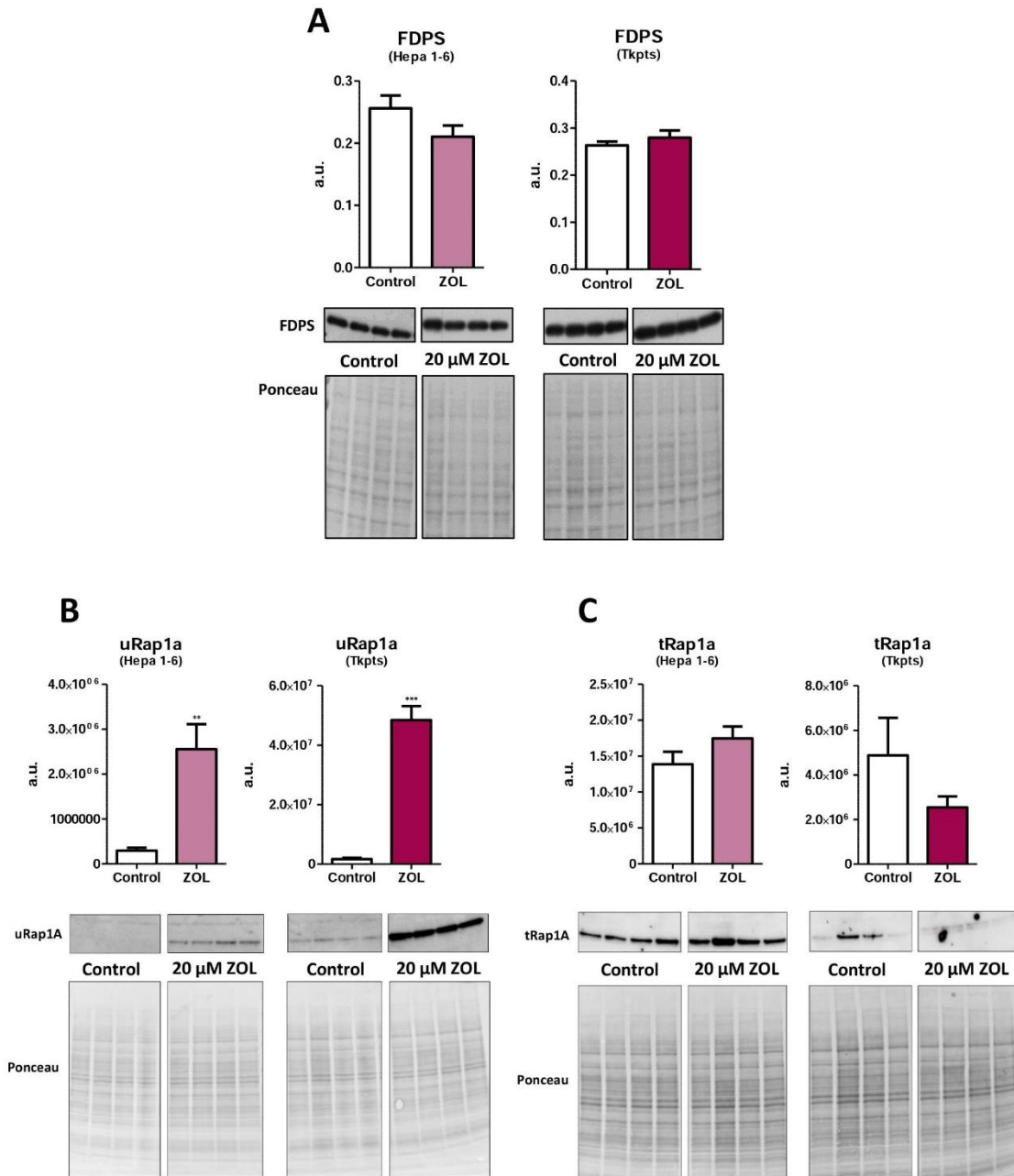
Figure R35. FDPS and Rap1A levels in cells treated with zoledronic acid. Specific antibodies were used to detect protein levels after treatment with ZOL. **(A) FDPS levels.** FDPS levels were not affected by ZOL in any of the cellular lines. **(B) Unprenylated Rap1a.** ZOL increased uRap1a levels in Hepa 1.6 and Tkpts cells, this increase being particularly high in Tkpts cells. **(C) Total Rap1A**. Total form of Rap1A was not influenced by ZOL in any cell line. Arbitrary units depicted in the graph relate directly to the immunoblots shown next to the graphics, and the immunoblots derive from the same film. Ponceau' staining is shown as loading control. Data are represented as mean ± SEM of 4 replicates**.** Differences with the corresponding control are represented as ** ($p < 0.01$) and *** ($p < 0.001$).

We next measured the accumulation of unprenylated Rap1A, a described biochemical indicator of the pharmacological activity of the NBPs [158, 159]. We indicated previously that Rap1A is specifically geranylgeranylated, so with this marker we actually measure the inhibition of the GGDPS mediated by NBPs, which has been also described in the literature [90, 160]. Rap1A levels are represented in Figure R35-B/C. Unprenylated Rap1A levels increased in presence of ZOL in both, Hepa 1.6 and Tkpts, indicating an inhibition of the geranylgeranylation and, thus, an inhibition of the GGDPS (Figure R35-B). Moreover, we should emphasize the dramatic increase of uRap1A observed in Tkpts cells treated with ZOL. Total Rap1A levels were also measured but no changes were observed in any cellular model (Figure R35-C). The analysis of the levels of total Rap1a reveals that under control conditions hepatic cells possesses significantly higher levels of this protein than cells from renal origin.

3.2.3. Effect of zoledronic acid on the Q system in different cell lines.

Having selected a suitable and functional ZOL concentration to treat each of the cells line of interest, we have studied the effect of this drug on Q levels. ZOL had a similar effect in all cell lines, with the exception of Tkpts cells. In Hepa 1.6, HEK 293 and HeLa cells ZOL treatment produced a general decrease in Q_9, Q_{10}, Q_9/Q_{10} ratio and total Q levels (Figure R36-A/C/D). Moreover, we should emphasize that the decrease in Q_{10} was always less pronounced that the observed for Q_9. Meanwhile, the response of Tkpts cells to the drug shared the decrease already described for Q_9 but, surprisingly, Q_{10} levels were dramatically increased after a treatment with ZOL (Figure R36-B). Higher levels of Q_{10} and lower levels of Q_9 in Tkpts treated with ZOL affected profoundly Q_9/Q_{10} ratio, which was reversed in comparison with the normal ratio of Q isoforms that characterizes murine cells, to become less than 1 (*i.e.* Q_{10} became the main isoform). Regarding total Q, the increase of Q_{10} resulted in a partial compensation of the Q_9 decrease. As a result, while total Q levels in Tkpts cells treated with ZOL were still lower than the levels measured in control cells, the overall effect of the drug on total Q was less pronounced than in the remaining cell lines.
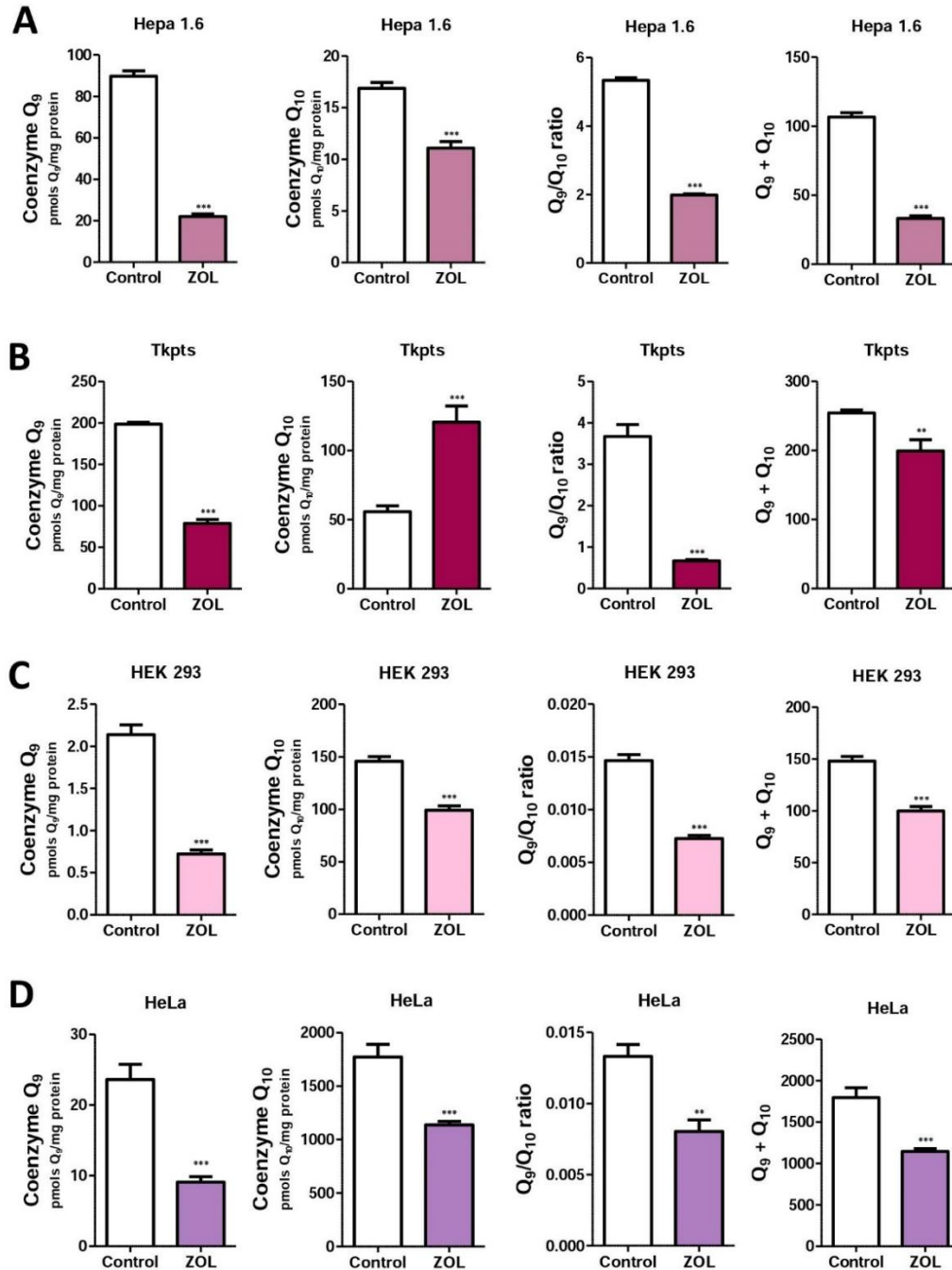
Figure R36. Effect of zoledronic acid on Q levels in several cell lines. Q_9, Q_{10}, Q_9/Q_{10} ratio and total Q levels are represented for each cellular line. **(A) Hepa 1.6 cells.** 20 µM ZOL significantly decreased all the parameters measured. **(B) Tkpts cells**. 20 µM ZOL decreased Q_9 but increased Q_{10} levels**.** The decrease of the Q_9/Q_{10} ratio in thus higher than the change observed for the rest of the cell lines. Total Q levels decreased, but overall inhibition was lower than the observed in the rest of the cells. **(C) HEK 293 cells**. 5 µM ZOL significantly decreased all the parameters measured. **(D) HeLa cells.** 10 µM ZOL significantly decreased all the parameters measured. Generally, Q_9 decreased to a greater degree than Q_{10}. Data are represented as mean ± SEM of 8 replicates**.** Differences with the corresponding control are represented as ** ($p < 0.01$) and *** ($p < 0.001$).

We previously have reported changes in Q levels with modifications in the biosynthetic rate of this molecule. Using ^{13}C-4HB, we wanted to study the biosynthesis of Q after a treatment with ZOL. Figure R37 summarize Q biosynthesis of Hepa 1.6 and Tkpts cells treated with 20 µM ZOL. The results so obtained were similar to those previously described for Q levels in both cellular lines, indicating that the general inhibition of Q observed with ZOL is consequence of an altered biosynthesis caused by the drug. Hepa 1.6 showed a decrease in ^{13}C-labeled Q_9, Q_{10} and total Q levels, as well as, a dramatic decrease of the Q_9/Q_{10} ratio in cells treated with ZOL (Figure R37-A). The inhibition of Q biosynthesis was lower for Q_{10} than for Q_9.

On the other hand, the amount of unlabeled Q_9 or Q_{10} (*i.e.*, the quinones synthesized from endogenous 4HB), Q_9/Q_{10} ratio and total Q did not change with the treatment, indicating that ZOL only affects newly synthesized Q. Interestingly, it was found that adding ^{13}C-4HB to the cells affected Q_9/Q_{10} ratio of newly synthesized Q in the absence of ZOL. As depicted in Figure R36-A, the normal Q_9/Q_{10} ratio in Hepa 1.6 is around 4, but adding ^{13}C-4HB raised this value to about 10 (Figure R37-A), indicating that supplementation with a Q ring precursor boost the preferential synthesis of Q_9 over Q_{10}. However, the presence of ZOL abated this effect and, under these conditions, Q_{10} was the preferred isoform synthesized by the cells.

In Tkpts we observed a decrease in ^{13}C-labelled Q_9, total Q and a dramatic decrease of the ratio. According to previous results described for Q_{10} in this cellular line, newly synthesized Q_{10} was enhanced in a treatment with ZOL (Figure R37-B). Here, we also found that ^{13}C-4HB affected the relative proportion of Q isoforms in the absence of ZOL. As depicted in Figure R36-B, the normal Q_9/Q_{10} ratio in Tkpts cells is around 4, but adding ^{13}C-4HB raised this value to about 35, indicating that supplementation with a Q ring precursor also boost the preferential synthesis of Q_9 in this cell line. Again, the presence of ZOL abated this effect and, under these conditions, Q_{10} was by far the preferred isoform synthesized by the cells. The Q system in Tkpts cells was extremely sensitive to modulation by ZOL, in such a way that the drug not only decreased the ratio of ^{13}C-labeled isoforms, but also that of the unlabeled quinones.
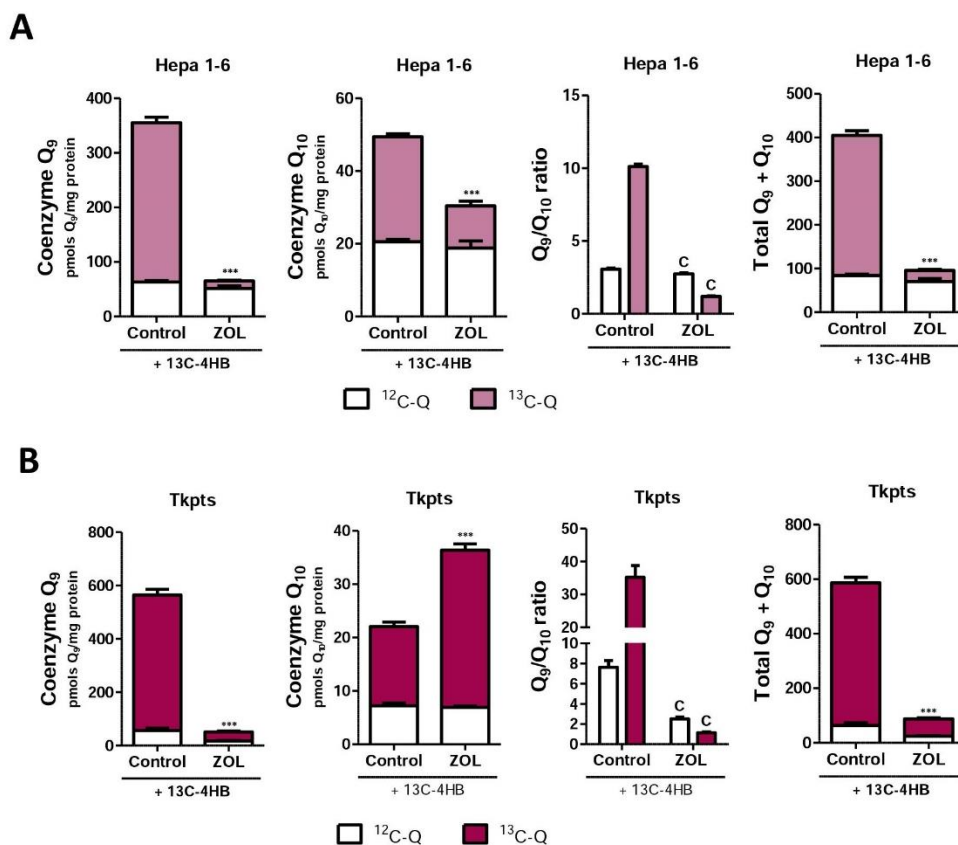
Figure R37. <u>Effect of zoledronic acid on Q biosynthesis of murine cells.</u> Q_9, Q_{10}, Q_9/Q_{10} ratio and total Q levels after a 48 hours incubation of ^{13}C-4HB are represented for each cell line. **(A) Hepa 1.6 cells.** 20 μM ZOL significantly decreased Q biosynthesis for all the parameters measured. The decrease observed for Q_{10} was less pronounced than the observed for Q_9. **(B) Tkpts cells**. 20 μM ZOL decreased Q_9 but increase Q_{10} biosynthesis**.** The decrease of the Q_9/Q_{10} ratio in this cell line was more pronounced than in the rest of the cell lines tested. Total Q biosynthesis decreased significantly. Data are represented as mean ± SEM of 6 replicates**.** Differences with the corresponding control are represented as *** (p < 0.001). **"C"** refers to significant differences (p<0.05) compared with the corresponding control.

Complementary, we also studied Q biosynthesis in human cell lines and similar results were observed in HEK 293 and HeLa (Figure R38-A/B). In both cell lines, Q_9 and to a lesser extent Q_{10} biosynthesis decreased with ZOL. Q_9 is a very minority isoform in human cells but, even so, a decrease in the ratio could be observed, confirming our observations of a lesser inhibition of Q_{10} biosynthesis. Finally, taking together all the results, total Q biosynthesis was significantly inhibited by treatment with ZOL.
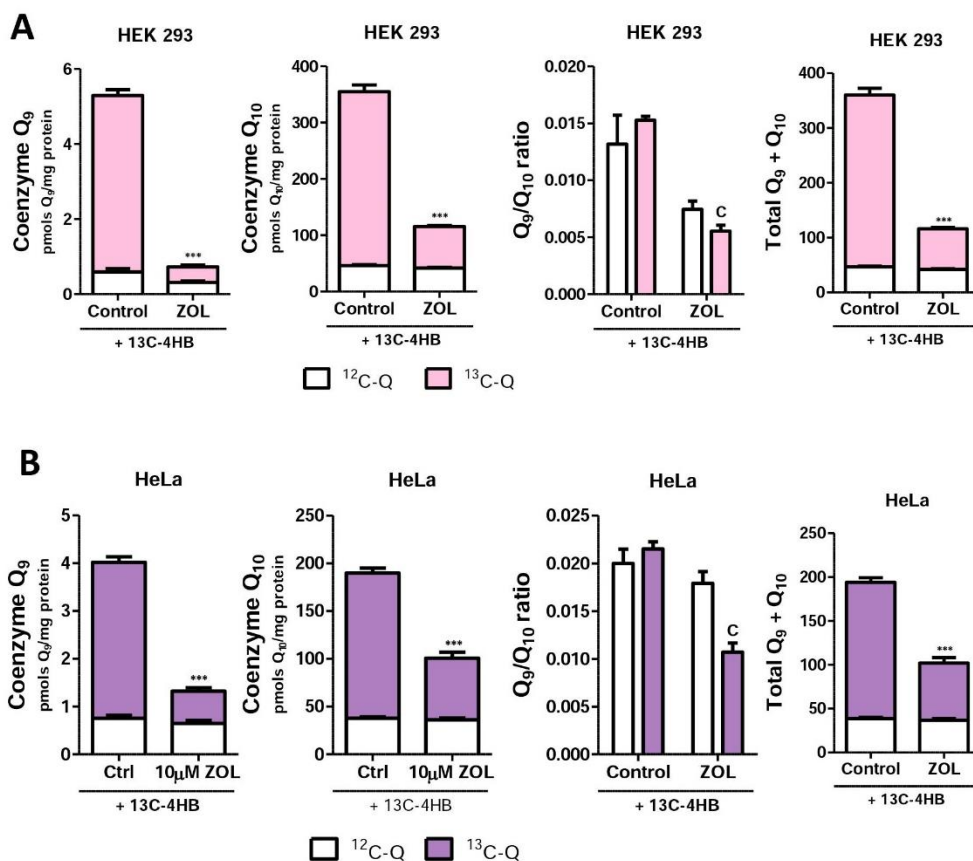
Figure R38. Effect of zoledronic acid on Q biosynthesis in human cells. Q_9, Q_{10}, Q_9/Q_{10} ratio and total Q levels after a 48 hours incubation with ^{13}C-4HB are represented for each cell line. **(A) HEK 293 cells.** 5 µM ZOL significantly decreased Q biosynthesis for all the parameters measured. **(B) HeLa cells**. 10 µM ZOL significantly decreased Q biosynthesis for all the parameters measured. Data are represented as mean ± SEM of 6 replicates**.** Differences with the corresponding control are represented as *** (p < 0.001). **"C"** refers to significant differences (p<0.05) compared with the corresponding control.

3.2.4. Effect of zoledronic acid at different levels of the mevalonate pathway.

ZOL alters different steps in the mevalonate pathway. It inhibits FDPS and GGDPS and produces a general decrease in Q levels. Due to these alterations, levels of isoprenoid intermediates of the mevalonate pathway could be influenced by this treatment. Thus, GPP and FPP levels were measured in both Hepa 1.6 and Tkpts cells and the results were represented in Figure R39-A/B. ZOL produced a huge increase in GPP levels of Hepa 1.6 cells whereas FPP levels were not modified (Figure R39-A). However, in Tkpts cells a treatment with ZOL did not modify neither GPP nor FPP levels, although, an upward trend was observed for GPP (Figure R39-B).

Complementary, we decided to study cholesterol as another branch end-product of the mevalonate pathway. ZOL is known to inhibit cholesterol biosynthesis [90, 161] acting as inhibitor of the SQS. We wondered whether cholesterol levels would be also decreased in our model after a treatment with ZOL and results are represented in Figure R39-C/D. Hepa 1.6 cells did not modify cholesterol levels after a 48 hours treatment with ZOL but, contrary, Tkpts cells decreased it significantly. Inhibition of SQS by ZOL seems to be dependent of the cellular line, being more effective in kidney-derived cells.
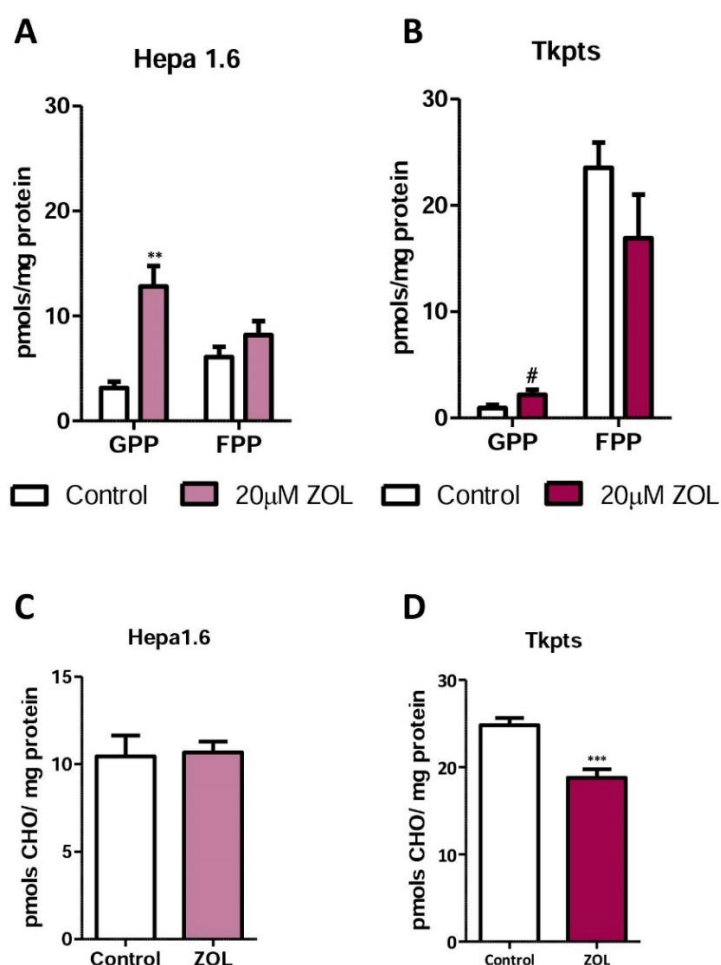
Figure R39. **Effect of zoledronic acid on GPP, FPP and cholesterol levels in mouse cell models.** **(A) GPP and FPP levels in Hepa 1.6 cells.** 20 μM ZOL significantly increased GPP levels but did not change FPP levels. **(B) GPP and FPP levels in Tkpts cells**. 20 μM ZOL did not change neither GPP nor FPP, although, an upward trend was observed for GPP. **(C) Cholesterol levels in Hepa 1.6 cells.** Treatment with ZOL did not affect cholesterol levels in this cell line. **(D) Cholesterol levels in Tkpts cells.** ZOL significantly decreased cholesterol levels. Data are represented as mean ± SEM of at least 4 replicates**.** Differences with the corresponding control are represented as ** (p < 0.01) and *** (p < 0.001). **"#"** represent a trend (p<0.05 in the one-tail statistical analysis) compared with the corresponding control.

3.2.5. Effect of upstream mevalonate pathway inhibitors on Q and CHO levels.

Statins and 4HB produce an upstream inhibition of the mevalonate pathway, contrary to all our previous strategies, so we thought a comparison of their effects on Q and cholesterol levels would be of interest.

Lovastatin was used as an example of the effect of the statins in our *in vitro* model. First, we performed a viability curve in order to choose the most suitable concentrations of this product for the cells. Figure R40 depicts of the results of MTT assays performed to reveal the tolerance of Hepa 1.6 and Tkpts cells to lovastatin. Hepa 1.6 viability was affected negatively by lovastatin at concentrations of 5 µM and higher, with concentrations above 20 µM being extremely toxic for the cells. On the other hand, deleterious effects in Tkpts appeared at concentrations of 20 µM and higher. In Tkpts cells, concentrations between 0.5 and 5 µM lovastatin produced significant increases of the MTT signal, which could be related with a possible improvement of the growth rate. According to these results, we decided to use the maximum concentration that did not cause any toxic effect. In Hepa 1.6 cells this concentrations is 1 µM lovastatin, so we decided to maintain the same concentration for both cellular lines.
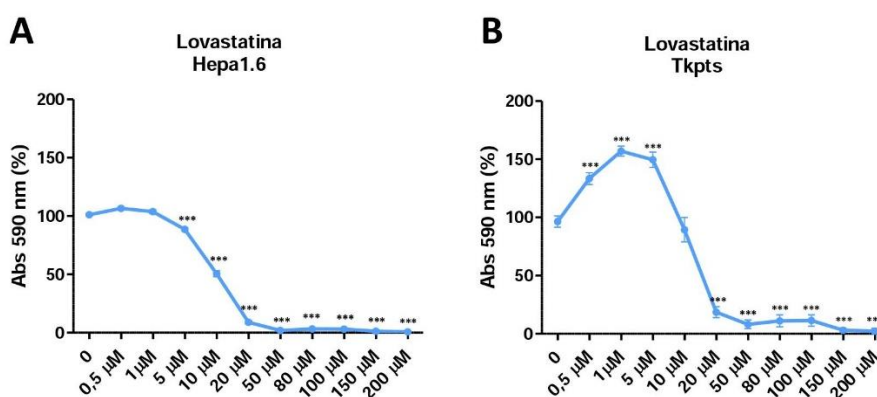
Figure R40. Effect on cell viability after a treatment with lovastatin. A MTT assay was performed for each cell line after treatment with lovastatin at different concentrations. **(A) Hepa 1.6 cells.** Lovastatin affected cellular viability at concentrations of 5 µM and higher. **(B) Tkpts cells**. Lovastatin affected cellular viability at concentrations of 20 µM and higher. The increase of absorbance observed at concentrations of lovastatin between 0.5 and 5 µM possibly reflects an improvement of the growth rate. Data are represented as mean ± SEM of 8 replicates. Differences with control are represented as *** ($p < 0.001$).

Q levels of cells treated with lovastatin are represented in Figure R41. Hepa 1.6 cells decreased Q_9, Q_{10} and Q total levels after a treatment with lovastatin, with a maintenance of Q_9/Q_{10} ratio (Figure R41-A). Meanwhile, in Tkpts, lovastatin decreased Q_9 and total Q levels without affecting Q_{10}. Lovastatin did not affect Q_9/Q_{10} ratio, although a downward trend was observed in this cell line (Figure R41-B).
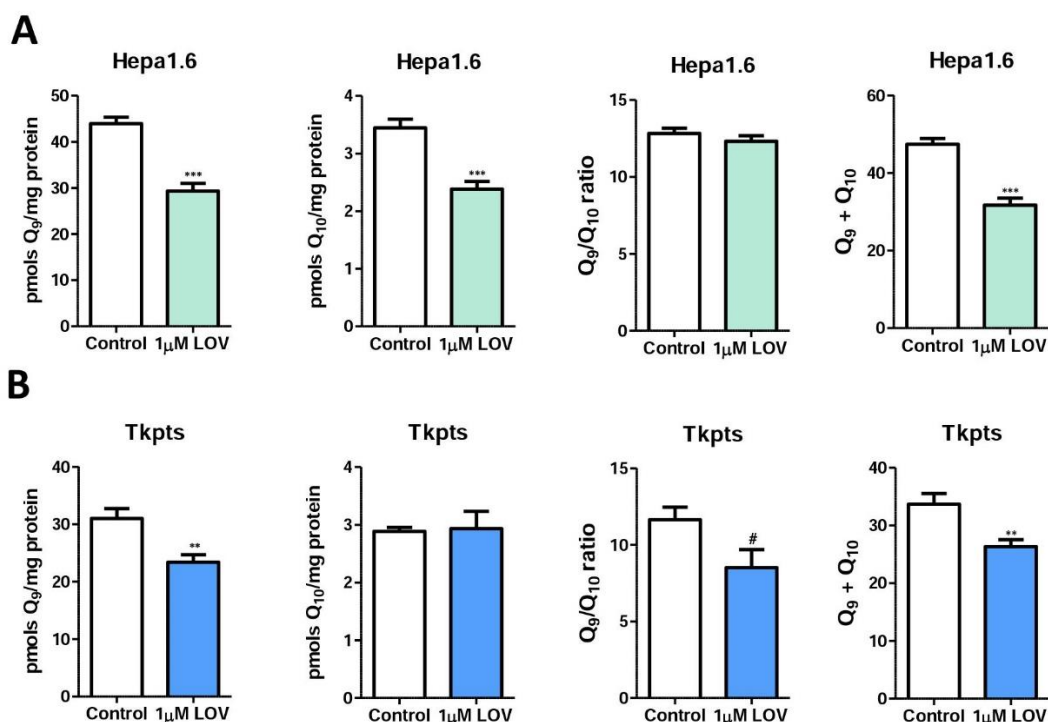
Figure R41. **Effect lovastatin on Q levels of hepatic and renal mouse cell lines.** Q_9, Q_{10}, Q_9/Q_{10} ratio and total Q levels are represented for each treatment. **(A) Hepa 1.6 cells treated with 1 μM lovastatin.** Lovastatin decreased Q_9, Q_{10} and Q total levels without affecting the Q_9/Q_{10} ratio. **(B) Tkpts cells treated with 1 μM lovastatin.** Lovastatin decreased Q_9 and Q total levels without changing Q_{10}. The Q_9/Q_{10} ratio displayed a downward trend. Data are represented as mean ± SEM of 6 replicates. Differences with the control are represented as ** ($p < 0.01$) and *** ($p < 0.001$). # represent a trend ($p < 0.05$) compared with the corresponding control.

We have studied 4HB as a Q precursor in Chapter 1 but this phenolic compound is also known to inhibit upstream enzymes of the mevalonate pathway when used at high concentrations. We have represented in Figure R42 the same dose-response curves of Hepa1.6 and Tkpts treated with different concentrations of 4HB (represented in Chapter 1, Figure R10) in order to evaluate complementary ideas not described previously.
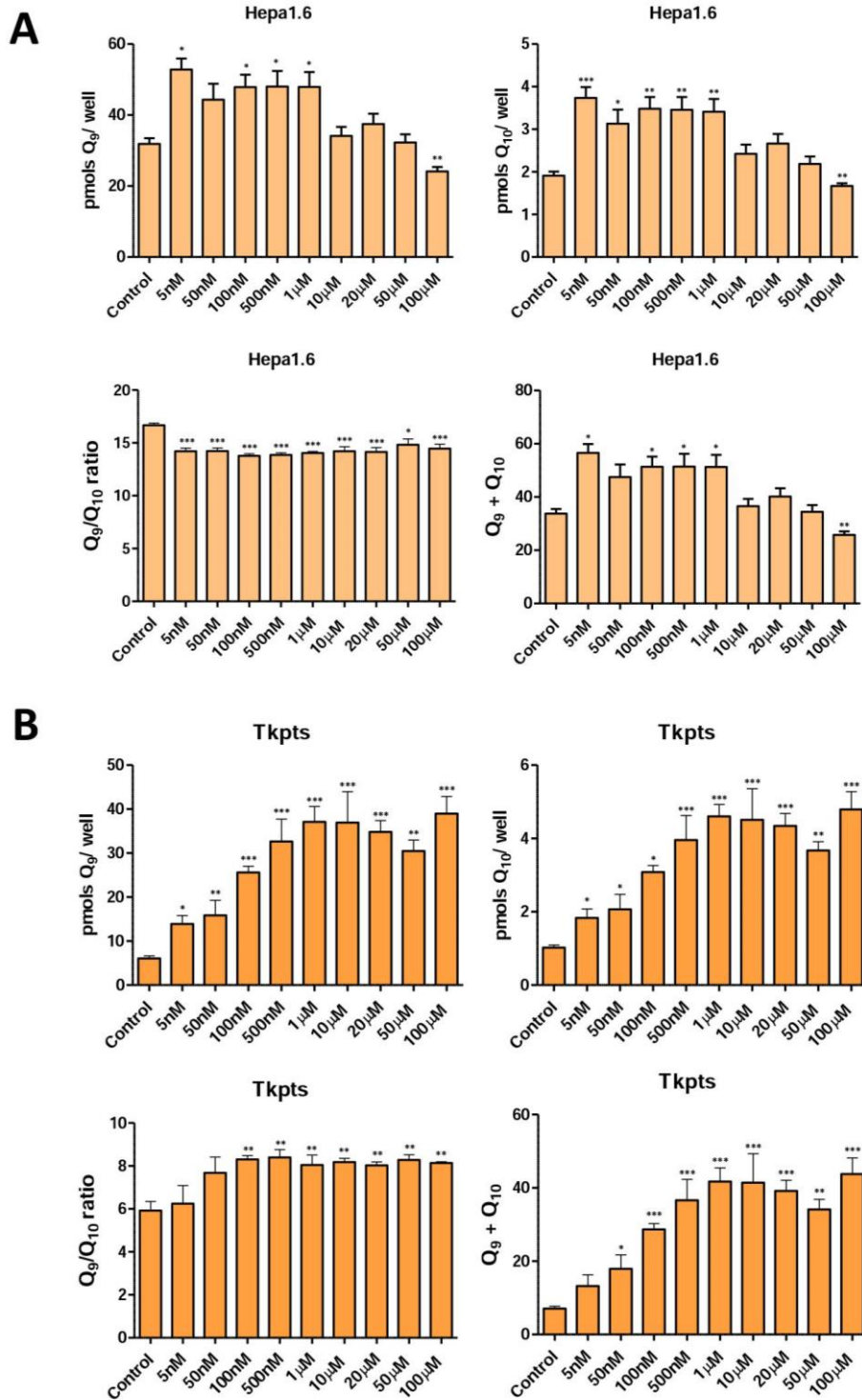
Figure R42. Effect 4HB on Q levels of hepatic and renal mouse cell lines. Q_9, Q_{10}, Q_9/Q_{10} ratio and total Q levels are represented for each treatment. **(A) Hepa 1.6 cells treated with 4HB.** 4HB increased Q levels at low concentrations and decreased it at high concentrations. Q_9/Q_{10} ratio decrease since 5nM onwards. **(B) Tkpts cells treated with 4HB.** 4HB increased Q_9, Q_{10} and Q total levels at concentrations of 50 nM and higher. Q_9/Q_{10} ratio increased since 100 nM onwards. Data are represented as mean ± SEM of 6 replicates. Differences with the control are represented as * ($p < 0.05$), ** ($p < 0.01$) and *** ($p < 0.001$).

In Hepa 1.6 cells, Q levels (both isoforms and the total levels) were increased by 4HB concentrations between 5 nM and 1 µM but this response was absent at concentration of 10 µM and higher and, even, an inhibition of Q level was observed at 100 µM (Figure R42-A). Q_9/Q_{10} ratio was inverted from concentration of 5 nM and higher. Conversely, in Tkpts Q_9, Q_{10} and total Q increased since very low concentrations of 4HB. Q_9/Q_{10} ratio increased from concentrations of 100 nM and higher (Figure R42-B). The behavior of Tkpts cells are in agreement with the role of 4HB as Q ring precursor, being identify previously as a limiting step in the biosynthesis of Q in kidney cells. However, in Hepa 1.6 this phenolic compound behave as Q ring precursor at low concentrations whereas at high concentrations its role change, acting as an inhibitor of the mevalonate pathway.
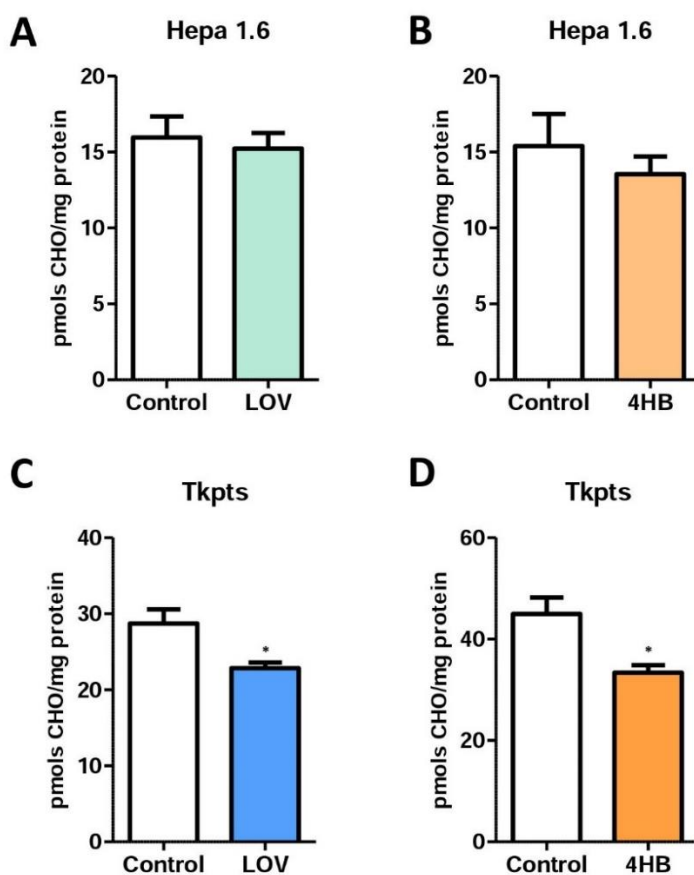
Figure R43. Effect lovastatin and 4HB on CHO levels of hepatic and renal mouse cell lines. (A) Hepa 1.6 cells treated with 1 µM lovastatin. Lovastatin did not change CHO levels. **(B) Hepa 1.6 cells treated with 1 µM 4HB.** 4HB did not change CHO levels **(C) Tkpts cells treated with 1 µM lovastatin.** Lovastatin decreased CHO levels, possibly by inhibiting SQS activity. **(D) Tkpts cells treated with 1 µM 4HB.** 4HB decreased CHO levels. Data are represented as mean ± SEM of 6 replicates. Differences with control are represented as * ($p < 0.05$).

Additionally, we have measured cholesterol levels in these cellular models after a treatment with 1 µM lovastatin and 1 µM 4HB (Figure R43). Neither lovastatin nor 4HB had any effect on CHO levels in Hepa 1.6 cells (Figure R43-A/B). Meanwhile, the same treatments carried out in Tkpts cells produced a significant decrease of CHO levels (Figure R43-C/D). These results indicate that the inhibition of SQS in Tkpts cell is more pronounced than in Hepa 1.6 cells.

Discussion

1. CHAPTER 1: <u>Effect of different phenolic compounds on Q metabolism</u>

1.1. Polyphenols as Q ring precursors

Polyphenols, widely present in foods and beverages of plant origin, have received great interest during the last years due to their positive effects on human health as, for example, the prevention of diseases like cancer or chronic inflammation [101]. The beneficial properties of polyphenols have been partially linked to their antioxidant activity as well as to their ability to modulate molecular targets and signaling pathways. Another important factor is the molecular structure of these compounds, which can modulate their properties and functions. To this sense, the 3-hydroxyl group in flavonols is considered as an especially important determinant for their antioxidant activities [98].

As a lipid-soluble antioxidant that can be endogenously synthesized by all organisms, Q plays a major role in antioxidant defense [10]. The stilbene, resveratrol, and some phenolic compounds such as 4HB, vanillic acid, protocatechuic acid and *p*-coumarate have been described as Q ring precursors in *S. cerevisiae* and mammal cells [52, 56], but the possibility that polyphenols could actually increase the levels of this lipid antioxidant in cells has not been explored. The capacity to increase Q levels endogenously could be a promising approach to palliate Q deficiencies associated with aging or disease. Kidney cells are especially sensitive to a decrease of Q levels, and a nephrotic syndrome is a major clinical phenotype in Q deficiencies [162]. For this reason, we selected two kidney-derived lines, murine Tkpts and human HEK 293 cells, to study the putative capacity of different polyphenols to increase Q levels.

Two stilbenes: resveratrol and piceatannol, and two flavonols: quercetin and kaempferol, were selected in the first phase of our studies. Resveratrol has been the subject of intense research due to its purported cardiovascular protective, antiplatelet, antioxidant, anti-inflammatory, blood glucose-lowering and anti-cancer activities (reviewed in [163]). Piceatannol is a hydroxylated analogue of resveratrol and shares the structural motif and biological activities, being even more potent in some studies [164]. Apart from the beneficial effects of stilbenes, the regular consumption of flavonoids is related to reduced risk of a number of chronic diseases, including cancer, cardiovascular disease and neurodegenerative disorders (reviewed in [165]). Flavonoids are divided into several groups, with flavonols being those containing the 3-hydroxy group that has been

considered very important for antioxidant activity. Thus, for our determinations we also chose quercetin and kaempferol, the two most common compounds in this group. Among these four compounds, only kaempferol efficiently increased Q levels in kidney cells and, interestingly, the effects were observed at concentrations that can be attainable physiologically both by consumption of flavonoids-containing food and by oral supplementation [166-168]. Since this ability may derive from its chemical structure, we also tested additional structurally related flavonoids in a second phase of our studies. In this case, we chose two flavones, apigenin and luteolin, and one flavanone, naringenin. Of these, only apigenin caused a slight increase in Q_9 and Q_{10} at selected concentrations, although its effects were extremely limited in comparison with kaempferol and moreover, a slight inhibition was even observed at one of the concentrations tested.

In addition, kaempferol has been previously described as a Sirt3 activator. This mitochondrial sirtuin mediates the adaptation of increased energy demand during adverse conditions to increase the production of energy equivalents, and also deacetylates and activates mitochondrial enzymes involved in fatty acid β-oxidation, amino acid metabolism, the electron transport chain, and antioxidant defense [150]. Our results have shown that mitochondrial levels of Sirt3 were indeed increased after kaempferol treatment, confirming these effects also take place in renal cells. However, treatment of kidney cells with NAM, a general inhibitor of sirtuin activity, did not affect the kaempferol-induced increase of Q levels, indicating that Sirt3 activation does not mediate kaempferol effects on Q system. Furthermore, Q levels measured in different tissues obtained from Sirt3 knockout mice did not differ from those measured in their wild-type littermates, indicating that Sirt3 does not modulate Q biosynthesis.

The increase in Q levels by kaempferol in kidney cells depends directly on the stimulation of Q biosynthesis. The kaempferol-mediated increase in Q was blocked by the Q biosynthesis inhibitor PABA and a competitive behavior against the incorporation of the ^{14}C-labelled ring precursor 4HB was found for this polyphenol. Moreover, cells treated with ^{13}C-kaempferol generated newly synthesized $^{13}C_6$-Q, demonstrating that kaempferol actually behaves as a novel Q ring precursor in mammalian cells. However, the exact metabolism of kaempferol that is responsible for its incorporation into the Q biosynthetic pathway remains to be established, although two possibilities can be proposed: (1) kaempferol could act directly as Q precursor being itself a substrate for the COQ2

transferase and would be subsequently metabolized and modified by different COQ proteins until it reaches the final structure of Q; or alternatively (2) kaempferol could be cleaved in the cell before entering the Q biosynthetic pathway to yield potential precursors which would be then integrated into this route.

Previous studies have described that flavonoids can be transformed into phenolic acids by colonic microflora. However, the type of metabolic products depends on what phenolic compound is metabolized and its specific structure [169]. Cleavage of kaempferol by colonic microflora occurs between C-3 and C-4 carbons of ring C, forming 4HPAA [152, 153] derived from the B ring, which is then rapidly decarboxylated to form *p*-cresol [170]. Moreover, Serra *et al.* [169] have detected 4HB derived from the metabolic pathway of kaempferol in rat microflora, possibly as a result of further 4HPAA processing. If renal cells were able to perform a fragmentation of kaempferol similar to that described for colonic bacteria, this metabolism might be an efficient source of Q precursors. However, in Tkpts cells neither 4HPAA nor *p*-cresol increased Q levels or competed with ^{14}C-4HB, demonstrating that these compounds do not act as Q ring precursors in our *in vitro* model. Therefore, even if kaempferol is cleaved in renal cells before entering the Q biosynthetic pathway, these known metabolites are not involved in augmenting Q levels.

A non-flavonoid compound like curcumin, which contains two ferulic acid moieties linked via a methylene bridge at the carbonyl group C atoms, also undergoes metabolism in animals, possesses antioxidant capacity and produces beneficial effects on diabetes, inflammation and neurodegenerative disease by modulating multiple signal molecules (transcription factors, enzymes, *etc.*) and controlling gene expression [171]. Structure of curcumin and ferulic acid differs substantially from that of flavonoids and stilbenoids, so testing their effect on Q system was also of considerable interest. However, our data indicate that neither curcumin nor ferulic acid increase Q levels, and only ferulic produced a small but detectable signal of D$_3$-labeled Q in kidney cells.

As part of this research, the effect of polyphenols as potential precursors of Q biosynthesis in *S. cerevisiae* was also studied at the University of California, Los Angeles. These results showed that Q$_6$ levels were not enhanced with any of the compounds tested (kaempferol, ferulic acid, vanillin or curcumin). Moreover, studies performed with ^{13}C-labelled compounds showed that neither kaempferol nor vanillin are used efficiently in Q biosynthesis, in contrast with ^{13}C$_6$-4HB that is rapidly incorporated into ^{13}C$_6$-Q$_6$

increasing significantly the total Q content in yeast (see Figure 7 in Appendix II) [172] . This complementary study allowed us to describe the previous results obtained with kaempferol as specific of mammalian cells.

As indicated above, chemical structure is a key factor that define the functions and the effect of the different polyphenols. In our study, flavonoids were more efficient used in Q biosynthesis than other non-flavonoid compounds like stilbenoids and curcuminoids. Moreover, one member of the flanovol group (kaempferol) and one member from the flavone group (apigenin) were the ones that displayed the strongest effect increasing Q_9 and Q_{10} levels in renal cells. The difference between flavonols and flavones is distinguished by the presence of a hydroxyl group in the C3 position. This group seems to be very important because kaempferol (that possesses this group) is much more efficient in increasing Q levels than apigenin and, interestingly, this specific OH group has been previously linked to an increase of antioxidant activity [98]. However, kaempferol and apigenin have a common characteristic that also seems to be an important determinant for their effect on Q biosynthesis: both compounds only possess one hydroxyl group in the B ring. The presence of two hydroxyl groups in this ring, as it is the case for quercetin and luteolin, abolishes the effect of these flavonoids on Q system. One study that compared the anxiolytic effect of different flavonols noted that this activity decreases with an increasing number of hydroxyl groups in the B ring: kaempferol revealed again the strongest effect, whereas myricetin (which possesses three hydroxyl groups) did not have any effect [173].

1.2. 4HB as a limiting step in the biosynthesis of Q

Whatever the metabolic route involved, an increase of alternative Q ring precursors in cells will only turn into higher Q levels if cells have low availability of endogenous 4HB. Pierrel *et al.* [54] described 4HB as a limiting step in the biosynthesis of Q in *S. cerevisiae* cells and, as we have demonstrated here, this also holds true for kidney cells, although not for other cell lines such as MEFs, Hep G2 or HL-60. The increase of Q observed after a treatment with nM concentrations of 4HB or kaempferol confirms that the endogenous availability of this precursor is very low in kidney cells of both mouse and human origin. The fact that many cell types do not show increased Q levels in response to exogenous 4HB is in agreement with the early demonstration that 4HB may be present at saturating

concentrations in liver, as determined by *in vitro* assays with liver tissue slices [174]. Tissue-specificity of ring precursor supplementation on Q biosynthesis is also supported by the observations of Wang et al. [58]. These investigators demonstrated that adding the ring precursor 2,4-dihydroxybenzoic acid (2,4-DHB) to the drinking water of wild-type mice resulted in an increase of Q_9 levels in mitochondrial kidney but a decrease in heart mitochondria as well as in liver and muscle homogenates. The specific increase of Q_9 levels in kidney but not in other tissues is in agreement with our results obtained with renal cell lines, thus confirming that the availability of ring precursors is a tissue-specific feature. Moreover, these researchers showed that giving 2,4-DHB to Q-deficient Mclk1 KO mice resulted in a healthier phenotype, an increase in Q levels and an improvement of the mitochondrial respiratory capacity in heart, kidney and skeletal muscle [58], indicating that the addition of Q ring precursor could improve the endogenous synthesis of this lipid in a disease phenotype.

In a previous report [154], we demonstrated maximal levels of COQ2 polypeptide in those organs displaying the highest Q concentrations, such as kidney and heart. In accordance, the murine kidney-derived Tkpts cells also showed significantly higher levels of both Q and COQ2 polypeptide than murine hepatic Hepa 1.6 cells. Moreover, Tkpts cells showed lower ratio than Hepa 1.6, as also occurs in kidney and liver tissues, revealing that the maintenance of a given Q_9/Q_{10} ratio might be important for proper function of each tissue and this property is maintained in cell lines derived from these tissues. Higher levels of the COQ2 transferase might maintain low cellular concentrations of the ring precursor 4HB due to its rapid use by the Coq2 prenyltransferase activity. Higher COQ2 levels could also account for making these cells particularly responsive to supplementation with ring precursors as 4HB or kaempferol, leading to a significant increase of Q levels. Further experiments will be needed to fully understand how kaempferol is metabolized to take part directly in the biosynthesis of Q.

Usually Q levels are a direct reflect of the amount of inner mitochondrial membrane present in the cells and, since this membrane is the most abundant in mitochondria, the amount of Q is a good marker of mitochondria abundance. Based on our previous observations of the levels of Q and COQ2 in Tkpts and Hepa 1.6 cells we also focused our research towards the determination of more specific mitochondrial markers as VDAC and the different complexes of the respiratory chain. Our results showed that VDAC

levels were drastically decreased in Tkpts cells whereas complexes I, III and IV were increased, comparing to Hepa 1.6. Taken together these results might suggest that Tkpts cells might have less or smaller mitochondria (as deduced from dramatically decreased levels of VDAC), but they contain more surface of mitochondrial cristae inside this organelle that could explain the highest levels of Q observed, as well as a higher abundance of electron transport chain complexes.

Nevertheless, although VDAC is widely used as mitochondrial marker [175], its use could be quite controversial. In mammalian cells, there are three isoforms of VDAC (VDAC1, VDAC2 and VDAC3) but previous studies have shown that they are not equally abundant, with VDAC1 being 10 times more abundant than VDAC2 and 100 times more abundant than VDAC3 [176]. Thus the majority of VDAC expressed inside cells is VDAC1 [177], which is mainly localized in the outer mitochondrial membrane. However, its exclusively mitochondrial location is still debated because VDAC has been also found on the cell surface and in the endoplasmic reticulum [178]. The specific antibody we used to detect VDAC is specifically designed against the 3 isoforms of the protein, so a variation in the proportion of the isoforms between the renal and the hepatic cell lines could influence our results. Moreover, VDAC levels were measured in total cell extracts so the abundance of the endoplasmic reticulum in the two cell lines tested is another factor to take into account. According to these observations, more direct approaches will be needed to determine the relative mitochondrial abundance in Tkpts and Hepa 1.6 cells.

1.3. Concluding remarks and perspectives

Taken all the results together, we have demonstrated that some components of a healthy diet can influence Q levels in renal cells. The flavonol kaempferol is identified here to have the strongest effect on increasing Q levels due to its action as a novel ring precursor in Q biosynthesis. The ability of kaempferol to simultaneously increase Q and Sirt3 levels links several of the beneficial effects previously described for this molecule. Moreover, we described 4HB as a limiting step in the biosynthesis of Q in mouse and human renal cells. Indeed, this knowledge can represent a step forward in the design of new treatments to alleviate the symptoms of Q deficiencies. Further experimentation is warranted to elucidate whether dietary kaempferol supplementation also increases Q levels in animals, both under normal and Q-deficient conditions. Extensive metabolism of kaempferol when

administered with the diet results in very low levels of circulating kaempferol in mice [179], which could hamper potential beneficial effects on Q biosynthesis. However, given the specific response of kidney to small amounts of ring precursors, it is still possible that dietary kaempferol could lead to increased Q levels in this organ, as previously observed for 2,4-DHB [58]. Increasing the availability of Q precursors in cells could move the metabolic flux in favor of the synthesis of Q, helping to ameliorate the phenotype associated with certain Q deficiencies, at least for some organs such as kidney.

CHAPTER 2: <u>Role of different fatty acids in Q metabolism</u>

2.1. Fatty acids as regulators of Q levels

Dietary fat, which contributes to food palatability and preservation, is an essential component of diet, and the presence of different types and quantities of fat is strongly associated with different culture and culinary traditions [180]. Dietary fat is classically defined as triglycerides (fats and oils), phospholipids, and sterols (cholesterol), including various classes of fatty acids (saturated and unsaturated). In the human body, fat is an energy and essential fatty acids source, an efficient energy long-term storage, and also a carrier of the fat-soluble vitamins A, D, E, and K. Moreover, fat provides insulation against temperature and protects vital organs from physical trauma [181]. Dietary fat and it associated nutrients play a critical role in health and, therefore, a bad nutrition could be related with some disorder such as cardiovascular diseases, obesity, diabetes and, even, cancer.

Membranes are plastic structures that can adapt their lipid composition according to the principal dietary fat source, which also influences Q levels and its biosynthesis. To deepen into the regulatory effects that different lipid sources could exert on Q metabolism we have designed an *in vitro* model in which mouse liver hepatoma cells (Hepa 1.6 cells) were treated with three different lipid emulsions that differ in their fatty acid composition. The composition of these lipid emulsions is based on n-3 PUFA (*Lipoplus*), n-6 PUFA (*Lipofundin*) or n-9 MUFA (*ClinOleic*). Including an emulsion based on saturated lipids would have been also very interesting, but no lipid emulsion with this composition is available [182]. Q determinations in Hepa 1.6 cells treated with the three emulsions showed a clear effect of different lipid source on the levels of this antioxidant molecule. *Lipoplus* and *Lipofundin* (and, therefore, PUFAs), and to a lesser extent, ClinOleic (MUFA source) contribute to the regulation of Q levels in the cells, increasing Q_{10} and, hence, decreasing considerably the Q_9/Q_{10} ratio. These emulsions also increase Q_9 levels as well as total Q content but the effect on Q_9 is more variable and always of lower magnitude than the effect exerted on Q_{10}. It is expected that cells treated with PUFAs would have more unsaturation in their membranes being thus more sensitive to oxidative stress. The increase of Q levels could be the consequence of high request of antioxidant defense in these cells containing high levels of PUFA in their membranes. Conversely, cells treated with MUFA did not increase Q levels as those cultured in the presence of

PUFA, possibly due to the lower levels of unsaturation of these membranes. However, this hypothesis solely cannot explain the different regulation of the two Q isoforms that leads to the alteration of the Q_9/Q_{10} ratio.

The effects of fatty acids on Q levels described above take place both under high-glucose and low-glucose conditions, although the effects were of less magnitude under conditions of restricted carbohydrate availability. A smaller magnitude of fatty acids effects in low-glucose can be explained by the existence of a regulation of Q levels by glucose availability itselfsince in low-glucose conditions, Q levels in control cells were significantly higher than in the corresponding control cells grown in high-glucose medium. Calorie restriction (CR) is a dietary regimen that reduces calorie intake without incurring in malnutrition, and it is the only non-pharmacological intervention know to retard aging and its deleterious symptoms in many model organisms [183]. Attending to Q, previous studies came up with the idea that alterations in Q biosynthesis are part of the metabolic adaptation to CR in mice [154], so our results agree with an adaptative response of cells towards a limited carbon source. In a parallel study performed in our research group other parameters associated with CR were also measured in cells grown under the same conditions as those used for Q determinations. Although the levels of mitochondrial ROS as well as mitochondrial membrane potential are known to be decreased in CR conditions [184, 185], in our cellular model these parameters were not altered (Gutiérrez-Casado, personal communication). These results suggest that culturing cells with limiting amounts of glucose and decreased insulin (because of the use of 10% FBS) does not mimic CR *in vitro* in the case of hepatic cells. This model has been previously proposed to mimic CR in skeletal muscles dissected from rats [186]. It remains for further investigation to study the effects of low glucose and lipid emulsions on Q system in insulin-responsive cells [187].

Since most of the cellular Q is located in mitochondria, the structure, number, size and distribution of this organelle greatly influences the overall content of this antioxidant in cells. For instance, cold adaptation and exercise increase mitochondrial number in the liver and skeletal muscle and, thereby, the total content of Q in these tissues is also increased [95]. We decided to study the ultrastructure and the abundance of this organelle in order to evaluate whether the regulation of Q levels by fatty acids involved an alteration of mitochondrial ultrastructure and/or mitochondrial abundance. Stereological

measurements carried out using electron microscopy micrographs of Hepa 1.6 cells treated with *Lipoplus* showed that n-3 PUFA significantly increased mitochondrial volume and the number of mitochondria *per* cell in glucose standard conditions. These data agree with previous results that described increased number of mitochondria *per* cell in hepatocytes of mice fed with a PUFA-enriched diet in calorie-restricted conditions, especially with a diet containing fish oil-as the predominat fat source [136]. However, changes observed under conditions of restricted glucose availability were less clear in our model. The increase of mitochondria in size and number could explain, at least partially, the increase of Q levels previously described. However, these changes at the level of mitochondrial ultrastructure could not explain the alteration of the Q_9/Q_{10} ratio. Additional experimentation is thus necessary to go deeper into the regulation of this antioxidant molecule by exogenous fatty acids.

Autoxidation of unsaturated fatty acids is a deleterious process to cells that can occur as consequence of exposure to an oxygen-enriched atmosphere. In mammalian cells, PUFAs are substrates for complex enzymatic systems that oxidize and convert them into a variety of lipid mediators [156]. Due to its antioxidant function, the increase of Q levels previously observed with the lipid emulsions containing high levels of PUFA could represent a protective response against this phenomenon. Furthermore, it was previously reported that Q is needed for providing protection against oxidative stress caused by PUFA autoxidation in yeasts [128]. In a previous study, antioxidants such as BHT, Trolox or vitamin E were used satisfactory to rescue the cellular toxicity that a treatment with PUFAs at elevated temperature causes in wild-type yeast [156]. Therefore, we decided to test whether the previous observed increase of Q mediated by fatty acids was influenced by lipid autoxidation. Cells were co-treated with *Lipoplus* and BHT or Trolox and Q levels were then measured. Results so obtained were generally similar to the previous effects observed after a treatment with *Lipoplus* alone, suggesting that lipid autoxidation is not influencing the increase of Q caused by PUFA.

2.2. Effect of fatty acids in Q biosynthesis and the mevalonate pathway

We wondered if the fatty acid-mediated increase of Q would be influenced by an alteration of its biosynthesis rate. Thus, we decided to measure directly Q biosynthesis by providing the labeled precursor ^{13}C-labelled 4HB to cells cultured in the presence of lipid

emulsions. This ^{13}C-labelled precursor allowed us to quantify the ^{13}C-Q produced during 48 hours of treatment with *Lipoplus* and *ClinOleic*. The PUFA-containing emulsion increased Q_9, total Q and, specially, Q_{10} biosynthesis, and therefore produced a decrease in the ^{13}C-Q_9/^{13}C-Q_{10} ratio. However, the emulsion containing MUFA did not affect Q_9 or total Q biosynthesis, but even decreased Q_{10} levels, thus increasing the ^{13}C-Q_9/^{13}C-Q_{10} ratio. These results demonstrate that enhancement of Q biosynthesis accounts for the increase of Q levels in cells treated with PUFA. However, putative changes of the Q biosynthesis rate cannot explain the increase of Q levels described with MUFA.

Q, as well as others polyisoprenoid lipids such as cholesterol, dolichol or ergosterol, is synthetized in a branch derived from the mevalonate pathway [188]. Little is known about Q metabolic regulation by PUFA, in contrast with the widely studied mechanism that regulates cholesterol. This lipid homeostasis is regulated by a family of membrane-bound transcriptional factors designated sterol regulatory element binding protein (SREBP) [189]. In human, hamsters and mice there are three isoforms of SREBP. Two of them, designated SREBP-1a and SREBP-1c, are produced from a single gene (*SREBF1*) by using alternative transcriptional start sites. The third member, called SREBP-2, is encoded by a separate gene (*SREBF2*) and shares approximately 50 % homology with the SREBP-1 isoforms [190]. This family of transcription factors regulate transcription of many genes that encode enzymes of the mevalonate pathway: HMG-CoA synthase, HMG-CoA reductase, FDPS and SQS. Moreover, SREBPs modulate the transcription of genes encoding enzymes of fatty acid synthesis and uptake, including acetyl CoA carboxylase, fatty acid synthase, stearoyl CoA desaturase-1, and lipoprotein lipase [191]. Although there is some overlap in their targets, SREBP-2 preferentially enhances transcription of genes that control cholesterol synthesis, whereas SREBP-1 enhances genes of the fatty acid synthetic pathway [190].

Previous studies have revealed that fatty acids and cholesterol, the final products of the pathway regulated by SREBPs, are themselves regulators of the same pathway by an auto-loop regulatory circuit. Moreover, they are also regulated by a superfamily of nuclear hormone receptors, called liver X receptor (LXRs), that are ligand-activated transcription factors [192]. Sterols activate LXR and, therefore, their role as regulators of SREBP-1c mRNA levels has been also described [193]. Concretely, it is proposed that fatty acids can act as competitive antagonists of LXR in cultured rat hepatoma and human HEK 293

cells. This antagonism appears to explain, at least partially, the ability of unsaturated fatty acids to lower the levels of mRNA for SREBP-1c, which transcription has been shown to depend on an endogenous sterol LXR ligand. The lowered SREBP-1c, in turn, leads to a fall in mRNAs for enzymes responsible for synthesizing unsaturated fatty acids, thus completing the feedback loop [192, 193]. The ability of unsaturated fatty acids to inhibit SREBP-1 expression seems to be related to chain length and degree of unsaturation. The longer the chain length and the higher degree of unsaturation, the more potent the fatty acid is in suppressing SREBP-1 expression [190]. Unsaturated fatty acids also appear to lower SREBP-1 mRNA by accelerating its degradation in hepatocytes [193] or by reducing the maturation of SREBP-1 proteins [194]. However, the effect of MUFA downregulating SREBP-1 is quite controversial in cellular models. While in some studies the effects of n-9 MUFA are similar to those observed with PUFA [193, 195], other studies have related the ability to decrease SREBP-1 levels exclusively with PUFA [190, 196]. Moreover, intestinal epithelial cells treated with SFA, MUFA or PUFA suppressed *de novo* fatty acid synthesis but only PUFA decreased SREBP-1 protein and SREBP-1c mRNA levels [190]. This study suggests that MUFA effects might be carried out by a different mechanism that do not involve SREBP mRNA levels, possibly accelerating the degradation of the mRNA or impairing the maturation of SREBP proteins. This controversy does not exist *in vivo*, where it is described that uniquely dietary n-6 and n-3 PUFA, but not saturated nor n-9 unsaturated fatty acids, reduce the hepatic abundance of SREBP-1c mRNA [197]. Thus, the *in vivo* regulation of SREBP-1 metabolism by fatty acids appears to differ from that of the cell line models.

PUFA inhibit SREBP-responsive genes such as HMG-CoA reductase and FDPS. Inhibition of FDPS (FDPS mRNA and protein levels) was described in hepatoma cells and also in liver from mice fed with n-3 PUFA, resulting in a decrease of cholesterol levels [198]. Cholesterol and FDPS levels in Hepa 1.6 cells treated with lipid emulsions were thus measured in this study, and a general decrease mediated by unsaturated fatty acids was observed. These results agree with the previous effects mediated by PUFA on cholesterol and FDPS levels, but also suggest a similar response to n-9 MUFA, since similar inhibition was observed with *ClinOleic*. However, despite the effect of MUFA and PUFA on cholesterol levels is similar, a different regulation is clearly observed in Q levels and Q biosynthesis, indicating a regulation of the mevalonate pathway at different levels.

The response of Q system to fatty acids differs from that described for cholesterol, despite both lipids share several steps in the mevalonate pathway. Despite PUFA strongly inhibited FDPS and, in accordance, we observed a decrease of cholesterol, this treatment led to an increase of Q_9, Q_{10} as well as total Q. Bentinger and collaborators reported that lipid epoxides can alter the biosynthesis of lipids in cell cultures *via* the mevalonate pathway in a very similar way [199]. Lipid epoxides enhanced Q biosynthesis at the gene level and, therefore, elevated cellular content of this lipid while, simultaneously, inhibited cholesterol synthesis at the level of oxidosqualene cyclase, a necessary enzyme in the cholesterol branch of the pathway. Epoxides have been also reported to increase Q_9/Q_{10} ratio in human hepatic cells, possible due to altered levels of IPP. Complementary treatments aimed to alter IPP levels, either towards an increase or to a decrease, allowed these authors to propose that low levels of IPP in the cells result in increased Q_9 levels while high levels of this intermediate favors the synthesis of Q_{10} [95]. However, contrary to the effect observed with the epoxides, in our mouse hepatocellular model PUFAs caused a decrease of the Q_9/Q_{10} ratio. The regulation of the ratio will be evaluated in depth in the discussion referred to Chapter 3 (see later).

Complementary, we have also focused our research towards the study of the effect of different fatty acids in other metabolites and enzymes of the mevalonate pathway. Using HPLC with fluorescence detection, we quantified cellular levels of GPP and FPP, the two metabolites produced by FDPS. The synthesis of FPP is catalyzed through two consecutive condensation reactions between, first, DMAPP and IPP to form GPP, and second, between GPP and another IPP unit to yield FPP [89]. Contrary to our expectations, GPP levels were significantly increased with both PUFA and MUFA while PUFA also increased FPP levels. A similar increment of these metabolites was observed in previous studies using NBPs [146, 147], leading to the proposal that GPP is not only a transient intermediate in the FDPS-catalyzed synthesis of FPP, as previously thought, but a metabolite that can be regulated to perform additional functions within the cells. GPP is used to elongate the polyisoprenyl chain of Q in yeast [200], and it was previously proposed as a precursor in the biosynthesis of Q polyisoprenyl chain in rat liver microsomes, even better than FPP [201]. However, no evidence is available for demonstrated functions of GPP in mammalian cells. The downregulation that fatty acids exerts on FDPS levels might affect upstream metabolites in the pathway such as IPP. Moreover, according with previous study with epoxides carried out by Bentinger *et al.*

[95], high levels of IPP would stimulate the biosynthesis rate of Q_{10} over Q_9. Thus, the decrease in the Q_9/Q_{10} ratio observed in our cells could be a direct consequence of the increased IPP levels. We have referred previously HMG-CoA reductase as a target of SREBP, the transcription factor specifically inhibited by PUFA. If a decrease of SREBP affected HMG-CoA reductase equally as FDPS, that upstream enzyme would be inhibited and then it is expected that IPP would not accumulate within the cells treated with PUFA. However, it has to be taken into account that HMG-CoA reductase is specifically regulated by SREBP-2 [202], and this isoform of the SREBP family exhibits a different regulation by fatty acids. Experiments performed in HEK 293 cells, have revealed that unsaturated fatty acids decreased the nuclear content of SREBP-1, but not SREBP-2 [195]. Moreover, *in vivo* experiments have shown that the response of SREBP-1 and -2 to PUFA clearly diverge [197]. After approximately 24 h of PUFA consumption, the nuclear concentration of mature SREBP-1 and the abundance of SREBP-1 mRNA decreased comparing with rats fed with fat-free diet, but the nuclear content of mature SREBP-2 and the abundance of SREBP-2 mRNA did not differ from the controls. In a longer intervention (> 48 h), the pool of SREBP-1 decreased while the content of mature SREBP-2 increased and, hence, the levels of HMG-CoA synthase, another target enzyme. Our results suggest that a different regulation of SREBP isoforms, able to maintain high levels of IPP, is also happening in our hepatocellular model.

Isopentenyl-diphosphate isomerase (IDI), found in all free-living eukaryotes examined, convert IPP to its highly nucleophilic isomer dimethylallyl diphosphate (DMAPP) [203]. Therefore, if IPP levels are increased in Hepa 1.6 cells as a response to the fatty acid treatment, the levels of DMAPP should be consequently increased too. Previous studies about FDPS kinetics have proposed that, when DMAPP levels are high the GPP formed in the first reaction catalyzed by FDPS can leave the catalytic site of the enzyme and can be replaced by DMAPP prior to the second step of the reaction. Only after the DMAPP concentration is reduced does the reaction proceed towards FPP synthesis [89]. In other words, high levels of DMAPP could inhibit the condensation of GPP to FPP. In our model, the high levels of DMAPP could promote its binding to the FDPS enzyme remainingin cells treated with PUFA, thus inhibiting the second reaction and leading to an accumulation of GPP.

On the other hand, the accumulation of FPP could be also influenced by the inhibition of FPP-consuming downstream enzymes. The decrease of SREBP-1c levels mediated by fatty acids could explain the specific inhibition of the cholesterol synthesis branch and, therefore, the increased FPP levels. Another FPP-consuming enzyme is GGDPS, which catalyze the condensation of one unit of FPP with one unit of IPP to yield GGPP [204]. Along with FPP, GGPP is in charge of the isoprenylation of several proteins, a process which in this case is specifically known as geranylgeranylation [205]. To study GGDPS status in our model we used an indirect approach measuring unprenylated Rap1A level, a small GTPase that is exclusively geranylgeranylated [90]. Our results showed that total levels of Rap1A were not affected by unsaturated fatty acids, but *ClinOleic* enhanced the non-prenylated form of this protein. This increase suggests an inhibitory effect on GGDPS mediated by MUFAs. However, cellular FPP levels in cells treated with *ClinOleic* were similar to those measured in control conditions, indicating that a partial inhibition of GGDPS does not influence the FPP pool. Moreover, this increased pool of FPP is not expected to be the cause of the enhancement Q biosynthesis mediated by unsaturated fatty acids because the transprenyl transferase (i.e., the enzyme that utilizes FPP in the branch of the mevalonate pathway related with the synthesis of Q isoprenoid chain) is known to have a low Km for FPP, and thus this metabolite would not be rate-limiting in Q biosynthesis [81, 206]. Taken together, our results suggest that, apart from inhibiting several enzymes in the mevalonate pathway, fatty acids could also have additional targets specifically in the branch that produce Q, resulting in the increase of Q levels.

2.3. Regulatory role of fatty acids in Q and FDPS levels of CR-mice fed with different lipid sources

During the last years, our group focused part of its research activity on studying how different predominant fat sources affected the outcome of CR in mice [207]. For this project, four dietary groups were established: one control group fed 95 % of a pre-determined *ad libitum* intake (control) and three CR groups fed 40 % less than *ad libitum* intake. Lipid source for the control and one of the CR groups was soybean oil (high in n-6 PUFA) whereas the two remaining CR groups were fed with diets enriched in fish oil (high in n-3 PUFA) or lard (high in saturated and monounsaturated fatty acids). Complementary, as CR is an intervention known to extend lifespan in many organisms,

our model included three blocks of sample collection: 1, 6 and 18 months, in order to study the effect of aging in these dietary groups. Using this model, our group performed a longitudinal lifespan study [208], as well as numerous determinations to evaluate several mitochondrial parameters such us fatty acid composition, H^+ leak, activities of electron transport chain enzymes, ROS generation, lipid peroxidation, mitochondrial ultrastructure, and mitochondrial apoptotic signaling in liver and skeletal muscle [135-138, 209, 210]. These approaches applied to different cohorts of mice have indicated independently that lard as a fat source often maximizes the beneficial effects of 40 % CR on mice, for example increasing lifespan or lowering level of liver DNA fragmentation in old mice [207]. The Membrane Theory of Aging proposes that lifespan is inversely related to the degree of unsaturation of membrane phospholipids [211, 212]. Thus, long-live animals possesses more saturated membranes and, hence, are less sensitive to oxidative stress. The beneficial effects described for lard could be due to significant increases of SFA and MUFA levels in membranes. A lipidomic study let us to better understand the diminished susceptibility of membranes to peroxidation, which relies on a redistribution of the type of unsaturation. CR increased MUFA in liver, whereas the levels of PUFA were decreased without any change in SFA. These changes could be the consequence of a metabolic reprogramming that would minimize the oxidative damage and could contribute to an increase of the lifespan in CR mice [213].

Q levels, *COQ* gene expression as well as Q-dependent antioxidant systems are CR targets in cellular systems and in mice in a tissue-specific way, with skeletal muscle exhibiting an early response (1 month) to this intervention [154]. In this study, skeletal muscle of CR-lard animals showed lower levels of Q_9 and Q_{10} comparing with the *ad libitum* controls, whereas the diet based in soybean oil displayed the opposite response. Liver did not reflect any change influenced by the CR or the dietary fat after 1 month of nutritional intervention [123]. Changes in Q content observed in CR skeletal muscle could be related with the described decrease of protein oxidation and ROS generation in this organ [184].

As part of the present work, we performed complementary studies in animals after medium (6-month) and long-term (18-month) intervention using this same model. The thought that Q levels decrease with aging is some tissues is extended [21], but in PUFA-enriched diets our results showed that liver and skeletal muscle actually augmented Q

levels, probably as a protective mechanism against a potentially prooxidant enrichment of membranes with PUFA. Meanwhile, CR abolished these age-induced changes of Q levels in liver and skeletal muscle from mice fed PUFA-enriched diets. In longer interventions, liver and skeletal muscle showed a different response, being liver the most affected organ in its Q levels. Moreover, our results have indicated that liver and skeletal muscle tissues are able to adapt to a PUFA-enriched CR diet by increasing Q levels and decreasing Q_9/Q_{10} ratio. Highest levels of Q in liver are observed in a RC-fish diet while RC-lard showed the lower levels. These observations again agree with the described protective effect of a saturated fat source in calorie-restricted conditions.

Additionally, we have studied the effect of CR and different fat sources in FDPS levels of both, liver and skeletal muscle. Our results have shown that this central enzyme of the mevalonate pathway is highly influenced in liver by age and by CR when animals are fed with a soybean oil-enriched diet. However, lard- or fish oil-enriched diet in CR conditions did not influence FDPS levels in liver. The influence of CR and age in skeletal muscle was milder but still some changes were observed. The possible relation between Q and FDPS levels in liver or skeletal muscle is not completely clear. In our cellular model, we have related the decrease in FDPS levels with the large increase of Q_{10} levels and the significant decrease of the Q_9/Q_{10} ratio caused by PUFA. However, in an *in vivo* model this correlation cannot be readily established. In both liver and skeletal muscle, we observed a decrease of the Q_9/Q_{10} ratio in a CR-fish diet, and under these conditions FDPS levels were also lower. Nevertheless, we have observed several modifications of Q and FDPS levels that cannot be related in this way. PUFA, and also MUFA, could have multiple targets when used in a cellular model, and these could be augmented exponentially in an *in vivo* model due to the intrinsic complexity of a living organism. Moreover, it is described that SREBP fatty acid regulation differed between cellular and animal models [197] and, hence, the same type of regulation could be found at the FDPS level. In Chapter 3 we will try to deepen in the regulation of Q levels through the mevalonate pathway using simpler cellular models.

2.4. Concluding remarks and perspectives

Unsaturated fatty acids are basic components of the diet and have, among others, several targets in the mevalonate pathway. Using a hepatocellular model, our results have shown

that unsaturated fatty acids are able to increase Q levels and Q biosynthesis as well as to decrease cholesterol levels. Moreover, unsaturated fatty acids regulated the different Q isoforms in a different way, promoting the biosynthesis of Q_{10} over Q_9 and leading to increased levels of Q_{10} and a decreased Q_9/Q_{10} ratio. The regulation of the ratio could be influenced by the decrease of FDPS produced by these compounds, which might lead to the accumulation of IPP and DMAPP within the cell. The accumulation of IPP would in turn promote the biosynthesis of Q_{10} over Q_9, a mechanism already proposed previously [95]. However, additional targets of unsaturated fatty acids are necessary to understand the differential regulation of cholesterol and Q by fatty acids. GPP and FPP, the two metabolites produced by FDPS, are accumulated in presence of PUFA indicating that FDPS activity do not regulate directly its metabolites, at least under our experimental conditions, but possibly these levels are mostly affected by the activities of GPP/FPP-consuming enzymes. Since GGDPS was not affected by PUFA, it is very likely that SQS, the major FPP-consuming enzyme, or other enzyme in the cholesterol branch, are directly regulated by PUFA in our hepatocellular system. Decreased levels of cholesterol confirmed this hypothesis but additional experiments are needed to point the concrete enzyme. Possibly IDI is also a target of fatty acids and this regulation could enhance DMAPP levels that might inhibit the second catalytic reaction of FDPS producing an accumulation of GPP. Finally, our results also suggest that unsaturated fatty acid did not regulate HMG-CoA reductase in our system.

A previous model of CR-restricted animals of different ages allowed us to study the effect of supplementation with different types of fat. We observed that CR abolished these age-induced changes of Q levels in liver and skeletal muscle from mice fed PUFA-enriched diets. In a CR context, liver and skeletal muscle tissues were able to adapt to a PUFA-enriched diet by increasing Q levels and decreasing Q_9/Q_{10} ratio. Taken together, these observations agree with the described protective effect of a saturated fat source in calorie-restricted conditions previously described by our research group. Additionally, it was observed that FDPS is also regulated in calorie restriction and influenced by the different fat source, but in a different way from how it is regulated in the hepatocellular model.

Further experiments are needed to fully understand the exact regulation that fatty acids exert in, both, cellular and animal models.

CHAPTER 3: <u>Regulation of Q system through the mevalonate pathway</u>

3.1. Regulation of Q levels and Q_9/Q_{10} ratio by inhibition of FDPS

Our previous results with different lipid sources in Hepa 1.6 cells have shown that fatty acids regulate the biosynthesis of Q by modulating the mevalonate pathway. However, many questions still remain regarding the mechanisms that are involved. A key point may be the inhibition that fatty acids exert over the FDPS. Thus, we wondered if we could obtain more information by inhibiting more selectively this enzyme in a cellular model. We decided to accomplish this task by using two different approaches: genetic and pharmacological. Moreover, we thought it could be interesting to test the effect of this inhibition, besides the hepatocellular model previously used with lipid emulsions (see Chapter 2), in another cellular line from mouse such as Tkpts that revealed very useful in elucidating the role of polyphenols as novel biosynthetic ring precursors (see Chapter 1). We previously indicated our attempt to use this cell line also to test the effect of lipid emulsions on Q system, but the non-tolerance of these cells to supplementation with exogenous lipids did not allowed us to do that. Our genetic approach consisted in inhibiting FDPS using specific siRNAs. Prior to investigate the effect of FDPS gene silencing on the Q system, the transfection index was tested in both Tkpts and Hepa 1.6 cells using a plasmid construct containing the GFP gene. These preliminary determinations indicated us that efficient transfections could be only obtained in liver- but not in kidney-derived cells.

The silencing of FDPS revealed some similarities with our previous observations after a treatment with lipid emulsions. In this way, a decrease of FDPS levels caused a large increase in Q_{10} levels and the alteration of the Q_9/Q_{10} ratio towards a decrease in both models. However, the increase of Q_9 and total Q previously observed upon treatment with PUFA was not observed when the FDPS was selectively silenced by siRNAs, indicating the existence of at least two levels of regulation, with FDPS activity controlling Q_9/Q_{10} ratio, and another step, still to be identified, that influences total levels of Q. As we proposed before, fatty acids could have additional targets in the Q biosynthesis branch of the mevalonate pathway that could produce an increase of Q levels.

We have studied the metabolites produced by FDPS, GPP and FPP, in FDPS-depleted Hepa 1.6 cells model but no significant changes were observed. These results indicate

that FPDS activity by itself does not regulate directly the levels of its reaction products, but additional factors are needed to be taken into account. Attending to our previous results with fatty acids, we observed that PUFA increased GPP and FPP levels while MUFA increased GPP. According to the results obtained by gene silencing, we can postulate that this increment is not related directly with the inhibition of the FDPS, because the specific depletion of this enzyme with a siRNA did not reproduce the changes in GPP or FPP. This would indicate that PUFA have additional targets that influence the levels of metabolites of the mevalonate pathway as we have previously proposed. Moreover, measuring unprenylated Rap1A levels we confirmed indirectly that the specific inhibition of FDPS did not influence GGDPS function.

Complementary to the studies described above, we decided to perform a combined experiment with *Lipoplus* and siRNA against FDPS. We observed that, although, the FDPS levels measured in cells transfected only with siRNA B and those measured in cells that, in addition, had been further treated with *Lipoplus* did not differ significantly, the combined treatment produced marked differences in the Q system comparing with the single siRNA treatment. Co-treatment with both PUFA and siRNA against FDPS produced a higher decrease of Q_9, an enhanced increase of Q_{10}, and hence, a higher decrease of the Q_9/Q_{10} ratio. This apparent discrepancy could be explained on the basis of a different sensitivity of the techniques used: western-blot for measuring FDPS and HPLC with electrochemical detection for measuring Q. We have described that *Lipoplus* did not contribute to a further inhibition of FDPS levels when siRNA B was present, however, a slightly non-significant decrease in the combined treatment was indeed observed (from an inhibition of 74% in the former case to one of 76% in the latter). The possibility exists that this difference does not reach statistical significance because of the use of a semiquatitative technique as the western-blot, which relies on densitometric evaluation of chemiluminescence due to antibody binding. However, minor differences might be easily demonstrated by the use of a more sensitive technique, as HPLC with electrochemical detection, which would allow to demonstrate actual differences in the combined treatment. In addition, we cannot forget that, in this experiment, if we focus on the control cells transfected with the scramble siRNA and then cultured in the presence of *Lipoplus*, no significant effect of the emulsion was apparent in this case, whereas in the previous experiments *Lipoplus* produced a consistent increase of Q_{10} and a large decrease of the Q_9/Q_{10} ratio. It is possible that the agent used for transfections could

influence this difference. Lipofectamine® 2000 is a cationic lipid and after its use cells might be already loaded with lipids making our treatment with *Lipoplus* partially ineffective. In this case, another transfection technique such as electroporation, which do not use cationic lipids, would be useful to avoid this interaction.

The described effects observed in the Q system in FDPS-depleted Hepa 1.6 cells could be explained due to the increase of upstream metabolites such as IPP. Low levels of FDPS will led to a decrease in the consumption rate of IPP and, therefore, to its accumulation within the cells. The length of Q side chain is precisely defined by PDSS1-PDSS2 in mammals cells but possibly the availability of isoprene units would also influence the length of the tail. The existence of an increased pool of IPP in cells could force PDSS1-PDSS2 to introduce an additional isoprene to produce, preferably, Q_{10} and, therefore, to decrease the Q_9/Q_{10} ratio. Unsaturated fatty acids as well as epoxides [95] produced, among others, similar alterations of Q_{10} and Q_9/Q_{10} ratio. However, our study with siRNA points out FDPS by the first time as the central regulator of Q_9/Q_{10} ratio in mediating effects since, according to our observations, the specific inhibition of FDPS would be sufficient to alter upstream metabolites (IPP) increasing Q_{10} levels and decreasing the Q_9/Q_{10} ratio.

The increase of GPP and FPP observed previously in Hepa 1.6 treated with fatty acids was not observed when we used specific siRNAs designed against FDPS. Our previous studies carried out with PUFA suggested that additional targets might account for the accumulation of these metabolites and, clearly, these targets are not affected by the specific siRNA used to inhibit FDPS expression. Indeed, the siRNA we used for this study were specifically designed against FDPS, so in this model the rest of IPP-FPP consuming enzymes would maintain their normal function. The residual FDPS activity that still remains in silenced cells would be still able to produce the FPP necessary to maintain a stable FPP pool in these cells to be used by these downstream enzymes. Previously, in the fatty acids model, we proposed DMAPP might take part in the accumulation of GPP by inhibiting the second reaction of FDPS. Of note, the accumulation of GPP did not take place after silencing of FDPS with specific siRNAs. If higher levels of IPP (and hence, of DMAPP) are also produced in this model (which could explain the lowering of Q_9/Q_{10} ratio), this would imply that high levels of DMAPP are not sufficient to produce the augmentation of GPP levels, but unsaturated fatty acids should have additional targets

that influence this phenomenon, for example, by affecting IDI or a GPP-consuming enzyme. In cells, IPP levels are higher than DMAPP levels; for instance, in MEFs the IPP:DMAPP proportion is approximately 750:100 pg/mg protein [214]. An increase in IPP levels would produce an increase of DMAPP to maintain the correct proportion within the cell. If IDI was upregulated by fatty acids, then the IPP:DMAPP ratio might change in favor of DMAPP. This increased availability of DMAPP might be the responsible of the inhibition of the second catalytic step of FDPS and, therefore, of the increase of GPP. Another possibility if that unsaturated fatty acid inhibit selectively an unidentified GPP-consuming enzyme.

We also performed additional experiments by following a pharmacological approach to inhibit FDPS levels. Nitrogen containing bisphosphonates, such as ZOL, are known to inhibit FDPS, presumably in a specific way [157]. Thus, we selected ZOL to treat cells in order to study its effect on the Q system. However, this inhibition does not take place at the transcriptional level, as we previously described by PUFA and siRNAs, but it is due to a slow, tight binding process which results in the inactivation of FPDS activity. In this way, ZOL binds to the GPP/DMAPP site in FDPS, the enzyme undergoes a conformational change that results in the trapping of the molecule and then, IPP will stabilize the complex in such a way that the inhibition persists [87, 88]. However, FDPS is not the only target of these compounds. ZOL also inhibits, GGDPS [85, 91, 92] and SQS [93]. In this case, experiments were performed using Hepa 1.6 cells but also, Tkpts, a kidney-derived cell model. Although an activity assay to confirm the inhibition of FDPS was not carried out, the analysis of unprenylated levels of Rap1A allowed us to confirm the inhibition produced by ZOL on GGDPS in both cell lines. The effect of ZOL in the unprenylated form of Rap1A is dramatically higher in kidney-derived cells than in hepatocellular model. Cholesterol levels were also determined to study the effect of this compound on SQS. In this case, cholesterol levels were decreased in Tkpts but not in Hepa 1.6 cells. Together, these results suggest that Tkpts are more sensitive to ZOL than cells of other origins.

Little is known about the effect that ZOL exerts on the Q system, apart from some studies that suggested a general decrease of Q levels [94, 96]. Thus, we studied the effect of ZOL on Q system in several cell lines, including two murine lines: Hepa 1.6 and Tkpts cells, as well as two human cell lines: HEK 293 and HeLa. Our results are in agreement with

the previous observations since a decrease in total Q levels was generally observed. Moreover, we should emphasize the general decrease observed in Q_9/Q_{10} ratio, particularly in Tkpts cells where Q_{10} levels after a treatment with ZOL rose significantly over those of control cells. Additional experimentation indicated that the decrease in Q levels was caused by a decrease of the biosynthesis, being the inhibition in Q_9 stronger than in Q_{10}, especially in Tkpts. The preference of Q_{10} over Q_9 in cells treated with ZOL, which led to a substantial decrease of the Q_9/Q_{10} ratio, was previously described in treatments with fatty acids and siRNAs against FDPS. In this case, the explanation is based on similar concepts: the increase of IPP levels mediated by the inhibition of the FDPS would stimulate the production of Q_{10} over Q_9. This increase of IPP has been confirmed in different mammalian cell lines after a treatment with ZOL [215, 216]. However, the general decrease of Q levels cannot be explained merely by the inhibition of FPDS nor the inhibition of GGDPS. Based on these results, we suggest that ZOL might have an additional target in the biosynthesis branch of Q of the mevalonate pathway, similarly to unsaturated fatty acids, despite their effects are totally opposite. Guo *et al.* described NBPs as inhibitors of hexaprenyl diphosphate synthase (from *Sulfolobus solfataricus*) and octaprenyl diphosphate synthase (from *E. coli*) [91]. Whether these long-chain prenyltransferases are potently inhibited by bisphosphonates, PDSS1-PDSS2 becomes a strong candidate to be the additional target of ZOL that whose inhibition results a a decrease of Q levels in mouse and human cells.

We additionally studied the effect of ZOL on the metabolites produced by FDPS. Results showed that while FPP levels were not affected by ZOL, GPP levels substantially increased in Hepa 1.6 and displayed an upward trend in Tkpts. In addition, we should indicate that basal levels of FPP were significantly higher in renal than in liver cells , indicating that the mevalonate pathway is regulated differentially in cells from different lines or tissues. The increased levels of GPP caused by ZOL agrees with the previous studied published by Holstein *et al.* [146]. The fact that FPP levels were not increased by ZOL disagrees with previous results described by Tong *et al.* [215]. ZOL binds and remains the DMAPP/GPP site during FDPS inhibition impairing the binds of GPP to it active site and this might lead to an accumulation within the cell. This GPP pool could contribute to the cellular functions described for NBPs. Discrepancies in FPP levels could be explained on the basis of the use of different cell types, since previous studied used human cells whereas our studies were performed in mouse cell lines. Moreover, the

duration of the treatments, which also differs from 24 [215] to 48 hours in our experiments, could influence the response of the cells.

3.2. Upstream inhibitors of the mevalonate pathway and their effect on Q system

Other group of compounds, statins, are well known as inhibitors of the mevalonate pathway. Statins, which inhibit specifically HMG-CoA reductase, are widely used in clinical practices to lower cholesterol levels. Several examples of these products, such as rosuvastatin, atorvastatin, simvastatin, lovastatin, pravastatin and fluvastatin, are available in the clinic, with different efficiency in the inhibition of cholesterol levels [217]. Since the effects of statins in general, and lovastatin in particular, on Q metabolism are extensively described [60, 70, 77-81] we decided to study the effect of lovastatin in our cellular models in order to compare with our previous results. As expected, we observed a general decrease of total Q, Q_9 and Q_{10} levels in Hepa 1.6 and Tkpts cells treated with lovastatin, with the only exception of Q_{10} in Tkpts which did not change. Lovastatin, as an upstream inhibitor of the mevalonate pathway, produced an effect on Q levels that differed from our previous treatments, which acted at the levels of FDPS. Moreover, lovastatin did not produce any change in the Q_9/Q_{10} ratio. These results would indicate that an upstream inhibition of the mevalonate pathway, as that caused by lovastatin, has different effects of Q system comparing with a downstream inhibition, as that caused by ZOL, fatty acids or specific siRNA against FDPS. The inhibition of HMG-CoA reductase produces a general decrease of Q without affecting the Q_9/Q_{10} ratio, while inhibition of the mevalonate pathway at the FPDS step strongly affects Q_9/Q_{10} ratio. The inhibition of HMG-CoA reductase would produce a general inhibition of all the downstream metabolites of the pathway, including IPP. The decrease of IPP would lead to lower levels of GPP, FPP and GGPP [146, 147] affecting downstream enzymes of the pathway. Lower levels of cholesterol indicated a decrease of SQS activity, while lower levels of Q would indicated a decrease of PDSS1-PDSS2 activity. However, it has to be noted that the decrease in Q levels occurred in both Tkpts and Hepa 1.6 cells, whereas the decrease of cholesterol was exclusively observed in the kidney-derived cell line, indicating that the effects produced by inhibitors of the mevalonate pathway on several branchs is cell-specific. Additional experiments, for instance aimed to measure directly SQS activity, will be necessary to uncover the mechanisms underlying this specificity.

In Chapter 1, we have described 4HB, the main ring precursor of Q, as a limiting step in the Q biosynthesis in kidney-derived cells. However, at high concentrations this compound has been reported to compete with the substrate mevalonate 5-pyrophosphate and so, to inhibit mevalonate pyrophosphate decarboxylase [105], the enzyme that catalyzes the decarboxylation of mevalonate pyrophosphate to isopentenyl pyrophosphate. Moreover, 4HB is known to decrease HMG-CoA reductase activity decreasing cholesterol levels in rat plasma [218], indicating the existence of a crosstalk between the pathways that originate the ring and the isoprenoid chain precursors of Q.

Dose-response curves with 4HB were performed in different cell lines and the increased levels of Q allowed us to conclude that kidney cells, but not cells from other origins, have a low endogenous availability of Q ring precursors. Of note, in the hepatocellular model Q levels were increased by 4HB at low concentrations (nM) but this effect disappeared at elevated concentrations of 4HB, or this compound became even inhibitory. 4HB has been described to be present at saturating concentrations in liver, as determined by *in vitro* assays with liver tissue slices [174] and, so, a putative function as modulator of Q levels as ring precursor would not be expected. Nevertheless, the decrease of Q we observed at 100 µM 4HB could be possibly due to its properties as mevalonate pathway inhibitor. Another difference between these cell lines to take into account is the different response in terms of the Q_9/Q_{10} ratio: while Tkpts increased the ratio upon treatment with 4HB, this value was decreased in Hepa 1.6 cells, indicating the existence of a tissue-dependent regulation of Q biosynthesis also at this level. Furthermore, cholesterol levels measured after treatments with statins and 4HB decreased in Tkpts cells, but they did not display any change in Hepa 1.6, further supporting the fact that different braches of the mevalonate pathway are differently regulated in different cell types.

3.3. Concluding remarks and perspectives

In this chapter we have deepen into the regulation of the Q system using different inhibitors of the mevalonate pathway. Specific siRNA against FPDS showed that the specific inhibition of this enzyme is sufficient to alter upstream metabolites of the mevalonate pathway (especially IPP) increasing Q_{10} levels and decreasing the Q_9/Q_{10} ratio. However, the inhibition of this enzyme did not alter the levels of its products, GPP and FPP, which did not change even when the enzyme levels were very low. On the other

hand, NBPs, and concretely ZOL, are inhibitors of some enzymes in the mevalonate pathway: FDPS, SQS and GGDPS. Thus, cells treated with ZOL generally decrease Q biosynthesis and Q levels, but also decrease the Q_9/Q_{10} ratio. The same upregulation of IPP seems to be the cause of the regulation of the Q_9/Q_{10} ratio, whereas an additional target in the Q biosynthetic branch of the pathway should be necessary to explain the lower levels of Q since FPP levels did not decrease. Using lovastatin, an inhibitor of the HMG-CoA reductase, we have observed the different Q regulation of the mevalonate pathway when using an upstream inhibitor. Cells treated with lovastatin decrease Q but did not alter the ratio Q_9/Q_{10}. Further investigation is warranted to understand the mechanisms underlying the differential cell-specific effects of several inhibitors on the products of different branches of the mevalonate pathway as Q and cholesterol. This may be of great importance, since side-effects of some of these inhibitors, as statins, on Q system are proposed to be involved in several deleterious alterations associated with their long-term use.

General conclusions

1. Kaempferol strongly increases coenzyme Q levels in kidney cells by acting as a novel precursor of the benzoquinone ring, independently to its effect as upregulator of sirtuins. Other phenolics are much less active in our model.

2. Limited availability of endogenous biosynthetic ring precursors of coenzyme Q is a feature of renal cells that determines enhanced sensitivity to supplementation with exogenous precursor substances, in comparison with cells of different origins.

3. Farnesyl diphosphate synthase is identify as a key enzyme in the regulation of the Q_9/Q_{10} ratio. Those interventions aimed to decrease its expression or inhibit its enzymatic activity produce a decrease in the Q_9/Q_{10} ratio.

4. The supplementation with monounsaturated fatty acids and polyunsaturated fatty acids exerts a differential action on the mevalonate pathway, particularly in the coenzyme Q biosynthesis branch.

5. Polyunsaturated fatty acids are demonstrated as novel modulators that target coenzyme Q biosynthesis pathway by increasing the biosynthetic rate and decreasing the Q_9/Q_{10} ratio. The alteration of the Q_9/Q_{10} ratio can be explained on the basis of their role as inhibitors of the farnesyl diphosphate synthase expression whereas the increase of Q biosynthesis implied additional target(s) still to be identified.

6. Zoledronic acid is identify by the first time as a drug that target the coenzyme Q biosynthesis by decreasing both, total coenzyme Q levels and the Q_9/Q_{10} ratio. The alteration of the Q_9/Q_{10} ratio can be explained by its action as a well-known enzymatic inhibitor of the farnesyl diphosphate synthase. The lack of a decrease of FPP levels implies the involvement of additional target(s) to explain the overall inhibition of coenzyme Q biosynthesis.

7. Impairment of coenzyme Q biosynthesis pathway by zoledronic acid should be considered to understand the pharmacological and side effects produced in the administration of this nitrogen-containing bisphosphonate.

8. The action of the different effectors that modify the coenzyme Q system through the mevalonate pathway is cell-specific.

Conclusiones generales

1. El kaempferol incrementa los niveles de coenzima Q en células de riñón actuando como un nuevo precursor del anillo benzoquinónico, independientemente de su afecto como activador de sirtuinas. Otros compuestos fenólicos son mucho menos activos en nuestro modelo.

2. La limitada disponibilidad de precursores endógenos de anillo del coenzima Q es una característica típica de células renales que potencia su sensibilidad a la suplementación con precursores exógenos, en comparación con la de células de diferentes orígenes.

3. La farnesil difosfato sintasa se identifica como una enzima clave en la regulación del ratio Q_9/Q_{10}. Las intervenciones enfocadas a disminuir sus niveles o su actividad producen un descenso del Q_9/Q_{10}.

4. La suplementación con ácidos grasos mono y poliinsaturados produce una regulación diferencial sobre la ruta del mevalonato, particularmente en la rama de la biosíntesis de coenzima Q.

5. Los ácidos grasos poliinsaturados actúan como moduladores de la ruta de biosíntesis de coenzima Q incrementando su tasa biosintética y disminuyendo el ratio Q_9/Q_{10}. La alteración del ratio Q_9/Q_{10} se explica debido a su papel como inhibidores de la expression de la farnesil difosfatos sintasa mientras que el incremento de la biosíntesis implica dianas adicionales aún por identificar.

6. El ácido zoledrónico ha sido identificado por primera vez como una droga que afecta de forma específica la biosíntesis de coenzima Q disminuyendo sus niveles totales así como el ratio Q_9/Q_{10}. La alteración del ratio Q_9/Q_{10} se explica en base a su bien conocida acción inhibidora sobre la actividad de la farnesil difosfato sintasa. La ausencia de un descenso de los niveles de FPP implica la acción de dianas adicionales para explicar la inhibición observada sobre la biosíntesis de coenzima Q.

7. La disfunción de la ruta de biosíntesis de coenzima Q mediada por ácido zoledrónico debe ser considerada para comprender los efectos farmacológicos y colaterales de la administración este bisfosfonato.

8. La acción de los diferentes efectores que modifican el sistema de coenzima Q a través de la ruta del mevalonato es específica de cada tipo celular.

Bibliography

1. Festenstein, G.N., et al., *A constituent of the unsaponifiable portion of animal tissue lipids (λ(max.) mμ.)*. Biochemical Journal, 1955. **59**(4): p. 558-566.
2. Crane, F.L., et al., *Isolation of a quinone from beef heart mitochondria*. Biochim Biophys Acta, 1957. **25**(1): p. 220-1.
3. Wolf, D.E., et al., *Coenzyme Q. I. Structure studies on the coenzyme Q group*. J. Am. Chem. Soc., 1958. **80**(17): p. 4752-52.
4. Kawamukai, M., *Biosynthesis and bioproduction of coenzyme Q10 by yeasts and other organisms*. Biotechnol Appl Biochem, 2009. **53**(Pt 4): p. 217-26.
5. Hayashi, K., et al., *Functional conservation of coenzyme Q biosynthetic genes among yeasts, plants, and humans*. PLoS One, 2014. **9**(6): p. e99038.
6. Kawamukai, M., *Biosynthesis of coenzyme Q in eukaryotes*. Biosci Biotechnol Biochem, 2015: p. 1-11.
7. Basselin, M., et al., *Ubiquinone synthesis in mitochondrial and microsomal subcellular fractions of Pneumocystis spp.: differential sensitivities to atovaquone*. Eukaryot Cell, 2005. **4**(8): p. 1483-92.
8. Wang, Y. and S. Hekimi, *Understanding Ubiquinone*. Trends Cell Biol, 2016. **26**(5): p. 367-78.
9. Saito, Y., et al., *Characterization of cellular uptake and distribution of coenzyme Q10 and vitamin E in PC12 cells*. J Nutr Biochem, 2009. **20**(5): p. 350-7.
10. Turunen, M., J. Olsson, and G. Dallner, *Metabolism and function of coenzyme Q*. Biochimica et Biophysica Acta (BBA) - Biomembranes, 2004. **1660**(1-2): p. 171-199.
11. Bentinger, M., K. Brismar, and G. Dallner, *The antioxidant role of coenzyme Q*. Mitochondrion, 2007. **7 Suppl**: p. S41-50.
12. Takahashi, T., et al., *Distribution of ubiquinone and ubiquinol homologues in rat tissues and subcellular fractions*. Lipids, 1993. **28**(9): p. 803-9.
13. Morre, D.J. and D.M. Morre, *Non-mitochondrial coenzyme Q*. Biofactors, 2011. **37**(5): p. 355-60.
14. Aberg, F., et al., *Distribution and redox state of ubiquinones in rat and human tissues*. Arch Biochem Biophys, 1992. **295**(2): p. 230-4.
15. Tang, P.H., et al., *Measurement of reduced and oxidized coenzyme Q9 and coenzyme Q10 levels in mouse tissues by HPLC with coulometric detection*. Clin Chim Acta, 2004. **341**(1-2): p. 173-84.
16. Mitchell, P., *Protonmotive redox mechanism of the cytochrome b-c1 complex in the respiratory chain: protonmotive ubiquinone cycle*. FEBS Lett, 1975. **56**(1): p. 1-6.
17. Lenaz, G. and M.L. Genova, *Structural and functional organization of the mitochondrial respiratory chain: a dynamic super-assembly*. Int J Biochem Cell Biol, 2009. **41**(10): p. 1750-1772.
18. Alcazar-Fabra, M., P. Navas, and G. Brea-Calvo, *Coenzyme Q biosynthesis and its role in the respiratory chain structure*. Biochim Biophys Acta, 2016.
19. Acin-Perez, R. and J.A. Enriquez, *The function of the respiratory supercomplexes: the plasticity model*. Biochim Biophys Acta, 2014. **1837**(4): p. 444-50.
20. Lapuente-Brun, E., et al., *Supercomplex assembly determines electron flux in the mitochondrial electron transport chain*. Science, 2013. **340**(6140): p. 1567-70.
21. Bentinger, M., M. Tekle, and G. Dallner, *Coenzyme Q--biosynthesis and functions*. Biochem Biophys Res Commun, 2010. **396**(1): p. 74-9.
22. Norenberg, M.D. and K.V. Rao, *The mitochondrial permeability transition in neurologic disease*. Neurochem Int, 2007. **50**(7-8): p. 983-97.
23. Nagy, M., F. Lacroute, and D. Thomas, *Divergent evolution of pyrimidine biosynthesis between anaerobic and aerobic yeasts*. Proc Natl Acad Sci U S A, 1992. **89**(19): p. 8966-70.
24. Crane, F.L., et al., *Transplasma-membrane redox systems in growth and development*. Biochim Biophys Acta, 1985. **811**(3): p. 233-64.
25. Kishi, T., D.M. Morre, and D.J. Morre, *The plasma membrane NADH oxidase of HeLa cells has hydroquinone oxidase activity*. Biochim Biophys Acta, 1999. **1412**(1): p. 66-77.

26. Morre, D.J. and D.M. Morre, *Cell surface NADH oxidases (ECTO-NOX proteins) with roles in cancer, cellular time-keeping, growth, aging and neurodegenerative diseases.* Free Radic Res, 2003. **37**(8): p. 795-808.

27. Cadenas, E. and K.J. Davies, *Mitochondrial free radical generation, oxidative stress, and aging.* Free Radic Biol Med, 2000. **29**(3-4): p. 222-30.

28. Lee, S., et al., *Mitochondrial H2O2 generated from electron transport chain complex I stimulates muscle differentiation.* Cell Res, 2011. **21**(5): p. 817-34.

29. Ris-Stalpers, C., *Physiology and pathophysiology of the DUOXes.* Antioxid Redox Signal, 2006. **8**(9-10): p. 1563-72.

30. Lambeth, J.D., T. Kawahara, and B. Diebold, *Regulation of Nox and Duox enzymatic activity and expression.* Free Radic Biol Med, 2007. **43**(3): p. 319-31.

31. Drummond, G.R., et al., *Combating oxidative stress in vascular disease: NADPH oxidases as therapeutic targets.* Nat Rev Drug Discov, 2011. **10**(6): p. 453-71.

32. Shimada, M., J. Cheng, and A. Sanyal, *Fatty Liver, NASH, and Alcoholic Liver Disease A2 - McManus, Linda M*, in *Pathobiology of Human Disease*, R.N. Mitchell, Editor. 2014, Academic Press: San Diego. p. 1817-1824.

33. Droge, W., *Free radicals in the physiological control of cell function.* Physiol Rev, 2002. **82**(1): p. 47-95.

34. Halliwell, B., *Antioxidant defence mechanisms: from the beginning to the end (of the beginning).* Free Radic Res, 1999. **31**(4): p. 261-72.

35. Tomasetti, M., et al., *In vivo supplementation with coenzyme Q10 enhances the recovery of human lymphocytes from oxidative DNA damage.* Faseb j, 2001. **15**(8): p. 1425-7.

36. Ernster, L. and G. Dallner, *Biochemical, physiological and medical aspects of ubiquinone function.* Biochim Biophys Acta, 1995. **1271**(1): p. 195-204.

37. Villalba, J.M., et al., *Insigths in cellular protecction against oxidative stress: the necessity for extramitochondrial coenzyme Q.* Mitochondrial ubiquinone (Coenzyme Q$_{10}$). Biochemical, functional, medical, and therapeutic aspects in human health and diseases. Vol.2. PROMINENT PRESS, 2001: p. 89-120.

38. Gomez-Diaz, C., et al., *Antioxidant ascorbate is stabilized by NADH-coenzyme Q10 reductase in the plasma membrane.* J Bioenerg Biomembr, 1997. **29**(3): p. 251-7.

39. Gomez-Diaz, C., et al., *Ascorbate stabilization is stimulated in rho(0)HL-60 cells by CoQ10 increase at the plasma membrane.* Biochem Biophys Res Commun, 1997. **234**(1): p. 79-81.

40. Santos-Ocana, C., et al., *Coenzyme Q6 and iron reduction are responsible for the extracellular ascorbate stabilization at the plasma membrane of Saccharomyces cerevisiae.* J Biol Chem, 1998. **273**(14): p. 8099-105.

41. Maguire, J.J., et al., *Succinate-ubiquinone reductase linked recycling of alpha-tocopherol in reconstituted systems and mitochondria: requirement for reduced ubiquinone.* Arch Biochem Biophys, 1992. **292**(1): p. 47-53.

42. Stoyanovsky, D.A., et al., *Ubiquinone-dependent recycling of vitamin E radicals by superoxide.* Arch Biochem Biophys, 1995. **323**(2): p. 343-51.

43. Acosta, M.J., et al., *Coenzyme Q biosynthesis in health and disease.* Biochim Biophys Acta, 2016. **1857**(8): p. 1079-1085.

44. Miziorko, H.M., *Enzymes of the mevalonate pathway of isoprenoid biosynthesis.* Arch Biochem Biophys, 2011. **505**(2): p. 131-43.

45. Henneman, L., et al., *Inhibition of the isoprenoid biosynthesis pathway; detection of intermediates by UPLC-MS/MS.* Biochim Biophys Acta, 2011. **1811**(4): p. 227-33.

46. Ericsson, J. and G. Dallner, *Distribution, biosynthesis, and function of mevalonate pathway lipids.* Subcell Biochem, 1993. **21**: p. 229-72.

47. Szkopinska, A. and D. Plochocka, *Farnesyl diphosphate synthase; regulation of product specificity.* Acta Biochim Pol, 2005. **52**(1): p. 45-55.

48. Saiki, R., et al., *Characterization of solanesyl and decaprenyl diphosphate synthases in mice and humans.* FEBS J, 2005. **272**(21): p. 5606-22.

49. Dallner, G. and P.J. Sindelar, *Regulation of ubiquinone metabolism.* Free Radic Biol Med, 2000. **29**(3-4): p. 285-94.

50. Tran, U.C. and C.F. Clarke, *Endogenous synthesis of coenzyme Q in eukaryotes.* Mitochondrion, 2007. **7 Suppl**: p. S62-71.

51. Block, A., et al., *The Origin and Biosynthesis of the Benzenoid Moiety of Ubiquinone (Coenzyme Q) in Arabidopsis.* Plant Cell, 2014. **26**(5): p. 1938-1948.

52. Nambudiri, A.M., et al., *Alternate routes for ubiquinone biosynthesis in rats.* Biochem Biophys Res Commun, 1976. **76**(2): p. 282-8.

53. Marbois, B., et al., *para-Aminobenzoic acid is a precursor in coenzyme Q6 biosynthesis in Saccharomyces cerevisiae.* J Biol Chem, 2010. **285**(36): p. 27827-38.

54. Pierrel, F., et al., *Involvement of mitochondrial ferredoxin and para-aminobenzoic acid in yeast coenzyme Q biosynthesis.* Chem Biol, 2010. **17**(5): p. 449-59.

55. Wang, Y. and S. Hekimi, *Molecular genetics of ubiquinone biosynthesis in animals.* Crit Rev Biochem Mol Biol, 2013. **48**(1): p. 69-88.

56. Xie, L.X., et al., *Resveratrol and para-coumarate serve as ring precursors for coenzyme Q biosynthesis.* J Lipid Res, 2015. **56**(4): p. 909-19.

57. Wang, Y., et al., *Pathogenicity of two COQ7 mutations and responses to 2,4-dihydroxybenzoate bypass treatment.* J Cell Mol Med, 2017. **[Epub ahead of print]**.

58. Wang, Y., D. Oxer, and S. Hekimi, *Mitochondrial function and lifespan of mice with controlled ubiquinone biosynthesis.* Nat Commun, 2015. **6**: p. 6393.

59. Xie, L.X., et al., *Overexpression of the Coq8 kinase in Saccharomyces cerevisiae coq null mutants allows for accumulation of diagnostic intermediates of the coenzyme Q6 biosynthetic pathway.* J Biol Chem, 2012. **287**(28): p. 23571-81.

60. Hargreaves, I.P., *Coenzyme Q10: From fact to fiction.* Pharmacology - Research, Safety Testing and Regulation., ed. I.P. Hargreaves and A.K. Hargreaves. 2015: Nova Science Publishers.

61. Mugoni, V., et al., *Ubiad1 is an antioxidant enzyme that regulates eNOS activity by CoQ10 synthesis.* Cell, 2013. **152**(3): p. 504-18.

62. Nakagawa, K., et al., *Vitamin K2 biosynthetic enzyme, UBIAD1 is essential for embryonic development of mice.* PLoS One, 2014. **9**(8): p. e104078.

63. He, C.H., et al., *Yeast Coq9 controls deamination of coenzyme Q intermediates that derive from para-aminobenzoic acid.* Biochim Biophys Acta, 2015. **1851**(9): p. 1227-39.

64. Allan, C.M., et al., *A conserved START domain coenzyme Q-binding polypeptide is required for efficient Q biosynthesis, respiratory electron transport, and antioxidant function in Saccharomyces cerevisiae.* Biochimica et Biophysica Acta (BBA) - Molecular and Cell Biology of Lipids, 2013. **1831**(4): p. 776-791.

65. Allan, C.M., et al., *Identification of Coq11, a new coenzyme Q biosynthetic protein in the CoQ-synthome in Saccharomyces cerevisiae.* J Biol Chem, 2015. **290**(12): p. 7517-34.

66. Marbois, B., et al., *The yeast Coq4 polypeptide organizes a mitochondrial protein complex essential for coenzyme Q biosynthesis.* Biochim Biophys Acta, 2009. **1791**(1): p. 69-75.

67. He, C.H., et al., *Coenzyme Q supplementation or over-expression of the yeast Coq8 putative kinase stabilizes multi-subunit Coq polypeptide complexes in yeast coq null mutants.* Biochim Biophys Acta, 2014. **1841**(4): p. 630-44.

68. Gonzalez-Mariscal, I., et al., *Regulation of coenzyme Q biosynthesis in yeast: a new complex in the block.* IUBMB Life, 2014. **66**(2): p. 63-70.

69. Ogasahara, S., et al., *Muscle coenzyme Q deficiency in familial mitochondrial encephalomyopathy.* Proc Natl Acad Sci U S A, 1989. **86**(7): p. 2379-82.

70. Laredj, L.N., F. Licitra, and H.M. Puccio, *The molecular genetics of coenzyme Q biosynthesis in health and disease.* Biochimie, 2014. **100**: p. 78-87.

71. Ozaltin, F., *Primary coenzyme Q10 (CoQ 10) deficiencies and related nephropathies.* Pediatr Nephrol, 2014. **29**(6): p. 961-9.

72. Trevisson, E., et al., *Coenzyme Q deficiency in muscle.* Curr Opin Neurol, 2011. **24**(5): p. 449-56.

73. Fernandez-Ayala, D.J., et al., *Survival transcriptome in the coenzyme Q10 deficiency syndrome is acquired by epigenetic modifications: a modelling study for human coenzyme Q10 deficiencies.* BMJ Open, 2013. **3**(3).

74. Doimo, M., et al., *Effect of vanillic acid on COQ6 mutants identified in patients with coenzyme Q10 deficiency.* Biochim Biophys Acta, 2014. **1842**(1): p. 1-6.

75. Hennessy, E., et al., *Is There Potential for Repurposing Statins as Novel Antimicrobials?* Antimicrob Agents Chemother, 2016. **60**(9): p. 5111-21.

76. Buhaescu, I. and H. Izzedine, *Mevalonate pathway: a review of clinical and therapeutical implications.* Clin Biochem, 2007. **40**(9-10): p. 575-84.

77. Appelkvist, E.L., et al., *Effects of inhibitors of hydroxymethylglutaryl coenzyme A reductase on coenzyme Q and dolichol biosynthesis.* Clin Investig, 1993. **71**(8 Suppl): p. S97-102.

78. Langsjoen, P.H. and A.M. Langsjoen, *The clinical use of HMG CoA-reductase inhibitors and the associated depletion of coenzyme Q10. A review of animal and human publications.* Biofactors, 2003. **18**(1-4): p. 101-11.

79. Low, P., et al., *Effects of mevinolin treatment on tissue dolichol and ubiquinone levels in the rat.* Biochim Biophys Acta, 1992. **1165**(1): p. 102-9.

80. Banach, M., et al., *Statin therapy and plasma coenzyme Q10 concentrations--A systematic review and meta-analysis of placebo-controlled trials.* Pharmacol Res, 2015. **99**: p. 329-36.

81. Littarru, G.P. and P. Langsjoen, *Coenzyme Q10 and statins: biochemical and clinical implications.* Mitochondrion, 2007. **7 Suppl**: p. S168-74.

82. Drake, M.T., B.L. Clarke, and S. Khosla, *Bisphosphonates: mechanism of action and role in clinical practice.* Mayo Clin Proc, 2008. **83**(9): p. 1032-45.

83. Li, E.C. and L.E. Davis, *Zoledronic acid: a new parenteral bisphosphonate.* Clin Ther, 2003. **25**(11): p. 2669-708.

84. Luhe, A., et al., *Preclinical evidence for nitrogen-containing bisphosphonate inhibition of farnesyl diphosphate (FPP) synthase in the kidney: implications for renal safety.* Toxicol In Vitro, 2008. **22**(4): p. 899-909.

85. Jiang, P., et al., *Anti-cancer effects of nitrogen-containing bisphosphonates on human cancer cells.* Oncotarget, 2016.

86. Dunford, J.E., et al., *Structure-activity relationships for inhibition of farnesyl diphosphate synthase in vitro and inhibition of bone resorption in vivo by nitrogen-containing bisphosphonates.* J Pharmacol Exp Ther, 2001. **296**(2): p. 235-42.

87. Rondeau, J.M., et al., *Structural basis for the exceptional in vivo efficacy of bisphosphonate drugs.* ChemMedChem, 2006. **1**(2): p. 267-73.

88. Kavanagh, K.L., et al., *The molecular mechanism of nitrogen-containing bisphosphonates as antiosteoporosis drugs.* Proc Natl Acad Sci U S A, 2006. **103**(20): p. 7829-34.

89. Glickman, J.F. and A. Schmid, *Farnesyl pyrophosphate synthase: real-time kinetics and inhibition by nitrogen-containing bisphosphonates in a scintillation assay.* Assay Drug Dev Technol, 2007. **5**(2): p. 205-14.

90. Goffinet, M., et al., *Zoledronic acid treatment impairs protein geranyl-geranylation for biological effects in prostatic cells.* BMC Cancer, 2006. **6**: p. 60.

91. Guo, R.T., et al., *Bisphosphonates target multiple sites in both cis- and trans-prenyltransferases.* Proc Natl Acad Sci U S A, 2007. **104**(24): p. 10022-7.

92. Zhang, Y., et al., *Lipophilic bisphosphonates as dual farnesyl/geranylgeranyl diphosphate synthase inhibitors: an X-ray and NMR investigation.* J Am Chem Soc, 2009. **131**(14): p. 5153-62.

93. Amin, D., et al., *Bisphosphonates used for the treatment of bone disorders inhibit squalene synthase and cholesterol biosynthesis.* J Lipid Res, 1992. **33**(11): p. 1657-63.

94. Coscia, M., et al., *Zoledronic acid repolarizes tumour-associated macrophages and inhibits mammary carcinogenesis by targeting the mevalonate pathway.* Journal of Cellular and Molecular Medicine, 2010. **14**(12): p. 2803-2815.

95.   Bentinger, M., et al., *Effects of various squalene epoxides on coenzyme Q and cholesterol synthesis.* Biochim Biophys Acta, 2014. **1841**(7): p. 977-86.

96.   Kalyan, S., et al., *Nitrogen-bisphosphonate therapy is linked to compromised coenzyme Q10 and vitamin E status in postmenopausal women.* J Clin Endocrinol Metab, 2014. **99**(4): p. 1307-13.

97.   Anantharaju, P.G., et al., *An overview on the role of dietary phenolics for the treatment of cancers.* Nutr J, 2016. **15**(1): p. 99.

98.   Tsao, R., *Chemistry and Biochemistry of Dietary Polyphenols.* Nutrients, 2010. **2**(12): p. 1231-1246.

99.   Hatia, S., et al., *Evaluation of antioxidant properties of major dietary polyphenols and their protective effect on 3T3-L1 preadipocytes and red blood cells exposed to oxidative stress.* Free Radic Res, 2014. **48**(4): p. 387-401.

100.   Crozier, A., I.B. Jaganath, and M.N. Clifford, *Dietary phenolics: chemistry, bioavailability and effects on health.* Nat Prod Rep, 2009. **26**(8): p. 1001-43.

101.   Del Rio, D., et al., *Dietary (poly)phenolics in human health: structures, bioavailability, and evidence of protective effects against chronic diseases.* Antioxid Redox Signal, 2013. **18**(14): p. 1818-92.

102.   Du, Y., H. Guo, and H. Lou, *Grape seed polyphenols protect cardiac cells from apoptosis via induction of endogenous antioxidant enzymes.* J Agric Food Chem, 2007. **55**(5): p. 1695-701.

103.   Sandoval-Acuna, C., J. Ferreira, and H. Speisky, *Polyphenols and mitochondria: an update on their increasingly emerging ROS-scavenging independent actions.* Arch Biochem Biophys, 2014. **559**: p. 75-90.

104.   Zhang, H. and R. Tsao, *Dietary polyphenols, oxidative stress and antioxidant and anti-inflammatory effects.* Current Opinion in Food Science, 2016. **8**: p. 33-42.

105.   Shama Bhat, C. and T. Ramasarma, *Inhibition of rat liver mevalonate pyrophosphate decarboxylase and mevalonate phosphate kinase by phenyl and phenolic compounds.* Biochem J, 1979. **181**(1): p. 143-51.

106.   Schaffer, S., et al., *Effects of polyphenols on brain ageing and Alzheimer's disease: focus on mitochondria.* Mol Neurobiol, 2012. **46**(1): p. 161-78.

107.   Sandoval-Acuna, C., et al., *Inhibition of mitochondrial complex I by various non-steroidal anti-inflammatory drugs and its protection by quercetin via a coenzyme Q-like action.* Chem Biol Interact, 2012. **199**(1): p. 18-28.

108.   Carrasco-Pozo, C., et al., *Differential protective effects of quercetin, resveratrol, rutin and epigallocatechin gallate against mitochondrial dysfunction induced by indomethacin in Caco-2 cells.* Chem Biol Interact, 2012. **195**(3): p. 199-205.

109.   Lagoa, R., et al., *Complex I and cytochrome c are molecular targets of flavonoids that inhibit hydrogen peroxide production by mitochondria.* Biochim Biophys Acta, 2011. **1807**(12): p. 1562-72.

110.   Moyad, M.A., *An introduction to dietary/supplemental omega-3 fatty acids for general health and prevention: part II.* Urol Oncol, 2005. **23**(1): p. 36-48.

111.   Innis, S.M., *Essential fatty acids in growth and development.* Prog Lipid Res, 1991. **30**(1): p. 39-103.

112.   Barr, L.H., G.D. Dunn, and M.F. Brennan, *Essential fatty acid deficiency during total parenteral nutrition.* Annals of Surgery, 1981. **193**(3): p. 304-311.

113.   Logan, A.C., *Omega-3 fatty acids and major depression: A primer for the mental health professional.* Lipids in Health and Disease, 2004. **3**: p. 25-25.

114.   Hooper, L., et al., *Risks and benefits of omega 3 fats for mortality, cardiovascular disease, and cancer: systematic review.* Bmj, 2006. **332**(7544): p. 752-60.

115.   Sacks, F.M. and H. Campos, *Polyunsaturated fatty acids, inflammation, and cardiovascular disease: time to widen our view of the mechanisms.* J Clin Endocrinol Metab, 2006. **91**(2): p. 398-400.

116. Huertas, J.R., et al., *Changes in mitochondrial and microsomal rat liver coenzyme Q9 and Q10 content induced by dietary fat and endogenous lipid peroxidation.* FEBS Lett, 1991. **287**(1-2): p. 89-92.

117. Ochoa-Herrera, J.J., et al., *Dietary oils high in oleic acid, but with different non-glyceride contents, have different effects on lipid profiles and peroxidation in rabbit hepatic mitochondria.* J Nutr Biochem, 2001. **12**(6): p. 357-364.

118. Lopez-Dominguez, J.A., *Efecto de la restricción calórica, el envejecimiento y el componente graso de la dieta sobre la señalización apoptótica en tejidos mitóticos y postmitóticos de ratón.* Doctoral Thesis. University of Cordoba, 2013.

119. Ramsey, J.J., et al., *Influence of mitochondrial membrane fatty acid composition on proton leak and H2O2 production in liver.* Comp Biochem Physiol B Biochem Mol Biol, 2005. **140**(1): p. 99-108.

120. Mataix, J., et al., *Tissue specific interactions of exercise, dietary fatty acids, and vitamin E in lipid peroxidation.* Free Radic Biol Med, 1998. **24**(4): p. 511-21.

121. Mataix, J., et al., *Coenzyme Q content depends upon oxidative stress and dietary fat unsaturation.* Mol Aspects Med, 1997. **18 Suppl**: p. S129-35.

122. Quiles, J.L., et al., *Olive oil supplemented with vitamin E affects mitochondrial coenzyme Q levels in liver of rats after an oxidative stress induced by adriamycin.* Biofactors, 1999. **9**(2-4): p. 331-6.

123. Parrado-Fernandez, C., *Biosíntesis del coenzima Q: Mantenimiento de la homeostasis redox y adaptación metabólica.* Doctoral Thesis. University of Cordoba, 2010.

124. Quiles, J.L., et al., *Coenzyme Q supplementation protects from age-related DNA double-strand breaks and increases lifespan in rats fed on a PUFA-rich diet.* Exp Gerontol, 2004. **39**(2): p. 189-94.

125. Ochoa, J.J., et al., *Coenzyme Q10 protects from aging-related oxidative stress and improves mitochondrial function in heart of rats fed a polyunsaturated fatty acid (PUFA)-rich diet.* J Gerontol A Biol Sci Med Sci, 2005. **60**(8): p. 970-5.

126. Quiles, J.L., et al., *Coenzyme Q addition to an n-6 PUFA-rich diet resembles benefits on age-related mitochondrial DNA deletion and oxidative stress of a MUFA-rich diet in rat heart.* Mech Ageing Dev, 2010. **131**(1): p. 38-47.

127. Gomez-Diaz, C., et al., *Effect of dietary coenzyme Q and fatty acids on the antioxidant status of rat tissues.* Protoplasma, 2003. **221**(1-2): p. 11-7.

128. Do, T.Q., J.R. Schultz, and C.F. Clarke, *Enhanced sensitivity of ubiquinone-deficient mutants of Saccharomyces cerevisiae to products of autoxidized polyunsaturated fatty acids.* Proc Natl Acad Sci U S A, 1996. **93**(15): p. 7534-9.

129. Ernest, S. and E. Bello-Reuss, *Expression and function of P-glycoprotein in a mouse kidney cell line.* Am J Physiol, 1995. **269**(2 Pt 1): p. C323-33.

130. Todaro, G.J. and H. Green, *Quantitative studies of the growth of mouse embryo cells in culture and their development into established lines.* J Cell Biol, 1963. **17**: p. 299-313.

131. Hayon, T., et al., *Appraisal of the MTT-based assay as a useful tool for predicting drug chemosensitivity in leukemia.* Leuk Lymphoma, 2003. **44**(11): p. 1957-62.

132. Gonzalez-Aragon, D., et al., *Coenzyme Q and the regulation of intracellular steady-state levels of superoxide in HL-60 cells.* Biofactors, 2005. **25**(1-4): p. 31-41.

133. Cimen, H., et al., *Regulation of succinate dehydrogenase activity by SIRT3 in mammalian mitochondria.* Biochemistry, 2010. **49**(2): p. 304-11.

134. Kuzma-Kuzniarska, M., et al., *Lovastatin-Mediated Changes in Human Tendon Cells.* J Cell Physiol, 2015. **230**(10): p. 2543-51.

135. Chen, Y., et al., *The influence of dietary lipid composition on liver mitochondria from mice following 1 month of calorie restriction.* Biosci Rep, 2012. **33**(1): p. 83-95.

136. Khraiwesh, H., et al., *Mitochondrial ultrastructure and markers of dynamics in hepatocytes from aged, calorie restricted mice fed with different dietary fats.* Exp Gerontol, 2014. **56**: p. 77-88.

137. Lopez-Dominguez, J.A., et al., *Dietary fat modifies mitochondrial and plasma membrane apoptotic signaling in skeletal muscle of calorie-restricted mice.* Age (Dordr), 2013. **35**(6): p. 2027-44.

138. Lopez-Dominguez, J.A., et al., *Dietary fat and aging modulate apoptotic signaling in liver of calorie-restricted mice.* J Gerontol A Biol Sci Med Sci, 2015. **70**(4): p. 399-409.

139. Lombard, D.B., et al., *Mammalian Sir2 homolog SIRT3 regulates global mitochondrial lysine acetylation.* Mol Cell Biol, 2007. **27**(24): p. 8807-14.

140. Stoscheck, C.M., *Quantitation of protein.* Methods Enzymol, 1990. **182**: p. 50-68.

141. Bradford, M.M., *A rapid and sensitive method for the quantitation of microgram quantities of protein utilizing the principle of protein-dye binding.* Anal Biochem, 1976. **72**(1-2): p. 248-54.

142. Arnezeder, C., W. Koliander, and W.A. Hampel, *Rapid determination of ergosterol in yeast cells.* Anal. Chim. Acta 1989. **225**: p. 129-136.

143. Clarke, C.F., W. Williams, and J.H. Teruya, *Ubiquinone Biosynthesis in Saccharomyces cerevisiae.* J Biol Chem, 1991. **266**(25): p. 16636-44.

144. Cordoba-Pedregosa Mdel, C., J.M. Villalba, and F.J. Alcain, *Determination of coenzyme Q biosynthesis in cultured cells without the necessity for lipid extraction.* Anal Biochem, 2005. **336**(1): p. 60-3.

145. Reiss, Y., et al., *Inhibition of purified p21ras farnesyl:protein transferase by Cys-AAX tetrapeptides.* Cell, 1990. **62**(1): p. 81-8.

146. Holstein, S.A., et al., *Quantitative determination of geranyl diphosphate levels in cultured human cells.* Lipids, 2009. **44**(11): p. 1055-62.

147. Tong, H., S.A. Holstein, and R.J. Hohl, *Simultaneous determination of farnesyl and geranylgeranyl pyrophosphate levels in cultured cells.* Anal Biochem, 2005. **336**(1): p. 51-9.

148. Weibel, E.R., *Stereological methods. Vol.1.* Practical Methods for Biological Morphometry. Academic Press, 1979. **1**: p. 26-46.

149. Marfe, G., et al., *Kaempferol induces apoptosis in two different cell lines via Akt inactivation, Bax and SIRT3 activation, and mitochondrial dysfunction.* J Cell Biochem, 2009. **106**(4): p. 643-50.

150. Kincaid, B. and E. Bossy-Wetzel, *Forever young: SIRT3 a shield against mitochondrial meltdown, aging, and neurodegeneration.* Frontiers in Aging Neuroscience, 2013. **5**: p. 48.

151. Weir, H.J., J.D. Lane, and N. Balthasar, *SIRT3: A central regulator of mitochondrial adaptation in health and disease.* Genes Cancer, 2013. **4**(3-4): p. 118-24.

152. Winter, J., et al., *C-ring cleavage of flavonoids by human intestinal bacteria.* Appl Environ Microbiol, 1989. **55**(5): p. 1203-8.

153. Moradi-Afrapoli, F., et al., *Validation of UHPLC-MS/MS methods for the determination of kaempferol and its metabolite 4-hydroxyphenyl acetic acid, and application to in vitro blood-brain barrier and intestinal drug permeability studies.* J Pharm Biomed Anal, 2016. **128**: p. 264-74.

154. Parrado-Fernandez, C., et al., *Calorie restriction modifies ubiquinone and COQ transcript levels in mouse tissues.* Free Radic Biol Med, 2011. **50**(12): p. 1728-36.

155. Mazure, N.M., *VDAC in cancer.* Biochim Biophys Acta, 2017.

156. Hill, S., et al., *Isotope-reinforced polyunsaturated fatty acids protect yeast cells from oxidative stress.* Free Radic Biol Med, 2011. **50**(1): p. 130-8.

157. van Beek, E., et al., *Farnesyl pyrophosphate synthase is the molecular target of nitrogen-containing bisphosphonates.* Biochem Biophys Res Commun. , 1999. **264**(1): p. 108-11.

158. Das, S., et al., *Upregulation of endogenous farnesyl diphosphate synthase overcomes the inhibitory effect of bisphosphonate on protein prenylation in Hela cells.* Biochim Biophys Acta, 2014. **1841**(4): p. 569-73.

159. Raikkonen, J., et al., *Mevalonate pathway intermediates downregulate zoledronic acid-induced isopentenyl pyrophosphate and ATP analog formation in human breast cancer cells.* Biochem Pharmacol, 2010. **79**(5): p. 777-83.

160.   Wiemer, A.J., et al., *Digeranyl bisphosphonate inhibits geranylgeranyl pyrophosphate synthase.* Biochem Biophys Res Commun, 2007. **353**(4): p. 921-5.

161.   Wasko, B.M., et al., *A novel bisphosphonate inhibitor of squalene synthase combined with a statin or a nitrogenous bisphosphonate in vitro.* J Lipid Res, 2011. **52**(11): p. 1957-64.

162.   Quinzii, C.M. and M. Hirano, *Primary and secondary CoQ(10) deficiencies in humans.* Biofactors, 2011. **37**(5): p. 361-5.

163.   Kursvietiene, L., et al., *Multiplicity of effects and health benefits of resveratrol.* Medicina (Kaunas), 2016. **52**(3): p. 148-55.

164.   Arai, D., et al., *Piceatannol is superior to resveratrol in promoting neural stem cell differentiation into astrocytes.* Food Funct, 2016. **7**(10): p. 4432-4441.

165.   Kozlowska, A. and D. Szostak-Wegierek, *Flavonoids--food sources and health benefits.* Rocz Panstw Zakl Hig, 2014. **65**(2): p. 79-85.

166.   Manach, C., et al., *Polyphenols: food sources and bioavailability.* Am J Clin Nutr, 2004. **79**(5): p. 727-47.

167.   Scalbert, A. and G. Williamson, *Dietary intake and bioavailability of polyphenols.* J Nutr, 2000. **130**(8S Suppl): p. 2073s-85s.

168.   Calderon-Montano, J.M., et al., *A review on the dietary flavonoid kaempferol.* Mini Rev Med Chem, 2011. **11**(4): p. 298-344.

169.   Serra, A., et al., *Metabolic pathways of the colonic metabolism of flavonoids (flavonols, flavones and flavanones) and phenolic acids.* Food Chemistry, 2012. **130**(2): p. 383-393.

170.   Labib, S., et al., *Use of the pig caecum model to mimic the human intestinal metabolism of hispidulin and related compounds.* Mol Nutr Food Res, 2006. **50**(1): p. 78-86.

171.   Ghosh, S., S. Banerjee, and P.C. Sil, *The beneficial role of curcumin on inflammation, diabetes and neurodegenerative disease: A recent update.* Food Chem Toxicol, 2015. **83**: p. 111-24.

172.   Fernandez-del-Rio, L., et al., *Kaempferol increases levels of coenzyme Q in kidney cells and serves as a biosynthetic ring precursor.* Free Radic Biol Med, 2017. **In press**.

173.   Vissiennon, C., et al., *Route of administration determines the anxiolytic activity of the flavonols kaempferol, quercetin and myricetin--are they prodrugs?* J Nutr Biochem, 2012. **23**(7): p. 733-40.

174.   Ranganathan, S. and T. Ramasarma, *The regulation of the biosynthesis of ubiquinone in the rat.* Biochem J, 1975. **148**(1): p. 35-9.

175.   Brahimi-Horn, M.C. and N.M. Mazure, *Hypoxic VDAC1: a potential mitochondrial marker for cancer therapy.* Adv Exp Med Biol, 2014. **772**: p. 101-10.

176.   De Pinto, V., et al., *Characterization of human VDAC isoforms: a peculiar function for VDAC3?* Biochim Biophys Acta, 2010. **1797**(6-7): p. 1268-75.

177.   Jitobaom, K., N. Tongluan, and D.R. Smith, *Involvement of voltage-dependent anion channel (VDAC) in dengue infection.* Sci Rep, 2016. **6**: p. 35753.

178.   Shoshan-Barmatz, V., et al., *Subcellular localization of VDAC in mitochondria and ER in the cerebellum.* Biochim Biophys Acta, 2004. **1657**(2-3): p. 105-14.

179.   Zabela, V., et al., *Pharmacokinetics of dietary kaempferol and its metabolite 4-hydroxyphenylacetic acid in rats.* Fitoterapia, 2016. **115**: p. 189-197.

180.   Del Razo Olvera, F.M., et al., *Setting the Lipid Component of the Diet: A Work in Process.* Adv Nutr, 2017. **8**(1): p. 165S-172S.

181.   Lichtenstein, A.H., et al., *Dietary fat consumption and health.* Nutr Rev, 1998. **56**(5 Pt 2): p. S3-19; discussion S19-28.

182.   Adolph, M., et al., *Lipid emulsions – Guidelines on Parenteral Nutrition, Chapter 6.* GMS German Medical Science, 2009. **7**: p. Doc22.

183.   Speakman, J.R. and S.E. Mitchell, *Caloric restriction.* Mol Aspects Med, 2011. **32**(3): p. 159-221.

184.   Bevilacqua, L., et al., *Effects of short- and medium-term calorie restriction on muscle mitochondrial proton leak and reactive oxygen species production.* Am J Physiol Endocrinol Metab, 2004. **286**(5): p. E852-61.

185. Hagopian, K., et al., *Long-term calorie restriction reduces proton leak and hydrogen peroxide production in liver mitochondria.* Am J Physiol Endocrinol Metab, 2005. **288**(4): p. E674-84.

186. Arias, E.B. and G.D. Cartee, *In vitro simulation of calorie restriction-induced decline in glucose and insulin leads to increased insulin-stimulated glucose transport in rat skeletal muscle.* Am J Physiol Endocrinol Metab, 2007. **293**(6): p. E1782-8.

187. Mueckler, M. and B. Thorens, *The SLC2 (GLUT) family of membrane transporters.* Mol Aspects Med, 2013. **34**(2-3): p. 121-38.

188. Goldstein, J.L. and M.S. Brown, *Regulation of the mevalonate pathway.* Nature, 1990. **343**(6257): p. 425-30.

189. Nakakuki, M., et al., *A novel processing system of sterol regulatory element-binding protein-1c regulated by polyunsaturated fatty acid.* J Biochem, 2014. **155**(5): p. 301-13.

190. Field, F.J., et al., *Polyunsaturated fatty acids decrease the expression of sterol regulatory element-binding protein-1 in CaCo-2 cells: effect on fatty acid synthesis and triacylglycerol transport.* Biochem J, 2002. **368**(Pt 3): p. 855-64.

191. Brown, M.S. and J.L. Goldstein, *The SREBP pathway: regulation of cholesterol metabolism by proteolysis of a membrane-bound transcription factor.* Cell, 1997. **89**(3): p. 331-40.

192. Murthy, S., H. Tong, and R.J. Hohl, *Regulation of fatty acid synthesis by farnesyl pyrophosphate.* J Biol Chem, 2005. **280**(51): p. 41793-804.

193. Ou, J., et al., *Unsaturated fatty acids inhibit transcription of the sterol regulatory element-binding protein-1c (SREBP-1c) gene by antagonizing ligand-dependent activation of the LXR.* Proc Natl Acad Sci U S A, 2001. **98**(11): p. 6027-32.

194. Kim, H.J., et al., *Sterol regulatory element-binding proteins (SREBPs) as regulators of lipid metabolism: polyunsaturated fatty acids oppose cholesterol-mediated induction of SREBP-1 maturation.* Ann N Y Acad Sci, 2002. **967**: p. 34-42.

195. Hannah, V.C., et al., *Unsaturated fatty acids down-regulate srebp isoforms 1a and 1c by two mechanisms in HEK-293 cells.* J Biol Chem, 2001. **276**(6): p. 4365-72.

196. Xu, J., et al., *Sterol regulatory element binding protein-1 expression is suppressed by dietary polyunsaturated fatty acids. A mechanism for the coordinate suppression of lipogenic genes by polyunsaturated fats.* J Biol Chem, 1999. **274**(33): p. 23577-83.

197. Xu, J., et al., *Dietary polyunsaturated fats regulate rat liver sterol regulatory element binding proteins-1 and -2 in three distinct stages and by different mechanisms.* J Nutr, 2002. **132**(11): p. 3333-9.

198. Le Jossic-Corcos, C., et al., *Hepatic farnesyl diphosphate synthase expression is suppressed by polyunsaturated fatty acids.* Biochem J, 2005. **385**(Pt 3): p. 787-94.

199. Bentinger, M., et al., *Polyisoprenoid epoxides stimulate the biosynthesis of coenzyme Q and inhibit cholesterol synthesis.* J Biol Chem, 2008. **283**(21): p. 14645-53.

200. Mollet, J., et al., *Prenyldiphosphate synthase, subunit 1 (PDSS1) and OH-benzoate polyprenyltransferase (COQ2) mutations in ubiquinone deficiency and oxidative phosphorylation disorders.* J Clin Invest, 2007. **117**(3): p. 765-72.

201. Teclebrhan, H., et al., *Biosynthesis of the side chain of ubiquinone-trans-prenyltransferase in rat liver microsomes.* J Biol Chem, 1993. **286**(31): p. 23081-86.

202. Wu, N., et al., *Activation of 3-hydroxy-3-methylglutaryl coenzyme A (HMG-CoA) reductase during high fat diet feeding.* Biochim Biophys Acta, 2013. **1832**(10): p. 1560-8.

203. Breitling, R., et al., *Isopentenyl-diphosphate isomerases in human and mouse: evolutionary analysis of a mammalian gene duplication.* J Mol Evol, 2003. **57**(3): p. 282-91.

204. Sagami, H., T. Korenaga, and K. Ogura, *Geranylgeranyl diphosphate synthase catalyzing the single condensation between isopentenyl diphosphate and farnesyl diphosphate.* J Biochem, 1993. **114**(1): p. 118-21.

205. McTaggart, S.J., *Isoprenylated proteins.* Cell Mol Life Sci, 2006. **63**(3): p. 255-67.

206. Grunler, J. and G. Dallner, *Investigation of regulatory mechanisms in coenzyme Q metabolism.* Methods Enzymol, 2004. **378**: p. 3-17.

207. Villalba, J.M., et al., *The influence of dietary fat source on liver and skeletal muscle mitochondrial modifications and lifespan changes in calorie-restricted mice.* Biogerontology, 2015. **16**(5): p. 655-70.

208. Lopez-Dominguez, J.A., et al., *The Influence of Dietary Fat Source on Life Span in Calorie Restricted Mice.* J Gerontol A Biol Sci Med Sci, 2015. **70**(10): p. 1181-8.

209. Khraiwesh, H., et al., *Alterations of ultrastructural and fission/fusion markers in hepatocyte mitochondria from mice following calorie restriction with different dietary fats.* J Gerontol A Biol Sci Med Sci, 2013. **68**(9): p. 1023-34.

210. Chen, Y., et al., *The Influence of Dietary Lipid Composition on Skeletal Muscle Mitochondria From Mice Following 1 Month of Calorie Restriction.* The Journals of Gerontology Series A: Biological Sciences and Medical Sciences, 2012. **67**(11): p. 1121-1131.

211. Hulbert, A.J., *The links between membrane composition, metabolic rate and lifespan.* Comp Biochem Physiol A Mol Integr Physiol, 2008. **150**(2): p. 196-203.

212. Hulbert, A.J., et al., *Life and death: metabolic rate, membrane composition, and life span of animals.* Physiol Rev, 2007. **87**(4): p. 1175-213.

213. Jove, M., et al., *Caloric restriction reveals a metabolomic and lipidomic signature in liver of male mice.* Aging Cell, 2014. **13**(5): p. 828-37.

214. Mourier, A., et al., *Mitofusin 2 is required to maintain mitochondrial coenzyme Q levels.* J Cell Biol, 2015. **208**(4): p. 429-42.

215. Tong, H., et al., *Quantitative determination of isopentenyl diphosphate in cultured mammalian cells.* Anal Biochem, 2013. **433**(1): p. 36-42.

216. Ashihara, E., et al., *Isopentenyl pyrophosphate secreted from Zoledronate-stimulated myeloma cells, activates the chemotaxis of gammadeltaT cells.* Biochem Biophys Res Commun, 2015. **463**(4): p. 650-5.

217. Chung, Y.H., et al., *Statins of high versus low cholesterol-lowering efficacy and the development of severe renal failure.* Pharmacoepidemiol Drug Saf, 2013. **22**(6): p. 583-92.

218. Jeon, S.M., et al., *Hypocholesterolemic and antioxidative effects of naringenin and its two metabolites in high-cholesterol fed rats.* Transl Res, 2007. **149**(1): p. 15-21.

Appendix I: Commercial brands

Product	Brand
(U-^{14}C)-tyrosine	Amersham
^{13}C-kaempferol	Iso-life
^{13}C-vanillin	Cambridge Isotopes
3-(4,5-dimethylthiazol-2-yl)-2,5-diphenyl tetrazolium bromide	Sigma Aldrich
4-hydroxybenzoic acid	Sigma Aldrich
4-hydroxyphenolacetic acid	Sigma Aldrich
Antipain	Sigma Aldrich
Apigenin	Santa Cruz Biotechnology
Bradford reagent	Bio-Rad
Butylated hydroxytoluene	Sigma Aldrich
Cell Dissociation Solution (non-enzymatic)	Sigma Aldrich
Cholesterol	Sigma Aldrich
Chymostatin	Sigma Aldrich
ClinOleic 20%	Baxter (Spain)
Coenzyme Q_{10}	Sigma Aldrich
Coenzyme Q_4	Sigma Aldrich
Coenzyme Q_6	Sigma Aldrich
Coenzyme Q_9	Sigma Aldrich
Curcumin	Santa Cruz Biotechnology
D_3-ferulic acid	Syninnova
D_6-curcumin	Syninnova
Dansyl labeled peptide GCVLS	BioNova científica, s.l.
Fdps Trilencer-27 Mouse siRNA	Origene
Ferulic acid	Santa Cruz Biotechnology
Fetal bovine serum	Sigma Aldrich
Gentamicin	Thermo Fisher Scientific
Hanks' Balanced Salt Solution	Sigma Aldrich
Kaempferol	Santa Cruz Biotechnology
Leupeptin	Sigma Aldrich
L-glutamine	Sigma Aldrich
Lipofectamine® 2000	Thermo Fisher Scientific
Lipofundin MTC/LCT 20%	B. Braun Melsungen AG, Germany
Lipoplus 20%	B. Braun Melsungen AG, Germany
Luteolin	Santa Cruz Biotechnology
Naringenin	Santa Cruz Biotechnology
Nicotinamide	Sigma Aldrich
Nicotinamide	Sigma Aldrich
Opti-MEM	Thermo Fisher Scientific
p-aminobenzoic acid	Sigma Aldrich
p-cresol	Sigma Aldrich
Pepstatin	Sigma Aldrich

Piceatannol	Santa Cruz Biotechnology
Phenylmethylsulfonyl fluoride	Sigma Aldrich
Quercetin	Santa Cruz Biotechnology
Resveratrol	Santa Cruz Biotechnology
Trolox	Sigma Aldrich
Vanillin	Sigma Aldrich
Zoledronic acid	Santa Cruz Biotechnology
γ-globulin	Sigma Aldrich

Appendix II: Article derived from the present work

Original article

Kaempferol increases levels of coenzyme Q in kidney cells and serves as a biosynthetic ring precursor

Lucía Fernández-del-Río[a], Anish Nag[b], Elena Gutiérrez Casado[a], Julia Ariza[a], Agape M. Awad[b], Akil I. Joseph[c], Ohyun Kwon[b], Eric Verdin[d], Rafael de Cabo[e], Claus Schneider[c], Jorge Z. Torres[b], María I. Burón[a], Catherine F. Clarke[b], José M. Villalba[a], *

[a] Departamento de Biología Celular, Fisiología e Inmunología, Universidad de Córdoba, Campus de Excelencia Internacional Agroalimentario, ceiA3, Spain
[b] Department of Chemistry and Biochemistry and the Molecular Biology Institute, UCLA, Los Angeles, CA, USA
[c] Department of Pharmacology, and the Vanderbilt Institute of Chemical Biology, Vanderbilt University Medical School, Nashville, TN, USA
[d] Buck Institute for Research on Aging, Novato, CA, USA
[e] Translational Gerontology Branch, National Institute on Aging, National Institutes of Health, Baltimore, MD, USA

ARTICLE INFO

ABSTRACT

Coenzyme Q (Q) is a lipid-soluble antioxidant essential in cellular physiology. Patients with Q deficiencies, with few exceptions, seldom respond to treatment. Current therapies rely on dietary supplementation with Q_{10}, but due to its highly lipophilic nature, Q_{10} is difficult to absorb by tissues and cells. Plant polyphenols, present in the human diet, are redox active and modulate numerous cellular pathways. In the present study, we tested whether treatment with polyphenols affected the content or biosynthesis of Q. Mouse kidney proximal tubule epithelial (Tkpts) cells and human embryonic kidney cells 293 (HEK 293) were treated with several types of polyphenols, and kaempferol produced the largest increase in Q levels. Experiments with stable isotope ^{13}C-labeled kaempferol demonstrated a previously unrecognized role of kaempferol as an aromatic ring precursor in Q biosynthesis. Investigations of the structure-function relationship of related flavonols showed the importance of two hydroxyl groups, located at C3 of the C ring and C4' of the B ring, both present in kaempferol, as important determinants of kaempferol as a Q biosynthetic precursor. Concurrently, through a mechanism not related to the enhancement of Q biosynthesis, kaempferol also augmented mitochondrial localization of Sirt3. The role of kaempferol as a precursor that increases Q levels, combined with its ability to upregulate Sirt3, identify kaempferol as a potential candidate in the design of interventions aimed on increasing endogenous Q biosynthesis, particularly in kidney.

1. Introduction

Coenzyme Q (Q) is the only lipid-soluble antioxidant synthesized endogenously and present in all cellular membranes. It plays an important role in cellular metabolism and protects membranes and lipoproteins from protein oxidation and lipid peroxidation [1]. The biosynthesis of Q is still not completely characterized. Its biosynthesis is divided into three steps: the synthesis of the polyisoprenoid tail, the attachment of the tail to the benzoquinone ring precursor, followed by subsequent modifications of the ring. In higher eukaryotes, synthesis of the poly-

isoprenoid tail depends on the cytosolic mevalonate pathway and on polyisoprenyl-diphosphate synthases located within the mitochondria [2,3]. The number of isoprene units (designated as the subscript n, Q_n) in the polyisoprenyl tail varies in different organisms. While *Saccharomyces cerevisiae* synthesize Q_6 and humans mainly Q_{10}, mice have two major isoforms, Q_9 and Q_{10} [4]. The polyprenyltransferase Coq2 joins the quinone ring precursor to the polyisoprenoid tail inside mitochondria, and then the ring is modified by distinct enzymes encoded by several *COQ* genes [5]. These modifications include three hydroxylations, one decarboxylation, two *O*-methylations and one *C*-methylation.

4-Hydroxybenzoic acid (4HB) was considered to function as the only confirmed ring precursor of Q for more than 40 years. In 2010 Marbois et al. and Pierrel et al. characterized *p*-aminobenzoic acid (PABA) as a novel Q precursor in yeasts [6,7]. In 2014, Block et al. showed that *Arabidopsis* is able to use *p*-coumarate, but not PABA, as another ring precursor in Q biosynthesis [8]. Recently, in 2015, Xie et al. have described that human and *E. coli* cells do not utilize PABA as precursor in the biosynthesis of Q while both *p*-coumarate and resveratrol, another polyphenol structurally similar to *p*-coumarate, can serve as a ring precursors of Q biosynthesis in *E. coli*, yeasts and human cells [9].

A decrease of Q biosynthesis and total Q levels correlates with physiological aging in some tissues [10]. Q_{10} deficiencies related to distinct diseases are observed in patients, and fortunately some patients with Q deficiencies respond to treatment with dietary supplementation of Q_{10} [5,11]. However, the long polyisoprenoid chain renders Q_{10} highly lipophilic and difficult to absorb by cells. Thus, the poor bioavailability of exogenous Q_{10} often results in treatments that are ineffective [12]. To develop more successful strategies, efforts should also focus on identifying molecules that enhance the endogenous synthesis of Q.

A traditional view is that plant polyphenols constitute a principal source of antioxidants in human diet. However, polyphenols are redox active compounds that elicit cellular signaling and modulate pathways that determine activity of the mitochondrial electron transport chain, membrane potential and biogenesis, intra-mitochondrial oxidative status and, ultimately, mitochondria-triggered cell death [13]. The more than 5000 polyphenol molecules identified have been classified into five major chemical families, namely flavonoids, phenolic acids, stilbenes, lignans and curcuminoids [14]. Studies reveal that their specific chemical structure affects their biological properties [14,15], and some of them can act as Q ring precursors [9].

In the present study, we determined the effect of several polyphenols on Q content and biosynthesis. Among the several polyphenols tested, kaempferol produced the strongest increase in Q content and acted as a novel ring precursor of Q biosynthesis in mammalian cells. The effect of kaempferol on Q biosynthesis may be linked to the numerous beneficial effects attributed to flavonoids. Our studies indicate a novel potential biosynthetic pathway leading to aromatic ring precursors of Q and also suggest new strategies that can help to alleviate the symptoms associated with Q deficiency in aging or disease states.

2. Material and methods

2.1. Chemicals and reagents

Non-labeled kaempferol, resveratrol, quercetin, piceatannol, apigenin, luteolin, naringenin, curcumin, and ferulic acid were obtained from Santa Cruz Biotechnology, Inc. All these compounds were checked in the Mass Spectrometry & Chromatography Service of the University of Córdoba and contamination with 4HB, vanillic or protocatechuic acid was not detected at levels higher than 0.01% of solid material. PABA, 4HB, vanillin, nicotinamide (NAM), 4-hydroxyphenylacetic acid and *p*-cresol were purchased from Sigma-Aldrich. ^{13}C-kaempferol was obtained from IsoLife and D_6-curcumin and D_3-ferulic acid were purchased from SynInnova. $^{13}C_{12}$-curcumin was synthesized from $^{13}C_6$-vanillin (Cambridge Isotopes Laboratories Inc) following a published procedure [16]. Standards of Q_4, Q_6, Q_9 and Q_{10} were purchased from Sigma-Aldrich. Dipropoxy-Q_{10} was synthesized essentially as described by Edlund [17] for diethoxy-Q_{10}, except 1-propanol was substituted for ethanol while maintaining the other reagents and conditions.

2.2. Cell cultures

Mouse kidney proximal tubule epithelial (Tkpts) cells [18], were provided by Dr. Elsa Bello-Reuss (Texas Tech University Health Science Center) and Dr. Judit K. Magyesi (University of Arkansas for Medical Sciences, Little Rock, AR). Human embryonic kidney cells 293 (HEK 293), human liver hepatoma cells (Hep G2), human promyelocytic leukemia cells (HL-60), mouse liver hepatoma cells (Hepa 1.6) and mouse embryonic fibroblast (MEFs) were also used in some studies. These cell lines were obtained from ATCC, whereas MEFs were obtained in our own laboratory by repeated subculture of cells derived from mouse embryos following a standard 3T3 immortalization protocol [19]. Tkpts and Hepa 1.6 cells were grown in DMEM/F12 with 4.5 g/L glucose supplemented with 10% FBS, 2 mM L-glutamine, and gentamicin-amphotericin B (125 μg/ml and 5 mg/ml, respectively). The same media but containing 1 g/L of glucose was used to culture HEK 293 cells. MEFs were cultured in DMEM with 2 g/L glucose supplemented with 10% fetal bovine serum (FBS, Sigma-Aldrich), 2 mM L-glutamine and gentamicin. Hep G2 cells were maintained in MEM containing 1 g/L glucose and supplemented with 10% FBS, 1% sodium pyruvate, 1% L-glutamine and gentamicin-amphotericin B. HL-60 cells were grown in RPMI-1640 supplemented with 10% FBS, 2 mM L-glutamine and gentamicin-amphotericin B. All cultures were maintained at 37 °C in a humidified atmosphere with 5% CO_2.

Saccharomyces cerevisiae BY4741, with genotype MAT **a** *his3Δ1 leu2Δ0 met15Δ0 ura3Δ0* [20] was used in all the determinations involving yeasts. Cells were grown in drop-out-dextrose medium (DOD) composed of 2% dextrose, 6.8 g/L Bio101 yeast nitrogen base minus pABA minus folate with ammonium sulfate and 5.83 mM sodium monophosphate (pH adjusted to 6.0 with NaOH). The yeast colonies were maintained in solid plate yeast extract peptone dextrose (YPD) medium composed of 1% Bacto-Yeast extract, 2% Bacto-Peptone, 2% Dextrose and 2% Bacto agar.

2.3. Treatments of human and mouse cells with polyphenols, and viability assays

The same experimental conditions were used for all compounds when tested in mouse and human cells. Assays were performed in six-well plates with an initial amount of 50,000–100,000 cells/well. Cells were incubated with the tested compounds for 48 h under standard culture conditions (37 °C, 5% CO_2). Once the treatment was completed, cells were detached from culture plates and pelleted by low-speed centrifugation (approximately 1000*g*). Cell pellets were collected and stored at −80 °C until use. Final concentrations of each polyphenol in assays to determine Q content and biosynthesis were selected from the results of viability assays to ensure that experimental conditions did not jeopardize cell viability. To perform these assays, 50 μl/ml of a 5 mg/ml stock of 3-(4,5-dimethylthiazol-2-yl)-2,5-diphenyltetrazolium bromide (MTT, Sigma) was added to the cell cultures (previously plated in 24 well-plates). After 2 h of incubation at 37 °C in 5% CO_2, the medium was removed, the formazan solubilized with 0.04 M HCl in absolute isopropanol, and the absorbance measured at 590 nm in a plate reader (Optic Ivymen System 2000-C).

2.4. Growth and treatment of yeast cells with polyphenols

BY4741 yeast were grown in 50 ml precultures in DOD medium overnight in a shaking incubator (30 °C, 250 rpm). A sample of the yeast preculture was inoculated in 18 × 150 mm borosilicate test tubes containing 5 ml of DOD medium to give an initial cell density of 0.2 A_{600}. Incubations continued at 30 °C and 250 rpm until a cell density of

0.5 A_{600}. At that point, designated polyphenol compounds were added to attain a final concentration of 10 µM and incubation resumed. The tubes were removed from the shaker at 3 h. The A_{600} values were measured and the cell pellets were collected and stored at − 20 °C.

2.5. Preparation of cell and tissue extracts

Whole lysates were prepared from cells as described by Ariza et al. [21] and steady state protein levels were determined by Western blot (see below). Tissues were obtained from Sirt3 knockout mice and their corresponding genetic background-matched controls bred at the Gladstone Institute (San Francisco, CA, USA). Extracts from these tissues were prepared as described by Ariza et al. [21].

2.6. Lipid extractions

2.6.1. Lipid extractions for HPLC-electrochemical detection measurements

Mouse and human cell pellets (approx. 10^6 cells) from the different treatments or 20 mg of the tissue homogenate were collected and resuspended in 90 µl of Hanks' balanced salt solution. Samples were then solubilized using 10 µl of 10% SDS followed by 200 µl of 95:5 ethanol-isopropanol. After vigorous vortexing, 500 µl of hexane were added and the samples were centrifuged for 5 min at 12,500 rpm in an Eppendorf Minispin. Lipids were recovered within the upper hexane phase, and this extraction step was repeated twice. Hexane phases were combined and the solvent evaporated under vacuum. Lipid extracts were stored frozen at −80 °C until use.

2.6.2. Lipid extractions for HPLC-MS/MS measurements

Di-propoxy-Q_{10} was added to the pellets as internal standard in mouse and human samples while Q_4 was used in yeast samples. Cell pellets were vortexed in 1 ml of methanol and 1 ml of petroleum ether. The organic upper layer was transferred to a new tube. Another 1 ml of petroleum ether was added to the original methanol layer, and samples were vortexed again. The organic phase was removed, and the combined organic phase was dried under a stream of nitrogen gas.

2.7. Measurements of Q levels by HPLC

HPLC analysis was carried out with a Beckman Gold System (Beckman Coulter, USA) connected to a Coulochem II electrochemical detector (ESA, Chemsfold, MA, USA). The chromatographic separation was performed with a C18 reverse phase analytical column (4.6 mm × 25 cm, Ultrasphere ODS, 5 µm particle). The mobile phase was composed of methanol/isopropanol/1 M ammonium acetate, pH 4.4, (53:45:2), and a flow rate of 1 ml/min. The analytical cell (ESA, Model 5010) was set at potentials of −500 mV and +300 mV in electrodes 1 and 2, respectively. The entire procedure was performed at room temperature. Lipid extracts were dissolved in 30 µl of methanol, and the sample was subjected then to a reduction step by adding 1 µl of freshly prepared 50 mM sodium borohydride just before injection into the system. This procedure results in the reduction of the quinones (Q) to their corresponding hydroquinones (QH$_2$), which are detected at the second electrode with maximal sensitivity, and allows for a shorter chromatography time. Retention times were 10–11 min for reduced Q_9H_2 and 14–15 min for reduced $Q_{10}H_2$. The area units of hydroquinone peaks were integrated and referred to the reduced $Q_{10}H_2$ standard. Normalized values were obtained by referring to the amount of protein of each sample, calculated previously with a Bradford assay [22].

2.8. Assays of Q biosynthesis

2.8.1. Assays with a radiolabeled precursor

Q biosynthesis was measured with the radiolabeled precursor 4-hydroxy-(U-^{14}C) benzoate (^{14}C-4HB) synthesized from (U-^{14}C)-tyrosine (Amersham) essentially as described by Clarke et al. [23] with a minor modification: aqueous tyrosine was dissolved in 25 µl of 10 M KOH and 12.5 µl of 10 M NaOH before blown to near dryness under nitrogen. ^{14}C-4HB (100,000 CPM) was added to the cells during the 48 h incubation with the treatment. Samples were processed as described previously by Córdoba-Pedregosa et al. [24]. Briefly, cells were rinsed twice with Hanks' balanced salt solution and fixed for 15 min in 1 ml of 5% trichloacetic acid (TCA). After thoroughly washing with TCA to remove the non-incorporated precursor, the radioactivity from the TCA-insoluble Q-containing fraction was directly extracted with 1 ml of 1 M NaOH for 2 h at room temperature with gentle stirring. Radioactivity was quantified in a Beckman scintillation counter by mixing 900 µl of each sample with 4 ml of scintillation liquid. The CPM values so obtained were then referred to the total amount of protein in each sample.

2.8.2. Assays with stable isotope-labeled compounds

Lipid extracts were measured by HPLC-tandem mass spectrometry (MS/MS) analyses as previously described by Xie et al. [9] with minor modifications. Samples were resuspended in 200 µl of ethanol containing 1 mg/ml benzoquinone in order to oxidize all the lipids prior to chromatographic separation with a mobile phase composed of 90% solvent A (95:5 mixture of methanol:isopropanol containing 2.5 mM ammonium formate) and 10% solvent B (isopropanol containing 2.5 mM ammonium formate) at a constant flow rate of 1 ml/min. Transitions monitored are described in Table 1. The area value of each peak, normalized with the correspondent standard curve and internal standard, was referred either to the initial amount of protein in the case of determinations carried out in murine and human cells, or to the total OD present in the yeast cell pellet (as determined by measurements of A_{600}).

2.9. Polyacrylamide gel electrophoresis and Western blot immunodetection

The procedure was performed as described by Ariza et al. [21] with samples of whole cell extracts (50 µg of protein) applied per gel lane. The following primary antibodies were used: Anti-Sirt3 (Santa Cruz Biotechnology, Inc) at 1:1000 dilution, anti-acetyl lysine (Cell Signaling) at 1:1000 dilution, and anti-Coq2 [25] at 1:1000 dilution. In all cases, horseradish peroxidase-conjugated secondary antibodies were used to reveal immunoreactivity by enhanced chemiluminescence. An anti-rabbit secondary antibody (at 1:2000 dilution, Santa Cruz Biotech-

Table 1

HPLC-MS-MS transitions for each analyte. We summarize here the transitions used for each molecule in the HPLC-MS/MS. We monitored both the protonated and the ammoniated transitions.

Molecule	m/z (+ H)	m/z (+ NH$_3$)
Q_4	455.3/197.08	472.3/197.08
Q_6	591.4/197.08	608.4/197.08
$^{13}C_6$-Q_6	597.4/203.08	614.4/203.08
Q_9	795.6/197.08	812.6/197.08
D_3-Q_9	798.6/200.08	815.6/200.08
$^{13}C_6$-Q_9	801.6/203.08	818.6/203.08
Q_{10}	863.6/197.08	880.6/197.08
D_3-Q_{10}	866.6/200.08	883.6/200.08
$^{13}C_6$-Q_{10}	869.6/203.08	886.6/203.08
Dipropoxy-Q_{10}	919.7/253.1	936.7/253.1

nology, Inc) was used for Sirt3 and acetyl lysine, while an anti-chicken secondary antibody (at 1:5000 dilution, Sigma-Aldrich) was used for Coq2.

2.10. Statistical analyses

Statistical analyses were performed using GraphPad Prism 5.03 (GraphPad Software Inc., San Diego, CA, USA). All the data shown are mean ± standard error (SEM) from at least five replicates. Normality of data was checked by Kolmogorov-Smirnov test with the Dallal-Wilkinson-Lilliefor corrected p value. Means were compared using either the parametric two-tail Student's *t*-test or non-parametric Mann-Whitney test depending on the results of the normality test. Significant differences were referred as $*p < 0.05$, $**p < 0.01$ and $***p < 0.001$.

3. Results

3.1. Kaempferol increases Q in cultured kidney cells

We determined the effect of several polyphenols on Q content and biosynthesis. Each compound used in this study was first added to cells at concentrations ranging from 5 nM to 100 μM over a period of 48 h, and tested with the MTT assay to determine effects on cellular viability (see Supplementary Fig. S1). Based on these data, we chose to test phe-

nolic compounds at concentrations ranging from 5 nM to 10 μM to detect possible effects on Q content. Within this range, none of the polyphenols under study decreased viability significantly, and only a small increase in viability was observed at 1 μM piceatannol.

Next, we tested how two stilbenoids (resveratrol and piceatannol) and two flavonols (quercetin and kaempferol) affected Q levels in Tkpts cells. As shown in Fig. 1A, resveratrol produced a slight increase of Q_9 and Q_{10} levels at most concentrations above 50 nM, whereas the other stilbenoid tested, piceatannol, and the flavonol quercetin had no effect on Q levels (either Q_9 or Q_{10}) at any of the concentrations tested. In contrast, kaempferol produced a dramatic increase of both Q_9 and Q_{10} at 100 nM and higher concentrations, producing a plateau at concentrations between 500 nM and 10 μM (Fig. 1B). We also confirmed a substantial increase of Q_9 and Q_{10} levels in Tkpts cells treated with kaempferol at concentrations above 100 nM when specific values were calculated on a protein basis (Supplementary Fig. S2).

Given the differential effects of kaempferol and quercetin (which differ only in one hydroxyl group), we hypothesized that the chemical structure of the flavonoids could influence their effect on Q content (see chemical structures of the compounds used in Supplementary Fig. S1 and the basic chemical skeleton of flavonoids in Fig. 1E). Thus, we tested how additional polyphenols of the flavonoid group affected Q levels in Tkpts cells. For these experiments, we chose two flavones: apigenin, luteolin (Fig. 1C), and one flavanone: naringenin (Fig. 1D).
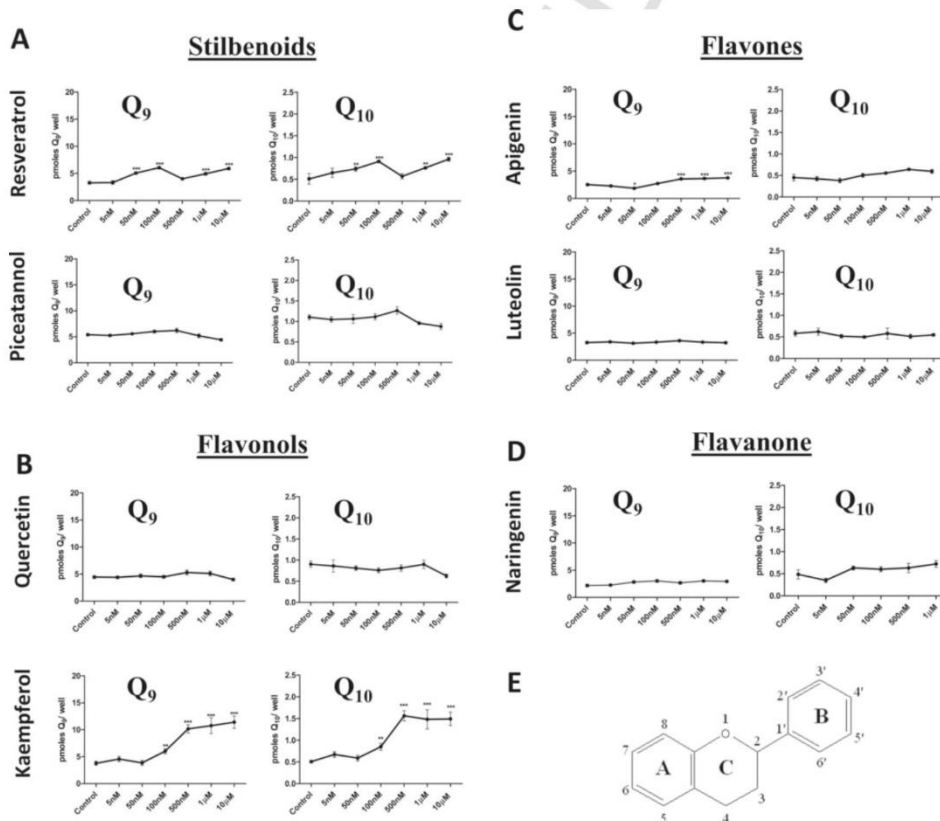
Fig. 1. Kaempferol strongly increases Q levels in Tkpts cells. Q_9 and Q_{10} levels were determined in Tkpts cells treated with different polyphenols at the given concentrations for 48 h. After the incubation period, lipids were extracted and Q levels quantified. **(A)** Stilbenoids. Resveratrol, but not piceatannol, produced a modest increase of Q_9 and Q_{10} levels. **(B)** Flavonols. Quercetin did not affect Q levels, but kaempferol produced a dramatic increase of both Q_9 and Q_{10}. **(C-D)** Flavones and a flavanone. Apigenin, but not luteolin or naringenin, slightly increased Q_9 and Q_{10} levels. **(E)** Basic chemical skeleton of flavonoids. Statistically significant differences between control and treatments are represented by $*p < 0.05$, $**p < 0.01$ and $***p < 0.001$.

Among these three flavonoids, only apigenin produced a slight increase in Q at concentrations between 500 nM and 10 µM, although a concentration of 50 nM was found inhibitory and statistically significant differences were observed for Q_9 but not for the Q_{10} isoform (Fig. 1C).

The following experiments, aimed to elucidate how flavonoids function to increase Q levels, were focused on kaempferol, as this polyphenol was by far the most efficient in augmenting the amounts of cellular Q.

3.2. Kaempferol activation of the mitochondrial sirtuin Sirt3 is unrelated with the increased Q levels

Kaempferol has been reported to up-regulate Sirt3 [26,27], a mitochondrial sirtuin that plays an important role in regulating cellular processes like homeostasis, oxidative stress and aging [28]. Up-regulation of mitochondrial Sirt3 optimizes redox processes linked to the electron transport chain and boosts antioxidant defense in this organelle by activating ROS-scavenging systems [29]. Thus, it seemed

possible that Sirt3-mediated changes might affect Q levels by providing an antioxidant environment that would diminish oxidative Q degradation. To investigate this, Tkpts cells were treated with kaempferol and the up-regulation of mitochondrial Sirt3 was then assessed. As depicted in Supplementary Fig. S3A, treatment of Tkpts cells with kaempferol increased significantly the levels of the mitochondrially-targeted (cleaved) form of Sirt3 at concentrations that also increased Q_9 and Q_{10} levels. We next proceeded to verify whether this up-regulation of Sirt3 mediated the increase in Q levels or, on the contrary, it was an independent event. To this purpose, we tested whether simultaneous treatment with NAM, a well-known inhibitor of sirtuin deacetylase activity [27], impacted Q levels in Tkpts cells treated with kaempferol. As shown in Fig. 2A, treatment with 10 mM NAM did not alter basal levels of Q in Tkpts cells, and the kaempferol-mediated increase of Q_9 and Q_{10} was completely unaffected by NAM. A western-blot using an anti-acetyl lysine antibody confirmed that, under our experimental conditions, deacetylase activity was significantly inhibited by 10 mM NAM since this treatment produced a substantial increase of protein acetyla-
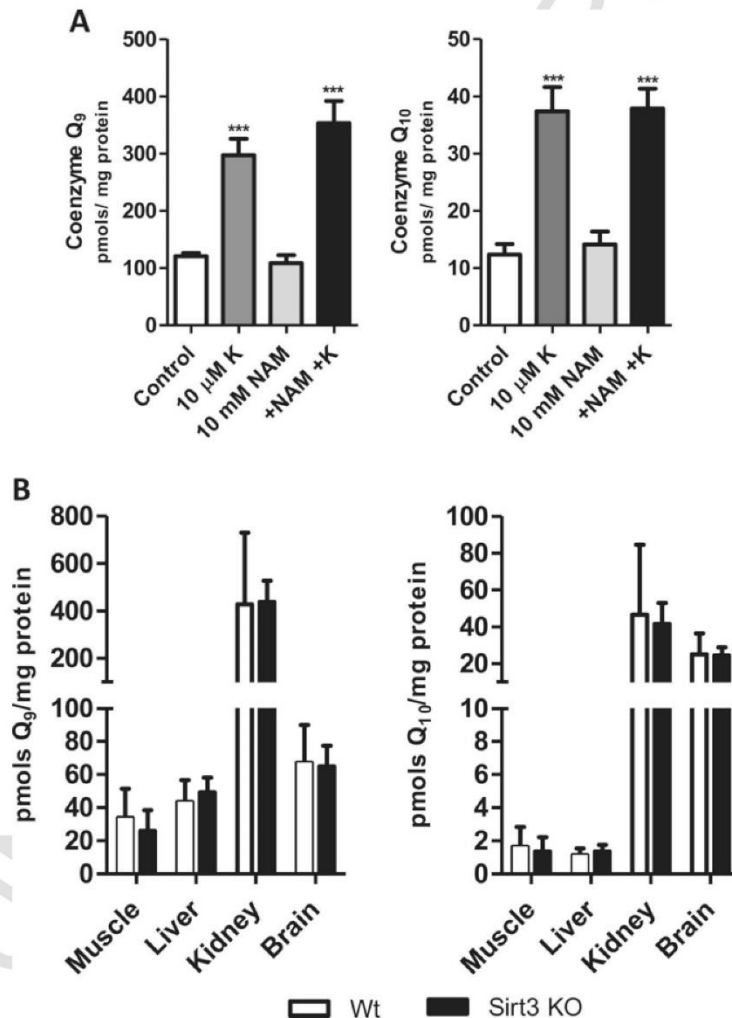
Fig. 2. **The mitochondrial sirtuin Sirt3 does not participate in the regulation of Q levels. (A)** General inhibition of sirtuin deacetylases by nicotinamide (NAM) at 10 mM did not prevent the increase of Q levels in Tkpts cells treated kaempferol (K) at 10 µM. **(B)** Q levels are not altered in tissues (skeletal muscle, liver, kidney and brain) obtained from Sirt3 knockout mice in comparison with age-matched controls. Asterisks denote statistically significant differences (***p < 0.001).

tion (Supplementary Fig. S3B). Furthermore, we also determined Q levels in several tissues obtained from Sirt3 knockout mice. In each tissue examined, including muscle, liver, kidney, and brain, Q levels from Sirt3 knockout mice were not significantly different from their background-matched controls (Fig. 2B). Thus, although similar concentrations of kaempferol can indeed up-regulate Sirt3-dependent mitochondrial functions and increase amounts of Q, the increase in Q content does not appear to be related to the upregulation of Sirt3 activity.

3.3. Kaempferol activates endogenous Q biosynthesis by acting as a ring precursor in mouse and human kidney cells

We considered the possibility that the increase of Q levels caused by kaempferol could be a consequence of a higher Q biosynthetic rate. To test this possibility, we followed two different approaches. First, we studied how PABA, a well-characterized inhibitor of Coq2 activity in animal cells [30,31], affected Q levels in control and in Tkpts cells that had been treated simultaneously with kaempferol. As expected, PABA

decreased Q levels in the control cells. Moreover, PABA abolished the increase of Q in response to kaempferol treatment, indicating a direct link between kaempferol and Q biosynthesis (Fig. 3A).

Secondly, we measured Q biosynthesis with an assay based on the incorporation of exogenous ^{14}C-labeled 4HB as Q ring precursor. Our results showed that kaempferol produced a substantial decrease in the incorporation of ^{14}C-4HB (Fig. 3B). The simultaneous increase of Q levels and decrease of ^{14}C-4HB incorporation into Q by kaempferol, implies that this compound competes with the substrate 4HB to behave as a ring precursor for Q biosynthesis. To confirm this possibility, we cultured Tkpts cells in the presence of ^{13}C-labeled kaempferol and then measured the levels of ^{12}C-Q and $^{13}C_6$-Q with HPLC-MS-MS. This technique allows the simultaneous measurement of the amount of cellular Q derived from endogenous 4HB (^{12}C-Q) and the amount of newly synthesized Q derived from ^{13}C-kaempferol ($^{13}C_6$-Q). Total levels of Q obtained in the presence of ^{13}C-kaempferol were also compared with those obtained when cells were grown in the presence of the non-labeled polyphenol. We found that Q_9 and Q_{10} levels increased equally with both non-labeled and ^{13}C-kaempferol. Of note, when the ^{13}C-la-
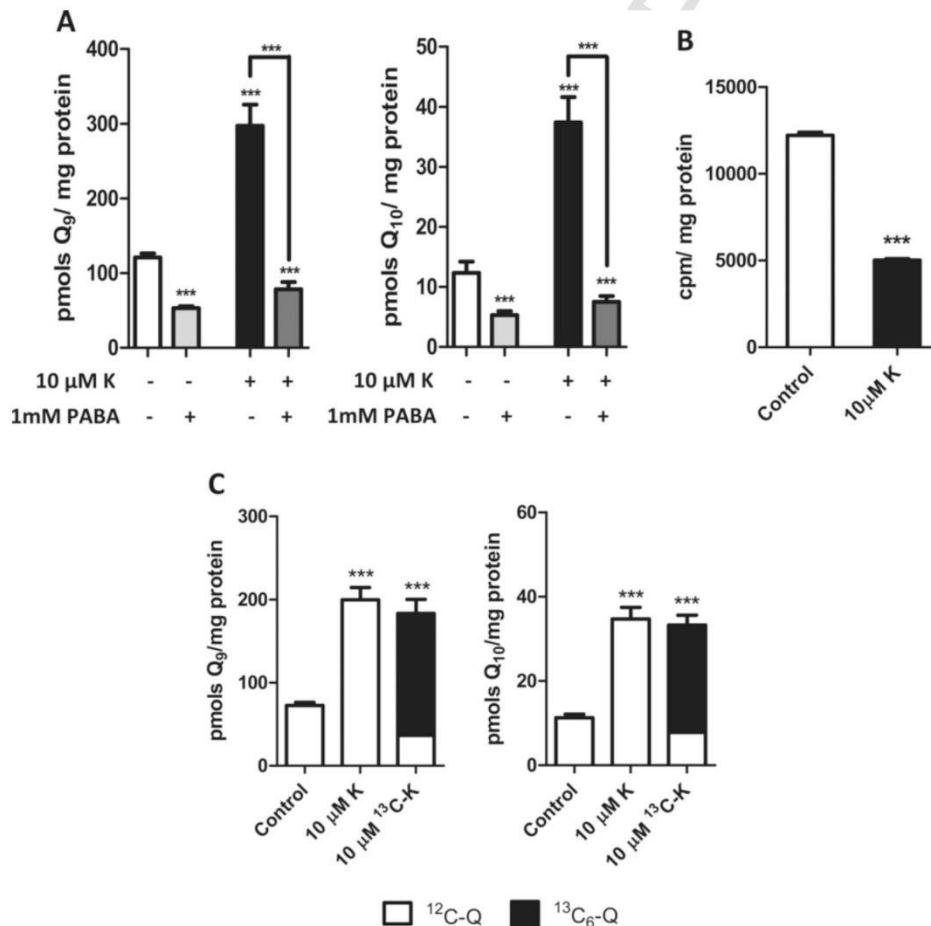
Fig. 3. Kaempferol augmentation of Q levels is related to the enhancement of Q biosynthesis. (A) Inhibition of the Coq2 polyprenyltransferase with PABA decreased Q levels in control Tkpts cells and abolished the increase of Q_9 and Q_{10} in cells treated with kaempferol (K). Cells were cultured for 48 h in the presence of kaempferol at 10 μM and /or PABA at 1 mM. Lipids were then extracted for quantification of Q by HPLC. (B) Competition assay of ^{14}C-4HB incorporation into Q. Treatment of cells with 10 μM kaempferol (K) inhibited the incorporation of ^{14}C-4HB into Q, which indicates competition of kaempferol and 4HB as Q ring precursors. (C) Demonstration of the role played by kaempferol as a Q ring precursor in Tkpts cells. Cells were cultured for 48 h in the presence of unlabeled (K) or ^{13}C-labeled kaempferol (^{13}C-K) at 10 μM. Unlabeled (^{12}C, open bars) and $^{13}C_6$-labeled (closed bars) Q were then measured with HPLC-MS/MS. The majority of Q measured in cells treated with ^{13}C-kaempferol was $^{13}C_6$-Q, demonstrating a role for kaempferol as a novel Q ring precursor. Asterisks denote statistically significant differences (***p < 0.001).

beled precursor was used, nearly all the Q present in Tkpts cells was $^{13}C_6$-Q, identifying kaempferol as an efficient novel Q ring precursor (Fig. 3C). Similar experiments were carried out to test the effects of kaempferol in human HEK 293 cells, another kidney cell line and, as observed for Tkpts cells, Q levels were also increased by kaempferol treatment. Furthermore, when ^{13}C-kaempferol was used, almost all the Q present in HEK 293 cells was $^{13}C_6$-Q (Supplementary Fig. S4A). In sum, our results demonstrate a role for kaempferol as a Q ring precursor both in murine and human kidney cell lines.

Colonic microflora metabolize kaempferol to 4-hydroxyphenylacetic acid (4HPAA) and 4-methyphenol (or *p*-cresol) [32,33]. Moreover, Serra et al. [34] have detected 4HB derived from the metabolic pathway of kaempferol in rat microflora, possibly as a result of further 4HPAA processing. To investigate if kidney cells could directly transform kaempferol in a similar way, we tested whether 4HPAA or p-cresol could serve as Q ring precursors. A MTT assay ruled out any toxicity of these compounds in concentrations ranging from 5 nM to 100 μM (data not shown). Thus, we used both 4HPAA and *p*-cresol at a similar concentration as that used in our previous experiments with kaempferol (10 μM). Our results showed that neither 4HPAA nor *p*-cresol increased Q levels, and they were also unable to compete with ^{14}C-4HB in a Q biosynthesis competition assay (Supplementary Fig. S5). Together, these results argue against 4HPAA and *p*-cresol as metabolites mediating the effect of kaempferol on Q biosynthesis in kidney cells.

### 3.4. Role of other phenolic compounds as Q ring precursors

To further study the ability of other dietary phenolic substances to act as precursors in Q biosynthesis we tested curcumin and ferulic acid, which have a quite different structure in comparison with the stilbenoids and flavonoids we already tested. We also analyzed vanillin, a simpler molecule that shares the same ring structure as curcumin, and ferulic acid (see Supplementary Fig. S1). Vanillic acid, which also bears hydroxyl and methoxy groups in the same position of the ring, has been previously described as a Q ring precursor in mammals [35]. As shown in Fig. 4A, total Q_9 levels were decreased when Tkpts cells were treated with both unlabeled or $^{13}C_{12}$-labeled curcumin, with no $^{13}C_6$-Q being detected in the latter case. The same trend was observed for Q_{10} levels, although a statistically significant decrease was observed only in the case of $^{13}C_{12}$-labeled curcumin. Similar results were obtained using D_6-curcumin in Tkpts cells (data not shown). Vanillin also produced a

decrease of Q_9 levels, and the same trend was observed for Q_{10} although without statistical significance. Strikingly, even when total Q levels were decreased, we were able to detect a signal for $^{13}C_6$-Q_9 although not for $^{13}C_6$-Q_{10} in lipid extracts obtained from cells cultured in the presence of $^{13}C_6$-vanillin (Fig. 4A). However, the proportion of $^{13}C_6$-Q_9 present in cells treated with $^{13}C_6$-vanillin was only about 2%, which is much lower than that produced by ^{13}C-kaempferol (see Fig. 3C). Ferulic acid did not produce any significant change of total Q levels, and deuterated forms of Q_9 or Q_{10} only accounted for a minor portion of total Q after treatment of Tkpts cells with D_3-ferulic acid (Fig. 4B).

Treatments were also carried out in human HEK 293 cells and, in this case, we found that both curcumin and vanillin increased Q levels. We were unable to detect any $^{13}C_6$-Q_{10} in cells cultured for 48 h in the presence of $^{13}C_{12}$-labeled curcumin (Supplementary Fig. S4B), which indicated that the increase of Q levels is not related to augmented Q biosynthesis. Total amounts of Q were also increased in HEK 293 cells cultured in the presence of $^{13}C_6$-labeled vanillin, but $^{13}C_6$-Q_{10} was only about 1% of total Q (Supplementary Fig. S4B), making it unlikely that augmented Q biosynthesis plays a prominent role for the increase of Q levels observed in this cell type. Treatment with ferulic acid did not alter Q levels and the deuterated form of Q_{10} (D_3-Q_{10}) was not detected. In summary, we demonstrate that neither curcumin nor ferulic acid serve as ring precursor for the Q biosynthetic pathway in mouse or human kidney cells, whereas vanillin plays only a minor role in comparison with kaempferol or with the endogenous substrate 4HB.

3.5. 4HB availability is a limiting step for Q biosynthesis in kidney cells

The efficient utilization of kaempferol by kidney cells as a Q ring precursor could be linked to a limited availability of endogenous ring precursors in these cells. In accordance, Pierrel et al. [7] described that availability of the ring precursor (4HB or PABA) was a rate-limiting step for the biosynthesis of Q_6 in yeasts cultured in PABA-free medium. To test whether the effect of kaempferol-mediated increase in Q levels in mammalian cells resulted from limiting amounts of endogenous ring precursors, we measured Q levels in cells that had been treated with exogenous 4HB. For these determinations, we compared the response of the two kidney-derived cell types (mouse Tkpts and human HEK 293) with that of non-kidney cell lines, including mouse liver hepatoma Hepa 1.6, MEFs, human liver hepatoma Hep G2, and human
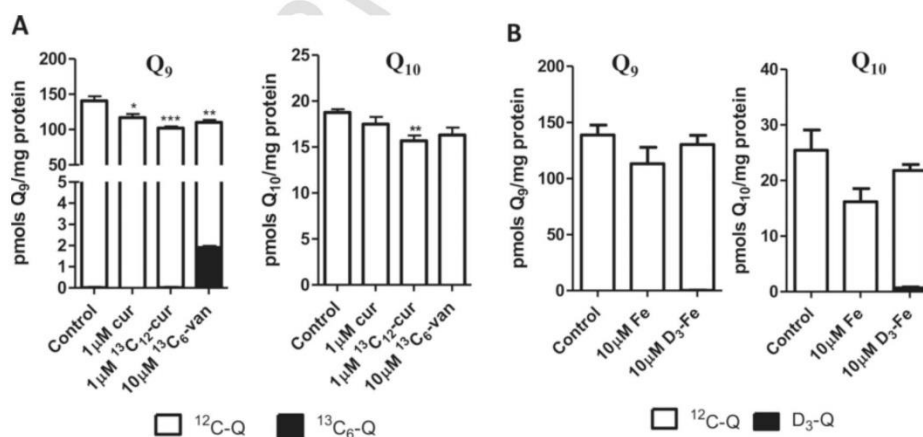
Fig. 4. **Effect of curcumin, ferulic acid and vanillin on Q biosynthesis in Tkpts cells.** (A) Q levels were slightly decreased in Tkpts cells treated with curcumin and vanillin. A small amount of $^{13}C_6$-Q was detected when Tkpts cells were treated with $^{13}C_6$-vanillin, but not when treated with $^{13}C_{12}$-curcumin, indicating that curcumin does not act as a Q ring precursor. (B) Ferulic acid did not alter Q levels and no deuterated signal was recovered after the treatment with D_3-ferulic acid, indicating that ferulic acid does not serve as a Q ring precursor. Statistically significant differences in total Q_9 or Q_{10} between control and treatments are represented by *p < 0.05, **p < 0.01 and ***p < 0.001.

promyelocytic leukemia HL-60 cells. As depicted in Fig. 5, Q levels were dramatically increased in the two kidney-derived cell lines when cultured in the presence of 4HB, and attained levels four- to six-fold higher as compared to the corresponding no addition control. HEK 293 cells were particularly sensitive to supplementation of culture medium with 4HB, with a close to maximal response being already achieved at concentrations as low as 5 nM 4HB. In the mouse Hepa 1.6 cell line, Q levels were increased two-fold by 4HB concentrations between 5 nM and 1 µM but, strikingly, this response was lost at concentration of 10 µM and higher. In the case of MEFs, a slight increase was obtained for the Q_9 isoform at concentrations of 4HB between 50 nM and 1 µM, but no significant changes were observed for Q_{10}. Except for a slight increase of Q_{10} levels at 50 nM 4HB in Hep G2 cells, no further alteration of Q levels by exogenous 4HB supplementation was observed in this cell line or in HL-60 cells at any concentration.

Taken together, these results indicate that availability of endogenous 4HB is a limiting step for Q biosynthesis in kidney cells, and that incorporation of exogenously applied ring precursors, such as kaempferol is favored. This could be due to a rapid flow of metabolites towards Q biosynthesis, which maintains very low levels of upstream substrates such as endogenous 4HB in kidney cells. This interpretation was further supported by the comparison of Q levels in Tkpts and Hepa 1.6 cells, the former containing much higher amounts of Q, particularly Q_{10} (Fig. 6A), and of the polyprenyltransferase Coq2, the enzyme that catalyzes the condensation reaction between ring and hydrophobic tail precursors, which was found also significantly enriched in Tkpts in comparison with Hepa 1.6 cells (Fig. 6B). This situation resembles that of kidney and liver tissues in the mouse [25].

3.6. Kaempferol is not utilized as a Q ring precursor by yeast cells as efficiently as 4HB

Since yeast utilize several ring precursors alternative to 4HB for Q biosynthesis, such as PABA [6,7], *p*-coumarate and resveratrol [9], we investigated whether kaempferol might also serve as a biosynthetic Q precursor in *S. cerevisiae*. In this study, we also investigated the effects of ferulic acid, vanillin, and curcumin, which had not been tested previously as putative Q biosynthetic ring precursors. As stated above, all of these compounds share the same ring structure as vanillic acid. Results obtained with these compounds were compared with those obtained with the endogenous substrate 4HB. Importantly, for these experiments yeast cells were cultured in minus PABA medium, since the presence of PABA in the medium could mask a role for the phenolics as putative Q biosynthetic precursors [6,7]. Yeast cells were grown for 3 h in the presence of each compound at 10 µM concentration, and lipids were extracted for Q_6 quantification. As depicted in Fig. 7A, no significant differences could be observed in the Q_6 levels between cells treated with the unlabeled compounds compared to the control cells.

We next cultured yeast cells in the presence of ^{13}C-labeled kaempferol to test whether kaempferol might still serve as a ring precursor of Q_6 in yeast. Although [13]C_6-Q_6 was detected, it comprised only two to four percent of the total Q content (Fig. 7B). In contrast, [13]C_6-
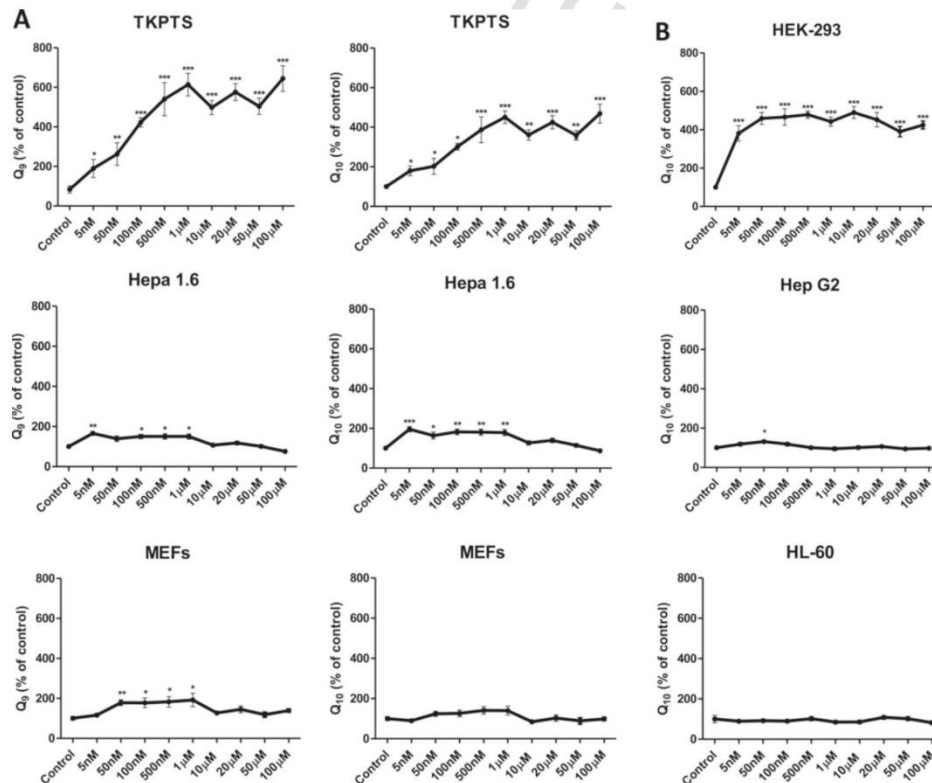
Fig. 5. 4HB is a limiting step in the biosynthesis of Q in kidney cells. (A) Different types of murine cells were treated with increasing concentrations of 4HB. Tpkts cells exhibited a dramatic increase in Q_9 and Q_{10} levels. However, only a slight increase at some concentrations of 4HB was observed for Hepa 1.6 and MEFs. (B) Similar experiments were performed in human cell lines. Human kidney-derived cells (HEK 293) displayed a significant increase of Q_{10} levels, but this effect was not found in human lines from another origin, such as Hep G2 or HL 60. The dramatic increase of Q levels in Tkpts and HEK 293 supports that availability of 4HB is a limiting step for the Q biosynthetic pathway in kidney cells. Statistically significant differences in total Q_9 or Q_{10} between control and treatments are represented by *p < 0.05, **p < 0.01 and ***p < 0.001.
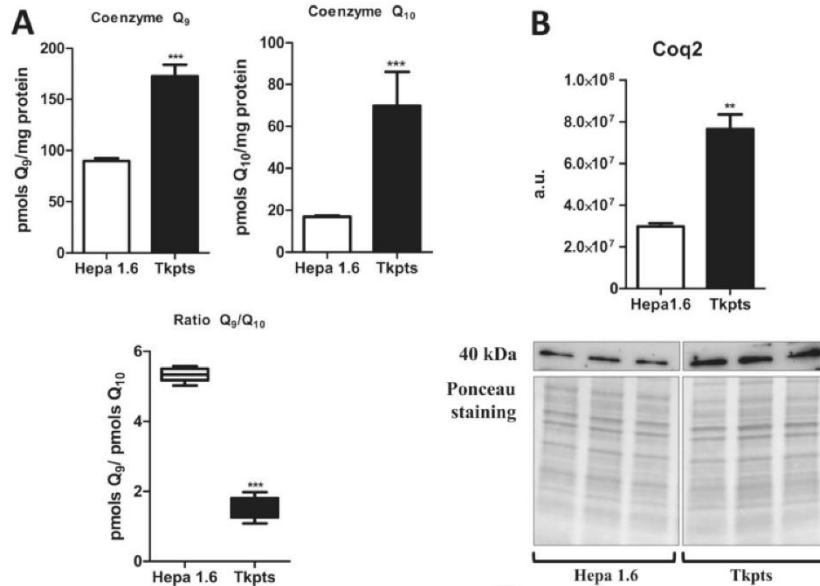
Fig. 6. Kidney-derived Tkpts cells display increased levels of Q and Coq2 in comparison with hepatic Hepa1.6 cells. (A) Q levels and Q_9/Q_{10} ratio. Q levels were higher and Q_9/Q_{10} ratio lower in Tkpts than in Hepa 1.6 cells. **(B)** Coq2 prenyltransferase levels. Arbitrary units depicted in the graph relate directly to the immunoblots shown underneath, which derive from the same film. Statistically significant differences between both cell types are represented by **$p < 0.01$ and ***$p < 0.001$.
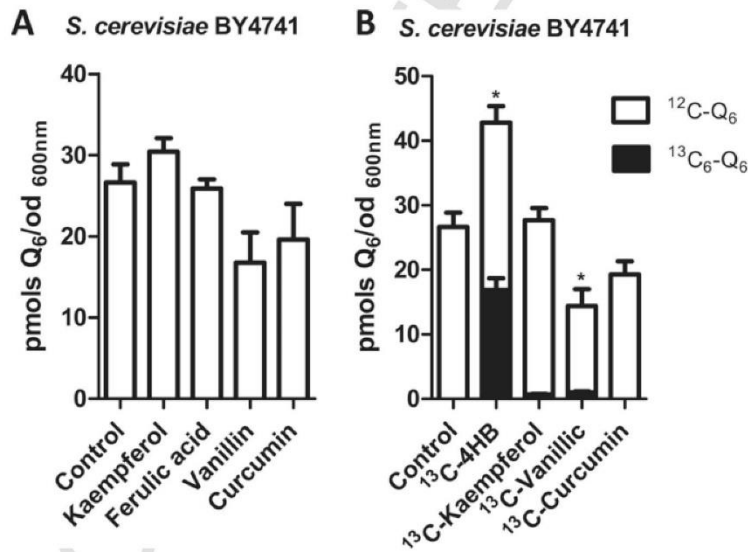
Fig. 7. Kaempferol, ferulic acid, vanillin and curcumin are not utilized as Q ring precursors as efficiently as 4HB in yeast. (A) Effect of kaempferol, ferulic acid, vanillin and curcumin on Q_6 levels. BY4741 yeast cells were treated with these compounds at 10 μM concentrations each, or with EtOH to establish the vehicle control. Yeast were subsequently grown for 3 h in PABA-minus folate-minus medium. **(B)** Effect of ^{13}C ring-labeled compounds on *de novo* Q_6 biosynthesis. BY4741 yeast cells were treated with $^{13}C_6$-4HB, ^{13}C-kaempferol, $^{13}C_6$-vanilin, $^{13}C_{12}$-curcumin, or with EtOH to establish the vehicle control. Significant differences refer to the control condition and are represented by *$p < 0.05$.

4HB was readily incorporated into $^{13}C_6$-Q_6, and also significantly enhanced the total Q content (Fig. 7B) indicating that, compared to kaempferol, yeast can utilize 4HB as a Q ring precursor with a substantially higher efficacy. As we previously observed in kidney cells, despite the decrease of Q_6 levels produced by vanillin, some $^{13}C_6$-labeled Q_6 could be detected when yeast cells were grown in the presence of $^{13}C_6$-labeled vanillin. Finally, as also found previously for kidney cells, no $^{13}C_6$-labeled Q_6 was detected when yeast cells were cultured in the presence of $^{13}C_{12}$-curcumin, suggesting this compound does not serve as a Q ring precursor.

4. Discussion

Polyphenols, which are widely present in foods and beverages of plant origin, have received great interest during the last years due to their positive effects on human health. Several studies have strongly

Appendix II: Article derived from the present work

L. Fernández-del-Río et al.   *Free Radical Biology and Medicine xxx (2017) xxx-xxx*

supported a role for polyphenols in the prevention of important diseases such as cancer, cardiovascular disease, chronic inflammation and neurodegenerative disease [36]. The beneficial properties of polyphenols have been partially attributed to a role as antioxidants as well as to their ability to modulate molecular targets and signaling pathways. Their antioxidant capacity is widely linked to their ability to reduce free radical formation and to scavenge free radicals, but other mechanisms of action serving to elevate endogenous antioxidants are also important. For example, polyphenols can induce antioxidant enzymes such as glutathione peroxidase, catalase and superoxide dismutase and inhibit the expression of enzymes such as xanthine oxidase [37]. Another important factor is the molecular structure of these compounds, which can modulate their properties and functions. Of note, the 3-hydroxyl group in flavonols is considered especially important for their antioxidant activities [38].

As a lipid-soluble antioxidant that can be endogenously synthesized by all organisms, Q plays a major role in antioxidant defense [30]. Resveratrol and *p*-coumarate have been described as Q ring precursors in *E. coli*, *S. cerevisiae* and human cells, but the possibility that polyphenols could actually increase the levels of this lipid antioxidant in cells has not yet been explored. A capacity to increase endogenous Q levels could be a very important finding to palliate Q deficiencies associated with aging or disease. Kidney cells are especially sensitive to a decrease of Q levels, and a nephrotic syndrome is a major clinical phenotype in Q deficiencies [39]. For this reason, we selected two kidney-derived lines, murine Tkpts and human HEK 293 cells, to study the capacity of different polyphenols to increase Q levels.

Two stilbenes, (resveratrol and piceatannol), and two flavonols, (quercetin and kaempferol), were selected in the first phase of our studies. Resveratrol has been the subject of intense research due to its purported cardiovascular protective, antiplatelet, antioxidant, anti-inflammatory, blood-glucose-lowering and anti-cancer activities (reviewed in [40]). Piceatannol is a hydroxylated analogue of resveratrol and shares the structural motif and biological activities, being even more potent in some studies [41]. Apart from the beneficial effects of stilbenes, the regular consumption of flavonoids is related to reduced risk of a number of chronic diseases, including cancer, cardiovascular disease and neurodegenerative disorders (reviewed in [42]). Flavonoids are divided into several groups, with flavonols being those containing the 3-hydroxy group, which has been considered very important for antioxidant activity. For our determinations, we chose quercetin and kaempferol, the two most common compounds in this group. Among these four compounds, only kaempferol efficiently increased Q levels in kidney cells and, interestingly, the effects were observed at concentrations that can be attainable physiologically both by consumption of flavonoids-containing food and by oral supplementation [15,43,44]. Since this ability may derive from its chemical structure, we also tested additional structurally related flavonoids. We chose two flavones, apigenin and luteolin, and one flavanone, naringenin. Of these, only apigenin caused a slight increase in Q_9 and Q_{10} at select concentrations, although its effects were extremely limited in comparison with kaempferol and a slight inhibition was also observed for one of the concentrations tested.

The increase in Q levels by kaempferol in kidney cells depends directly on the stimulation of Q biosynthesis. The kaempferol-mediated increase in Q was blocked by the Q biosynthesis inhibitor PABA; conversely addition of kaempferol competed with incorporation of ^{14}C-4HB into ^{14}C-labeled Q. Cells treated with ^{13}C-kaempferol generated newly synthesized $^{13}C_6$-Q, and demonstrated that kaempferol behaves as a novel Q ring precursor in mammalian cells. The metabolism of kaempferol responsible for its incorporation into the Q biosynthetic pathway remains to be established, although two possibilities can be proposed: (1) kaempferol could act directly as a Q precursor being itself a substrate for the Coq2 transferase and would be subsequently

metabolized and modified by different Coq proteins until it reaches the final structure of Q; or alternatively (2) kaempferol could be cleaved in the cell to yield potential ring precursors which would be then integrated into this pathway. Indeed, previous studies have shown that flavonoids can be transformed by colonic microflora into phenolic acids. However, the type of metabolic products depends on what phenolic compound is metabolized and its specific structure [34]. Cleavage of kaempferol by colonic microflora occurs between C-3 and C-4 carbons of ring C, forming 4HPAA [32,33] derived from the B ring, 4HPAA is then rapidly decarboxylated to form *p*-cresol [45]. If kidney cells were able to perform a biochemical transformation of kaempferol similar to that described for colonic microflora, this would provide an efficient source of Q precursors. However, neither 4HPAA nor *p*-cresol increased Q levels nor competed with ^{14}C-4HB, demonstrating that these compounds do not act as Q ring precursors. Therefore, even if kaempferol is cleaved in renal cells before entering the Q biosynthetic pathway, these known metabolites are not involved in augmenting Q levels.

Whatever the metabolic route involved, an increase of alternative Q ring precursors in cells will only result in higher Q levels if cells have low availability of endogenous 4HB. Pierrel et al. [7] described 4HB as a limiting step in the biosynthesis of Q in *S. cerevisiae* cells and, as we have demonstrated here, this also holds true for kidney cells, although not for other cell lines such as MEFs, Hep G2 and HL-60. The increase of Q observed after a treatment with nanomolar concentrations of 4HB or kaempferol confirms that the availability of endogenous ring precursors is very low in kidney cells of both mouse and human origin. The fact that many cell types do not show increased Q levels in response to exogenous 4HB is in agreement with the early demonstration that 4HB may be present at saturating concentrations in liver, as determined by *in vitro* assays with liver tissue slices [46]. Tissue-specificity regarding the effect of supplementation with ring precursors on Q biosynthesis is further supported by the observations of Wang et al. [47], who demonstrated that adding the ring precursor 2,4-dihydroxybenzoic acid (2,4-DHB) to the drinking water of Q-deficient Mclk1 KO mice resulted in a healthier phenotype, an increase in Q levels and an improvement of the mitochondrial respiratory capacity in heart, kidney and skeletal muscle, although no statistically significant differences were observed in small intestine. Moreover, when 2,4-DHB was given to wild-type mice an increase of Q_9 levels was still detected in kidney mitochondria, but no increase was observed in mitochondria isolated from heart, liver, skeletal muscle or intestine, which agrees with the idea that, even under normal (non deficient) conditions, availability of Q ring precursors is a limiting step in kidney.

In a previous report [25], we demonstrated maximal levels of Coq2 polypeptide in those organs displaying the highest Q concentrations, such as kidney and heart. In accordance, the murine kidney-derived Tkpts cells also showed significantly higher levels of both Q and Coq2 polypeptide than murine hepatic Hepa 1.6 cells. Higher levels of the Coq2 transferase might maintain low cellular concentrations of the ring precursor 4-HB due to its rapid use *via* the Coq2 prenyltransferase activity. Higher Coq2 levels could also account for making these cells particularly responsive to ring precursors as 4HB or kaempferol, leading to a significant increase of Q levels upon supplementation. Further experiments will be needed to fully understand how kaempferol is metabolized to take part directly in the biosynthesis of Q.

Experiments carried out with *S. cerevisiae* demonstrated that kaempferol is not effective in increasing Q_6 levels or acting as a Q ring precursor in this eukaryotic cell model, even when ring precursors are limiting the biosynthesis of Q. Previous studies indicate that yeast cultured under PABA limiting conditions show increased Q_6 content when supplemented with either 4HB or PABA (6). The lack of an effect of kaempferol indicates that yeast cannot utilize flavonoids in the same manner as mammalian cells.

10

The non-flavonoid compound curcumin, which contains two ferulic acid moieties linked *via* a methylene bridge at the carbonyl group C atoms, undergoes metabolism in animals, possesses antioxidant capacity and produces beneficial effects on diabetes, inflammation and neurodegenerative disease by modulating multiple signal molecules (transcription factors, enzymes, *etc.*) and controlling gene expression [48]. Structure of curcumin and ferulic acid differs substantially from that of flavonoids and stilbenoids, so testing their effect on Q system was of considerable interest. However, our data indicate that neither curcumin nor ferulic acid increase Q levels, and only ferulic produced a small but detectable signal of D_3-labeled Q in kidney cells. Similar results were obtained in yeast cells. Chemical structure is a key factor that define the functions and the effect of the different polyphenols. In our study, flavonoids were more efficient used in Q biosynthesis than other non-flavonoid compounds like stilbenoids and curcuminoids. Moreover, one member of the flavonol group (kaempferol) and one member from the flavone group (apigenin) were the ones that displayed the strongest effect increasing Q_9 and Q_{10} levels in renal cells.

The difference between flavonols and flavones is distinguished by the presence of a hydroxyl group in the C3 position. This group seems to be critical because kaempferol (that possesses this group) is much more efficient in increasing Q levels than apigenin and, interestingly, this specific OH group has been linked to an increase of antioxidant activity [38]. However, kaempferol and apigenin have a common characteristic that also seems to be an important determinant for their effect on Q biosynthesis: both compounds possess one hydroxyl group in the B ring. The presence of two hydroxyl groups in this ring, as is the case for quercetin and luteolin, abolishes the effect of these flavonoids on Q biosynthesis. One study that compared the anxiolytic effect of different flavonols noted that this activity decreased with an increasing number of hydroxyl groups in the B ring: kaempferol revealed again the strongest effect, whereas myricetin (which possesses three hydroxyl groups) did not have any effect [49].

In addition, kaempferol has been previously described as a Sirt3 activator. This mitochondrial sirtuin mediates the adaptation of increased energy demand during adverse conditions to increase the production of energy equivalents, and also deacetylates and activates mitochondrial enzymes involved in fatty acid β-oxidation, amino acid metabolism, the electron transport chain, and antioxidant defense [28]. Our results have shown that mitochondrial levels of Sirt3 were indeed increased after kaempferol treatment, confirming these effects also take place in renal cells. However, treatment of kidney cells with NAM, a general inhibitor of sirtuin activity, did not affect the kaempferol-induced increase of Q levels, indicating that Sirt3 activation does not mediate kaempferol effects on Q biosynthesis. Furthermore, Q levels measured in different tissues obtained from Sirt3 knockout mice did not differ from those measured in their wild-type littermates, indicating that Sirt3 does not modulate Q biosynthesis.

Further experimentation is warranted to elucidate whether dietary kaempferol supplementation also increases Q levels in animals, both under normal and Q-deficient conditions. Extensive metabolism of kaempferol when administered with the diet results in very low levels of circulating kaempferol in mice [50], which could hamper potential beneficial effects on Q biosynthesis. However, given the specific response of kidney to small amounts of ring precursors, it is still possible that dietary kaempferol could lead to increased Q levels in this organ, as previously observed for 2,4-DHB [47]. Increasing the availability of Q precursors in cells could move the metabolic flux in favor of the synthesis of Q, helping to ameliorate the phenotype associated with certain Q deficiencies, at least for some organs such as kidney.

In conclusion, we demonstrate that some components of a healthy diet can influence the levels of Q in renal cells. The flavonol kaempferol is identified here as having the strongest effect on increased Q levels due to its action as a novel ring precursor in Q biosyn-

thesis. The ability of kaempferol to simultaneously increase Q and Sirt3 levels, link several of the beneficial effects previously described for this molecule. Further experiments, both *in vitro* and *in vivo*, will be needed to elucidate the exact metabolic pathway by which kaempferol participates in Q biosynthesis, as well as to test its potential beneficial effects *in vivo*.

Acknowledgements

Appendix A. Supplementary material

Supplementary data associated with this article can be found in the online version at doi:10.1016/j.freeradbiomed.2017.06.006.

References

[1] J.M. Villalba, C. Parrado, M. Santos-Gónzalez, F.J. Alcaín, Therapeutic use of coenzyme Q10 and coenzyme Q10-related compounds and formulations, Expert Opin. Invetig. Drugs 19 (4) (2010) 1–20.

[2] J. Ericsson, G. Dallner, Distribution, biosynthesis, and function of mevalonate pathway lipids, Sub-Cell. Biochem. 21 (1993) 229–272.

[3] M.A. Desbats, G. Lunardi, M. Doimo, E. Trevisson, L. Salviati, Genetic bases and clinical manifestations of coenzyme Q10 (CoQ 10) deficiency, J. Inherit. Metab. Dis. 38 (1) (2015) 145–156.

[4] K. Hayashi, Y. Ogiyama, K. Yokomi, T. Nakagawa, T. Kaino, M. Kawamukai, Functional conservation of coenzyme Q biosynthetic genes among yeasts, plants, and humans, PLoS One 9 (6) (2014) e99038.

[5] M.J. Acosta, L. Vazquez Fonseca, M.A. Desbats, C. Cerqua, R. Zordan, E. Trevisson, L. Salviati, Coenzyme Q biosynthesis in health and disease, Biochim. Et. Biophys. Acta 1857 (8) (2016) 1079–1085.

[6] B. Marbois, L.X. Xie, S. Choi, K. Hirano, K. Hyman, C.F. Clarke, para-Aminobenzoic acid is a precursor in coenzyme Q6 biosynthesis in Saccharomyces cerevisiae, J. Biol. Chem. 285 (36) (2010) 27827–27838.

[7] F. Pierrel, O. Hamelin, T. Douki, S. Kieffer-Jaquinod, U. Muhlenhoff, M. Ozeir, R. Lill, M. Fontecave, Involvement of mitochondrial ferredoxin and para-aminobenzoic acid in yeast coenzyme Q biosynthesis, Chem. Biol. 17 (5) (2010) 449–459.

[8] A. Block, J.R. Widhalm, A. Fatihi, R.E. Cahoon, Y. Wamboldt, C. Elowsky, S.A. Mackenzie, E.B. Cahoon, C. Chapple, N. Dudareva, G.J. Basset, The Origin and Biosynthesis of the Benzenoid Moiety of Ubiquinone (Coenzyme Q) in Arabidopsis, Plant Cell 26 (5) (2014) 1938–1948.

[9] L.X. Xie, K.J. Williams, C.H. He, E. Weng, S. Khong, T.E. Rose, O. Kwon, S.J. Bensinger, B.N. Marbois, C.F. Clarke, Resveratrol and para-coumarate serve as ring precursors for coenzyme Q biosynthesis, J. Lipid Res. 56 (4) (2015) 909–919.

[10] R.S. Sohal, M.J. Forster, Coenzyme Q, oxidative stress and aging, Mitochondrion 7 (Suppl) (2007) S103–S111.

[11] F. Ozaltin, Primary coenzyme Q10 (CoQ 10) deficiencies and related nephropathies, Pediatr. Nephrol. 29 (6) (2014) 961–969.

[12] Y. Wang, S. Hekimi, Understanding Ubiquinone, Trends Cell Biol. 26 (5) (2016) 367–378.

[13] C. Sandoval-Acuna, J. Ferreira, H. Speisky, Polyphenols and mitochondria: an update on their increasingly emerging ROS-scavenging independent actions, Arch. Biochem. Biophys. 559 (2014) 75–90.

[14] S. Hatia, A. Septembre-Malaterre, F. Le Sage, A. Badiou-Beneteau, P. Baret, B. Payet, C. Lefebvre d'hellencourt, M.P. Gonthier, Evaluation of antioxidant properties of major dietary polyphenols and their protective effect on 3T3-L1 preadipocytes and red blood cells exposed to oxidative stress, Free Radic. Res. 48 (4) (2014) 387–401.

[15] A. Scalbert, G. Williamson, Dietary intake and bioavailability of polyphenols, J. Nutr. 130 (8S Suppl) (2000) 2073s–2085ss.

[16] O.N. Gordon, L.A. Graham, C. Schneider, Facile synthesis of deuterated and [(14)C]labeled analogs of vanillin and curcumin for use as mechanistic and analytical tools, J. Label. Compd. Radiopharm. 56 (14) (2013) 696–699.

[17] P.O. Edlund, Determination of coenzyme Q10, alpha-tocopherol and cholesterol in biological samples by coupled-column liquid chromatography with coulometric and ultraviolet detection, J. Chromatogr. 425 (1) (1988) 87–97.

[18] S. Ernest, E. Bello-Reuss, Expression and function of P-glycoprotein in a mouse kidney cell line, Am. J. Physiol. 269 (2 Pt 1) (1995) C323–C333.

[19] G.J. Todaro, H. Green, Quantitative studies of the growth of mouse embryo cells in culture and their development into established lines, J. Cell Biol. 17 (1963) 299–313.

[20] C.B. Brachmann, A. Davies, G.J. Cost, E. Caputo, J. Li, P. Hieter, J.D. Boeke, Designer deletion strains derived from Saccharomyces cerevisiae S288C: a useful set of strains and plasmids for PCR-mediated gene disruption and other applications, Yeast 14 (2) (1998) 115–132.

[21] J. Ariza, J.A. Gonzalez-Reyes, L. Jodar, A. Diaz-Ruiz, R. de Cabo, J.M. Villalba, Mitochondrial permeabilization without caspase activation mediates the increase of basal apoptosis in cells lacking Nrf2, Free Radic. Biol. Med. 95 (2016) 82–95.

[22] M.M. Bradford, A rapid and sensitive method for the quantitation of microgram quantities of protein utilizing the principle of protein-dye binding, Anal. Biochem. 72 (1–2) (1976) 248–254.

[23] C.F. Clarke, W. Williams, J.H. Teruya, Ubiquinone Biosynthesis in Saccharomyces cerevisiae, J. Biol. Chem. 266 (25) (1991) 16636–16644.

[24] C. Cordoba-Pedregosa Mdel, J.M. Villalba, F.J. Alcain, Determination of coenzyme Q biosynthesis in cultured cells without the necessity for lipid extraction, Anal. Biochem. 336 (1) (2005) 60–63.

[25] C. Parrado-Fernandez, G. Lopez-Lluch, E. Rodriguez-Bies, S. Santa-Cruz, P. Navas, J.J. Ramsey, J.M. Villalba, Calorie restriction modifies ubiquinone and COQ transcript levels in mouse tissues, Free Radic. Biol. Med. 50 (12) (2011) 1728–1736.

[26] G. Marfe, M. Tafani, M. Indelicato, P. Sinibaldi-Salimei, V. Reali, B. Pucci, M. Fini, M.A. Russo, Kaempferol induces apoptosis in two different cell lines via Akt inactivation, Bax and SIRT3 activation, and mitochondrial dysfunction, J. Cell. Biochem. 106 (4) (2009) 643–650.

[27] H. Cimen, M.J. Han, Y. Yang, Q. Tong, H. Koc, E.C. Koc, Regulation of succinate dehydrogenase activity by SIRT3 in mammalian mitochondria, Biochemistry 49 (2) (2010) 304–311.

[28] B. Kincaid, E. Bossy-Wetzel, Forever young: SIRT3 a shield against mitochondrial meltdown, aging, and neurodegeneration, Front. Aging Neurosci. 5 (2013) 48.

[29] H.J. Weir, J.D. Lane, N. Balthasar, SIRT3: a central regulator of mitochondrial adaptation in health and disease, Genes Cancer 4 (3–4) (2013) 118–124.

[30] M. Turunen, J. Olsson, G. Dallner, Metabolism and function of coenzyme Q, Biochim. Et. Biophys. Acta (BBA) - Biomembr. 1660 (1–2) (2004) 171–199.

[31] D. Gonzalez-Aragon, M.I. Buron, G. Lopez-Lluch, M.D. Herman, C. Gomez-Diaz, P. Navas, J.M. Villalba, Coenzyme Q and the regulation of intracellular steady state levels of superoxide in HL-60 cells, BioFactors 25 (1–4) (2005) 31–41.

[32] J. Winter, L.H. Moore, V.R. Dowell Jr., V.D. Bokkenheuser, C-ring cleavage of flavonoids by human intestinal bacteria, Appl. Environ. Microbiol. 55 (5) (1989) 1203–1208.

[33] F. Moradi-Afrapoli, M. Oufir, F.R. Walter, M.A. Deli, M. Smiesko, V. Zabela, V. Butterweck, M. Hamburger, Validation of UHPLC-MS/MS methods for the determination of kaempferol and its metabolite 4-hydroxyphenyl acetic acid, and application to in vitro blood-brain barrier and intestinal drug permeability studies, J. Pharm. Biomed. Anal. 128 (2016) 264–274.

[34] A. Serra, A. Macià, M.P. Romero, J. Reguant, N. Ortega, M.J. Motilva, Metabolic pathways of the colonic metabolism of flavonoids (flavonols, flavones and flavanones) and phenolic acids, Food Chem. 130 (2) (2012) 383–393.

[35] A.M. Nambudiri, D. Brockman, S.S. Alam, H. Rudney, Alternate routes for ubiquinone biosynthesis in rats, Biochem. Biophys. Res. Commun. 76 (2) (1976) 282–288.

[36] D. Del Rio, A. Rodriguez-Mateos, J.P. Spencer, M. Tognolini, G. Borges, A. Crozier, Dietary (poly)phenolics in human health: structures, bioavailability, and evidence of protective effects against chronic diseases, Antioxid. Redox Signal. 18 (14) (2013) 1818–1892.

[37] Y. Du, H. Guo, H. Lou, Grape seed polyphenols protect cardiac cells from apoptosis via induction of endogenous antioxidant enzymes, J. Agric. Food Chem. 55 (5) (2007) 1695–1701.

[38] R. Tsao, Chemistry and biochemistry of dietary polyphenols, Nutrients 2 (12) (2010) 1231–1246.

[39] C.M. Quinzii, M. Hirano, Primary and secondary CoQ(10) deficiencies in humans, BioFactors 37 (5) (2011) 361–365.

[40] L. Kursvietiene, I. Staneviciene, A. Mongirdiene, J. Bernatoniene, Multiplicity of effects and health benefits of resveratrol, Medicina 52 (3) (2016) 148–155.

[41] D. Arai, R. Kataoka, S. Otsuka, M. Kawamura, H. Maruki-Uchida, M. Sai, T. Ito, Y. Nakao, Piceatannol is superior to resveratrol in promoting neural stem cell differentiation into astrocytes, Food Funct. 7 (10) (2016) 4432–4441.

[42] A. Kozlowska, D. Szostak-Wegierek, Flavonoids–food sources and health benefits, Rocz. Panstw. Zakl. Hig. 65 (2) (2014) 79–85.

[43] C. Manach, A. Scalbert, C. Morand, C. Remesy, L. Jimenez, Polyphenols: food sources and bioavailability, Am. J. Clin. Nutr. 79 (5) (2004) 727–747.

[44] J.M. Calderon-Montano, E. Burgos-Moron, C. Perez-Guerrero, M. Lopez-Lazaro, A review on the dietary flavonoid kaempferol, Mini Rev. Med. Chem. 11 (4) (2011) 298–344.

[45] S. Labib, S. Hummel, E. Richling, H.U. Humpf, P. Schreier, Use of the pig caecum model to mimic the human intestinal metabolism of hispidulin and related compounds, Mol. Nutr. Food Res. 50 (1) (2006) 78–86.

[46] S. Ranganathan, T. Ramasarma, The regulation of the biosynthesis of ubiquinone in the rat, Biochem. J. 148 (1) (1975) 35–39.

[47] Y. Wang, D. Oxer, S. Hekimi, Mitochondrial function and lifespan of mice with controlled ubiquinone biosynthesis, Nat. Commun. 6 (2015) 6393.

[48] S. Ghosh, S. Banerjee, P.C. Sil, The beneficial role of curcumin on inflammation, diabetes and neurodegenerative disease: a recent update, Food Chem. Toxicol.: Int. J. Publ. Br. Ind. Biol. Res. Assoc. 83 (2015) 111–124.

[49] C. Vissiennon, K. Nieber, O. Kelber, V. Butterweck, Route of administration determines the anxiolytic activity of the flavonols kaempferol, quercetin and myricetin–are they prodrugs?, J. Nutr. Biochem. 23 (7) (2012) 733–740.

[50] V. Zabela, C. Sampath, M. Oufir, F. Moradi-Afrapoli, V. Butterweck, M. Hamburger, Pharmacokinetics of dietary kaempferol and its metabolite 4-hydroxyphenylacetic acid in rats, Fitoterapia 115 (2016) 189–197.